# INVESTIGATING THE PRODUCTION AND SECRETION OF PEPITEM, A REGULATOR OF LEUKOCYTE TRAFFICKING

by

Poppy Ysabel Nathan

A thesis submitted to the University of Birmingham for the degree of

DOCTOR OF PHILOSOPHY

Institute of Cardiovascular Sciences

College of Medical and Dental Sciences

University of Birmingham

September 2023

# ABSTRACT

Leukocyte trafficking is an essential part of the inflammatory response. Immune cells need to migrate to areas of inflammation to initiate pathogen clearance and mediate tissue repair. It is vital that this process is tightly regulated, as aberrant lymphocyte recruitment contributes to immune-mediated inflammatory diseases (IMIDs). PEPITEM (PEPtide Inhibitor of TransEndothelial Migration) is an immuno-regulatory peptide secreted by adiponectin-stimulated B-cells and acts to suppress T-cell transendothelial migration. It is known that PEPITEM is derived from the parent protein 14-3-3ζ, however the mechanisms behind PEPITEM production and secretion are currently unknown.

In this thesis, we explored proteases involved in PEPITEM production. Using genetic silencing and blockade with inhibitors, we identified the matrix metalloproteinases MMP-2 and MMP-9 are both required for cleavage of 14-3-3ζ into functional peptide. We also found inflamed endothelial cells upregulate MMP-9 expression and MMP-2 activity in parallel, with a concomitant downregulation of expression of their endogenous inhibitors, TIMP1 and TIMP2. This represents a novel mechanism of regulation of the PEPITEM pathway in inflammatory conditions.

We explored mechanisms of PEPITEM secretion and identified B-cells secrete whole 14-3-3ζ protein in response to adiponectin, which is then proteolytically cleaved once in the extracellular environment. We investigated extracellular vesicle release from B-cells and observed constitutive release of vesicles that was not regulated by adiponectin. Importantly, these vesicles did not contain 14-3-3ζ and therefore do not

represent the mechanism of 14-3-3ζ release from B-cells. Despite 14-3-3ζ lacking the signal recognition particle required for trafficking to the endoplasmic reticulum, we identified inhibition of the classical secretory pathway suppressed 14-3-3ζ secretion. Therefore, it is likely 14-3-3ζ is transported out of the cell coupled with a classically secreted protein.

Thus, we report that 14-3-3ζ is secreted via the classical secretory pathway and subsequently cleaved by MMP-2 and MMP-9 to yield PEPITEM once in the extracellular milieu. Data from this thesis offer a novel understanding of the mechanisms and regulation of PEPITEM production, which will support the development of PEPITEM as a therapeutic agent.

# ACKNOWLEDGMENTS

*Firstly, I would like to thank the Wellcome Trust for funding this project, and to Steve Watson, Robin May and Graham Wallace for obtaining the grant that enabled this work to be carried out.*

*Thank you to my supervisors, Ed Rainger and Helen McGettrick, for your endless support over the last 3 years. Your guidance, advice, and enthusiasm for the project even in the face of setbacks has been greatly appreciated. I would not have been able to complete this project without you.*

*I also want to say a huge thank you to Myriam Chimen, for your supervision during the start of this project. Without your encouragement, I would not have thought myself capable of doing a PhD. You have been greatly missed since your departure from UoB, and I wish you all the best in your new adventures.*

*Thank you to all the blood donors who volunteered for these studies, I promise my vampiric days are behind me.*

*To every member of LTG with whom I have had the pleasure of working, thank you all for the laughs and memories we have shared together. A particular thank you must go to Sophie, you have been with me on this journey since my masters', and you have been both an invaluable lab mentor and a wonderful friend. Thank you to Jenefa, for your constant positivity, kindness, and all the chocolate that you have shared with me during our time working together. To Dean Kavanagh, for your positive nihilism and ridiculous office chats and to Sam Weaver, for quite literally providing a shoulder for me to cry on. To Kathryn, Ladi, Mustafa, Adel and Julia, you have all been an invaluable part of this experience and I am incredibly thankful I got to share it with you.*

*To the MIDAS gang, I am so grateful we got put on this journey together. Abbey, Lisa, David, Sofia and Rachel, you have been the greatest cohort I could have asked for. To all of you, and to Tristan, Tom, and Gillian, I am so thankful for your friendships, which I have no doubt will last a lifetime.*

*Most importantly, thank you to my family. To my parents, for your unconditional love and support. And to Ed, my oldest friend.*

*Finally, to Kyle. I can never repay the support you have given me over the last 3 years, but I intend to spend the rest of my life trying.*

*To everyone, thank you.*

# OUTPUTS FROM THIS THESIS

**First author manuscripts** (in draft)

**Nathan, P.,** Chimen, M**.,** McGettrick, H. M., Rainger, G.E. (2023) MMP-2 and MMP-9 are required for cleavage of 14-3-3ζ to produce functional PEPITEM, a regulator of T-cell transmigration

**Reviews**

**Nathan, P.** Gibbs, JE. Rainger, GE., Chimen, M. (2021) Changes in Circadian Rhythms Dysregulate Inflammation in Ageing: Focus on Leukocyte Trafficking, *Frontiers in Immunology*

**Science Communication Publications**

**Nathan, P**., Hopkin, S., Wilson, I., Lightfoot, A., Begum, J., Lezama, D., Manning, J., Frost, K., Abudu, O., Wahid, M., Sevim, M., (2022) Hitting the road at last: ECRs at an international conference, BSI Immunology News

**Nathan, P**., Hopkin, S., Wilson, I., Lightfoot, A., Begum, J., Lezama, D., Manning, J., Frost, K., Abudu, O., Wahid, M., Sevim, M., (2022) Meeting report: 15th World Congress on Inflammation, British Inflammation Research Association

**Nathan, P.** (2021) New ways to study the elusive exosome, Proteintech Blog

**Nathan, P.** (2021) The Covid Timeline, MIDAS UoB Blog

**Oral Presentations**

PEPITEM Symposium, Mechanisms of PEPITEM production, UK (2023)

MIDAS, The PEPITEM pathway, UK (2022)

WCI, Mechanisms and secretion of PEPITEM, a novel immuno-regulatory peptide, Italy (2022)

MIDAS, The role of MMP-9 in PEPITEM cleavage, UK (2021)

**Poster Abstracts**

BSI 2022, Investigating secretion of B cell derived vesicles, UK (2022)

BSI B Cell Meeting, Mechanisms of secretion of a B-cell derived immuno-regulatory peptide, UK (2022)

# COVID-19 MITIGATION STATEMENT

The COVID-19 pandemic significantly impacted the research originally planned for this thesis. My experiments were delayed or impacted due to limited access to the laboratory, the need to modify ethics and risk assessments involved in blood collection, and access to blood donors who had fully completed their vaccination course. This thesis focuses on leukocyte trafficking and B-cell characterisation, therefore the research relies heavily on access to blood donors. In addition, there were several implications of COVID-19 on access to training, limited allowed working hours, and self-isolation periods that all contributed to delayed research required for this thesis between October 2020 and July 2021.

# Table of Contents

# List of Figures

# List of Tables

# ABBREVIATIONS LIST

| | |
|---|---|
| ABC | ATP-binding cassette |
| ACTB | β-actin |
| ADAM | A disintegrin and metalloproteinase |
| ADAMTS | A disintegrin and metalloproteinase with thrombospondin motifs |
| AKT | Protein kinase B |
| ANOVA | Analysis of Variance |
| AQ | Adiponectin |
| AR | Adiponectin receptor |
| BBE | Bovine brain extract |
| BCR | B cell receptor |
| BEC | Blood endothelial cells |
| BMDM | Bone marrow derived macrophages |
| BSA | Bovine serum albumin |
| BVEC | Blood vascular endothelial cells |
| CCL | C-C chemokine ligand |
| CCR | C-C chemokine receptor type |
| CD | Cluster of differentiation |
| CDH | Cadherin |
| CLA | Cutaneous lymphocyte antigen |
| CNS | Central nervous system |
| COP | Coat protein complex |
| CRP | Collagen related peptide |
| CTL | Cytotoxic T lymphocyte |
| CTLA | Cytotoxic T-lymphocyte-associated protein |
| CXCL | C-X-C chemokine ligand |
| CXCR | C-X-C chemokine receptor |
| DLEC | Dermal lymphatic endothelial cells |
| DMSO | Dimethyl sulfoxide |
| DNA | Deoxyribonucleic acid |
| dNTP | Deoxynucleotide triphosphate |
| EAE | Experimental autoimmune encephalomyelitis |
| EBV | Epstein–Barr virus |
| EC | Endothelial cell |
| ECGS | Endothelial cell growth supplement |
| EDTA | Ethylenediaminetetraacetic acid |
| EGF | Epidermal growth factor |
| ELISA | Enzyme-linked immunosorbent assay |
| EPO | Erythropoietin |
| ER | Endoplasmic reticulum |

| | |
|---|---|
| ESCRT | Endosomal sorting complex required for transport |
| ESL | E-selectin ligand |
| EV | Extracellular vesicles |
| FACS | Fluorescence-activated cell sorting |
| FBS | Fetal bovine serum |
| FCS | Fetal calf serum |
| FDC | Follicular dendritic cells |
| FGF | Fibroblast growth factor |
| GAPDH | Glyceraldehyde-3-phosphate dehydrogenase |
| GP | Glycoprotein |
| HAEC | Human aortic endothelial cells |
| HDBEC | Human dermal blood endothelial cells |
| HDMEC | Human Dermal Microvascular Endothelial Cells |
| HIV | Human immunodeficiency virus |
| HLA-DR | Human Leukocyte Antigen – DR isotype |
| HLMVEC | Human lung microvascular endothelial cells |
| HMEC | Human microvascular endothelial cell |
| HSEC | Hepatic sinusoidal endothelial cells |
| HUVEC | Human umbilical vein endothelial cells |
| IC50 | Half-maximal inhibitory concentration |
| ICAM | Intercellular adhesion molecule |
| IFN | Interferon |
| IHC | Immunohistochemistry |
| IL | Interleukin |
| IMID | Immune-mediated inflammatory disorders |
| ITAC | Interferon-inducible T cell α chemoattractant |
| JAM | Junctional adhesion molecule |
| LAD | Leukocyte adhesion deficiency |
| LAMP1 | Lysosomal-associated membrane glycoprotein |
| LCL | Lymphoblastoid cell lines |
| LFA | Lymphocyte function-associated antigen |
| LN | Lymph node |
| LPS | Lipopolysaccharide |
| LRS | Leukocyte reduction cone |
| MADCAM | Mucosal addressin cell adhesion molecule |
| MAPK | Mitogen-activated protein kinases |
| MBEC | Murine brain endothelial cells |
| MEC | Microvascular endothelial cells |
| MFI | Mean fluorescence intensity |
| MHC | Major histocompatibility complex |
| MIP | Macrophage inhibitory protein |
| MISEV | Minimal Information for Studies of Extracellular Vesicles |

| | |
|---|---|
| MLEC | Murine lymphoid endothelial cells |
| MMP | Matrix metalloproteinase |
| MS | Multiple sclerosis |
| MT-MMP | Membrane type matrix metalloproteinase |
| NFκB | Nuclear factor kappa beta |
| NK | Natural killer cells |
| NTA | Nanoparticle tracking analysis |
| PAEC | Pulmonary arterial endothelial cells |
| PBL | Peripheral blood lymphocytes |
| PBMC | Peripheral blood mononuclear cells |
| PBS | Phosphate buffered saline |
| PCR | Polymerase chain reaction |
| PEPITEM | PEPtide Inhibitor of TransEndothelial Migration |
| PEV | Platelet derived extracellular vesicles |
| PI3K | Phosphoinositide 3-kinases |
| PKA | Protein kinase A |
| PM | Plasma membrane |
| PMA | Phorbol myristate acetate |
| PNA | Peripheral node addressin |
| PSGL | P-selectin glycolipid ligand |
| RA | Rheumatoid arthritis |
| RNA | Ribonucleic acid |
| RT | Room temperature |
| S1P | Sphingosine-1-phosphate |
| S1PR | Sphingosine-1-phosphate receptor |
| SD | Standard deviation |
| SDF | Stromal cell-derived factor |
| SEM | Standard error of the mean |
| SLE | Systemic lupus erythematosus |
| SPHK1 | Sphingosine kinase 1 |
| SPNS2 | Spinster homolog 2 |
| SRP | Signal recognition peptide |
| T1D | Type-1-diabetes |
| TCR | T cell receptor |
| TEM | Tansendothelial migration |
| TGF | Transforming growth factor |
| TSP | Thrombospondin |
| TIMP | Tissue inhibitors of metalloproteinases |
| TLR | Toll-like receptor |
| TNF | Tumour necrosis factor |
| TNFR | Tumour necrosis factor receptor |
| VCAM | Vascular cell adhesion molecule |

| | |
|---|---|
| VEGF | Vascular endothelial growth facto |
| VLA | Very Late Antigen |
| WT | Wild type |

# Chapter 1. INTRODUCTION

## 1.1. Introduction

Inflammation is the protective sequence of events occurring in response to local tissue injury or infection (Kindt, Osborne and Goldsby, 2006). During an inflammatory response, circulating leukocytes are recruited to the site of inflammation and play key roles in pathogen clearance and tissue repair (Ryan and Majno, 1977). This thesis is broadly interested in the factors influencing T-cell trafficking into peripheral tissues, and trafficking of other leukocyte subsets, migration into lymphoid tissues or across lymphatic endothelial cells will not be discussed. For further information, these topics have been reviewed extensively elsewhere (Hunter, Teijeira and Halin, 2016).

A novel regulatory pathway of T-cell transendothelial migration, the PEPITEM pathway, which is defective in immune-mediated inflammatory diseases (IMIDs), was recently described in Birmingham (Chimen et al., 2015). PEPITEM (Peptide Inhibitor of TransEndothelial Migration), a proteolytic product of a larger protein (14-3-3ζ) is secreted from adiponectin-stimulated B-cells, however, the exact mechanisms involved in this secretion and which proteases are involved in mature PEPITEM processing are yet to be elucidated. In this thesis, we aimed to investigate the mode of PEPITEM secretion and cleavage and how this is modulated in areas of inflammation in order to take full advantage of the translational potential of PEPITEM.

## 1.2. Immune-mediated inflammatory disease

Immune-mediated inflammatory diseases (IMIDs) represent a host of multifactorial diseases including inflammatory bowel disease, psoriasis, systemic lupus erythematosus, type-1-diabetes (T1D) and rheumatoid arthritis (RA) (McInnes and Gravallese, 2021). These conditions are associated with systemic inflammation and inappropriate leukocyte trafficking (Manning *et al.*, 2021; Ortega *et al.*, 2022).

Importantly, these diseases have a significant impact on patients' quality of life as well as having a huge economic burden on both individuals and health care systems (Kuek, Hazleman and Östör, 2007). Current treatments aiming to reduce systemic inflammation are often expensive and have severe side effects (Bullock *et al.*, 2018). PEPITEM represents a novel therapeutic that acts to target the dysregulated leukocyte trafficking seen in these patients to help reduce inflammation (Chimen *et al.*, 2015)

### 1.3. Endothelial Cell Environmental Responses That Influence Trafficking

Lymphocyte trafficking is a tightly regulated process. A critical regulator of this process are blood vascular endothelial cells (BEC), which respond to local changes in their microenvironment to facilitate trafficking. In response to inflammatory mediators such as cytokines and histamine, BEC up-regulate the surface expression of adhesion molecules, chemokines and lipid mediators which are all required for efficient lymphocyte trafficking.

Inflamed BEC upregulate surface expression of adhesion molecules, E- and P-selectin, which are bound by their capture receptors P-selectin glycoprotein ligand 1 (PSGL1) on T-cells (Gotsch *et al.*, 1994; Strindhall, Lundblad and Pahlsson, 1997). P-selectin is stored in Weibel-Palade bodies in the BEC which can be rapidly released and localised to the EC surface upon activation (McEver *et al.*, 1989), E-selectin peaks 4-6 hours after activation following RNA and protein synthesis (Bevilacqua *et al.*, 1987; Pober and Cotran, 1990). Inflammation also induces secretion and surface immobilisation of chemokines CXCL9 (Mig) and CXCL10 (IP-10) (Piali *et al.*, 1998) and CXCL11 (I-TAC) (Mazanet, Neote and Hughes, 2000). mRNA transcripts of CXCL9 and CXCL10 were not detected before 4h of stimulation

and peaked at 8-16 hours (Piali *et al.*, 1998). Cytokine stimulation of BEC results in upregulation of surface expression of members of the immunoglobulin (Ig) superfamily; intercellular cell adhesion molecule 1 (ICAM-1) and vascular cell adhesion molecule 1 (VCAM-1). IL-1 and TNF- α treatment increased ICAM-1 and VCAM-1 surface expression following mRNA and protein synthesis which peaks at 6-8hr and lasts up to 72hr (Wong and Dorovini-Zis, 1992). Ligands of ICAM-1 and VCAM-1 are integrins, LFA-1 (αLβ2) and VLA-4 (α4β1) respectively and this interaction is essential for transendothelial migration and will be covered in more detail in section 1.4.2.

BEC activity is also influenced by the stromal microenvironment, which in turn can influence the process of leukocyte trafficking (reviewed in McGettrick, 2012; Manning, 2020). Stromal cells have tissue-specific effects on leukocyte adhesion and migration across EC (Bradfield *et al.*, 2003; McGettrick *et al.*, 2010; McGettrick *et al.*, 2010; Kuravi *et al.*, 2014). Hence, stromal 'address-codes' direct leukocyte recruitment during an inflammatory response (Parsonage *et al.*, 2005). Haemodynamic forces also regulate BEC phenotype which dictates where in the vasculature trafficking can occur due to the shear dynamics (Rainger *et al.*, 2001).

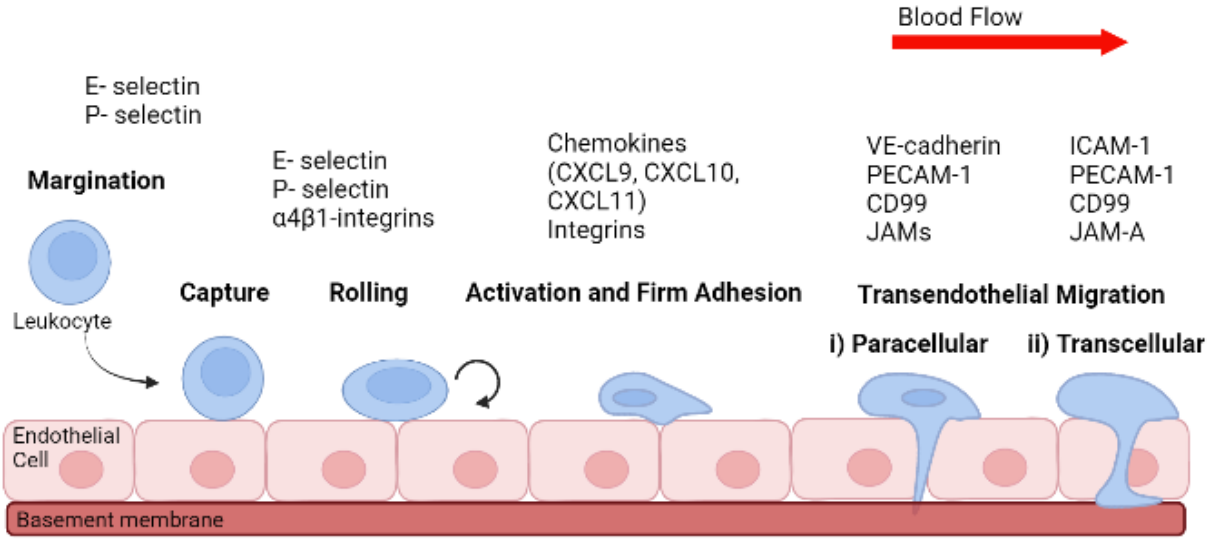


**Figure 1.1 – Leukocyte adhesion and migration across the endothelium**
For leukocyte emigration out of the vessel and into inflamed tissues, they undergo a process of i) margination ii) capture iii) rolling iii) activation and firm adhesion, and iv) transendothelial migration. Each step in leukocyte recruitment is governed by interactions between specific adhesion molecules and their counter-ligands. Cytokine stimulated endothelial cells upregulate varying adhesion molecules at different stages of the recruitment process as shown in the above diagram. CXCL, C-X-C Motif Chemokine Ligand; VE-cadherin, vascular endothelial-cadherin; PECAM-1, Platelet And Endothelial Cell Adhesion Molecule 1; cd99, cluster of differentiation 99 (MIC2); JAM, junctional adhesion molecule

## 1.4. Lymphocyte recruitment during inflammation

Temporal expression of adhesion molecules on the surface of lymphocytes and blood vascular endothelial cells (BVEC) mediates lymphocyte trafficking, in a process known as the leukocyte adhesion cascade (Springer, 1995). This paradigm can be separated into several key stages; margination, capture from flow, rolling, firm adhesion and arrest, before finally migrating across the BVEC layer (reviewed in Ley *et al.*, 2007) (Figure 1.1) and will be discussed in detail below. It is essential that leukocyte trafficking is tightly regulated, as aberrant lymphocyte recruitment contributes to the development and persistence of immune-mediated inflammatory diseases (IMIDs), such as systemic lupus erythematosus (SLE) and type-1-diabetes (T1D) (Wuthrich, 1992; Johnson et al., 1993; Pallis et al., 1993).

### *1.4.1. Margination*

T cells are required to be in close proximity to the inflamed BVEC to facilitate capture from flow. In standard blood flow, this proximity is favoured due to the natural kinetics of blood flow in a process termed margination, whereby red blood cells flow through the centre of the vessel forcing lymphocytes to flow along the periphery of the vessel by a simple mechanical characteristic of blood rheology (Goldsmith and Spain, 1984; Abbitt and Nash, 2003; Dimitrov *et al.*, 2009).

### *1.4.2. Capture from flow*

Selectins are a family of adhesion molecules containing a C-type lectin domain which can bind specific carbohydrate groups on their respective ligands (Table 1.1) (Springer, 1995; Middleton *et al.*, 2002). The three members of the selectin family (E-, P- and L-) form high-affinity interactions with their ligands with fast bond kinetics, resulting in constant rapid breaking and reforming of bonds that mediates dynamic,

rolling adhesion (Alon, Hammer and Springer, 1995). Interestingly, selectin-dependent adhesion is supported by shear stress and rolling lymphocytes detach from the endothelium when flow is removed (Finger *et al.*, 1996; Lawrence *et al.*, 1997). These high kinetic bonds reduce the velocity of the T-cell on the endothelium and results in their 'rolling' along the endothelium. Importantly, the reduction in flow speed allows sufficient time for the T-cells to undergo integrin mediated firm adhesion, which is covered in detail in section 1.3.3.

As previously mentioned, inflamed endothelial cells express E- and P-selectin that bind glycosylated ligands on T-cells (Gotsch *et al.*, 1994; Strindhall, Lundblad and Pahlsson, 1997). Under flow conditions, very few PBL adhered to unstimulated human HUVEC cultured on filters, however TNF-α and IFN-γ stimulation lead to much greater adherence (McGettrick *et al*., 2009). In a flow based *in vitro* model, primary CD4+ T-cell adhesion and rolling across TNF-α stimulated HUVEC was significantly blocked using an anti-P-selectin monoclonal antibody (mAb), however no effect on adhesion or rolling was seen using anti-E-selectin or anti-L-selectin mAbs (Luscinskas, Ding and Lichtman, 1995). This data suggests CD4+ T-cell adhesion is primarily mediated by P-selectin. However, blockade of P-selectin only lead to a partial (50%) decrease in adhesion, which can be explained by the supporting role of α4β1-integrin (Very Late Antigen-4; VLA-4) interaction with VCAM-1 (Luscinskas, Ding and Lichtman, 1995). Blockade of α4β1 or VCAM-1 led to significant reduction in adhesion, however the α4β1-VCAM1 interaction alone was not enough to induce rolling (Luscinskas, Ding and Lichtman, 1995). E-selectin is essential for adhesion of memory T-cells (Shimizu *et al.*, 1991). IL-1 stimulated HUVEC treated with anti-LFA1 and anti-VLA4 antibodies, which can only bind cells dependent on E-selectin, bind a

much greater amount of purified memory CD4+ T-cells compared to naïve CD4+ T-cells (Shimizu *et al.*, 1991).

*In vivo* models support a level of redundancy between selectins for lymphocyte rolling. In young mice pre-treated with an intrascrotal injection of TNF- α (0.5μg), intravital microscopy of the cremaster muscle revealed both E- and P- selectin need to be blocked, either using mAbs or genetic silencing, to significantly decrease lymphocyte rolling (Kunkel and Ley, 1996; Jung and Ley, 1999). Addition of either E- or P- selectin mAbs to TNF-α treated wildtype mice showed no decrease in percentage lymphocyte rolling, however addition of both of these antibodies decreased rolling by 80-90% (Kunkel and Ley, 1996). Interestingly, blockade of E-selectin alone either by addition of an E-selectin monoclonal antibody or in the E-selectin deficient mice had significantly increased percentage rolling following TNF-a stimulation compared to similarly treated wild-type controls, suggesting E-selectin may play other roles than in rolling, such as inducing firm adhesion or arrest (Kunkel and Ley, 1996). These models however only look at total lymphocyte populations and do not look at specific T-cell population trafficking.

L-selectin is found on all leukocytes except a subset of memory T-cells (Von Andrian et al., 1993), and is widely used as an activation marker as it is readily shed upon engagement of the T-cell receptor (Jung *et al.*, 1988). L-selectin deficient mice have only a slightly lower level of rolling lymphocytes compared to WT, however addition of a blocking P-selectin mAb, but interestingly not an E-selectin mAb, significantly reduced rolling. This suggests L-selectin deficient lymphocytes are more dependent on P-selectin for TNFα-induced rolling (Kunkel and Ley, 1996). Importantly, despite the redundancy between selectins that can be seen in *in vitro*

rolling experiments, the role of L-selectin in inflammatory responses cannot be overlooked as L-selectin deficient mice have impaired lymphocyte recruitment into inflammatory sites in models of peritonitis (Ley *et al.*, 1995), delayed type hypersensitivity (Tedder, Steeber and Pizcueta, 1995), and impaired CD8+ T-cell homing to sites of viral infections (Mohammed *et al.*, 2016). It is also worth noting L-selectin primarily regulates entry of naïve and central memory T-cells into lymph nodes which will not be discussed in detail here (reviewed in Mackay, Marston and Dudler, 1992).

The importance of selectins in lymphocyte trafficking is evidenced by leukocyte adhesion deficiency (LAD) type II. LAD II patients have impaired selectin ligand glycosylation resulting in a deficiency of LAD II leukocytes in binding to endothelial E- and P-selectins, resulting in recurrent infections and leukocytosis (Etzioni *et al.*, 1992).

**Table 1.1 Selectins involved in T-cell trafficking**

| Selectin | Distribution | Ligand | Role in T-cell Migration |
|---|---|---|---|
| L-selectin (CD62L) | All leukocytes<br>Readily shed upon activation | PSGL-1<br>PNA-d<br>CD34<br>GlyCAM-1<br>MADCAM-1 | Homing to lymphoid tissues |
| E-selectin (CD62E) | Endothelilal cells | PSGL-1<br>ESL-1<br>CLA | Migration to areas of inflammation<br><br>Memory T-cells homing to skin |
| P-selectin (CD62P) | Endothelial cells<br>Platelets | PSGL-1,<br>CD24,<br>PNA-d | Migration to areas of inflammation |

CLA: cutaneous lymphocyte antigen; EC: endothelial cells; ESL-1: E-selectin ligand-1; GlyCAM-1: glycosylation-dependent cell adhesion molecule-1; MAdCAM-1: mucosal addressin cell adhesion molecule-1; PNAd: peripheral node addressin and PSGL-1: P-selectin glycolipid ligand-1.
Adapted from (von Andrian and Mackay, 2000 and Kappelmayer *et al.*, 2004)

### *1.4.3. Activation and Firm Adhesion*

Chemokine activation of integrins is essential for firm adhesion of rolling lymphocytes to the endothelium. As mentioned in section 1.3, chemokines are upregulated by endothelial cells in response to pro-inflammatory stimuli and become immobilised to proteoglycans found on the extracellular matrix. Immobilised chemokines then act as chemo-attractants and attract rolling lymphocytes via haptotactic gradients (Kim and Broxmeyer, 1999). Chemokines interact through G-protein coupled receptors on the surface of T-cells that triggers activation of integrins via “inside-out signalling”. This is a process where integrins undergo a conformational change from a bent low-affinity conformation to an extended high-affinity conformation, exposing the ligand binding domain (Arnaout, Mahalingam and Xiong, 2005; Ley et al., 2007). Chemokines also induce reorganisation of integrins into clusters, increasing the number of interactions between lymphocytes and adhesion molecules on the endothelium (reviewed in Carman and Springer, 2003). *In vitro*, mouse lymphocytes stimulated with CXCL12 (SLC) underwent significant redistribution of the β2-integrin into clusters and large polar patches (Constantin et al., 2000).

Distinct chemokine – receptor interactions dictate lymphocyte trafficking, and expression of varying chemokine receptors by different T-cell subsets is important for their unique patterns of trafficking (reviewed in von Andrian and Mackay, 2000) (Table 1.2). CXCR4 is the only chemokine receptor expressed on all T-cells and facilitates their trafficking into bone marrow in response to CXCL12 (SDF-1) (Bleul *et al.*, 1996). CXCL12 is a ubiquitously expressed homeostatic chemokine and acts to

maintain survival and trafficking of many types of immune cell (reviewed in Pozzobon *et al.*, 2016).

The chemokine CXCR3 is selectively expressed on activated effector CD8+ T-cells and Th1 CD4+ T-cells and plays an important role in trafficking these cells to areas of peripheral inflammation (Groom and Luster, 2011). CXCL9 and CXCL10, which are upregulated by the endothelium in response to TNFα and IFNγ, induce rapid adhesion of IL-2 stimulated T-cells to immobilised ICAM-1 and VCAM-1 through the receptor CXCR3 (Piali *et al.*, 1998). Under flow conditions, addition of an anti-CXCR3 mAb reduced adhesion of T-cells to cytokine-stimulated endothelium (Piali *et al.*, 1998; Curbishley *et al.*, 2005).

CXCR3 and CCR5 are chemokine receptors which specifically bind inflammatory chemokines. Infiltrating T-cells in inflammatory lesions in patients with rheumatoid arthritis (RA) or multiple sclerosis (MS) are predominantly CXCR3+ CCR5+, despite their relatively low levels in blood or lymph node (Qin *et al.*, 1998; Balashov *et al.*, 1999). In parallel, ligands for CXCR3 or CCR5 are also highly expressed in inflammatory lesions in these conditions (Qin *et al.*, 1998; Balashov *et al.*, 1999). Therefore, CXCR3 and CCR5 act to home peripheral blood T-cells to Th1 type inflammatory sites. In contrast, Th2 T-cells express CCR3, a receptor for eotaxin, which are chemokines that are primarily expressed in hyper reactive airways and in areas of allergic responses (Jose *et al.*, 1994; Sallusto, Mackay and Lanzavecchia, 1997). Hence CCR3 expression regulates Th2 cell trafficking to areas of Th2 inflammatory responses. Therefore, the chemokine receptors expressed by varying T-cell subsets acts as traffic signals to control their differential recruitment to areas of inflammation.

Following activation, the T-cells change from a spherical shape to a more flattened morphology due to reorganisation of the actin cytoskeleton. The T-cell also becomes polarised, creating a leading edge rich in chemokine receptors CCR2 and CCR5 (Nieto Et al., 1997) and formation of a uropod (trailing edge) rich in ICAM adhesion molecules (Sánchez-Madrid and del Pozo, 1999). Localisation of chemokine and integrin receptors during cell polarisation guides cell mobility through detection of chemoattractant signals and haptotactic gradients (Miguel Angel *et al.*, 1998).

### *1.4.4. Transmigration*

There are two possible routes for T-cell endothelial migration; paracellular, where T-cells migrate through intercellular junctions between BVEC (Burns et al., 1997), or less frequently transcellular, where cells migrate through the BVEC directly (Feng et al., 1998). Junctional molecules concentrated between neighbouring BVEC are involved in paracellular T-cell diapedesis (Muller, 2003).

Junctional adhesion molecules are redistributed towards endothelial junctions following pro-inflammatory cytokine stimulation of the endothelium (Jaczewska *et al.*, 2014). *In vitro*, knockdown of endothelial JAM-A inhibits cytokine-dependent TEM of effector memory CD4+ T-cells (Manes and Pober, 2011) and JAM-A blockade reduced T-cell extravasation (Tsou *et al.*, 2018) (reviewed in Wang)

Originally, CD31 was not thought to be involved in T-cell TEM as it is not enriched on human T-cells that migrated across IL-1β treated HUVEC compared to the starting population (Bird et al, 1993). It is now known CD31 is involved in TCR-driven (antigen-dependent) TEM, but not in cytokine-driven TEM (Manes and Pober,

2011; Ma et al., 2012). In an in vivo adoptive transfer model, WT and CD31-/- T-cells were transferred into mice primed with IFNγ via intraperitoneal injection (Ma et al., 2012). Significantly more antigen-specific WT T-cells were recruited into the peritoneal lavage of antigenic mice compared to antigen-specific CD31-/- T-cells (Ma et al., 2012). Interestingly, antigen-specific T-cell extravasation was increased in mice lacking endothelial CD31 compared to WT mice, however in non-antigenic mice, T-cell extravasation was decreased in CD31-/- mice. These data show that loss of endothelial CD31 increases extravasation of antigen-specific T-cells, suggesting endothelial CD31 has a role in regulating antigen-specific T-cell transendothelial migration. This was found to be because CD31 signalling contributes to re-establishing endothelial integrity following endothelial-MHC:T-cell antigen engagement, which temporarily increases vascular permeability (Ma *et al.*, 2012). In disease models, CD31 knockout mice experience increased T-cell extravasation and subsequent enhanced disease severity in EAE and in collagen-induced arthritis models (Tada *et al.*, 2003; Wong *et al.*, 2005). Homophilic interactions between CD31 molecules is also important for targeted trafficking of the lateral border recycling compartment to the site of TEM (Gonzalez, Cyrus and Muller, 2016).

It has been shown *in vitro* CD31 acts upstream of CD99 to regulate leukocyte TEM (Sullivan 2013). CD99 is expressed along the borders of endothelial cells, and at a lower level on T-cells. Homophilic interactions between CD99 molecules regulate TEM (Muller, 2011). Antibodies against the murine homolog of CD99 inhibited migration of the T-cell line SJL.PLP7 across TNF-α stimulated endothelioma cells (Bixel *et al.*, 2004). In vivo, anti-CD99 antibodies inhibited T-cell recruitment to inflamed skin (Bixel *et al.*, 2004). *In vitro* it was shown siRNA knockdown of

endothelial CD99 in HDMEC cells inhibited antigen-dependent, but not cytokine-dependant, TEM of effector memory CD4+ T-cells (Manes and Pober, 2011). It has been shown *in vitro* CD31 acts upstream of CD99 via protein kinase A (PKA) to regulate leukocyte diapedesis.

**Table 1.2 - Chemokines and their receptors in T-cell migration**

| Biological Function | | Chemokine Receptor | Chemokines |
|---|---|---|---|
| Th1 Effector T-cells | Migration | CCR2 | CCL7 (MCP-3) |
| | | CCR5 | CCL5 (RANTES) |
| | | CXCR3 | CXCL9 (Mig), CXCL10 (IP-10) |
| Th2 Effector T-cells | Migration | CCR3 | CCL11, 24 (eotaxin-1,-2), CCL5 (RANTES), CCL8, 7, 13 (MCP-2,-3,-4), CCL15 (HCC-2) |
| | | CCR4 | CL22 (MDC-1) |
| | | CCR8 | CCL1 (I-309) |
| | | CXCR4 | CXCL12 (SDF-1α) |
| Memory T-cells | Migration to skin | CCR4 | CCL17 (TARC) |
| | Migration to the gut | CCR9 | CCL25 (TECK) |
| | Migration to areas of inflammation | CCR2 | CCL2 (MCP-1) |
| | | CCR5 | CCL5 (RANTES) |
| | Migration to lymphoid tissues | CCR7 | CCL21 (SLC) |
| Naïve T-cells | Migration of naive T-cells to LN and Peyer's patches | CCR7 | CCL19 (ELC) |
| | Migration of naive T-cells within lymphoid tissues | CXCR4 | CXCL12 (SDF-1α) |

ELC: Epstein-Barr virus-induced gene-1 ligand chemokine; HCC: human CC chemokine; IP: IFN-inducible protein; MCP: macrophage chemoattractant protein MDC: macrophage derived chemokine; Mig: monokine induced by IFNγ; MIP: macrophage inhibitory protein; RANTES: regulated on activation of normal T-cells expressed and secreted; SLC: secondary lymphoid tissue chemokine; TARC: thymus and activation regulated chemokine and TECK: thymus expressed chemokine.
Adapted from von Andrian & MacKay, 2000

### *1.4.5. PEPITEM Pathway*

Recently, Chimen et al (2015) identified a novel regulator of T-cell trafficking into inflamed tissues, the PEPITEM pathway. It was discovered that cultured media from adiponectin-stimulated B-cells can inhibit T-cell transendothelial migration *in vitro*. Mass spectrometry analysis identified a novel 14-amino acid peptide that was unique to B-cell supernatants that had been cultured with adiponectin. This peptide, termed PEPITEM (PEPtide Inhibitor of TransEndothelial Migration), showed complete sequence homology to amino acids 28-41 of the protein 14-3-3ζ. PEPITEM binds cadherin-15 on the surface of the endothelium and causes an intracellular signalling cascade resulting in phosphorylation of sphingosine to sphingosine-1-phosphate (S1P) by sphingosine kinase (SPHK1). S1P is translocated across the endothelium via spinster homolog 2 (SPNS2) and once in the vessel S1P can bind S1P receptors S1PR1/S1PR4 on the surface of T-cells. This interaction reduces the affinity of LFA-1 for its cognate ligand ICAM-1 on the surface of the endothelium, resulting in reduced T-cell extravasation (Chimen *et al.,* 2015) (Figure 1.2).

The PEPITEM pathway is dysregulated in patients with type-1-diabetes (T1D) and rheumatoid arthritis (RA) due to reduced expression of both adiponectin receptors on circulating B-cells compared to healthy controls (Chimen et al., 2015). This resulted in a reduced ability to produce PEPITEM in response to adiponectin in *ex vivo* migration assays, however the effects of adiponectin could be restored using exogenous PEPITEM (Chimen et al., 2015). Additionally, low concentrations of PEPITEM could be detected in serum from healthy controls however this was reduced in T1D patients. This suggests PEPITEM treatment in these patients could replace the inhibition on T-cell migration and act to reduce inflammation. Exogenous

PEPITEM has also been shown to inhibit T-cell infiltration into multiple organs in a mouse model of systemic lupus erythematosus (SLE) (Matsubara *et al.*, 2020). Recently, using *in vivo* models of obesity, it has been shown both prophylactic and therapeutic PEPITEM treatment could alleviate the effects of a high fat diet on pancreatic beta cell size, aberrant T-cell trafficking into visceral adipose tissue, and leukocyte trafficking from secondary lymphoid organs (Pezhman, L. et al, 2022).

Using *in vitro* static transmigration assays, addition of exogenous 14-3-3ζ or PEPITEM results in reduced lymphocyte trafficking across cytokine-stimulated endothelium to a similar efficacy as adiponectin (Chimen *et al.*, 2015). However, this inhibition seen with 14-3-3ζ is reversed when in the presence of a broad spectrum matrix metalloproteinase inhibitor (Apta, 2015). This suggests that PEPITEM has to be cleaved from the parent protein 14-3-3ζ in order to mediate its functional effects. In this thesis, I aim to elucidate the processing of PEPITEM and identify the protease(s) involved in cleavage of PEPITEM from 14-3-3ζ. I also aim to identify the mechanism of secretion of PEPITEM from the B-cell. Therefore, the remainder of my introduction will focus on 1) matrix metalloproteinase expression in endothelial cells (section 1.5) and 2) mechanisms of protein secretion from B-cells (section 1.6).

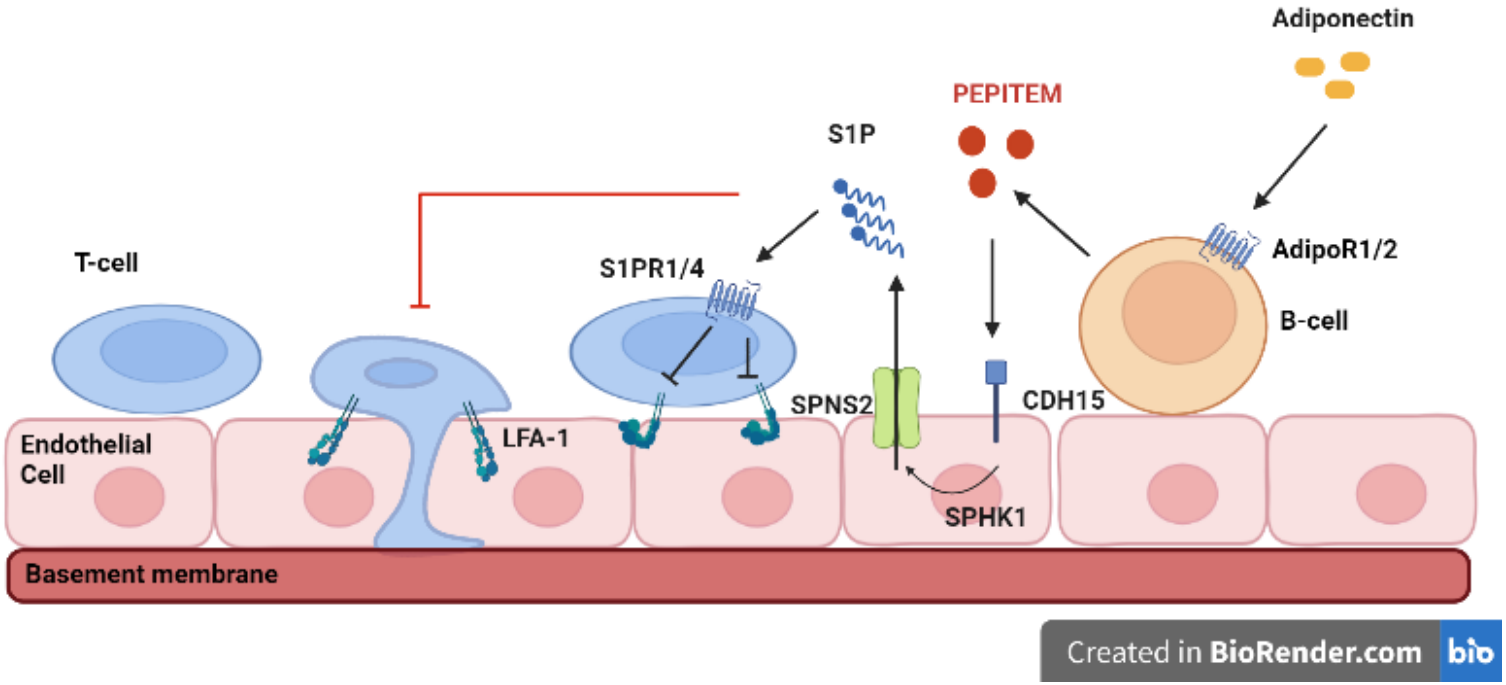


**Figure 1.2 – The PEPITEM Pathway**

Adiponectin binds adiponectin receptors (AdipoR1 / AdipoR2) on the surface of B-cells which induces release of PEPITEM. PEPITEM binds cadherin-15 (CDH-15) on the surface on endothelial cells and triggers an intracellular signalling cascade resulting in Sphingosine Kinase 1 (SPHK1) to phosphorylate sphingosine into sphingosine-1-phosphate (S1P). S1P translocates across the endothelial cell membrane via the transporter Spinster homolog 2 (SPNS2). Once in the blood vessel, S1P binds S1P receptors S1PR2 and S1PR4 on the surface on T-cells. This results in a reduction of affinity of the T-cell integrin adhesion receptor LFA1, disrupting levels of T-cell transendothelial migration.

## 1.5. Matrix Metalloproteinase

Matrix metalloproteinases (MMPs) are homeostatic proteases that degrade extracellular matrix proteins and regulate the extracellular matrix environment (Nagaset and Woessner, 1999). Activity of MMPs is tightly regulated under physiological conditions both transcriptionally and post-translationally, via activation of precursor zymogens and by endogenous inhibitors (Löffek, Schilling and Franzke, 2011). Dysregulation can contribute to several inflammatory diseases including arthritis, cardiovascular disease, cancers, and fibrosis (reviewed in Liu, Sun and Sader, 2006; Mehana, Khafaga and El-Blehi, 2019)

Twenty-four MMPs are found in humans, including two identical MMP-23 proteins which are both encoded by distinct genes (MMP23A and MMP23B) (Nagase, Visse and Murphy, 2006). All MMPs contain an N-terminal signal peptide, a pro-domain, and a catalytic domain (Laronha and Caldeira, 2020). The catalytic domain contains a highly conserved, zinc-dependent active site that contains three histidine residues bound to catalytic zinc (Laronha and Caldeira, 2020). MMPs can be further categorised according to substrate specificity and domain structures; 1) collegenases, 2) stromelysins, 3) gelatinases, 4) matrilysins and 5) membrane type MMPs (MT-MMPs) (Table 1.3).

MMPs are initially synthesised as pre-proenzymes (Nagase, 1997). During translation, the signal peptide is removed generating pro-MMPs, or zymogens. Many MMPs are secreted from the cell as zymogens that have to be proteolytically activated in the extracellular environment (Rosenblum *et al.*, 2007). The pro-domain contains a conserved “cysteine switch” sequence which is in close proximity to the catalytic domain. Interactions between the cysteine in the sequence and the free zinc

ion at the catalytic domain prevent substrate binding (Springman *et al.,* 1990). Cleavage of the pro-domain is an important regulatory step of MMP activity and requires proteolytic cleavage of the pro-domain by endopeptidases. These can include serine proteases, plasmin, furin, or other MMPs. Activities of MMPs are also regulated by endogenous inhibitors, tissue inhibitors of MMPs (TIMPs) (Rosenblum et al., 2007).

### *1.5.1. Tissue Inhibitors of MMPs*

Humans have four TIMP proteins (TIMP1-4) encoded by separate genes which share roughly 40% sequence similarity (Brew and Nagase, 2010). All of the TIMPs inhibit MMPs but with varying affinities. TIMP-1 has a relatively low affinity for the MT-MMPs (Hamze et al., 2007). TIMP-3 is unique amongst the TIMPs, as it is the only one with the ability to bind with high affinity to the extracellular matrix, but it also has the broadest substrate range and can inhibit several ADAM proteins (Fan and Kassiri, 2020). The balance between MMPs and TIMPs is tightly regulated and during inflammatory responses an imbalance between these molecules can contribute towards several pathological conditions such as arthritis, cancer, chronic pain and neurological conditions (Löffek, Schilling and Franzke, 2011; Knight et al., 2019; Mehana, Khafaga and El-Blehi, 2019). There are also non-inhibitory interactions between certain TIMPs and MMPs. TIMP-2 binds to pro-MMP-2, an interaction which is essential for the cell-surface activation of MMP-2 (covered in section 1.5.5), and TIMP-1 forms a complex with pro-MMP-9 through each of their C-terminal domains (Itoh, 2015). This TIMP-1/pro-MMP-9 complex leaves the TIMP-1 N-terminal free to inhibit other MMP molecules, although the exact function of this complex remains unsolved (Brew and Nagase, 2010).

**Table 1.3 – MMPs members and their substrates**

| Subgroup | MMP | Alternate Name | Substrate |
|---|---|---|---|
| Collagenases | MMP-1 | Collagenase-1 | Collagen types I, II, III, VII and X |
| | MMP-8 | Collagenase-2 | |
| | MMP-13 | Collagease-3 | |
| Stromelysins | MMP-3 | Stromelysin-1 | Gelatin, fibronectin, casein, |
| | MMP-10 | Stromelysin-2 | laminin, elastin, |
| | MMP-11 | Stromelysin-3 | MMP-2/TIMP-2 |
| Gelatinases | MMP-2 | Gelatinase A | Gelatin, collagen, fibronectin, |
| | MMP-9 | Gelatinase B | elastin, laminin |
| Matrilysins | MMP-7 | Matrilysin-1 | Fibronectin, laminin, gelatine, |
| | MMP26 | Matrilysin-2 | aggrecan, fibrin, fibrinogen |
| Membrane Type | MMP-14 | MT1-MMP | Pro MMP-2 |
| | MMP-15 | MT2-MMP | Pro-MMP-2 |
| | MMP-16 | MT3-MMP | Pro-MMP-2 |
| | MMP-17 | MT4-MMP | Gelatin, TNF-α precursor, fibrin |
| | MMP-24 | MT5-MMP | Gelatin, TNF-α precursor, fibrin |
| | MMP-25 | MT6-MMP | Collage IV, gelatine, laminin |

Adapted from Nijm and Jonasson, 2009

### *1.5.2. Gelatinases*

The gelatinases, MMP-2 (gelatinase-A) and MMP-9 (gelatinase-B), are the most extensively studied MMPs due to their roles in angiogenesis and cell metastasis (Björklund and Koivunen, 2005; Quintero-Fabián et al., 2019). The gelatinases are structurally unique from the rest of the MMP family as they contain three fibronectin-type II repeats in their catalytic domains which acts as a binding site for collagen (Murphy et al., 1994). MMP-2 is constitutively expressed across many tissues, whilst MMP-9 tends to be lowly expressed at basal levels and upregulated following cytokine and growth factor stimulation (Roomi et al., 2017; Yosef, Hayun and Papo, 2021). As well as their roles in cancer metastasis, MMP-2 and MMP-9 also contribute to immune cell recruitment by acting on chemokine gradients (Vergote et al, 2006; McQuibban et al., 2001), which can have either pro- or anti- inflammatory effects. In a murine model of EAE, MMP-2 and MMP-9 derived from infiltrating or tissue resident immune cells contributed to immune cell recruitment via inactivation of CXCL12 (Song *et al.*, 2015). CXCL12 plays an important anti-inflammatory role during EAE, localising CXCR4-expressing mononuclear cells to the perivascular space and preventing their infiltration into the CNS parenchyma (McCandless *et al.*, 2008). The importance of this MMP-2 and MMP-9 mediated leukocyte recruitment in EAE is evidenced as young MMP-9 knockout mice are resistant to EAE development (Dubois *et al.*, 1999), and MMP-2/-9 double knockout mice are resistant even in adulthood (Agrawal *et al.*, 2006). Conversely, using MMP2-/- mice with an asthma phenotype, MMP2 was found to be required for inflammatory cell egress from the lung, and in its absence immune cells accumulated in the lung parenchyma and left mice susceptible to lethal asphyixiation (Corry et al, 2002).

### *1.5.3. MMP expression in the endothelium*

Despite their central roles in endothelial homeostasis, MMP production by endothelial cells is not yet well characterised and literature about the factors that regulate their expression is limited and at times contradictory (Table 1.4). For example, Taraboletti et al (2002) detected MMP-2 and MMP-9 positive vesicles in HUVEC at passages (P)3-5, however several studies have been unable to detect MMP-9 expression in unstimulated endothelial cells (Yosef, Hayun and Papo, 2021) and *in vitro*, MMP-9 expression is dependent on passage number and rapidly decreases after P0 (Arkell and Jackson 2003).

### *1.5.4. Gelatinase storage in endothelial cells*

Other than the transmembrane-type MMPs which contain a transmembrane domain to allow their adhesion to cell membranes, the MMPs are generally considered to be rapidly secreted proteases. However, the MMP-2 and MMP-9 have been found to be stored intracellularly in cytosolic granules in human microvascular endothelial cells (MEC) (Nguyen, Arkell and Jackson, 1998), HUVEC (Taraboletti et al., 2002) and neutrophils (Kjeldsen et al., 1993). In MEC, electron microscopy revealed active-MMP-9 containing vesicles to be concentrated in pseudopodia, enabling rapid release and basement membrane digestion to help with EC migration. Interestingly, in culture media, MMP-9 is often found in complex with the inhibitor TIMP-1, however TIMP-1 was absent from these vesicles. In comparison, the gelatinase vesicles found in HUVEC contained both pro- and active forms of MMP-9 and MMP-2, and had the transmembrane MMP, MT-MMP1 associated on the external side of the vesicle membrane (Taraboletti et al., 2002). These vesicles were also positive for the inhibitors TIMP1 and TIMP2, although as TIMP2 and MT-MMP1

can act together in a complex as an activator for MMP-2, it might not be acting in an inhibitory capacity. Shedding of these vesicles was stimulated by angiogenic factors, fibroblast growth factor-2 (FGF2) and vascular endothelial growth factor (VEGF) and originated from specific localisations on the plasma membrane of HUVEC (Taraboletti et al., 2002). Gelatinase positive vesicles have also been found to be secreted from tumour cells (Ginestra et al., 1997; Dolo et al., 1999) however this shedding is constitutive and isn't confined to specific areas of release along the plasma membrane.

### *1.5.5. MMP2/MMP9 Cell Surface Attachment*

Despite neither of the gelatinases containing a transmembrane domain like the MT-MMPs, they can both interact with several cell surface integral membrane proteins and localise to the endothelial plasma membrane. Proteolytically active MMP-9 can bind to the hyaluronan receptor CD44 which promotes endothelial cell motility and tumour angiogenesis via activation of latent transforming growth factor-β (TGF-β) into the active form (Yu and Stamenkovic, 1999). This MMP-9-CD44 interaction also promotes tumour cell invasiveness and metastasis and targeting this interaction may be a useful therapeutic strategy against cancer (Yosef, Hayun and Papo, 2021). As previously mentioned, there is a well-defined interaction between surface bound MMP-14 (MT1-MMP), TIMP2 and MMP-2 (Figure 1.3). In this model, MMP-14 forms a homo-dimer on the cell surface (Itoh *et al.*, 2001). The catalytic site of one of these molecules binds to the N-terminal domain of TIMP-2, leaving an exposed C-terminal domain which can bind pro-MMP-2. The other molecule of MMP-14 that is not bound to TIMP-2 is then free to cleave pro-MMP-2 into the active form which is released from the complex (reviewed in Itoh, 2015). MMP-2 can also be

localised to the cell surface through its interaction with the integrin αvβ3 (Brooks et al., 1996). Importantly, this interaction is via the C-terminus of MMP-2, localising the enzyme to the cell surface in the proteolytically active form. This interaction is important for cell migration and invasion in angiogenic blood vessels and cancer metastasis *in vivo* (Brooks et al., 1996).

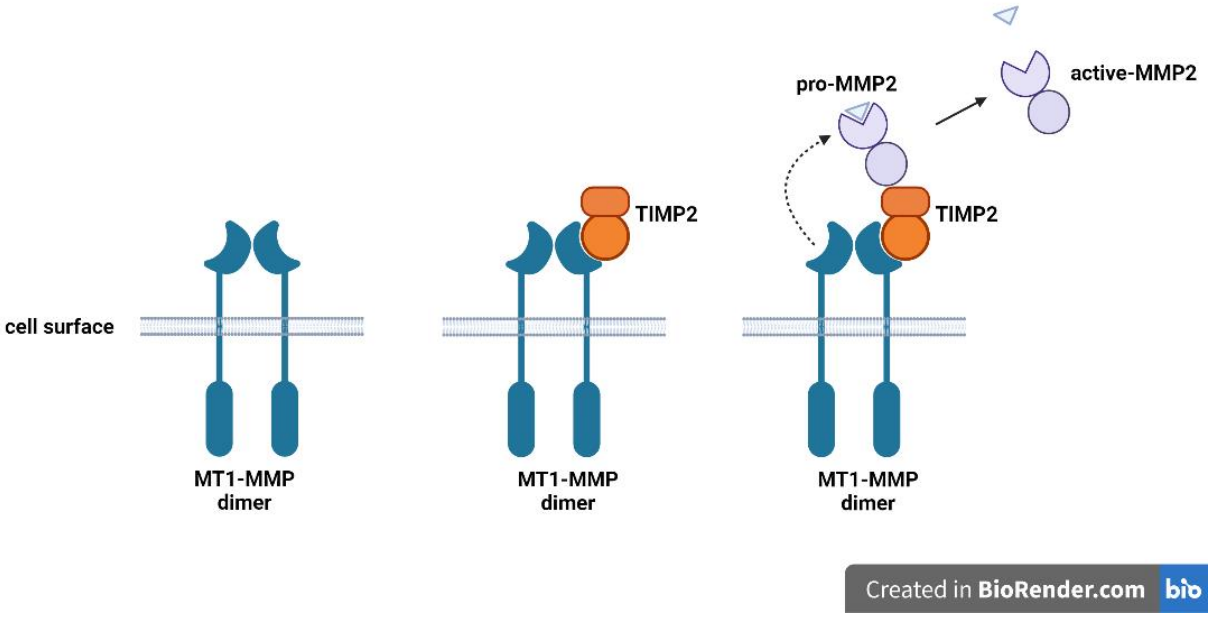


**Figure 1.3 - Mechanism of MMP-2 activation via MT1-MMP and TIMP2**

MT1-MMP monomers dimerise on the cell surface. One molecule of MT1-MMP binds the N-terminus of TIMP2. The C-terminal domain of TIMP2 binds pro-MMP-2. The catalytic domain of the unoccupied MT1-MMP monomer activates pro-MMP-2 by cleaving off the pro-domain and causes release of active MMP-2 from the complex.

**Table 1.4 – MMP-2 and MMP-9 expression in endothelial cells**

| Article | Cell Type | Passage | Media | Treatment | Detection Method | MMP9 expression |
|---|---|---|---|---|---|---|
| Magid, Murpy and Galis 2003 | MLEC | N/A | Serum free | Bidirectional shear / unidirectional flow | Gelatin Zymography | 3 fold higher MMP9 after 6 hour bidirectional shear compared to unidirectional flow |
| | | | | | qPCR | MMP9 message increased 3-fold and 8-fold after 3hr or 6hr bidirectional shear compared to uni |
| | | | | | MMP9 promoter activity | Unidirectional shear increased MMP9 promotor activity 3-fold over static, bidirectional shear resulted in 25 fold increase over static |
| Wang et al, 2006 | MBEC | 10-12 | Serum free, concentrated using centricon | Erythropoietin 24-48hr | Gel Zymography | MMP9 not detected in the basal supernatants, rhEPO showed induction of pro and active MMP9 |
| | | | | | qPCR | rhEPO treatment increased MMP2 and MMP9 mRNA levels compared with the control group |
| Taraboletti et al, 2002 | HUVEC | 3-5 | Medium depleted of MMP2/9 using gelatin Sepharose | FGF . VEGF, FCS | Gel Zymography | HUVEC-derived vesicles positive for pro MMP2 and MMP9<br>Increasing serum concentrations induced proMMP-9 compared to the absence of serum, FGF-2 and VEGF induced significant increases in proMMP-9 |
| | | | | | Western Blot | Bands seen at 150kd for complex with high molecular weight, and a truncated form (~60 kd) |

| | | | | | | |
|---|---|---|---|---|---|---|
| Arkell and Jackson 2003 | HUVEC | P0-2 | Media depleted of MMP2 / 9 using gelatin sepharose | Passaging | Gelatin Zymography | Pro-MMP9 detected at P0, rapid reduction in MMP9 expression in P1 and none in P2 |
| | | | | | ELISA | MMP9 detected in the conditioned media of P0 HUVEC ranged from 0.8 -1.6 ng/ml. None was detected in P2 |
| | | | | | IHC | MMP9 detected in cytoplasm of P0 HUVEC |
| Harkness et al, 2000 | RCEC | 8-12 | Serum-free media | TNF-α, IL-1β Dexamethasone | Gelatin Zymography | MMP-2 and MMP-9 constitutively expressed MMP-9 expression is upregulated following TNF-α and IL-1β stimulation |
| Liu et al, 2018 | Calf PAEC | 2-3 | DMEM + 20% FBS | Hypoxia | Gelatin Zymography | MMP-2 and MMP-9 detected in normoxia Hypoxia significantly upregulates synthesis and activation of MMP-2 and MMP-9 |
| Qin et al, 2012 | HUVEC | <5 | Serum free media | Melatonin Melatonin + IL1B | Gelatin Zymography RT-PCR | Low levels of MMP-9 present in control, upregulated by IL-1B. Constitutive high levels of MMP-2. |
| Kargozaran et al, 2007 | HLMVEC | N/A | Serum free media | MMP-2 siRNA | Gelatin Zymography | MMP-2 detected basal conditions |
| Yosef et al, 2002 | EAhy 926 cells line (hybridoma) | N/A | 10%FCS | Hypoxia | Gelatin Zymography | MMP-2 constitutively expressed, MMP-9 not detected |

MLEC: murine lymphoid endothelial cells, MBEC: murine brain endothelial cells, HUVEC: Human Umbilical Vein Endothelial Cell, RCEC: Rat cerebral endothelial cells, PAEC: pulmonary arterial endothelial cells, HLMVEC: human lung microvascular endothelial cells

## 1.6. B-cell Protein Secretion

One of the main roles of B-cells is to secrete antibodies that help mediate an immune response by neutralising pathogens, activating the complement system, and facilitating phagocytosis of foreign substances (Forthal, 2015). Following activation from antigen, naïve or memory B-cells proliferate and differentiate into plasma cells which can secrete vast quantities of antibodies (Alberts *et al.*, 2002). To accommodate the increased secretory load required, expansion of secretory organelles occurs during plasma cell differentiation to form a highly developed transport network (Kirk *et al.*, 2010). In addition to plasma cell differentiation and antibody secretion, B-cells also secrete different cytokines in response to different stimuli (Duddy et al, 2004). Seminal work in the early 2000s revealed primary human PBMC enriched B-cells activated by BCR cross-linking and T-cell costimulation via CD40 for 48 hours produced and secreted IL-6, TNF-α and lymphotoxin-α (Duddy et al, 2004). In contrast, B-cells stimulated with CD40 alone secreted the immunoregulatory cytokine, IL-10 (Duddy et al, 2004). Therefore, B-cells were found to be able to modulate the immune response not only through antibody secretion, but also by contributing to the cytokine micro-environment.

### *1.6.1. Classical and Non-classical Protein Secretion*

Antibodies, and most cytokines, are secreted via the classical secretory pathway (Stow and Murray, 2013; Coulet *et al.*, 2023). Classically secreted proteins express a signal recognition particle (SRP) which facilitates translocation into the endoplasmic reticulum (ER) (Walter and Blobel, 1982). Once in the ER, the proteins are transported to the golgi apparatus in COPII+ vesicles (Barlow*e et al*, 1994). Here, they are packed into secretory vesicles which fuse with the plasma membrane and

release the secretory proteins into the extracellular environment (reviewed in Viotti, 2016).

Several proteins destined for secretion however do not contain an SRP and are not directed to the classical secretory pathway. These proteins are known as unconventional or non-classically secreted proteins. Unlike the classical pathway, there is not one mechanism for unconventional protein secretion and several secretory pathways have been identified (Cohen, Chirico and Lipke, 2020). Some proteins, such as heat shock protein 70 (Hsp70) are translocated across the PM using an ABC transporter (Mambula and Calderwood, 2006). Other proteins such as FGF1 and FGF2 can directly cross the PM via formation of membrane pores (La Venuta et al., 2015).

Many members of the interleukin family represent unconventionally secreted cytokines. IL-1β is a non-classically secreted protein with several routes of secretion depending on biological context (Daniels and Brough, 2017). Pro-IL-1β is processed into the active, mature form by caspase-1, which itself is activated by recruitment to multi-protein complexes called inflammasomes. In macrophages, inflammasome mediated caspase-1 activation causes the cells to undergo pyroptotic death and cell lysis, which leads to release of mature IL-1β (Liu et al., 2014; Martin-Sanchez et al., 2016). Pyroptosis is mediated by gasdermin-D, the N-terminal cleavage product translocates to the plasma membrane and forms pores directly in the plasma membrane (He *et al.*, 2015; Ding *et al.*, 2016; Liu *et al.*, 2016). Apoptosis regulates IL-1β release dependent upon caspase-8 (England *et al.*, 2014). Additionally, alternative routes of IL-1β release have been found which allow the cells to remain intact. In HEK293T cells expressing pro-IL-1β and pro-caspase-1, IL-1β secretion

was regulated by autophagy induced by nutrient starvation (Zhang et al., 2015). IL-1β has also been found in monocyte-derived endolysosomal vesicles following ATP treatment (Andrei et al, 1999), and in exosomes released from murine macrophages following P2X7 receptor stimulation (Qu, 2009).

IL-1α secretion is similarly complicated, context dependent, and not fully understood. Multiple cell death stimuli regulate the processing and release of IL-1α (X. W. Cheng *et al.*, 2007; England *et al.*, 2014; Cohen, Chirico and Lipke, 2020; Ratitong, Marshall and Pearlman, 2021). IL-1α is released from necrotic human aortic vascular smooth muscle cells (VSMCs), and secondary necrosis causes release of both IL-1α and IL-1β (Clarke *et al.*, 2010). In turn, IL-1 proteins upregulate IL-6 and MCP-1 production from healthy VSMCs (Clarke *et al.*, 2010). In atherosclerosis, phagocytosis of apoptotic VSMCs is reduced, leading to increased secretion of IL-1 proteins and pro-inflammatory cytokines, contributing to the chronic inflammatory state seen in this condition (Clarke *et al.*, 2010). IL-1α and IL-1β are good examples of the complicated nature of non-classical secretory pathways of cytokines, and how this can contribute to inflammation in pathology.

### *1.6.2. 14-3-3 proteins*

The mammalian family of 14-3-3 proteins consists of seven highly conserved isoforms; beta (β), epsilon (ε), gamma (γ), eta (η), sigma (σ), tau (τ), and zeta (ζ) (Munier, Ottmann and Perry, 2021) They have over 1200 binding partners and have roles in various cellular processes including transcription, cell signalling, DNA repair, differentiation, cell adhesion and protein trafficking (Obsilova and Obsil, 2022). The PEPITEM pathway is the first identified link between 14-3-3 proteins and T-cell

migration, however previous roles have been identified in cell adhesion and integrin signalling. In fibroblasts, 14-3-3β can bind to β1 integrin cytoplasmic domain to facilitate cell spreading and wound healing (Han, Rodriguez and Guan, 2001). Cell adhesion induces 14-3-3ζ binding to the integrin signalling adaptor protein Cas (Garcia-Guzman et al., 1999). Overexpression of 14-3-3ζ in mammary epithelial cells led to reduced expression of E-cadherin, which promoted cell migration (Lu et al., 2009). Therefore, 14-3-3 proteins have varying roles in cell adhesion and migration in different cell contexts.

### *1.6.3. 14-3-3 Protein Secretion*

Proteins in the 14-3-3 family are generally considered cytosolic proteins and are expressed in almost all mammalian tissues (Munier, Ottmann and Perry, 2021). Despite this, they have also been found in extracellular environments. Extracellular 14-3-3 proteins are also being used as diagnostic markers for disease progression; 14-3-3 expression in cerebrospinal fluid is a diagnostic test for Creutzfeldt-Jakob disease (Huang et al, 2003) and patients with multiple sclerosis who are at high risk of developing severe disability (Colucci et al, 2004). Notably, 14-3-3 proteins lack a signal recognition particle therefore must be utilizing a non-classical method of secretion.

### *1.6.4. Extracellular Vesicles*

An increasingly well researched method of unconventional protein secretion is release via extracellular vesicles (EVs). EVs are membrane-bound nanoparticles that are released from nearly every cell type. Initially thought to be a waste removal system (Johnston*e et al.*, 1987), we now know they act as important signalling

molecules and can transfer proteins and nucleic acid from donor to recipient cell (Lo Cicero, Stahl and Raposo, 2015). EV research is at the forefront of immunology due to their roles in both homeostatic and pathological processes. The term “extracellular vesicle” encompasses a number of heterogenous vesicle populations which have different properties such as size, protein content, and developmental origin. EVs can be categorised into three main subtypes: microvesicles, apoptotic bodies, and exosomes (Doyle and Wang, 2019).

### *1.6.5. Exosomes*

Exosomes are the smallest subset of EV (30-150nm) and are key cellular communicators during inflammatory responses (Gurung *et al.*, 2021). Exosome biogenesis occurs via the endosomal system. Early endosomes, formed by inward budding of the plasma membrane, mature into multi-vesicular bodies which contain several intraluminal vesicles (Yáñez-Mó *et al.*, 2015). The multi-vesicular body gets transported to and docks with the plasma membrane, releasing the intraluminal vesicles (now exosomes) into the extracellular space (reviewed by Denzer 2000).

The exosome proteome is often used as an identification method to discriminate between exosomes and other EVs. Exosome formation is regulated by endosomal sorting complex required for transport (ESCRT) proteins, therefore these proteins (Alix and TSG101) are present in exosomes (Zhan*g et al*., 2019). Tetraspanin family members CD9, CD63 and CD81 are also enriched in exosomes and are frequently used as exosome markers, however they have since also been identified in microvesicles and apoptotic bodies (Rossella *et al*., 2013).

### *1.6.6. B-cell derived exosomes*

Exosome release from B-cells was first identified in 1996 where it was found B-lymphoblastoid cells contained major histocompatibility complex (MHC) class II enriched compartments that could fuse with the plasma membrane and release internal MHC class II containing exosomes into the extracellular space (Raposo *et al.*, 1996). These exosomes were isolated via differential centrifugation and western blot analysis revealed they were positive for LAMP1 and CD63, but negative for transferrin receptor, a plasma membrane and endosome marker, proving they were not merely shed plasma membrane caused by the centrifugation process (Raposo *et al.*, 1996). Importantly, antigen presentation assays revealed when these isolated exosomes were allowed to bind peptide, they could stimulate proliferation of a T-cell line which recognises the same peptide. This proliferation did not occur when using a B-cell line negative for the MHC class II surface receptor, HLA-DR, or when using a mAb against HLA-DR (Raposo *et al.*, 1996). Therefore, B-cell derived vesicles contain surface MHC class II proteins which can present antigen and can interact with other cells and initiate T-cell responses.

Since this seminal work, functional roles of B-cell derived exosomes have been extensively researched (reviewed in Hazrati *et al.*, 2022). B-cell derived exosomes are constitutively secreted at low levels but their release is significantly increased following cytokine or mitogen activation signals, such as signalling via CD40 and the IL-4 receptor, or by B-cell activation through the B-cell receptor (BCR) or toll-like receptor 9 (TLR9) (Muntasell, Berger and Roche, 2007; Arita *et al.*, 2008; Saunderson *et al.*, 2008). Inhibition of the NF-κB pathway significantly reduced activated B-cell exosome production, measured by exosomal HLA quantification,

identifying the NF-kB pathway important in B-cell derived exosome release (Arita *et al.*, 2008)

B-cell derived exosomes have several functional effects and can interact with several members of the immune system. *In vivo* studies have shown exosomes isolated from primary B-cells stimulated with ovalbumin protein can initiate a cytotoxic T lymphocyte (CTL) response (Saunderson *et al.*, 2014). Interestingly, and in contrast to the effects from dendritic cell derived exosomes, the CTL response is much greater when the B-cells incubated with full ovalbumin protein compared to peptide incubation (Qazi *et al.*, 2009; Saunderson *et al.*, 2014; Saunderson and McLellan, 2017). Importantly, this CTL immunity is mediated via collaboration between NK cells, CD4+ T-cells and CD8+ T-cells and depletion of any of these cell subsets abolished the B-cell derived exosome CTL response (Saunderson and McLellan, 2017). In an allergen model it was shown B-cell derived exosomes can bind peptides from the birch allergen, Bet v 1, and initiate Bet v 1-specific T-cell proliferation and cytokine production (Admyre *et al.*, 2007).

B-cell derived exosomes can also specifically bind to and coat follicular dendritic cells (FDCs) in human tonsil tissue (Denzer *et al.*, 2000). *Ex vivo*, co-culture of FDCs and activated B-cells isolated from primary human tonsil tissue lead to numerous MHC class II positive small vesicles associated with the FDC surface seen by immunoelectron microscopy (Denzer *et al.*, 2000). These vesicles were identical to the B-cell exosomes coined by Raposo (1996) in terms of size and protein composition. *In vitro* binding experiments then revealed B-cell derived exosomes could specifically bind to FDC but not to other cell types (Denzer *et al.*, 2000). As FDC cannot produce MHC class II molecules (Denzer *et al.*, 2000b), the attachment

of multiple MHC class II-positive vesicles to the FDC surface may be a way for FDC to be involved in recruitment and activation of specific T-cells. B-cell derived exosomes can also bind TNF-activated fibroblasts via β1 and β2 integrins on their surface (Clayton *et al.*, 2004)

### *1.6.7. B-cell derived exosome proteome profile*

Despite such extensive research into B-cell derived exosomes, there are disparities in the literature about the protein content of these exosomes. B-cell derived exosomes are known to be highly enriched for both MHC class I and MHC class II proteins, which enables them to participate in antigen presentation to other immune cells (Raposo *et al.*, 1996; Saunderson *et al.*, 2008). There is also evidence B-cell derived exosomes express certain B-cell markers including CD19, CD20, CD45R and Ig (Admyre *et al.*, 2007; Buschow *et al.*, 2010; Oksvold *et al.*, 2014; Saunderson and McLellan, 2017). Enrichment of CD63+ and CD81+ exosomes from B-cell lymphoma lines via magnetic beads revealed different cell lines have different levels of expression for B-cell markers and for tetraspanin expression (Oksvold *et al.*, 2014). Western blot analysis revealed CD63 and CD81 were present but no CD9 was found on any of the B-cell lymphoma lines. In contrast, exosomes isolated from primary human B-cells were found to be positive for CD9 and CD81, but negative for CD63 (Saunderso*n et al*., 2008; Saunderson and McLellan, 2017). These discrepancies could be due to the variation between cell types or due to the isolation methods. As the lymphoma cell line exosomes were isolated through pre-enrichment of CD63 and CD81 exosomes, one possibility could be the lack of overlap of tetraspanins on individual exosomes. Therefore, there could be CD9+ exosomes present in the samples but they do not co-express the other tetraspanins. Similarly,

CD63 may be expressed at low concentrations and cannot be detected without pre-enrichment of CD63+ vesicles.

### *1.6.8. 14-3-3 Protein Expression in Extracellular Vesicles*

Several proteins of the 14-3-3 family have been found expressed in exosomes of varying origin (Keerthikumar *et al.*, 2016). ExoCarta, a database of exosomal protein expression, identified both 14-3-3ε and 14-3-3ζ in the top 20 most often identified exosomal proteins (Keerthikumar *et al.*, 2016). Notably however, these proteins are frequently found upregulated in cancer (revied in Kindt, Osborne and Goldsby, 2006) and many exosome studies use cancerous cell lines which may contribute to their high expression level. 14-3-3ζ expression has been identified in exosomes derived from bladder cancer, colorectal cancer (Choi et al., 2007), hepatocellular carcinoma (Wang et al., 2018), melanoma cells (Peinado et al., 2012), neuroblastoma (Keerthikumar et al., 2015), ovarian cancer (Liang et al., 2013), prostate cancer (Hosseini-Beheshti et al., 2012) and squamous carcinoma (Park et al., 2010). Upregulation of 14-3-3ζ by cancer cells and its association with exosomes has important functional effects. Hepatocarcinoma cells release 14-3-3ζ+ vesicles which can be taken up by tumour infiltrating T-cells and impairs their anti-tumour activity (Wang et al., 2018)

Interestingly, mass spectrometry analysis identified 14-3-3ζ in exosomes derived from the EBV-transformed B-cell line (RN) via mass spectrometry (Buschow et al., 2010), however this hasn't been identified yet in exosomes derived from primary B-cells. However, this may represent a potential model for 14-3-3ζ release from B-cells during the PEPITEM pathway.

**Table 1.1 Protein expression in B-cell-derived exosomes**

| Family | Protein | Identified By | Exosomal Origin | Reference |
|---|---|---|---|---|
| Classical exosome tetraspanins | CD63 | Western Blotting<br>FACS<br>Mass Spec | Primary human B-cells, Raji Cells | (1-6,9) |
| | CD9 | Western Blotting<br>Mass Spec | Raji Cells | (5,6,7,8) |
| | CD81 | Western Blotting<br>FACS<br>Mass Spec | Human, Raji Cells | (1-9) |
| B-cell markers | CD19 | Mass Spec<br>Western Blotting | Human, B-cell lymphoma lines (Ramos, SUDHL-4, SUDHL-6, Ros-50) | (4,6, 8) |
| | CD20 | Western Blotting | | (6) |
| | CD24 | Western Blotting | | (6) |
| | CD37 | Western Blotting | | (6) |
| Major Histocompatibility Complex | MHC class I | Mass Spec | HLA-DR15+ B-cells | (2,4) |
| | HLA-DRA | Mass Spec | | |
| | HLA-DR2 | Mass Spec | | |
| | HLA-DR2.2 | Mass Spec | | |
| | HLA-DRQB1 | Mass Spec | | |
| | HLA-E | Mass Spec | | |
| | MHC class I | Flow Cytometry | Primary human B-cell | (7,8) |
| | MHC class II | Flow Cytometry | Primary human B-cells | (7,8) |

| | | | | |
|---|---|---|---|---|
| 14-3-3 proteins | 14-3-3ζ | Mass Spec | HLA-DR15+ B-cells | (6) |
| | 14-3-3β | Mass Spec | | |
| | 14-3-3η | Mass Spec | | |
| | 14-3-3γ | Mass Spec | | |
| | | Flow Cytometry | Primary human B-cells | (7) |
| | 14-3-3ε | Mass Spec | | |
| | 14-3-3θ | Mass Spec | | |

CD: cluster of differentiation; HLA: human leukocyte antigen (major histocompatibility complex [MHC]); HLA-DRA; Major Histocompatibility Complex, Class II, DR Alpha; HLA-DR2; Major histocompatibility complex, class II, DR2; HLA-DRQB1: Major histocompatibility complex, class II, DQ beta 1; HLA-E: Major Histocompatibility Complex, Class I, E. References: (1) ((Escola *et al.*, 1998) (2) (Wubbolts *et al.*, 2003) (3) (Admyre *et al.*, 2007) (4) (Buschow *et al.*, 2010) (5) (Mittelbrunn *et al.*, 2011) (6) (Oksvold *et al.*, 2014) (7) (Saunderson and McLellan, 2017) (8) (Saunderson *et al.*, 2008) (9) (Admyre *et al.*, 2007)

### *1.6.9. Aims and Objectives*

The PEPITEM pathway represents a novel mechanism of regulation of inflammation and could be a therapeutic target for inflammatory disease. However, not enough is yet known about the mechanisms of PEPITEM generation from 14-3-3ζ, or how PEPITEM is secreted from the B-cells. Therefore, we sought to elucidate the mechanisms of secretion and generation of PEPITEM to fully unleash its therapeutic potential. We intend to do this using the following aims:

1. Investigate protease expression in endothelial cells and how this is regulated by various inflammatory stimuli
2. Elucidate the protease(s) involved in cleavage of PEPITEM from 14-3-3ζ
3. Investigate mechanisms of PEPITEM release from B-cells
4. Assess the potential of a genetically tractable model for the PEPITEM pathway

# Chapter 2. MATERIALS AND METHODS

## 2.1. List of media and buffers

### *2.1.1. Human umbilical vein endothelial cells Complete Media:*

Medium 199 (M199; Gibco, Life Technologies, Paisley, UK, catalogue number #25300054) supplemented with 20% fetal bovine serum (FBS), 1µg/ml hydrocortisone, 10ng/ml epidermal growth factor (all Sigma-Aldrich, Paisley, UK), 100U/ml Penicillin-Streptomycin, and 2.5µg/ml amphotericin B (ThermoFisher; Paisley, UK).

### *2.1.2. HDBEC Growth Media:*

Low serum (2% v/w) endothelial cell growth medium MV (PromoCell, Heidelberg, Germany, catalogue number #C-22120), supplemented with fetal calf serum (FCS; PromoCell, catalogue number #C-37310), endothelial cell growth extracted from hypothalamic (ECGS/H; Promocell, catalogue number #C-30120).

### *2.1.3. MACS Buffer:*

Phosphate buffered saline with calcium and magnesium (PBS+; Sigma-Aldrich, catalogue number #14040141) supplemented with 0.1mM ethylenediaminetetraacetic acid (EDTA; Sigma-Aldrich, catalogue number #E8008) and 0.6% bovine serum albumin (BSA; Bovine Albumin Fraction V, 7.5% solution; Sigma-Aldrich, catalogue number #15260037).

### *2.1.4. Raji Culture Media:*

RPMI-1640 Medium with sodium bicarbonate without L-glutamine (Sigma-Aldrich, catalogue number #R0883) supplemented with 10% heat-inactivated FBS and 1% L-glutamine-Penicillin-Streptomycin solution (Sigma-Aldrich, catalogue number #G1146).

## 2.2. Ethics

All human samples were obtained with written, informed consent and approval in compliance with the Declaration of Helsinki. HUVEC were isolated from umbilical cords obtained from woman undergoing elective caesarean section at Sandwell and West Birmingham Hospitals NHS Foundation Trust and approved by NRES Committee North East – Tyne and Wear South (REC 15/NE/0285). Whole blood was taken with informed consent from healthy adult volunteers with approval from the University of Birmingham Local Ethical Review Committee (ERN_12-0079).

## 2.3. Culture and Isolation of Endothelial Cells

### *2.3.1. Human Umbilical Vascular Endothelial Cell Isolation and Culture*

HUVEC were isolated from umbilical cords using a collagenase digest as previously described (Munir *et al.*, 2015). Briefly, the vein was cannulated at one end and washed twice with phosphate buffered saline without calcium or magnesium (PBS-; Sigma-Aldrich, catalogue number #14040141) to remove any blood. The vein was incubated with 1mg/ml collagenase type Ia (Sigma-Aldrich, catalogue number #SCR103) diluted in PBS with calcium and magnesium ($PBS^+$) for 15 minutes at 37 °C and 5% $CO_2$. During this time, 25$cm^2$ flasks (T25 flasks; BD Falcon, UK) were coated with 2% bovine skin gelatin solution (Type B, Sigma, catalogue number #G1393) made up in PBS+ for 5 minutes prior to aspiration. The cord was massaged for 30 seconds and the endothelial cell suspension was collected by flushing the vein twice with PBS followed once by air to remove all remaining cell solution. The cell suspension was centrifuged at 250 g for 5 minutes and the pellet was re-suspended in 1ml HUVEC complete medium (see Section 2.3) before being added to the gelatin-coated T25 flask containing 3ml HUVEC complete medium. HUVEC were

cultured to confluence (approximately 5 days) before being subcultured as described (see Section 2.3.3) or frozen (see Section 2.3.6)

### *2.3.2. HDBEC Cell Culture*

Cryopreserved human dermal blood endothelial cells (HDBEC; PromoCell, catalogue number #C-12225, lot number #423Z004, #423Z048*)* were purchased at passage two. The cells were thawed at 37°C and cultured in 75cm$^2$ flasks (T75 flasks; BD Falcon) using HDBEC growth media as recommended by the manufacturer (see Section 2.1.2). HDBEC growth media was replaced every 3 days. The cells were subcultured at a 1:3 ratio (Section 2.3.3). The cells were used in experiments or cryopreserved (Section 2.3.6) at passage four.

### *2.3.3. Subculture*

Adherent endothelial cells were subcultured at 80% confluence. The media was aspirated and the cells were washed with 0.5mM EDTA for 30 seconds. EDTA was aspirated and cells were incubated with trypsin (Trypsin 0.05%-EDTA 0.53 mM; Life Technologies, Thermofisher, catalogue number #25300054) at room temperature for 2 minutes. Phase-contrast microscopy was used to visualise when the adherent cells had detached from the flask. Once detached, trypsin was neutralised by the addition of medium 199 supplemented with 20% FBS. The cell suspension was then centrifuged at 400 g for 5 minutes, and the remaining cell pellet was re-suspended in 1ml respective cell culture medium. The cells were counted in a 1:20 dilution using a Z2-series Coulter Counter (Beckman Coulter, High Wycombe, UK) and were either seeded for use in experiments (Section 2.3.6), or cryopreserved (Section 2.3.4).

### *2.3.4. Seeding of endothelial cells onto multi-well plates*

Endothelial cells were subcultured (Section 2.3.3) and re-suspended in $2x10^5$ cells/ml of respective cell media. One ml of cells ($2x10^5$ cells) were added to wells of a 12-well plate (BD Falcon, catalogue number #353043) and plates were incubated at 37°C and 5% $CO_2$ for 24 hours, after which time a confluent monolayer had been formed. Endothelial cells were treated with TNFα and IFNγ for 24h prior to experiments as previously described (M. McGettrick *et al*>, 2009). Briefly, the media was aspirated and replaced with 1ml media containing 10U/ml TNF-α (R&D systems, catalogue number #210-TA-010) and 10ng/ml IFN-γ (Peprotech, London, UK, catalogue number #300-02) for 24 hours prior to the experiment.

### *2.3.5. Short Interfering RNA knockdown of MMP-2 / MMP-9*

HDBEC were seeded as in Section 2.3.4 and left for 24 hours. For siRNA knockdown, 2.5µL of MMP-2 or MMP-9 specific siRNAs or AllStars Negative Control siRNA (Qiagen, catalogue number #1027280) were added to 167µLOpti-MEM (ThermoFisher, catalogue number #31985062) and incubated at RT for 10 minutes. A lipofectamine mix was created by diluting 3µL Lipofectamine RNAiMAX (Invitrogen, Hertford, UK, catalogue number #13778030) with 27µL Opti-MEM and incubated at RT for 10 minutes. The lipofectamine mix was added to the siRNA mix and incubated at RT for 10 minutes. The siRNA-lipofectamine complex was added to each well at a final concentration of 25nM of each siRNA/well and incubated at 37°C for 4 hours, before media was washed twice with PBS and replaced with HDBEC media. Cells were cultured for 24 hours before cytokine-stimulation. After 24 hours of cytokine stimulation, cells and supernatants were harvested and analysed for MMP-2 and MMP-9 expression by qPCR and ELISA (see Sections 2.6.3 and 2.7.9).

### *2.3.6. Cryopreservation of endothelial cells*

For cryopreservation, cells at 80% confluence were subcultured and the pellet re-suspended in cryo-SFM (PromoCell, catalogue number #29910) and split 1:3 into 1.5ml cryovials (Greiner Bio-One, catalogue number #123261). Cryovials were slowly cooled to -80°C using a Mr. Frosty™ freezing container with isopropanol (ThermoFisher, catalogue number #51001-0001) for 24 hours before being stored in liquid nitrogen.

## 2.4. Culture of Cell Lines

### *2.4.1. Culture of immortalised B-Cell lines*

Cryopreserved RAJI cells were purchased from Sigma-Aldrich (catalogue number #85011429-1VL). Cryopreserved RAMOS cells were kindly given to us by Professor Dagmar Toellner. The cells were thawed at 37°C, added to 10ml of Raji media (see Section 2.3.3) and centrifuged at 300 g for 6 minutes at room temperature. Supernatant was aspirated and the remaining cell pellet was re-suspended in 1ml media. Cells were counted in a 1:20 dilution using a Z2-series Coulter Counter (Beckman Coulter) and further diluted to a concentration of $0.5x10^6$ cells/ml in complete Raji media (Section 2.1.4.). Cells were cultured in $75cm^2$ flasks (T75, BD Falcon). RAJI cells were passaged every 2-3 days as described (Section 2.4.2) and used in experiments between passages 8-22.

### *2.4.2. Subculture of Raji cells*

Raji cells float in suspension. To passage, the media was collected into a 15ml propylene tube (BD Falcon). The flask was washed with complete Raji media, which was also collected and added to the 15ml tube. Cells were centrifuged at 200 g for 6 minutes, re-suspended in 1ml media and counted using a Z2-series Coulter

Counter (Beckman Coulter) using a 1:20 dilution. Cells were further diluted to a final concentration of $0.5x10^6$ cells/ml in complete Raji media and 10ml was placed in $75cm^2$ flasks.

### *2.4.3. Cryopreservation of cells in suspension*

Raji cells were subcultured and the pellet re-suspended in complete Raji media ($5 \times 10^6$ cells/ml) supplemented with 10% dimethyl sulfoxide (DMSO; Bio-Techne, Abingdon, UK; catalogue number #3176) and stored in 1.5ml cryovials (Greiner Bio-One). Cryovials were slowly cooled to -80°C using a Mr. Frosty™ freezing container for 24 hours before being stored in liquid nitrogen.

## 2.5. Collection and Preparation of Whole Blood

### *2.5.1. Peripheral Blood Mononuclear Cell Isolation*

Venous blood was collected from healthy volunteers <35 years old into vacutainer tubes coated with 1.6mg/ml potassium ethylenediaminetetraacetic acid ($K_2$EDTA) to inhibit coagulation (BD Vacutainer; Greiner Bio-One, Stonehouse, UK, catalogue number #455045). Peripheral blood mononuclear cells (PBMC) were isolated from whole blood as previously described (Rainger *et al*., 1996). Briefly, 5ml whole blood was gently layered on top of 5ml Histopaque 1077 (Sigma-Aldrich, catalogue number #10771) and centrifuged at 800 g for 30 minutes at room temperature. The PBMC layer sediments just beneath the plasma, and this layer was collected and washed twice in $PBS^+$ by centrifugation at 250 g for 5 minutes at room temperature. After the second wash, the PBMC pellet was re-suspended in 1ml M199 supplemented with 0.15% BSA (M199-BSA) and were counted using a 1:20 dilution using a Z2-series Coulter Counter and either used for experiments or used for isolation of peripheral blood lymphocytes (PBL) (Section 2.5.2).

### *2.5.2. PBL Isolation and Treatments*

PBMC were suspended in 5ml M199-BSA and added to a 25cm$^2$ flask and cultured for 30 minutes at 37°C and 5% $CO_2$ to allow the monocytes to adhere to the flask as previously described (Rainger et al. 2001). The remaining PBL in suspension were collected, washed with M199-BSA by centrifugation at 200 g for 5 minutes at room temperature, and re-suspended in 1ml M199-BSA. PBL were counted using a 1:20 dilution using a Z2-series Coulter Counter and further diluted to a concentration of 1x10$^6$ cells/ml in M199-BSA.

For adiponectin stimulation, 1 x 10$^6$ PBL were placed in 1.5ml Eppendorf microtubes (Sigma-Aldrich) and centrifuged at 200 g for 5 minutes. PBL were resuspended in 100µL M199-BSA and treated with 10µg/ml adiponectin (Enzo Life Sciences, Exeter, UK, catalogue number #ALX-522-063-C050) for 1 hour at room temperature with gentle agitation. PBL were washed by centrifugation at 200 g in M199-BSA for 5 minutes at room temperature before use. PBL pellets were re-suspended in 1x10$^6$ cells/ml M199-BSA for use in experiments.

For PEPITEM (20ng/ml; SVTEQGAELSNEER, Cambridge Research Biochemicals Limited, UK, Billingham) and 14-3-3ζ (10ng/ml; Stratech Scientific Limited, UK, Cambridgeshire, catalogue number #Y92-30N) stimulation, 1 x 10$^6$ PBLs were placed in 1.5ml Eppendorf microtubes and PEPITEM or 14-3-3ζ were added immediately before use in experiments.

Metalloproteinase inhibitors were used to investigate the cleavage of PEPITEM from 14-3-3ζ. The broad spectrum inhibitors GM6001 (10nM; Santa Cruz, catalogue number #SC-203979), TIMP1 (0.1uM), TIMP2 (0.1uM), marimostat (10uM), or the specific MMP-2 (17uM; Generon, Slough, UK, catalogue number

#C5615), MMP-9 (50nM; Merck, catalogue number #444278-500UG), and cathepsin-G inhibitors were pre-incubated with 1 x $10^6$ PBL/ml for 1 hour prior to use in experiments. These were not washed out before being added to the endothelium in order to inhibit proteases in both the PBL and the endothelium.

### *2.5.3. B-Cell Isolation*

B-cells were isolated from PBMCs using EasySep B-cell Human Isolation Kit (StemCell Technologies, EasySep, catalogue number #19054) according to the manufacturer's protocol. Briefly, PBMC ($5x10^7$ cells/ml) in MACS buffer were added to 14ml polystyrene round-bottom tube (EasySep, catalogue number #38008). Cells were incubated with 50µl/ml antibody cocktail (EasySep, catalogue number #19054) for 10 minutes at room temperature. Cells were then incubated with 75 µl/ml magnetic beads (EasySep, catalogue number #19054) for 5 minutes at room temperature. Cells were topped up to 5ml of MACS buffer and added to the magnet (The Big Easy, EasySep, catalogue number #18001) and left for 5 minutes at room temperature. All other lymphocytes were adhered to the walls of the tube and the remaining B cells were poured into a new 15ml tube (BD Falcon). Isolated B cells were centrifuged at 200 g for 5 minutes and re-suspended in 200µl M199-BSA. B cells were counted in a 1:10 dilution and used in experiments. Purity was determined by flow cytometry staining for CD19 (Section 2.7.1).

### *2.5.4. B-Cell Depletion*

B-cells were depleted from PBL using CD19 microbeads (Miltenyi Biotec, Germany) according to manufacturer's instructions. Briefly, PBL were resuspended in 80µl of buffer per $10^7$ cells and 20µl microbeads were added. The cell-bead suspension was incubated for 15 minutes at 4°C. Cells were washed with 2ml of

buffer per $10^7$ and centrifuged at 300 g for 10 minutes. Supernatant was aspirated and cells were resuspended in 500µl of buffer. A MACS LS Column was rinsed with 3ml of buffer. The cell sample was added to the column and total effluent was collected (CD19 depleted PBL). The column was washed with 3ml of buffer which was also collected. The depleted PBL fraction was centrifuged at 300 g for 10 minutes, supernatant was aspirated and cells were resuspended in 1ml M199-BSA. Cells were counted in a 1:40 dilution and used in experiments. Purity was determined by flow cytometry staining for CD19, CD3 and CD14 (Section 2.7.1).

## 2.5 Adhesion Assays

### *2.5.5. Static Adhesion and Migration Assay*

Static adhesion and migration assays were performed as previously described (McGettri*ck et al.*, 2009). In some experiments, cytokine-stimulated endothelium were pre-treated with 14-3-3ζ (10ng/ml) for one hour prior to the assay. Cytokine-stimulated endothelial cells were washed with M199-BSA to remove residual cytokines and non-adhered cells. Untreated or treated PBL (Section 2.5.2) ($1x10^6$ /ml) were added to each well and incubated at 37°C and 5% $CO_2$ for 20 minutes. Immediately after, EC were washed with M199-BSA to remove non-adherent PBL. Cells were fixed with 2% v/v glutaraldehyde (Sigma-Aldrich, #G5882) and imaged (Section 2.5.5) using a phase contrast microscope (Olympus IX71; Southend-on-Sea, UK).

### *2.5.6. Phase Contrast Microscopy*

PBL migration was imaged and analysed using Image Pro Plus (Media Cybernetics). Eight randomly selected fields were imaged using phase-contrast microscopy with an inverted bright-field microscope (Olympus IX71). Cells were

classed as either adhered or migrated as previously described (Chimen *et al*., 2015). Phase bright and phase grey lymphocytes on the surface of the EC monolayer were classified as adherent. Phase dark lymphocytes were classified as transmigrated, and typically appeared to be spread out under the EC monolayer (Figure 1.4 – Representative micrograph image of adhered and migrated PBL following static adhesion assay). The numbers of adhered and migrated PBL were counted and averaged across all fields. Total number of adherent cells was calculated by averaging the number of adhered cells over the eight fields and multiplying by the area of the field of view in $mm^2$ and the number of cells added to the well per $1 \times 10^6$. The number of PBL that had undergone transmigration were expressed at a percentage of the total number of cells that adhered.

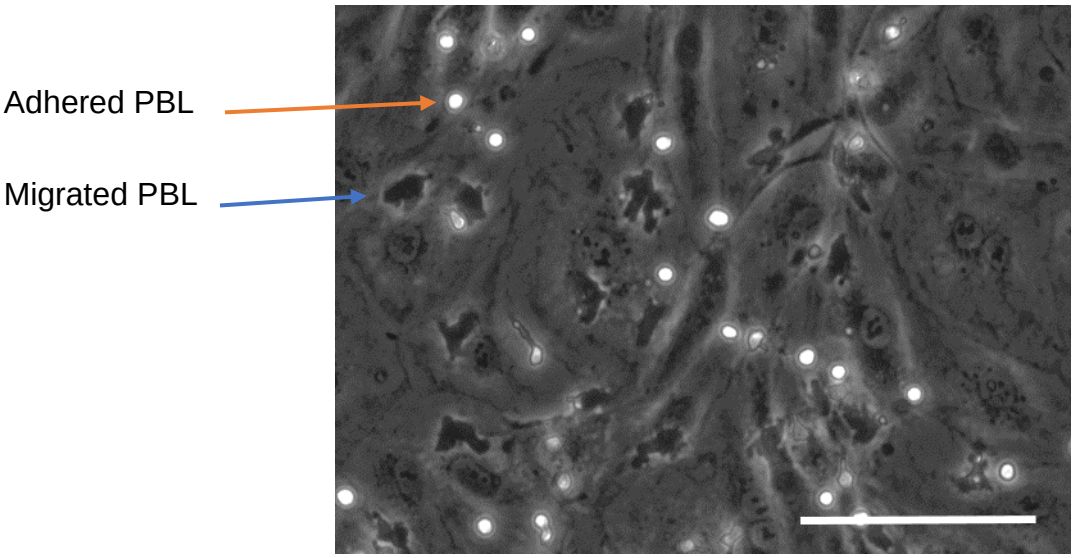


**Figure 1.4 – Representative micrograph image of adhered and migrated PBL following static adhesion assay**

Representative micrograph image of PBL adhesion and migration through inflamed endothelium observed using phase contrast microscopy. HDBEC were seeded onto 12-well plates for 24 hours prior to simulation with 10U/ml TNFα and 10ug/ml IFNγ for 24 hours. HDBEC were washed and incubated with $1x10^6$ PBL for 20 minutes at 37°C, 5% $CO_2$. Images of 8 random fields were acquired and analysed offline. Firmly adherent phase bright PBL (orange arrow) remain circular and are on top of the endothelium. The transmigrated phase dark PBL (blue arrow) appear flattened and irregular shaped underneath the endothelial cell layer. Magnification 20X, scale bar represents 100μM.

## 2.6. Gene Expression

**Table 1.5** Human TaqMan gene expression probes used for real-time PCR

| ***Assay ID*** | ***Primer Sequence*** |
|---|---|
| *ACTB* | Hs99999903_m1 |
| *THBS1* | Hs00962908_m1 |
| *MMP-1* | Hs00899658_m1 |
| *MMP-2* | Hs01548727_m1 |
| *MMP-9* | Hs00957562_m1 |
| *MMP-14* | Hs01037003_g1 |
| *TIMP1* | Hs01092512_g1 |

**All TaqMan probes were purchased from Thermofisher with catalog number 4331182**

### *2.6.1. RNA Extraction*

Total mRNA was extracted from cells using the RNasy Minikit (Qiagen, Manchester, UK; catalogue number #74104) according to user guide. Briefly, cell suspensions were centrifuged at 250 g for 5 minutes and remaining cell pellets were lysed with Buffer RLT. For adherent cells, cells were washed twice with $PBS^-$ and lysed by adding Buffer RLT directly to the cells. Ethanol (70% v/v) was added and the sample was collected in a 1.5ml Eppendorf tube and vortexed to disrupt cell membranes. The whole sample was added to a spin column for centrifugation at 8000 g. The flow-through was discarded and RW1 buffer was added to the collection tube before being centrifuged for 30s at 8000 g. The flow-through was discarded and RPE buffer was added to the collection tube before centrifugation for 30s at 8000 g. The flow-through was discarded and RPE buffer was added to the collection tube before centrifugation for 2 minutes at 8000 g. The spin column was placed into a new 2ml collection tube and dried by centrifugation for 2 min at 10000 g. mRNA was eluted from the spin column using 30µL RNase-free $dH_2O$ which was added to the

collection tube and centrifuged at 8000 g for 1 min. The RNase-free $dH_2O$ flow-through was collected and re-applied to the spin column for another centrifugation to increase RNA yield. RNA concentration and quality was immediately measured using Nanodrop spectrofluorimeter (LabTech). A 260/280 ratio of 1.80-2.20 was deemed acceptable for cDNA conversion. Samples were stored at -80°C for <72 hours before being converted to cDNA.

### *2.6.2. mRNA to cDNA conversion*

To convert the extracted RNA to cDNA, 1µg of total RNA was reverse transcribed using High Capacity cDNA Reverse Transcription Kit (Applied Biosystems, Warrington, UK; 4368814) following the user guide. A reaction volume of 20µl was used containing: 3.2µl RNase free $H_20$, 2µl RT buffer, 0.8µl dNTP mix (100mM), 2µl RT random primers, 1µl RNaseOUT, 1µl reverse transcriptase and 1µg of total RNA. RT was performed in a thermocycler at 25°C for 10 min, 37°C for 120 min, 85°C for 5 min, with a final hold at 4°C. cDNA was stored at -20°C before qPCR use.

### *2.6.3. Real-time Polymerase Chain Reaction*

TaqMan multiplex master mix (Applied Biosciences; 4461881) was used to replicate all cDNA and TaqMan probes (see Table 1.5) were used to identify the cDNA of interest (Thermofisher, 4331182). All probes were labels with FAM marker except for the human housekeeping GAPDH, which was labelled with VIC. Each reaction contained: 5.5µl of Taqman multiplex master mix, 3.9µl of RNase free $H_20$, 0.6µl of TaqMan probes, and 0.5µl of cDNA. PCR was performed using the 7900HT Fast Real-Time PCR System with 384-Well Block Module (Applied Biosystems, catalogue number #4329001). qPCR employed 40 cycles of: 50°C for 2 minutes,

95°C for 10 minutes, 95°C for 15 seconds, 60°C for 1 minute, with the final holding at 4°C. Each sample was run in technical duplicates and the mean cycle threshold (Ct) of the duplicates was calculated. Only values with standard deviation (SD) <1 were used for further analysis. To compare gene expression, the cycle threshold (Ct) was recorded and compared to the house keeping control to work out ΔCt (ΔCt = Ct target gene – Ct reference gene). Results are expressed as relative gene expression against the endogenous control ($2^{-\Delta Ct}$) or fold change between treated and untreated samples $2^{-\Delta\Delta Ct}$).

### *2.6.4. Analysis of EndoDB Datasets*

EndoDB is a freely-available online endothelial cell database that provides a collection of pre-analysed data collected from 360 datasets of endothelial transcriptomics. Bulk datasets of interest were selected by screening for keywords in the search feature. Results identified were screened and those that matched the inclusion criteria of; using the keyword as an endothelial cell stimulant without being used in conjugation with other factors, and including an unstimulated endothelial control, were selected for analysis. Normalised expression values for each study were exported and results are expressed as log2 fold change.

## 2.7. Protein Expression

### *2.7.1. Flow Cytometry*

Cells ($0.5 \times 10^6$) were added to a 5ml polypropylene tube (BD Falcon) and centrifuged at 300 g for 5 minutes and re-suspended in MACs buffer (see Section 2.1.3). Antibodies (see Table 1.6) diluted in PBS+ were incubated with the cells for 20 minutes in the dark at 4°C. Zombie aqua was used to stain for live/dead cells. Cells were washed with 4ml cold PBS+ and centrifuged at 300 g for 5 minutes. This

was repeated for any secondary staining steps. Cells were fixed with 2% formaldehyde (TAAB Laboratories Equipment Ltd; catalogue number #F003) diluted in deionized water for 10 minutes in the dark at 4°C. Cells were washed with 4ml cold PBS+ and centrifuged at 300 g for 5 minutes. Cells were re-suspended in PBS+ and kept in the dark at 4°C until ready for analysis. Flow cytometry was performed using a 4-laser Fortessa X20 flow cytometer with DIVA software. At least 10,000 total events were acquired per sample where possible.

### *2.7.2. Analysis of flow cytometry data*

During acquisition, gates were set up on FACSDiva (version 7; BD Biosciences) to gate for cells using forward (FSC) and side (SSC) scatter profiles. Doublets were excluded using forward scatter area (FSC-A) and forward scatter height (FSC-H), and dead cells were excluded using positive zombie aqua signal. Data were exported from FACSDiva and analysed using Flow Jo (version 10.7.1, BD Biosciences).

Human leukocyte populations were gated on PBMC as follows: T-cells (CD3+CD19-), B-cells (CD3-CD19+), NK cells (CD3-CD56+), and monocytes (CD14+). T-cells were further categorised based on CD4+ and CD8+ expression. For adiponectin receptor (AdiporR1/2) quantification, mean fluorescence intensity (MFI) and the percentage of cells that were positive and negative in the Alexa fluor 488 channel were exported for each sample. The isotype control values were subtracted from the AdipoR1/2 stained samples to determine the percentage of cells expressing AdipoR1/2 and the MFI. Flow cytometry was used to test purity after B-cell isolation and depletion.

**Table 1.6. List of antibodies used in flow cytometry**

| Reagent | Manufacturer | Catalogue Number | Clone | Working Concentration |
|---|---|---|---|---|
| FcR block | MACS (Bisley, Surrey) | 130-059-901 | N/A | 1:50 |
| AdipoR1 | Pheonix Pharma (Burlingame, California) | G-001-44 | IgG | 1:100 |
| AdipoR2 | Pheonix Pharma | G-001-23 | IgG | 1:100 |
| Goat anti-rabbit FITC | Invitrogen (Paisley, UK) | A11008 | IgG | 1:100 |
| CD56 PE | eBiosciences (Paisley, UK) | 12-0567-42 | CMSSB | 1:50 |
| CD3 PerCpCy5.5 | Invitrogen | 45-0037-42 | OKT3 | 1:100 |
| CD19 PECy7 | eBiosciences | 15520187 | HIB19 | 1:100 |
| CD14 APC | Invitrogen | 17-0149-42 | 61D3 | 1:50 |
| CD4 APCCy7 | Invitrogen | 56-0049-42 | RPA-T4 | 1:50 |
| CD8 PB | eBiosciences | 11-0048-42 | OKT4 | 1:100 |
| Normal Goat serum (block) | R&D Systems | DY005 | N/A | 1:50 |
| Zombie Aqua dye | BioLegend (Highgate, UK) | 77143 | N/A | 1:500 |

### *2.7.3. Generating Lysates for Western Blot and Gel Zymography*

Protein isolation from cells was performed using RIPA buffer (Sigma, catalogue number #R0278) containing 10% protease inhibitor cocktail (Sigma, catalogue number #P8340). Cells were washed twice with ice-cold PBS- and RIPA buffer was added. Cells were kept on ice for 30 minutes under gentle agitation before being scraped and collected into an Eppendorf. Cells were centrifuged at 12,000 g for 10 minutes, supernatants were collected and stored in -80°C until used in western blot (Section 2.7.6)

### *2.7.4. Generating Lysates for Proteome Array*

Protein isolation from cells was performed using Lysis Buffer 17 (R&D Systems, catalogue number #895943) containing 10% protease inhibitor cocktail (Sigma). Cells were washed twice with ice-cold PBS- solubilised at $1x10^6$ cells/ml in lysis buffer. Cells were pipetted up and down to re-suspend and were kept on ice for 30 minutes under gentle agitation. Cells were centrifuged at 14,000 g for 5 minutes, supernatants were collected and stored in -80°C until used in proteome array (section 2.7.5).

### *2.7.5. Protein Quantification*

Protein quantification was performed using the Pierce BSA Protein Assay (ThermoScientific, catalogue number #23225). Briefly, serial dilutions of BSA standards were made between concentrations 0µg/ml to 2000µg/ml by diluting in the same lysis buffer as the cell lysates. Samples and standards (25µL) were added to a 96-well tissue culture plate in duplicate. Working reagent was made by mixing 50 parts BCA reagent A with 1 part BCA reagent B, and 200µl was added to each well. Plates were covered in aluminium foil and incubated at 37°C for 30 minutes. Plates were allowed to cool to room temperature before being ran on a plate reader (BioTek, Synergy HT Microplate Reader) at wavelength 562nm. The blank read was subtracted from all other reads before analysis. The average absorbance for each known standard was used to generate a standard curve using GraphPad Prism 8.0.2. Concentrations of unknown samples were interpolated from this standard curve.

### *2.7.6. Western Blot*

HDBEC lysates from Section 2.7.3 were quantified (Section 2.7.5) and used for western blot. Samples (10µg) or PageRuler Plus Prestained Protein Ladder (Invitrogen, catalogue number #26616) were mixed 1:4 with 4x Laemmli sample buffer (BioRad, #161074) and heated to 95°C on the heatblock (Fisher Scientific, Techne Dri-block heater DB-2D) for 10 minutes. NuPAGE™ 4 to 12%, Bis-Tris, 1.0mm, Mini Protein Gels (Invitrogen, #NP0324BOX) were prepared by adding 1x NuPAGE™ MES SDS Running Buffer (Invitrogen, #NP0001) diluted in deionized water to an XCell SureLock Mini-Cell (Invitrogen, catalogue number #EI0001). Buffer was added to the tank until all the wells were submerged. The comb was removed and 4µl PageRuler Plus Prestained Protein Ladder or samples were loaded into respective wells. Proteins were separated using 125V for 10 minutes, 100V for 90 minutes, and 150V for 10 minutes. Following gel electrophoresis, the gel was transferred onto a PVDF membrane using the Trans Blot Turbo Midi 0.2mm (BioRad, #170415). The bottom half of the membrane was placed onto Trans-Blot Turbo transfer system (BioRad, #1704150). The gel cassette was opened and the gel was placed face up directly on the bottom half of the membrane. The top half of the membrane was then placed on top and air bubbles were removed using a roller. The transfer was run using the MINI gel settings for 10 minutes to transfer the protein. Membranes were blocked with 5% milk diluted in PBS-T for 1 hour with gentle agitation. Primary antibodies (Table 1.7) were diluted in 5% milk PBS-T and incubated with the membrane overnight at 4°C under gentle agitation. Membranes were washed with PBS-T before being incubated with a HRP conjugated secondary antibody (Table 1.7) for 90 minutes. Membranes were washed again in PBST and 2ml of Clarity Western Peroxide Reagent and Clarity Western Luminol/Enhancer

Reagent (BioRad, #1705060) mixed 1:1 was added to the membrane for 1 minute. Membranes were wrapped in cling film and placed in an autoradiography film cassette with the identification numbers facing up. Membranes were exposed to X-ray film and developed. If membranes needed to be stripped and reprobed, membranes were incubated with Restore PLUS Western Blot stripping buffer (Thermo Scientific, #46430) for 30 minutes at 37°C before staining for subsequent primary antibodies. Developed films were scanned into TIF files and quantified by comparison of band intensity of protein of interest and housekeeping protein using ImageJ.

**Table 1.7 – Antibodies used in western blot**

| Protein Target | Manufacturer | Catalogue Number | Host | Dilution |
|---|---|---|---|---|
| MMP-2 | Proteintech | 10373-2-AP | Rabbit | 1/1,000 |
| MMP-9 | Cell Signalling | 3852 | Rabbit | 1/1,000 |
| TIMP-1 | Cell Signalling | D10E6 | Rabbit | 1/1,000 |
| TIMP-2 | Cell Signalling | D18B7 | Rabbit | 1/1,000 |
| β-actin | Sigma-Aldrich | A2066 | Rabbit | 1/4,000 |
| CD63 | Invitrogen | 10628D | Mouse | 1/1,000 |
| CD81 | Invitrogen | 10630D | Mouse | 1/1,000 |
| CD9 | Invitrogen | 10626D | Mouse | 1/1,000 |
| Calnexin | Merck | AB2301 | Rabbit | 1/1,000 |
| Goat anti-rabbit IgG peroxidase conjugate | EMD Millipore Corp | 401393 | Goat | 1/10,000 |
| Anti-mouse secondary | EMD Millipore Corp | 401253 | Goat | 1/10,000 |

### *2.7.7. Gelatin Zymography*

HDBEC lysates from Section 2.7.3 were quantified (Section 2.7.5) and used for gelatin zymography. Samples were normalised to 5µg and added to 5µl tris-glycine SDS sample buffer (2X) (Invitrogen, catalogue number #LC2676). Standards were diluted to 20ng in glycine SDS sample buffer. Samples and standards were made up to 10µl with deionized water. Samples were not heated or reduced for zymography. Novex 10% zymogram plus (gelatin) protein gels 1.0mm (Invitrogen, catalogue number #ZY00105BOX) were prepared by adding 1x Tris-Glycine SDS running buffer (Invitrogen, catalogue number #LC2675) diluted in deionized water to an XCell SureLock Mini-Cell. Buffer was added to the tank until all the wells were submerged. The comb was removed and 4µl PageRuler Plus Prestained Protein Ladder or samples were loaded into respective wells. Proteins were separated using a constant 125V voltage polypack for 105 minutes. Following gel electrophoresis, the gel was incubated in 1x zymogram renaturing buffer (Invitrogen, catalogue number #LC2670) for 30 minutes at room temperature with gentle agitation. The buffer was decanted and replaced with 1x zymogram developing buffer and left to equilibrate for 30 minutes at room temperature with gentle agitation. The buffer was replaced with fresh 1x zymogram developing buffer and incubated at 37°C overnight. Following this incubation, gels were stained by incubating for 1 hour at room temperature with SimplyBlue Safe Stain (Thermofisher, #LC6060) before being destained with deionised water for 30 minutes at room temperature. Gels were imaged using Vilber Lourmat Fusion FX. Images were inverted and analysed by comparison of band intensity.

### *2.7.8. Proteome Array*

Expression of proteases was identified using the proteome profiler human protease array kit (R&D Systems, catalogue number #ARY021) according to the user guide. All reagents are provided with the kit were manufactured by R&D Systems. Array buffer 6 (#893573) was added to each well of a 4-well multi-dish (#607544). Membranes containing antibody capture chips against proteases were added to a well with the number of the membrane facing upwards. Membranes were incubated on a rocking platform for one hour at room temperature. B cell lysates and supernatants isolated as in Section 2.7.3-2.7.4 were thawed and adjusted to a final volume with 1.5ml with Array Buffer 6. Detection Antibody Cocktail (15µl; #894548) was added to each prepared sample and incubated at RT for one hour. Array Buffer 6 was removed from the wells by aspiration and the prepared sample-antibody mixture was added to the membrane and incubated overnight at 4$^{o}$C on a rocking platform shaker. Membranes were washed three times with 1x wash buffer (#895003) for 10 minutes on a rocking platform shaker. After washing, 1x streptavidin-HRP (893019) diluted in Array Buffer 6 was added to each membrane and incubated for 30 minutes at RT on a rocking platform shaker. Membranes were washed three times with 1 x wash buffer as previously described, before being removed from the wash container and blotted against a paper towel. Membranes were placed on cling film and Chemi Reagent 1 (894287) mixed 1:1 with Chemi Reagent 2 (894288) was added to the membrane to provide complete coverage before incubation for 1 minute. Membranes were wrapped in cling film and placed in an autoradiography film cassette with the identification numbers facing up. Membranes were exposed to X-ray film for 30 minutes and developed using the Compact X4 Automatic X-ray Film Processor (Xograph, UK).

Developed films were scanned into TIF files and quantified by comparison of band intensity of reference spots and antibody spots using ImageJ. For analysis, the images were inverted so the mean grey pixel value could be measured as a quantification of the amount of protease present in the sample. An ROI was created and used to measure the value of each protease spot. As each protease had duplicate spots, the values of these was averaged and the value of the negative control spot was subtracted. The data between untreated and AQ-stimulated samples was normalised by the reference spots and expressed as fold-change in protease abundance.

### *2.7.9. ELISA*

MMP-2 and MMP-9 concentration in B cell and EC supernatants was quantified using DuoSet ELISA Human MMP2 (R&D Systems, catalogue numbers DY902-05) and DuoSet ELISA Human MMP-9 (R&D Systems, catalogue numbers DY911-05). Firstly, a 96-well microplate was coated with capture antibody (part #844926) diluted to 1 µg/ml in PBS-. The plate was sealed and incubated overnight at RT. The next morning, wells were washed by addition and removal of 400µl of wash buffer (0.05% Tween 20 in PBS; R&D Systems, catalogue number #WA126) three times before blotting against a paper towel to remove any remaining wash buffer. Plates were then blocked by the addition of reagent diluent (1% BSA in PBS; R&D Systems, catalogue number #DY995) and incubating at RT for 1 hour. Plates were washed as above. Standards were made from the recombinant human MMP-9 standard (part #841030) by 2-fold serial dilution in reagent diluent to concentrations between 31.3pg/ml and 2000pg/ml. Standards and neat supernatants were added to a well in duplicate and incubated at RT for 2 hours. Plates were washed as above. Detection antibody (150ng/ml; part #844927) diluted in reagent diluent with 2%

normal goat serum (R&D Systems, catalogue number #DY005) was added to each well and incubated at RT for 2 hours. Plates were washed as above. Streptavidin-HRP (part #893975) diluted in reagent diluent was then added to wells and incubated for 20 minutes at RT in the dark. Plates were washed as above before addition of substrate solution (1:1 mixture of Color Reagent A ($H_2O_2$) and Color Reagent B (Tetramethylbenzidine) (R&D Systems®, catalogue number # DY999)) for 30 minutes in the dark. The reaction was stopped by addition of stop solution (2 N H2SO4, R&D Systems®, catalogue number #DY994). Plate absorbance was read on a microplate reader set to 450nm with wavelength correction at 570nm and the values were exported into a table.

To quantify the levels of MMP2 and MMP9 in the samples, readings at 570 were subtracted from the readings at 450nm to correct for optical imperfections in the plate. The readings from the background well were also subtracted from the samples. The average absorbance for each known standard was used to generate a standard curve using GraphPad Prism 8.0.2. The concentrations of unknown samples were interpolated from this standard curve using the y-intercept and slope derived from the standard curve.

## 2.1. Extracellular Vesicle Characterisation

### *2.1.1. PKH26 Staining*

Primary isolated B-cells were labelled with an intercalating lipid dye using the PKH26 Red Fluorescent Cell Linker Kit for General Cell Membrane Labelling (Sigma-Aldrich, MIDI26) following manufacturer's instructions. Briefly, $2x10^7$ cell/ml were added to a 15ml polypropylene tube (BD Falcon) and washed with $PBS^-$. Cells were centrifuged at 300 g for 10 minutes. Cells were re-suspended in Diluent C to

make a 2X Cell Suspension. In a fresh tube, PKH26 ethanolic dye was diluted in Diluent C to make a 2X Dye Suspension. The cell suspension was added to the cell solution and mixed well by pipetting, and left to incubate for 5 minutes at room temperature with periodic pipetting. An equal volume of sterile-filtered (0.22μm) FBS was added to stop the reaction and left to incubate for 1 minute. Cells were washed with sterile-filtered (0.22μm) PBS-BSA (0.15% BSA, PBS+) and centrifuged at 300 g for 10 minutes. Cells were re-suspended in sterile-filtered (0.22μm) PBS-BSA and transferred to a fresh 15ml polypropylene tube. Cells were washed twice more as above with PBS-BSA and re-suspended in 1ml PBS-BSA for counting. Cells were diluted 1:20 and counted using a Z2-series Coulter Counter. Cells were re-suspended in $10x10^6$ cells/ml PBS-Albumin solution and either immediately analysed using an Accuri C6 Flow Cytometer (BD Biolscience, Oxford, UK) or stimulated to release EV (Section 2.1.1) prior to analysis using a BD FacsVia flow cytometer.

During acquisition using BD FACSDiva Software (BD Biosciences), the size threshold was reduced to 20,000 FSC-H to enable detection of small extracellular vesicles. Gates were set up using unstimulated B-cells using forward (FSC) and side (SSC) scatter profiles. Data were exported from FACSDiva and analysed using Flow Jo (version 10.7.1, BD Biosciences). On Flow Jo, to eliminate high background seen as a result of reducing the sizing threshold, the detection threshold was increased to 2,500 fluorescence intensity of PKH26.

### *2.1.2. B-Cell Stimulation for Extracellular Vesicle Release*

B-cells ($10x10^6$ cells/ml) were suspended in PBS-BSA and stimulated with one of the following treatments: adiponectin (10μg/ml), IL-4 (50ng/ml; Enzo Life Sciences, catalogue number #ENZ-PRT180-0020) and CD40 (0.5mg/ml; Enzo Life Sciences, catalogue number #ENZ-ABS-130-0100), phorbol myristate acetate (PMA;

1ng/ml; Sigma, catalogue number #P1585) and ionomycin (1Mm; Sigma, catalogue number #I3909) on a shaker for 1 hour at room temperature. Cells were centrifuged at 500 g for 10 minutes, supernatants were collected and stored at -80°C until use in experiments.

### *2.1.3. Nanoparticle Tracking Analysis*

B cell supernatants were collected as described in Section 2.1.2 and used for nanoparticle tracking analysis (NTA). Total EV concentration and size distribution was measured using a Nanosight LM10 (Malvern Instruments, UK) as previously described (Chimen *et al*., 2020). Vesicle concentration was diluted with filtered PBS- to a concentration that fell within the linear range of the instrument (1-10 x $10^6$ particles/ml; 20-60 microspheres per field of view). Approximately 500µL of the diluted sample or solvent (PBS-BSA) were added to the Nanosight chamber mounted on the light microscope. A laser was used to illuminate particles with the samples and movement of individual particles was tracked. Sixty-second videos (30 frames per second) were recorded from six different fields of view per sample. Acquisition parameters were optimised according to Gardiner et al (2013) and maintained constant between samples. First, PBS-BSA was added to the sample chamber to check that it is free from particles and the chamber was clean. Samples were then loaded and the camera level was increased until the image was close to saturated, then slowly reduced the camera level until the vesicles are observed as single bright points with minimal blur or diffraction rings. Using this optimisation method, digitised sequences were recorded with the camera level set at 13 and camera gain set at 1, and analysed with detection threshold set at 8. Sequence captures were automatically analysed by NTA software 2.2.

### *2.1.4. ExoView*

Exosomes were quantified and characterised using the Exoview R100 and all reagents provided by the Exoview Tetraspanin Kit with Cargo (EV-Tetra-C-Car, Nanoview Bioscieces, Malvern, UK). Before sample capture and staining, Exoview cargo chip files (provided by the manufacturer) were loaded onto the ExoView computer. Chips were pre-scanned using nScan2 V 2.76 acquisition software. Chips were added to the centre of a well of a 24-well tissue culture plate with the chip ID facing up using tweezers to prevent touching the face of the chip. Edge wells were not used and surrounding areas between wells were filled with 0.22µm sterile-filtered deionized $H_20$ to maintain a humid environment (Figure 1.5). B-cell supernatant samples as produced in Section 2.1.2 were diluted 1:2 in incubation solution. Diluted sample (35µL) was loaded onto the centre of the chip and incubated for 16 hours at RT in the dark. Following incubation, chips were washed by adding 1ml 1X solution A and shaking at 300rpm for 3 minutes. After washing, 750µl of 1X solution A was removed from each well and replaced with fresh 750µl and put back on an orbital shaker for 3 minutes at 300rpm. This washing and shaking was repeated 3 times. After the last wash, 750µl of solution A was removed from the well and 250µl solution C was added. Chips were placed on an orbital shaker at 200rpm for exactly 10 minutes. After 10 minutes, 500µL of 1X solution A was added to each well and 750µL was immediately removed. The chips were then washed a further 3 times by addition of 750µL 1X solution A and shaking at 300rpm for 3 minutes. After these wash steps, 750µL was removed from each well and 250µL of solution D was added. Chips were placed on an orbital shaker at 200rpm for exactly 10 minutes. After 10 minutes, 500µL of 1X solution A was added to each well and 750µL of solution was immediately

removed. The chips were then washed a further 3 times by addition of 750µL 1X solution A and shaking at 300rpm for 3 minutes, and removal of 750µL of solution.

After the last wash, 750µL of solution was removed from each well and was replaced with 250µL of fluorescently labelled antibody mixture containing CD19-AF488 (1:200, eBiosciences, catalogue number #15520187) and 14-3-3ζ-CD647 (1:200, Biorbyt, catalog number #orb382906-CF647) in cargo blocking solution. The plate was covered with aluminium foil to prevent light, and placed on an orbital shaker at 300rpm for 1 hour. Following incubation with antibody mixture, chips were washed by the addition of 500µL of 1X solution A. Immediately 750µL of solution from each well was removed and 750µL of 1X solution B was added to each well. The plates were placed on an orbital shaker at 300rpm for 3 minutes and 750µL of solution was removed from each well. Chips were washing 3 times by the addition of 750µL 1X solution B, shaking at 300rpm for 3 minutes and removing 750µL of solution. After the final wash, 750µL of deoinized water was added to each well and plates were added to an orbital shaker at 500rpm for 3 minutes. Deionized water was added to a 10-cm Petri dish and chips were transferred one at a time to the water-filled Petri dish. Tweezers were used to hold the chip on either side, chips were maintained horizontal in order to prevent them from drying out. Chips were moved back and forth to circulate water without exposing the chip to any air. The chips were tilted to a 45° angle and slowly pulled out of the water. Chips were placed on absorbent paper towel with the chip ID facing up and allowed to dry. Interferometric images of the chips were acquired with an Exoview R100 reader using the ExoScan software. If not acquired immediately, chips were stored at 4°C until further use.

### *2.1.5. ExoView Analysis*

Pre-scan and post-scan chip files were exported and analysed on Exoview Analyser (Nanoview Biosciences). Vesicle binding was calculated by subtracting the signal measurement of the pre-scanned chips from the post-scanned chips. Exosomes captured by the chips appeared as bright spots, the light was quantified with sizing threshold set to 50-200nm. Size and number of exosomes was determined by the Exoview Analyser software. ExoView captured fluorescence of secondary antibodies against CD19 and 14-3-3ζ and total fluorescence was calculated by subtracted fluorescence intensity of the isotype controls from the samples.

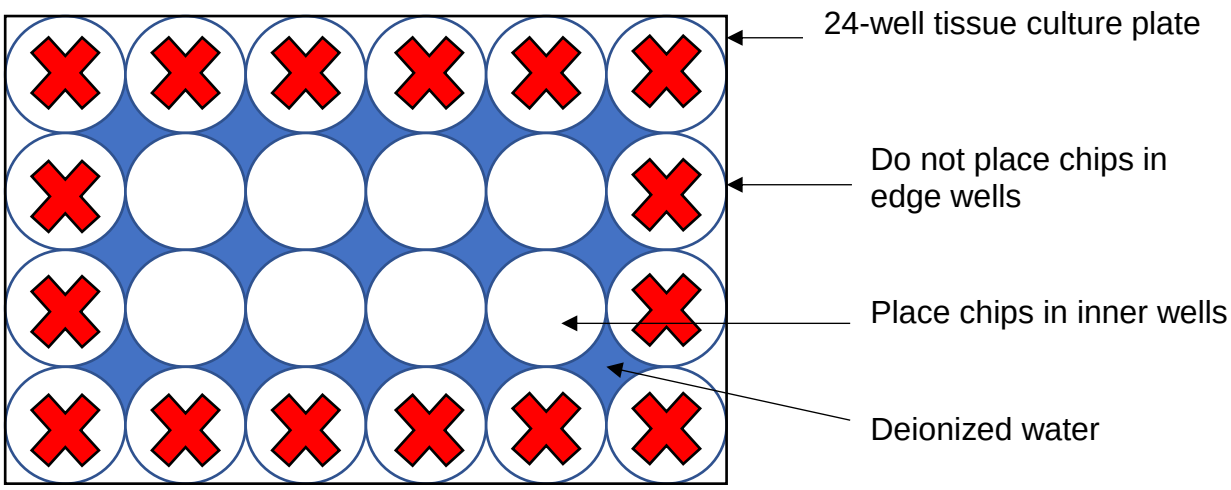


**Figure 1.5 – ExoView chip layout in 24-well tissue culture plate**

Chips are placed in middle wells of a 24-well tissue culture plate with chip ID facing up. Surrounding areas are filled with deionized water to maintain humidity. Diluted sample is added to the chip and incubated for 16 hours before washing, permeabilisation and staining. Chips are then dried and ran on the ExoView.

# Chapter 3. MMP EXPRESSION IN ENDOTHELIAL CELLS AND B CELLS

## 3.1. Introduction

PEPITEM is a 14-amino acid sequence cleaved from the parent protein 14-3-3ζ between amino acids 28 and 41. Importantly, 14-3-3ζ can inhibit lymphocyte transmigration to a similar efficacy as PEPITEM, however this is reversed in the presence of a broad-spectrum matrix-metalloproteinase (MMP) inhibitor (Apta, 2016). Therefore, cleavage of 14-3-3ζ into PEPITEM must occur to mediate the immuno-regulatory function, however it is not currently known which MMP is involved in this cleavage.

Matrix metalloproteinases (MMPs) are a family of proteases expressed by many cell types and associated with inflammatory disease (reviewed in Nissinen and Kahari, 2014). Despite their central roles in endothelium homeostasis, MMP production by endothelial cells is not yet well characterised and literature about the factors that regulate their expression is limited. Here, we are particularly interested in the gelatinases, MMP-2 and MMP-9, and their expression in B-cells and the endothelium as we identify them as proteases potentially involved in PEPITEM cleavage.

In this chapter, we aim to elucidate which protease(s) are involved in cleavage of 14-3-3ζ using an online webserver to identify potential cleavage sites flanking PEPITEM within the 14-3-3ζ amino-acid sequence. We also aim to elucidate the cellular origin of these proteases by investigating expression of proteases within the endothelium and in primary B cells and their regulation by pro-inflammatory stimuli.

## 3.2. Results

### *3.2.1. Identifying potential protease cleavage sites in the 14-3-3ζ sequence*

In order to identify proteases involved in cleaving 14-3-3ζ into PEPITEM, we screened the amino acid sequence of 14-3-3ζ using PROSPER, an online webserver for predicting protease cleavage sites within a sequence. Two proteases were identified that had potential cleavage sites flanking PEPITEM, MMP-9 and cathepsin-G (Figure 3.1A). Cleavage sites for MMP-9 (green residues) were identified that could cleave 14-3-3ζ releasing a 17-amino acid sequence, MKSVTEQGAELSNEERN, which contains PEPITEM (SVTEQGAELSNEER) (Figure 3.1A).

Cathepsin-G (red residues) cleavage sites could cleave 14-3-3ζ into two shorter sequences, SVTEQGAEL and SNEERNLL (Figure 3.1A). Previous data has shown that the broad spectrum MMP inhibitor, GM6001, prevents the immuno-modulatory effects of 14-3-3ζ (Apta, 2015). As GM6001 does not inhibit activity of cathepsin-G, it is likely that cathepsin-G is not essential for cleavage of 14-3-3ζ into a functional peptide. Glutamyl peptidase (pink residues) does not have cleavage sites flanking PEPITEM, however does have a potential cleavage site within the PEPITEM sequence, which could potentially be involved in further cleavage of PEPITEM into smaller peptides (Figure 3.1A). Therefore, MMP-9 or cathepsin-G are likely to be involved in cleavage of PEPITEM from 14-3-3ζ, and glutamyl pepitdase or cathepsin-G may be involved in further cleavage of PEPITEM into smaller fragments.

We also used a more novel *in silico* webserver, ProCleave, which provides probability scores for potential cleavage sites. Using ProCleave, we identified probability scores for the previously identified cleavage sites within the 14-3-3ζ

sequence (Figure 3.1B). Probability scores ranged from 0-1 with the higher numbers having higher probability of cleavage. The cleavage sites for cathepsin-G had probability scores ranging from 0.118 to 0.280, and the cleavage sites for MMP-9 had probability scores of 0.191 to 0.505 (Figure 3.1B). Interestingly, ProCleave also identified very high probability scores (0.983 and 0.996) for MMP-2 cleavage sites within the 14-3-3ζ sequence flanking PEPITEM, which would result in a 15-amino acid sequence, SVTEQGAELSNEERN (PEPITEM with one additional N amino acid group) (Figure 3.1B). The data from the Prosper and ProCleave software suggest the proteases most likely to be involved in cleavage of PEPITEM from 14-3-3ζ are the gelatinases, MMP-2 and MMP-9. Therefore, we were specifically interested in MMP-2 and MMP-9, when investigating expression of proteases in the endothelium and in B-cells.

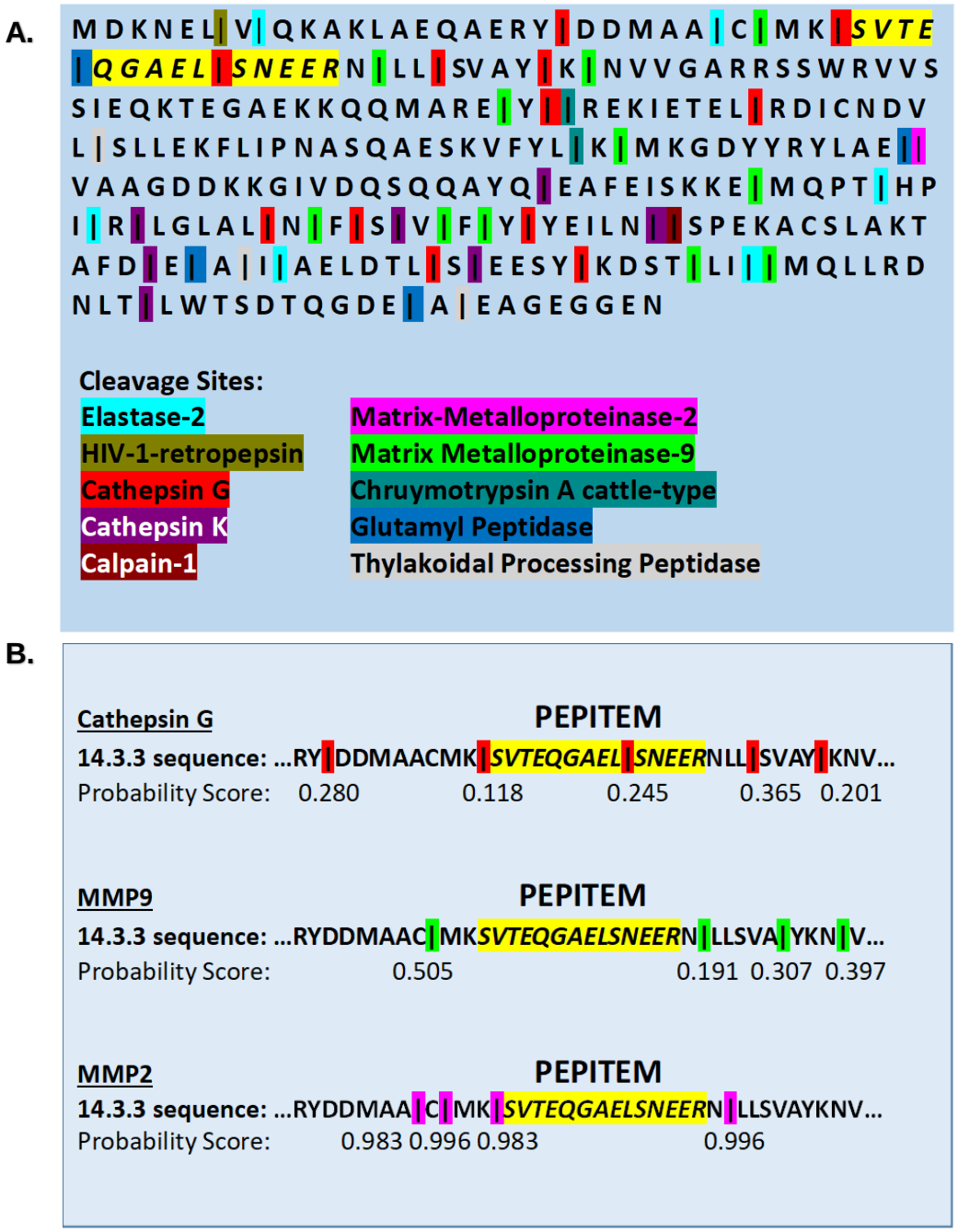


**Figure 3.1 – Predicted protease cleavage sites in the 14-3-3ζ sequence**

The sequence of 14-3-3ζ was screened using (A) PROSPER, a webserver for in silico prediction of protease substrates and their cleavage sites. Cleavage sites are shown for elastase-2 (light blue), HIV-1-retropepsin (khaki), cathepsin-G (red), cathepsin-K (purple), calpain-1 (brown), matrix metalloproteinase-2 (pink), matrix metalloproteinase-9 (green), chrymotyrpsin A cattle type (turquoise), glutamyl peptidase (blue) and thylakoidal processing peptidase (grey). (B) ProCleave probability scores for potential cleavage sites for cathepsin-G (red), MMP-9 (green) and MMP-2 (pink). PEPITEM sequence shown in yellow.

### *3.2.2. Investigating how inflammatory stimuli affect MMP expression in endothelium*

An extensive understanding of MMP expression within the endothelium is not fully known. MMPs are regulated at not only the level of transcription, but also post-translationally through activation of latent isoforms and through tight regulation by endogenous tissue inhibitor of metalloproteinases (TIMPs). Therefore, when investigating MMP expression it is equally important to investigate expression of TIMPs. Expression of MMPs and TIMPs vary depending on type of endothelium and following inflammatory stimuli. In recent years, technological advances have led to global profiling of transcript levels in endothelial cells via a range of high-throughput methods, including microarray analysis and RNA sequencing. A freely-available online endothelial cell database, EndoDB, provides a collection of pre-analysed data collected from 360 datasets of endothelial transcriptomes (Khan et al., 2019) (Figure 3.2). To investigate how pro-inflammatory stimulation affected MMP and TIMP gene expression in endothelial cells, we used EndoDB to mine these publicly available transcriptomics datasets. We searched through bulk datasets on EndoDB for the keywords “TNF”, “interferon”, “VEGF” and “shear stress”. Each of these searches led to several results which were screened and those that were applicable were selected for further analysis. Inclusion criteria included; using the keyword as an endothelial cell stimulant without being used in conjugation with other factors, and including an unstimulated endothelial control (Figure 3.3). The raw expression values for all MMP and TIMP genes were downloaded and analysed using GraphPad Prism 8.0.2.

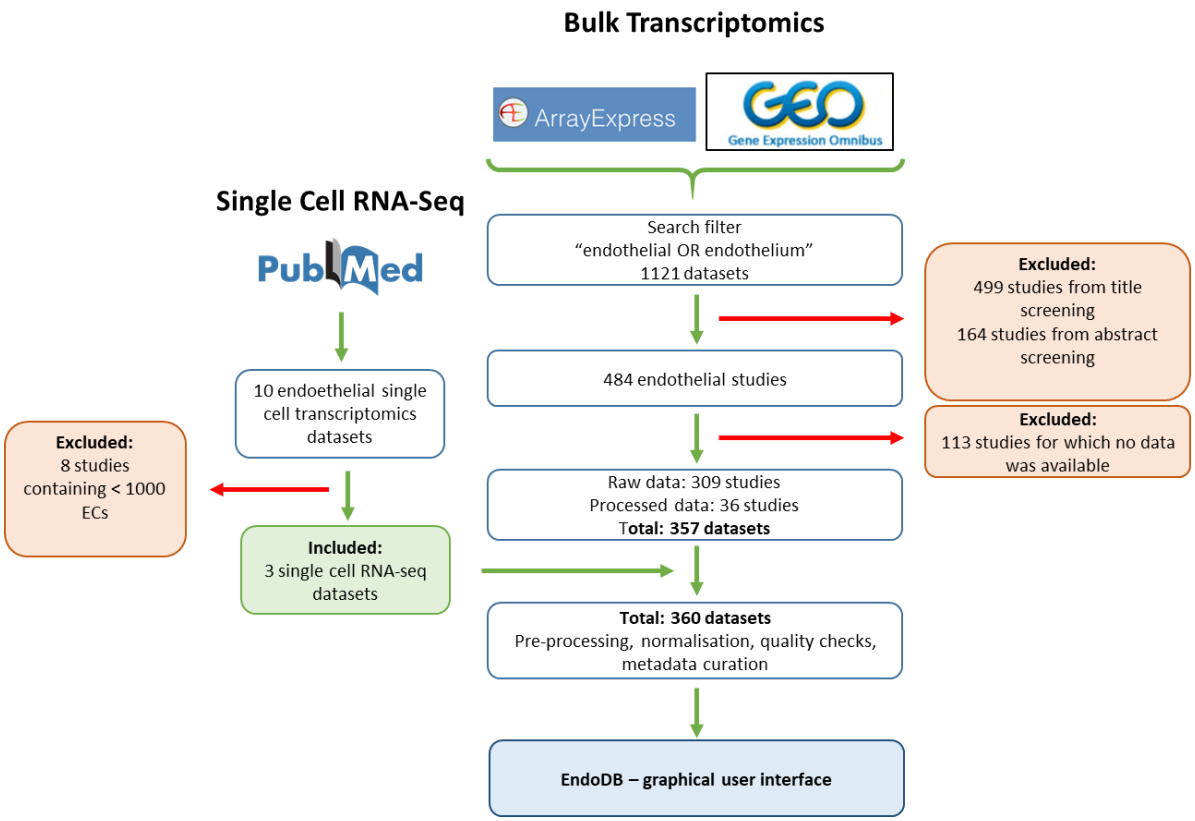


**Figure 3.2- Schematic diagram of transcriptomics database collection by EndoDB**

Endothelial cell transcriptomics datasets available in the public domain as of 1st June 2018 were identified and collected. The filter 'endothelial OR endothelium' was used to search through ArrayExpress and GEO. Title and abstract screening was performed to identify studies which performed gene expression profiling in endothelial cells. PubMed was screened for single-cell RNA sequencing studies and only those that had sequenced <1,000 ECs were selected. Adapted from Khan *et al.*, 2019.

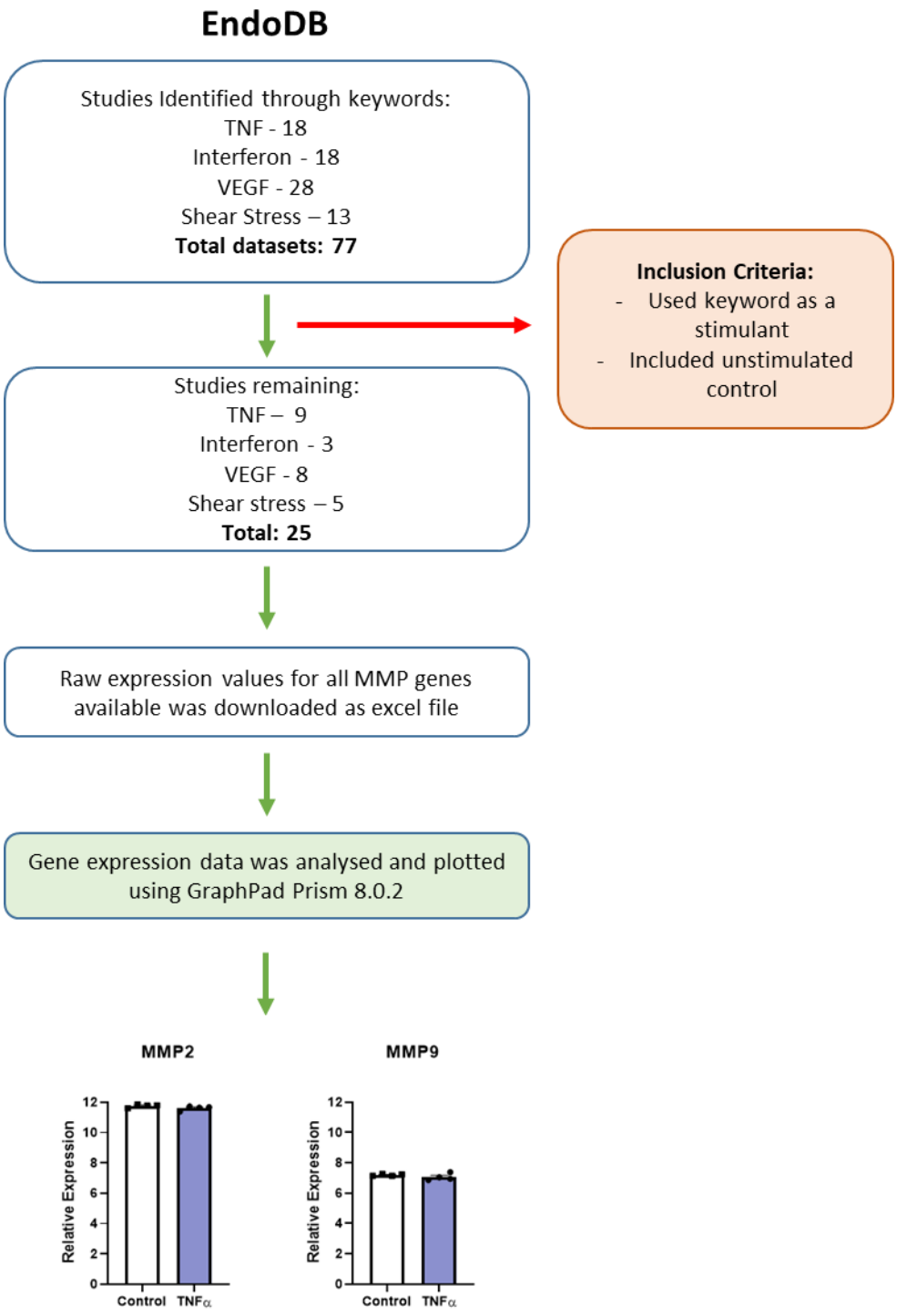


**Figure 3.3 - Schematic diagram of methods for screening EndoDB database**

Bulk datasets on EndoDB were screened for the keywords “TNF”, “interferon”, “VEGF” and “shear stress”. Datasets were excluded from further analysis if they had not used the keyword as a stimulant or did not include an unstimulated control. From the datasets that were selected, the raw expression values for all MMP genes were downloaded and analysed using GraphPad Prism 8.0.2.

Searching for the keywords “TNF”, “Interferon”, “VEGF” and “shear stress” led to 18, 18, 28, 13 results respectively and of these 9, 3, 8 and 5 were selected for further analysis. Overall, there was no significant fold change between unstimulated EC and EC stimulated with TNF, IFN or VEGF (Figure 3.4A-C). Similarly, no significant difference in *MMP-2* or *MMP-9* expression was observed between low and high shear stress (Figure 3.4D). These data suggest gelatinase expression is not regulated at the gene level in response to inflammatory stimuli.

Despite a lack of differences observed when we combined results from all studies, each of these studies utilised different cell types, passage number, serum concentration, concentration of stimulant, and time of treatment. Therefore, we also investigated MMP gene expression between control and stimulated endothelium within each study. Indeed, we did observe significant difference in *MMP-2* and *MMP-9* expression between control and stimulated-EC in individual studies. In one study, HUVECs were stimulated with 10ng/ml TNFα for 8 hours and RNA was extracted every 15 minutes and analysed using an Affymetrix GeneChip Human Genome U133 Plus 2.0 (E-GEOD-9055) (Wada *et al.*, 2009). *MMP-2* gene expression was downregulated after ≈ 4 hours, and *MMP-9* gene expression was upregulated from ≈ 1 hour (Figure 3.5). The endogenous MMP inhibitors, *TIMP1* and *TIMP2*, were also down regulated at the gene level after ≈ 5 hours (E-GEOD-9055) (Figure 3.5). This increase in *MMP-9* was also seen in HUVECs treated with TNF at 1ng/ml for 8 hours (Barker, 2008) (Table 3.1). In this study, there was also an increase in *MMP-10* and *MMP-12* expression after 8 hours (Barker, 2008) (Table 3.1). HUVECs stimulated with 2ng/ml TNF for 5 hours showed no change in *MMP-2* or *MMP-9* gene expression, but did show upregulation of *MMP-10* and downregulation of *MMP-16* (Table 3.1). *MMP-10* was also found to be increased in HUVECs treated with

20ng/ml for 20 hours. *MMP-2* was also found to be decreased in other endothelial cell types following TNF stimulation, including in human mammary epithelial cells and aortic endothelial cells (Table 3.1).

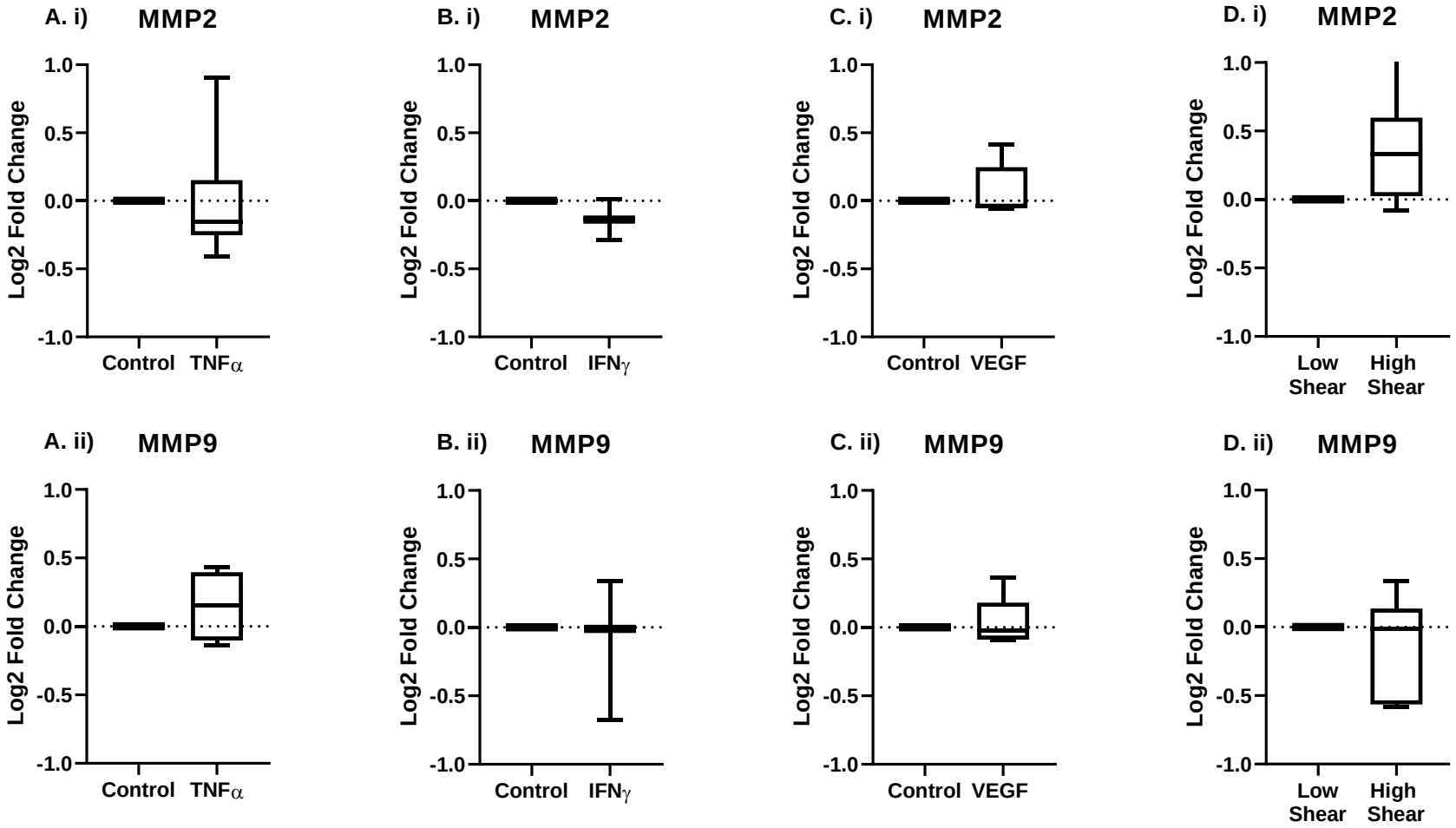


**Figure 3.4– Gene expression of MMP2 and MMP9 from bulk datasets on EndoDB**

*In silico* analysis - Bulk datasets on EndoDB were screened for the keywords “TNF”, “interferon”, “VEGF” and “shear stress”. Datasets were excluded from further analysis if they had not used the keyword as a stimulant or did not include an unstimulated control. From the datasets that were selected, the raw expression values for all MMP genes were downloaded and analysed using GraphPad Prism 8.0.2. Processed expression values from the searches for (A) TNF (n=9), (B) Interferon (n=3), (C) VEGF (n=8), and (D) shear stress (n=5) are shown for (i) MMP-2 and (ii) MMP-9. Data are displayed as mean Log2 fold change ± min and max.

**Table 3.1 – EndoDB results for "TNF" keyword search**

| ID | Cell Type Passage | Serum in Media | TNF concentration | Time of Treatment | Platform | MMP / TIMP Expression |
|---|---|---|---|---|---|---|
| E-GEOD-2638 (Viemann *et al.*, 2006) | HMEC P3-4 | 10% FCS gold | 2ng/ml | 5hr | Affymetrix GeneChip Human Genome HG-U133A | ↑MMP-1, MMP-14 ↓MMP-2 |
| E-GEOD-2639 (Viemann *et al.*, 2006) | HUVEC P3-4 | 2% FBS | 2ng/ml | 5hr | Affymetrix GeneChip Human Genome HG-U133A | ↑MMP-10 ↓MMP-16 |
| E-GEOD-34059 (Hottenrott et al., 2013) | HUVEC | 10% FBS | 50ng/ml (1000IU) | | Affymetrix GeneChip Human Genome U133 Plus 2.0 | No change |
| E-GEOD-35000 (Cheng and Kao, 2012) | HUVEC P<5 | | 20ng/ml | 20hr | Illumina HumanHT-12 V4.0 expression beadchip | ↑MMP-10 |
| E-GEOD-6257 (Johnson *et al.*, 2006) | DLEC | 5% FBS | 1ng/ml | 48hr | Affymetrix GeneChip Human Genome U133 Plus 2.0 | ↑MMP-19 |
| E-GEOD-8166 (Barker *et al.*, 2008) | HUVEC | 10% pooled human serum | 1ng/ml | 3hr / 8hr | Illumina HumanHT-12 V4.0 expression beadchip | ↑MMP-9, MMP-10, MMP-12 |
| E-GEOD-9055 (Wada *et al.*, 2009) | HUVEC | 0.5% FBS | 10ng/ml | 0-8hr | Affymetrix GeneChip Human Genome U133 Plus 2.0 | ↓MMP-2, TIMP1, TIMP2 ↑MMP-9 |
| E-MEXP-3540 | HAEC P4-8 | 1% FCS | 10ng/ml | | Affymetrix GeneChip Human Exon 1.0 ST Array version 1 | ↓MMP-2 ↑MMP-3, MMP-9, MMP-15 |

HMEC: human mammary epithelial cells; HUVEC: human umbilical vein endothelial cells; DLEC: normal dermal lymphatic endothelial cells; N-OD: N-Octanoyl Dopamine; FCS: fetal calf serum; FBS: fetal bovine serum; HC: hydrocortisone; hEGF: human epidermal growth factor; BBE: bovine brain extract

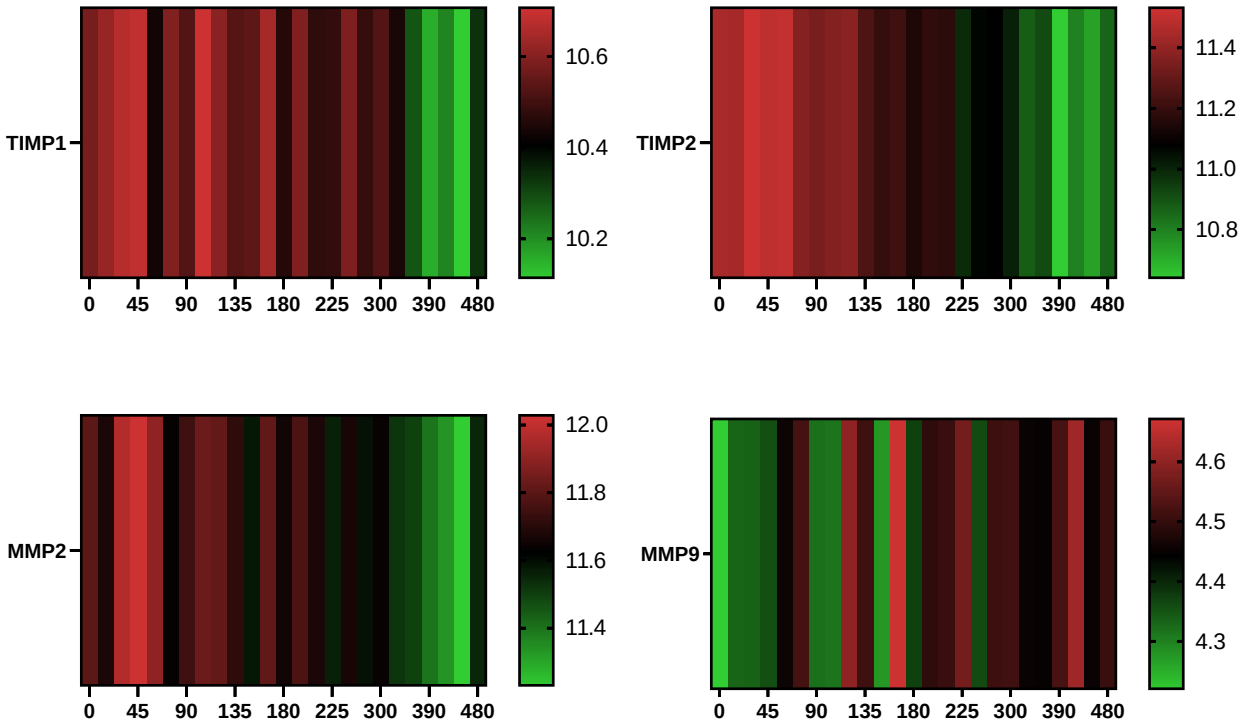


**Figure 3.5 – Gene expression of MMP-2, MMP-9, TIMP1 and TIMP2 over an 8-hour time course**

*In silico* analysis **-** RNA was extracted every 15 minutes from HUVECs treated with TNF 10ng/mL for 8 hours and quantified using an Affymetrix GeneChip Human Genome U133 Plus 2.0. Processed relative expression data for (A) TIMP1 (B) TIMP2 (C) MMP-2 and (D) MMP-9 was collected from assay E-GEOD-9055 and expressed as a heat map. Red signifies high relative expression, green signifies low relative expression. (n=1).

Our search for the keyword “interferon” on bulk datasets on EndoDB led to 18 results, of which only 3 used interferon as a stimulant and were therefore included in our analysis (Table 3.2).

In assay E-GEOD-3920, HUVECs were treated with 1000IU/mL of either IFNα, IFNβ, or IFNγ for 5 hours. Gene expression of *MMP-17* was decreased following IFNα or IFNβ treatment, whilst MMP gene expression remained unchanged following IFNγ treatment (Table 3.2). However, when HUVECs were treated with 100U/mL of IFNγ for 8 hours (E-GEOD-6092), gene expression of both *MMP-9* and *MMP-16* were significantly decreased. Interestingly, when HUVECs were co-stimulated with TNFα (10ng/ml) and IFNγ (10ng/ml) together for 24 hours (E-GEOD-78020) there was upregulation of *MMP-10, MMP-19, MMP-23* and *MMP-25,* and downregulation of *MMP-1, MMP-11, MMP-15, MMP-16* and *MMP-28*. There was no significant change in TIMP expression in any study using IFN (Table 3.2). Overall, IFNγ stimulation lead to significant changes in MMP but not TIMP expression, and more changes were seen when IFNγ was used in conjunction with TNFα.

In order to look for effects of other pro-inflammatory molecules on MMP expression, we also searched through bulk datasets on EndoDB for the keyword “VEGF” (vascular endothelial growth factors), which represents a family of secreted polypeptides that are potent angiogenic factors, as well as acting as pro-inflammatory cytokines. Twenty-eight results were identified from this initial search and from these 7 used VEGF as a stimulant and were selected for our analysis (Table 3.3).

HUVECs stimulated with VEGF have a tendency to increase *MMP-1* gene expression after time points of ≈ 6 hours (*Table 3.3*). Following 4 days of 16ng/ml

VEGF stimulation, HUVECs showed upregulation of *MMP-1* and downregulation of *MMP-2* (Liu *et al.*, 2015). In one study, treating HUVEC with 50ng/ml of VEGF for only 30 minutes was sufficient to upregulate *MMP-9 (Roukens et al., 2010)*, however this increase was not seen at any other time points or concentrations (Table 3). Overall, there was no common trend for changes in *MMP-2* or *MMP-9* gene expression following VEGF stimulation.

**Table 3.2 - EndoDB results for "interferon" keyword search**

| ID | Cell Type and Passage | Serum | IFN concentration | Time of Treatment | Platform | MMP Expression |
|---|---|---|---|---|---|---|
| E-GEOD-3920 (Indraccolo *et al.*, 2007) | HUVEC P4-7 | 20% FCS | IFN-α 1000IU/ml IFN-β 1000IU/ml IFNγ 1000IU/ml | 5hr | Affymetrix GeneChip Human Genome HG-U133A | ↓MMP-17 |
| E-GEOD-6092 (Dame *et al*., 2007) | HUVEC P1 | 20% FBS | IFNγ 100U/mL | 8hr | Affymetrix GeneChip Human Genome U133 Plus 2.0 | ↓MMP-2, MMP-16 |
| E-GEOD-78020 (Patten *et al.*, 2017) | HUVEC | 10% human serum | TNFα 10ng/ml IFN γ 10ng/ml | 24hr | Agilent-039494 SurePrint G3 Human GE v2 8x60K Microarray | ↑MMP-10, MMP-19, MMP-23B, MMP-25 ↓MMP-1, MMP-11, MMP-14, MMP-15, MMP-16, MMP-28, |
| E-GEOD-78020 (Patten *et al.*, 2017) | HSEC | 10% human serum | TNFα 10ng/ml IFN γ 10ng/ml | 24hr | Agilent-039494 SurePrint G3 Human GE v2 8x60K Microarray | ↑MMP-3, MMP-9 |

HUVEC: human umbilical vein endothelial cells; HSEC: human sinusoidal endothelial cells

**Table 3.3 - EndoDB results for "VEGF" keyword search**

| ID | Cell Type | Concentration | Time of Treatment | Platform | MMP Expression |
|---|---|---|---|---|---|
| E-GEOD-10778 | HUVEC | VEGF 100ng | 30, 60, 150, 360 minutes | Affymetrix GeneChip Human Genome HG-U133A | ↑MMP-1, MMP-10 |
| E-GEOD-10778 | HUVEC | EGF 50ng | 30, 60, 150, 360 minutes | Affymetrix GeneChip Human Genome HG-U133A | ↓MMP-14, MMP-16 |
| E-GEOD-15464 (Schweighofer *et al.*, 2009) | | 100ng VEGF-A165 | 30, 60, 150 minutes | Affymetrix GeneChip Human Genome U133 Plus 2.0 | ↓MMP-28 |
| E-GEOD-17777 (Hong *et al.*, 2007) | HMVEC | 100pg/ml | 4hr | Affymetrix GeneChip Human Genome U133 Plus 2.0 | No change |
| E-GEOD-18913 (Suehiro *et al.*, 2010) | HUVEC | | 0hr, 1hr, 4hr | Affymetrix GeneChip Human Genome U133 Plus 2.0 | No change |
| E-GEOD-19098 | HUVEC | 50ng/ml | 18hr | Affymetrix GeneChip Human Genome U133 Plus 2.0 | ↑MMP-1 |
| E-GEOD-19335 | HUVEC | VEGF 50ng/ml | 30 minutes | Illumina HumanHT-12 v3.0 Expression BeadChip | ↑MMP-9 |
| E-GEOD-71216 | HUVEC | 16 ng/mL VEGF | 4 days | RNA-seq | ↑MMP-1<br>↓MMP-2 |

HUVEC: human umbilical vein endothelial cells; HMVEC: human microvascular endothelial cells

Finally, we also explored the effect of shear stress on MMP expression in the endothelium. Vascular shear stress refers to the frictional force that the blood flow exerts on the vessel wall. Shear stress in venous laminar flow ranges from 0.1-0.6 Pa (Wrag*g et al*., 2014) which promotes endothelial cell survival and quiescence. Variation from this normal shear stress level or changing flow direction as found in turbulent flow at sites of vascular divergence, promotes proliferation and apoptosis and can cause endothelial cell dysfunction. Screening bulk endothelial datasets for the keyword “shear stress” led to 13 results and from these 5 were selected for our analysis (Table 3.3).

In both HUVEC and bovine aortic endothelial cells, high shear stress (75 dynes/cm$^2$ and 28.4Pa respectively) over 24 hours lead to a downregulation of gene levels of *MMP-1* and *MMP-11* (Table 3.4) (E-GEOD-23289, E-GEOD-37127*). In vivo,* disturbed blood flow was created by partially ligating the left carotid artery of 6-8 week old male mice, which lead to an increase in *MMP-12, MMP-13* and *MMP-14*, compared to the control non-ligated carotid artery (E-GEOD-56143). In conclusion, changes in shear stress appear to modulate MMP gene expression *in vitro* and *in vivo*.

**Table 3.4 – EndoDB results for "shear stress" keyword search**

| ID | Cell Type | Treatment | Time of Treatment | Platform | MMP Expression |
|---|---|---|---|---|---|
| E-GEOD-13712 (Mun *et al.*, 2009) | HUVEC Passage 4 / Passage 18 | Low shear stress at 12 dyn/cm2 | 24 hours | Affymetrix GeneChip Human Genome U133 Plus 2.0 | ↑MMP-28 young static to young shear<br>↑MMP-19 young static to old static<br>↓ MMP-28 young shear to old shear |
| E-GEOD-1518 (Andersson *et al.*, 2005) | HUVEC | Normal / High pressure (20 / 40mmHg)<br>Low / High shear (<4 / 25 dyn/cm2) | | Affymetrix GeneChip Human Genome HG-U133A | ↓MMP-1, MMP-9, MMP-10, MMP-12<br>↑MMP-2 |
| E-GEOD-23289 (White *et al.,* 2011) | HUVEC | Normal shear (15 dynes/cm2)<br>High shear (75 dynes/cm$^2$) | 24 hours | Illumina HumanRef-8 v2 Expression BeadChip | ↓MMP-1, MMP-11 |
| E-GEOD-37127 (Dolan *et al.,* 2013) | AEC | Uniform shear stress 3.5Pa, high shear stress 28.4Pa | 24 hours | Affymetrix GeneChip Bovine Genome Array | ↓MMP-1, MMP-11 |
| E-GEOD-46248 | HUVEC | Clockwise 15 dynes/cm$^2$<br>30 dynes/cm$^2$ in clockwise or reversed direction for 6 hours | 24 hour pre conditioning<br>6 hour acute increase | Affymetrix GeneChip Human Gene 1.0 ST Array | ↑MMP-3 non reversed, MMP-8 reversed,<br>↑MMP-12 non reversed,<br>↓MMP-26 non reversed |
| E-GEOD-56143 (Dunn *et al.*, 2014) | 6- to 8-week-old male C57Bl/6 mice | partial carotid ligation surgery to induce low and oscillatory blood flow in left carotid artery | | Illumina HumanHT-12 V4.0 expression beadchip | ↑MMP-12, MMP-13, MMP-14 |

HUVEC: human umbilical vein endothelial cells; HMVEC: Human microvascular endothelial cells; AEC: bovine aortic endothelial cells

### *3.2.3. Investigating protease expression in endothelial cell lysates and supernatants*

Through analysing publicly available transcriptomics datasets, we found MMP expression varied significantly with different inflammatory stimuli, thus we wanted to evaluate relative MMP expression in endothelial cells following our own stimulation protocol (24 hours stimulation with 10U/ml TNFα + 10ng/mL IFNγ). We had access to RNA sequencing data from cytokine-stimulated HUVEC our lab previously performed, which we mined to look for expression of all human MMPs (Figure 3.6). *MMP-2*, *MMP-1* and *MMP-14* were flagged as highly expressed relative to other MMPs (Figure 3.6). Therefore, we focussed on these three MMPs, plus our other protease of interest *MMP-9*, for further investigation.

Again, as data from the previous section highlighted how the time of stimulation affects MMP expression, we wanted to investigate how gene expression of these highly expressed MMPs (*MMP-2, MMP-1, MMP-14*) and our protease of interest *MMP-9*, changed over time with cytokine stimulation. As activity of MMPs are tightly regulated by endogenous inhibitors, we also looked at expression of TIMP1. *MMP-1, MMP-14*, and *TIMP1* gene expression didn't change following cytokine stimulation (Figure 3.7). *MMP-2* gene expression was significantly decreased at 16 hours of TNFα + IFNγ stimulation compared to unstimulated control (Figure 3.7B). *MMP-9* gene expression significantly increased following 16 and 24 hours of cytokine stimulation, and then returned back towards baseline levels after 72 hours of stimulation (Figure 3.7E). Of note, *MMP-9* and *MMP-2* transcripts were expressed at relatively low levels compared to MMP-1 (15-fold and 15,000-fold) at both 0 hours and 24 hours following cytokine-stimulation (Figure 3.7F).

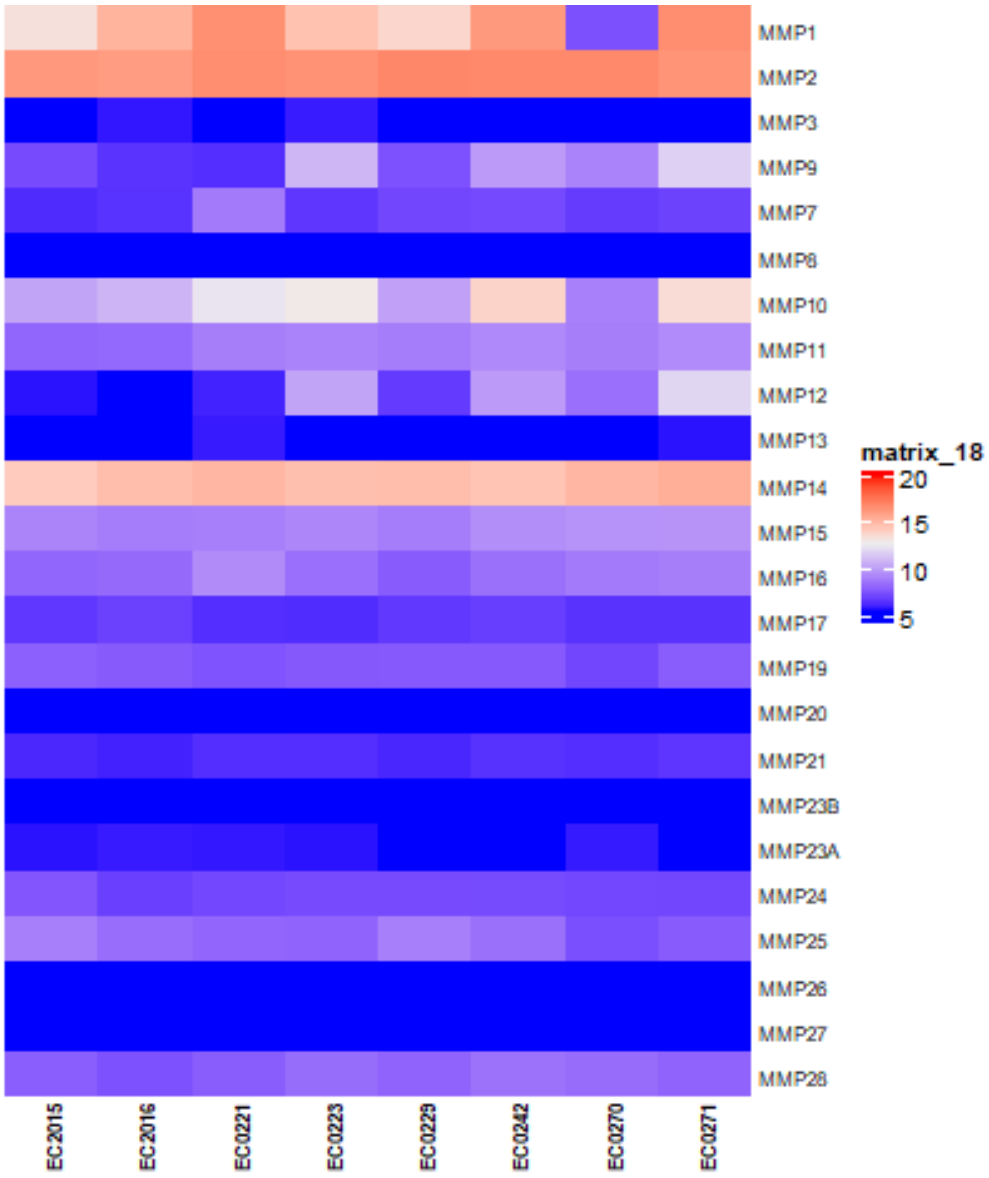


**Figure 3.6 – MMP expression in cytokine-stimulated HUVEC**

HUVEC were simulated with TNFα and IFNγ for 24 hours before being lysed and RNA extracted for RNA seq. Heatmap of the relative expression of human MMPs in cytokine-stimulated HUVEC calculated by variance stabilization transformed data. Read count data were provided by Dr Julia Manning (University of Birmingham) and analysis was performed using the web application iDEP (integrated Differential Expression and Pathway analysis). Individual sample IDs are shown on the X axis (N=8).

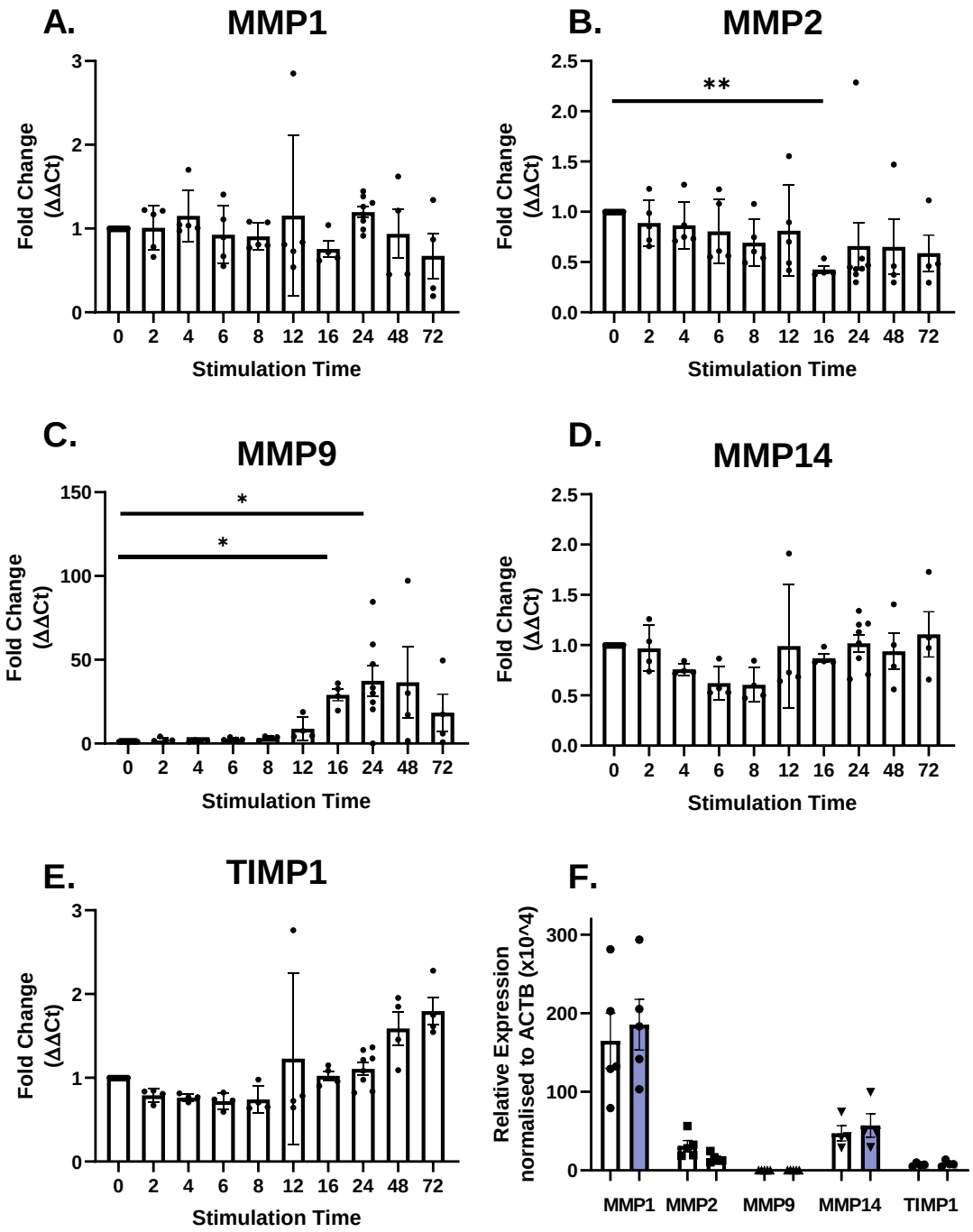


**Figure 3.7 – MMP and TIMP mRNA expression in cytokine-stimulated EC**

HDBEC were stimulated with TNFα + IFNγ for 0-72 hours. RNA isolated from cultures (n=4-8) were analysed by qPCR for expression of (A,F) MMP1, (B,F) MMP2, (C,F) MMP9, (D,F) MMP14 and (E,F) TIMP1 compared to unstimulated controls. Data are mean ± SEM. Data are displayed as (A-E) fold change ($2^{-\Delta\Delta Ct}$) to unstimulated control, or (F) relative expression ($2^{-\Delta\Delta Ct}$) where ΔCt is the relative expression compared to ACTB housekeeping gene. Significance determined by one-way ANOVA, *=P<0.05 by Dunnett's multiple comparison test.

As we saw significant changes in *MMP-2* and *MMP-9* gene expression following cytokine stimulation, we next measured protein expression of MMP-2 and MMP-9 in resting and cytokine-stimulated endothelial cell lysates and supernatants using western blot, gelatin zymography, and ELISA.

We found no significant change in total MMP-2 protein expression between resting and cytokine-stimulated endothelial cells or supernatants using western blot (Figure 3.8B) or ELISA (Figure 3.10A). Gelatin zymography is a technique which allows us to distinguish between the latent zymogen and active forms of the gelatinases. Interestingly, using this method we observed a reduction in pro-MMP-2 (73kDa) and an increase in active-MMP-2 (63kDa) in endothelial cell supernatants following cytokine stimulation (Figure 3.9). This data shows pro-inflammatory stimulation led to activation of pro-MMP-2 into the active form.

Notably, we could not detect MMP-9 expression in endothelial cell lysates using western blot (Figure 3.8C) nor in endothelial cell supernatants using gelatin zymography (Figure 3.9). Using ELISA, MMP-9 protein was increased following TNFα + IFNγ stimulation compared to unstimulated control (Figure 3.10B) although this was at the limits of detection.

To investigate what might be regulating the increase in MMP-2 activation, we looked for expression of the endogenous MMP-2 inhibitors, TIMP1 and TIMP2, in endothelial cell lysates. Expression of both TIMP1 and TIMP2 in endothelial cells was significantly decreased following cytokine-stimulation (Figure 3.11), suggesting MMP-2 may be becoming activated due to a reduction in inhibition from the TIMP proteins.

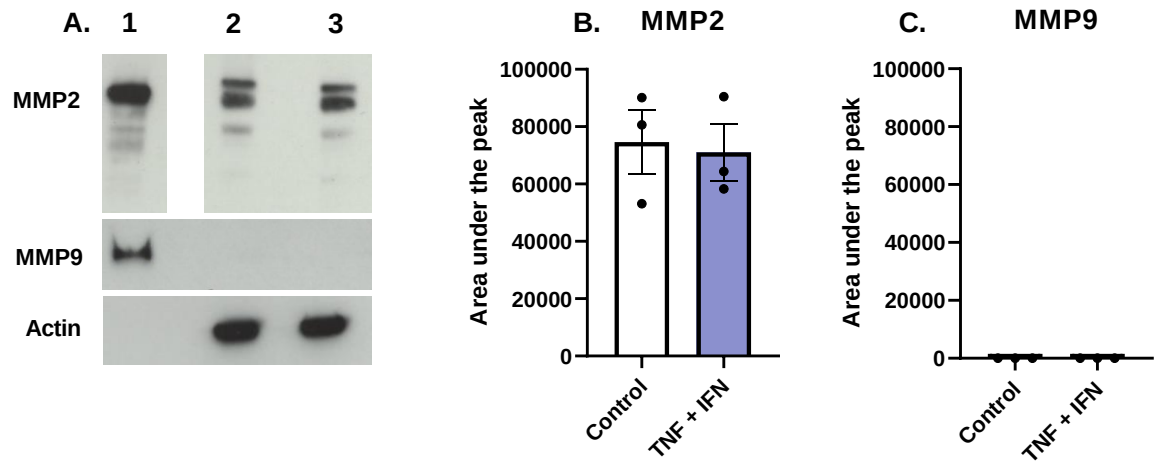


**Figure 3.8 – MMP2 and MMP-9 expression in resting and cytokine-stimulated EC lysates measured by Western Blot.**

Cell lysates were isolated from HDBEC stimulated with and without TNFα + IFNγ for 24 hours and analysed for total (A) MMP-9 and (B) MMP-2 content by western blot (representative of 3 independent experiments). Lanes: 1 = recombinant human MMP standards, 2 = unstimulated HDBEC, 3 = TNF+IFN stimulated HDBEC.

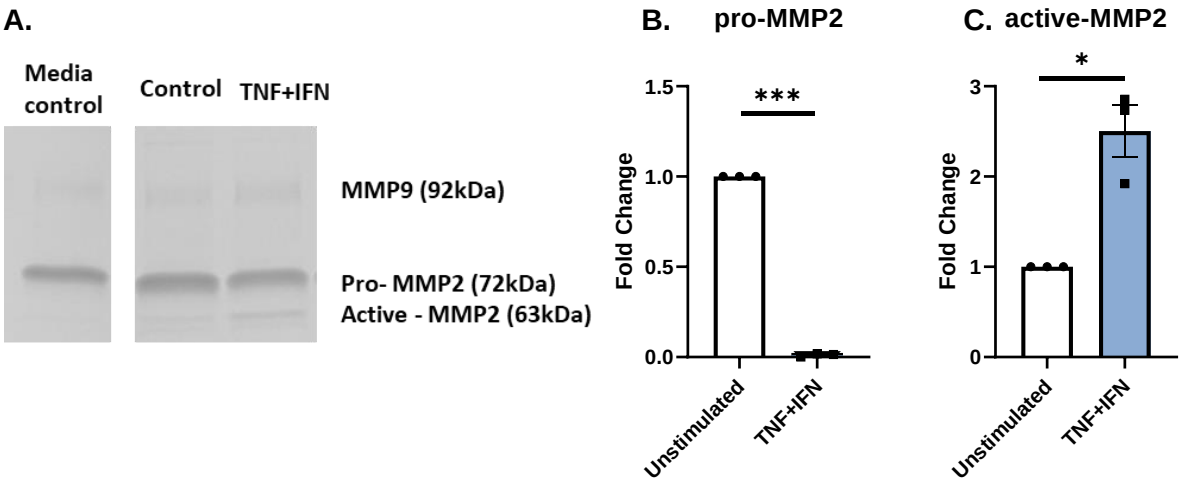


**Figure 3.9 – MMP-2 and MMP-9 expression in resting and cytokine-stimulated EC cell culture supernatants measured by Gelatin Zymography.**

Cell supernatants were collected from HDBEC stimulated with and without TNFα + IFNγ for 24 hours and analysed for pro and active forms of MMP-2 and MMP-9 by gelatin zymography. (A) Representative image of 3 independent experiments. Fold change of (B) pro-MMP2 (72kDa) and (C) active-MMP2 (63kDa) between unstimulated (white bars) and stimulated (blue bars) endothelial cell supernatants. Data are mean ± SEM. * = P≤0.05, and *** = P≤0.001 by paired student's t-test (n=3).

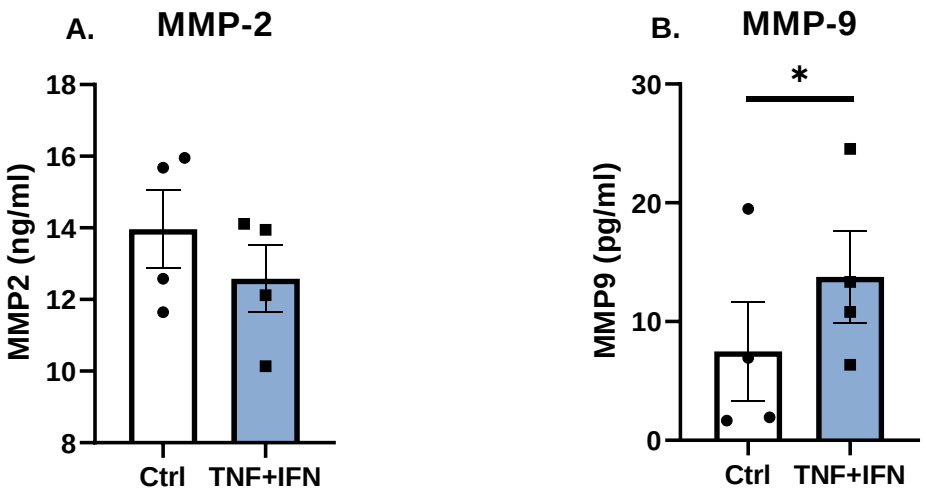


**Figure 3.10 – MMP-2 and MMP-9 expression in resting and cytokine-stimulated EC supernatants measured by ELISA**

Cell culture supernatants were collected from HDBEC that were either left untreated (white bars) or stimulated with TNFα + IFNγ for 24 hours (blue bars). Total (A) MMP-2 and (B) MMP-9 content was measured by ELISA. Data are mean ± SEM., * = P≤0.05 by paired student's t-test (n=4)

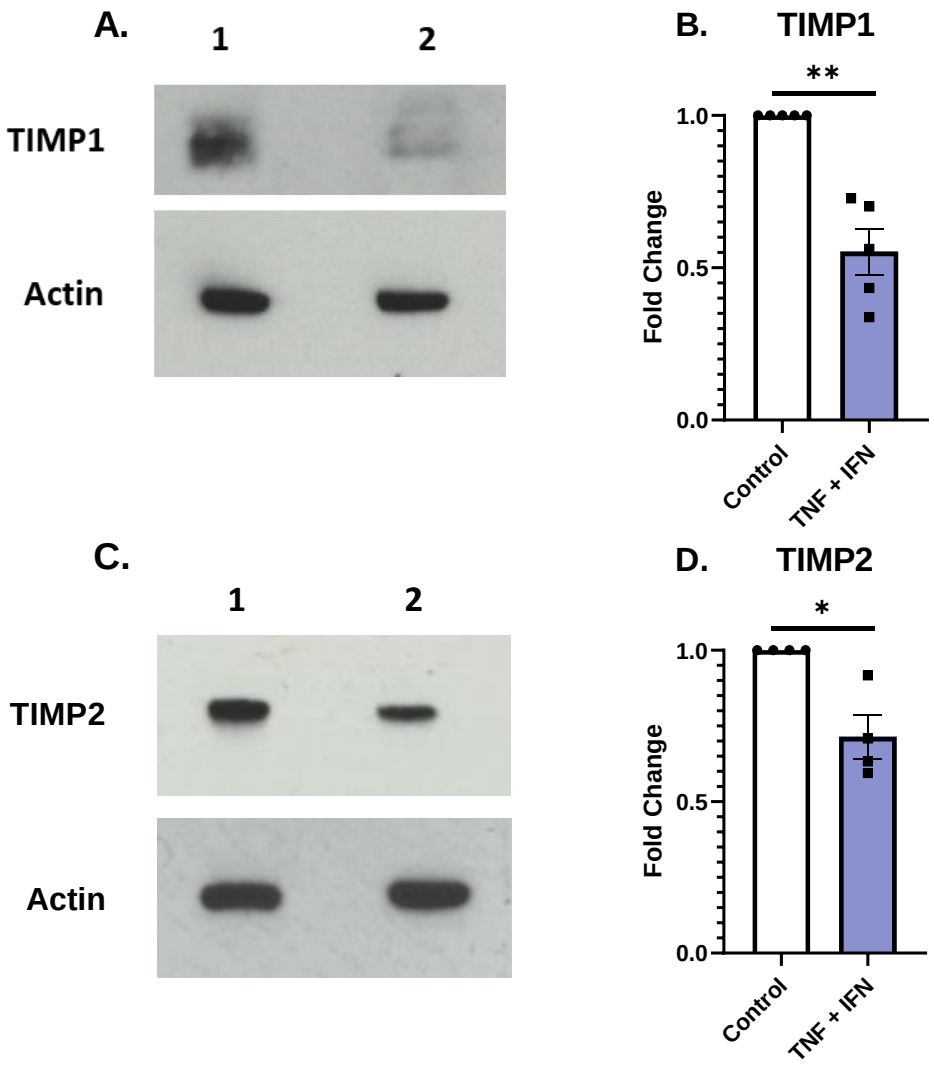


**Figure 3.11 – TIMP1 expression in resting and cytokine-stimulated EC lysates measured by western blot.**

Cell lysates were isolated from HDBEC either unstimulated (white bar) or stimulated with TNFα + IFNγ (blue bar) for 24 hours and analysed for total (A, B) TIMP1 and (C, D) TIMP2 content by western blot. (A, B) Representative image of 4 independent experiments. Fold change of (B) TIMP1 (n=5) and (D) TIMP2 (n=4) expression compared to unstimulated control. Data are mean ± SEM. * = P≤0.05, and ** = P≤0.01 by paired student's t-test (n=3).

### *3.2.4. Investigating protease expression in B cell lysates and supernatants*

We next aimed to identify whether the B-cells could be providing the protease required for 14-3-3ζ cleavage and whether expression of this protease was regulated by adiponectin, the inducer of PEPITEM release. Therefore, we screened unstimulated and adiponectin-stimulated B-cell lysates and supernatants using a protease array that could detect expression of 33 different proteases from one sample (Table 3.5). Leukocyte cones were used for this experiment due to the limiting numbers of B cells we were able to isolate from whole blood donated from healthy volunteers.

MMP-1, -7, -8, -9, -10 and -12, and cathepsin –A, -B, -D, -S, -V, -X/Z/P were expressed in both B cell lysates and supernatants, however there was no significant change in their expression following adiponectin stimulation (Figure 3.12, Figure 3.13). Proteinase-3, ADAM-8 and ADAMTS-13 were identified in B cell lysates, but not supernatants (Figure 3.13). MMP-2 was detected only in supernatants, but not in cell lysates (Figure 3.12). MMP-3, MMP-13, ADAM-9 and ADAM-TS1 were not detected in B cell lysates or supernatants (Figure 3.12, Figure 3.13). No kallikrein proteins, CD10, presenilin-1, proprotein convertase-3, or urokinase were detected in either supernatants or lysates (Figure 3.13).

As these experiments were performed in B cells isolated from leukocyte cones, we next aimed to confirm the results of our protease of interest, MMP-9, in primary B cells isolated from fresh whole blood. We investigated expression of MMP-9 using ELISA in untreated and adiponectin-stimulated B cells. We observed constitutive expression of MMP-9 in B cells (~180pg/mL), which remained unchanged following adiponectin stimulation (Figure 3.14).

**Table 3.5 – Proteases detected by Proteome Profiler Human Protease Array Kit**

| ADAMs | Cathepsins | Kallikreins | MMPs | Other |
|---|---|---|---|---|
| ADAM8 | Cathepsin A | Kallikrein 3/PSA | MMP-1 | Neprilysin/CD10 |
| ADAM9 | Cathepsin B | Kallikrein 5 | MMP-2 | Presenilin-1 |
| ADAMTS1 | Cathepsin C | Kallikrein 6 | MMP-3 | Proprotein Convertase 9 |
| ADAMTS13 | Cathepsin D | Kallikrein 7 | MMP-7 | Proteinase 3 |
| | Cathepsin E | Kallikrein 10 | MMP-8 | uPA/Urokinase |
| | Cathepsin L | Kallikrein 11 | MMP-9 | |
| | Cathepsin S | Kallikrein 13 | MMP-12 | |
| | Cathepsin V | | MMP-13 | |
| | Cathepsin X/Z/P | | | |

ADAM: a disintegrin and metalloproteases; ADAMTS: a disintegrin and metalloproteinase with thrombospondin motifs; MMP: matrix metalloproteinase; uPA; Urokinase-type Plasminogen Activator.

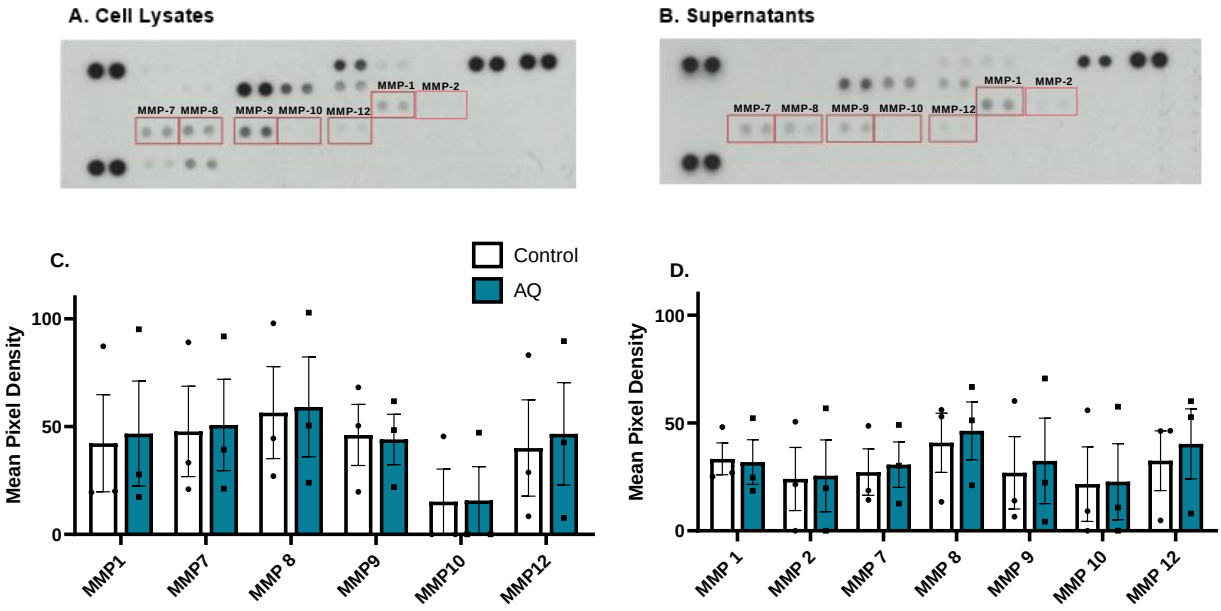


**Figure 3.12 – MMP expression in B-cell supernatants and lysates**

B cells were isolated from leukocyte cones and treated with (blue bars) or without adiponectin (white bars) (AQ; 10 ug/ml) for one hour. Cells were centrifuged and supernatants collected. Cells were lysed. MMP expression in (A, C) 150ug cell lysates and (B, D) supernatants quantified by Proteome Profiler Human Protease Array analysed by densitometry using ImageJ. Data are shown as mean ± SEM for n=3 independent experiments using a different blood donor in each experiment.

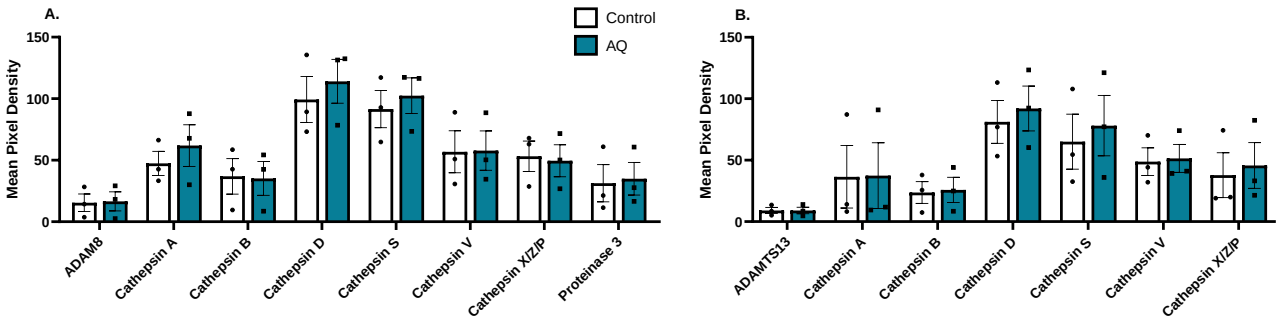


**Figure 3.13 - Protease expression in B-cell supernatants and lysates**

B cells were isolated from leukocyte cones and treated with (blue bars) or without adiponectin (white bars) (AQ; 10 ug/ml) for one hour. Cells were centrifuged and supernatants collected. Cells were lysed. Protease expression in (A) 150ug cell lysates and (B) supernatants quantified by Proteome Profiler Human Protease Array analysed by densitometry using ImageJ. Data are shown as mean ± SEM for n=3 independent experiments using a different blood donor in each experiment.

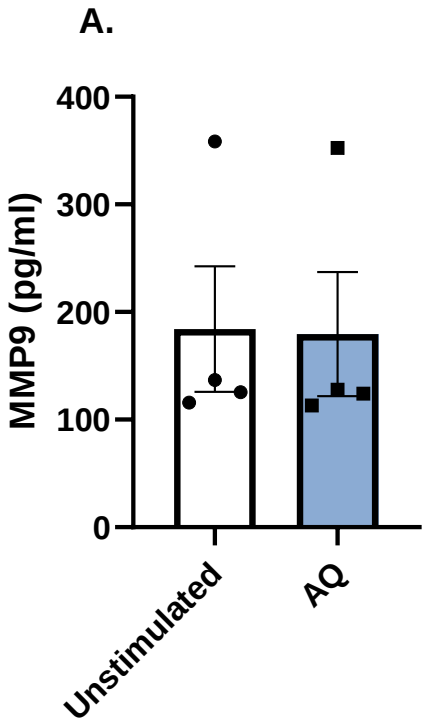


**Figure 3.14 – MMP-9 expression in B-cell supernatants measured by ELISA**

Cell culture supernatants were collected from B cells ($1x10^6$) that were either left untreated (white bars) or stimulated with adiponectin (AQ; 10µg/ml; blue bar) for 1 hour. Cells were pelleted and supernatants collected for ELISA. Total MMP-9 content was measured by ELISA. Data are mean ± SEM, n=4 independent experiments using different blood donors.

## 3.3. Discussion

The molecular mechanisms underpinning PEPITEM processing from 14-3-3ζ remain poorly understood. Here, we have identified a potential role for the proteases MMP-2 and MMP-9 in cleavage of 14-3-3ζ into PEPITEM and identified the cleavage products likely to be produced. Furthermore, little is known about expression of these proteases in endothelial cells. We have shown endothelial cell MMP-9 expression tends to be upregulated and MMP-2 tends to be downregulated following pro-inflammatory stimulation. We have also shown cleavage of MMP-2 from the pro- to the active- form is increased following cytokine stimulation in endothelial cells, in parallel with the reduction in expression of the endogenous inhibitors, TIMP1 and TIMP2. To investigate if B-cells could be the source of these proteases, we investigated expression of several proteases following adiponectin stimulation. We found that MMP-2 and MMP-9 were constitutively secreted by B-cells and this was not affected by adiponectin stimulation. Our data provide novel information on the expression of proteases in endothelium, and highlight a further potential mechanism of regulation of the PEPITEM pathway in the way of regulating protease expression.

### *3.3.1. Products of 14-3-3ζ cleavage*

Here, we identified the proteases MMP-2, MMP-9 and cathepsin-G as potential proteases involved in cleavage of PEPITEM from the parent protein, 14-3-3ζ. *In silico* analysis revealed cleavage by MMP-9 would yield a 17-amino acid sequence, MKSVTEQGAELSNEERN. As the 14-amino acid sequence of PEPITEM was first detected via mass spectrometry, a process that involves protein fragmentation, it is possible the PEPITEM sequence detected was actually part of the larger 17-amino acid sequence cleaved by MMP-9 (Chimen *et al.*, 2015). We also identified potential cleavage sites for cathepsin-G flanking PEPITEM which would result in a 17-amino

acid sequence SVTEQGAELSNEERNLL. Importantly, cathepsin-G also has a cleavage site within the PEPITEM sequence, meaning cleavage from this protease could result in two smaller peptides, SVTEQGAEL and SNEERNLL. However, we have previously shown the broad spectrum MMP inhibitor GM6001 prevents the immuno-modulatory effects of 14-3-3ζ (Apta, 2015). Cathepsin-G activity is not inhibited by GM6001, therefore it is unlikely that cathepsin-G is essential for cleavage of 14-3-3ζ into a functional peptide. Subsequent analysis using the more novel ProCleave software revealed that MMP-2 could cleave 14-3-3ζ directly at the start of the PEPITEM sequence and result in the 15-amino acid sequence, SVTEQGAELSNEERN. MMP-2 also had the highest probability score for cleavage compared to MMP-9 and cathepsin-G. Therefore, using *in silico* analysis we have identified MMP-2 as the most likely candidate for PEPITEM cleavage due to the high cleavage probability score, and would result in the cleavage product most similar to PEPITEM. As this work is all based on computer modelling, future work needs to test the function of MMP-2, MMP-9, and cathepsin-G on cleavage of 14-3-3ζ. This can be done using functional transmigration assays and blockade of specific proteases via genetic silencing or with the use of inhibitors.

### *3.3.2. MMP gene expression in endothelium*

Using publicly available endothelial cell transcriptomic datasets (Khan *et al.*, 2019), we saw a trend for upregulation of gene expression of *MMP-9* and a downregulation of *MMP-2, TIMP1 and TIMP2* following stimulation with TNFα. Notably, when we investigated changes in gene expression in all studies together by comparing the log2 fold change, no significant difference was found. As previously mentioned, each of these studies had different parameters including different EC cell types, passage number, serum concentration, concentration of stimulant, and time of

treatment, which is a significant caveat when trying to compare between transcriptomic datasets.

We validated this data in house using qPCR on blood vascular endothelial cells and we also saw an upregulation of *MMP-9* and downregulation of *MMP-2* following TNFα + IFNγ stimulation. MMP-2 is constitutively expressed in many tissues, whilst MMP-9 tends to be expressed in response to stimuli that induce activity of transcription factors (Morelli *et al.*, 2004). Despite their functional similarities, *MMP-2* and *MMP-9* have very distinct promoter sequences (Yan and Boyd, 2007). The promoter of MMP-9 is more similar to promoters of MMP-1,-3,-7,-10,-12,-13 and -19 in that they contain a TATA box and an AP-1 binding site, making them susceptible to regulation by cytokines and growth factors (Benbow and Brinckerhoff, 1997). MMP-9 also contains a NF-κB binding site in its promoter, which renders MMP-9 responsive to TNFα (Bond et al., 2001). MMP-2 on the other hand, likewise MMP-14 and -28, do not harbour a TATA box and therefore, transcription can start at multiple sites in the promoter sequence (Yoshizaki et al., 1998). Expression of MMP-2 is determined by the Sp-1 family of transcription factors, which are ubiquitously expressed across human cells (Briggs *et al.*, 1986; O'Connor, Gilmour and Bonifer, 2016), leading to the generally constitutive activity of MMP-2 across multiple tissues (Chakraborti et al., 2003). Indeed, both the mined data from EndoDB datasets and our in house data identified much higher expression of MMP-2 in unstimulated endothelial cells compared to MMP-9, which was expressed at very low levels.

### *3.3.3. Regulation of MMP-2 via TIMP1/2*

MMP activity is very tightly regulated at not only the level of production, but also post-translationally through activation of latent zymogens and regulation by inhibitors (Löffek, Schilling and Franzke, 2011). Following cytokine-stimulation, we observed a

reduction in expression of the endogenous MMP inhibitors, TIMP1 and TIMP2. Alongside this, we also observed an increase in active-MMP-2 and a reduction in pro-MMP-2 in endothelial cell secretome. TIMPs act as broad spectrum MMP inhibitors however TIMP1 and TIMP2 have highest affinities for MMP-9 and MMP-2 respectively (Costanzo et al, 2022). Our data suggest a novel method of regulation of PEPITEM production as TNFα/IFNγ stimulation leads to a reduction in TIMP1 and TIMP2 expression, which removes the inhibition on MMP2 activation.

Importantly, TIMP2 can also facilitate activation of MMP-2 through its interaction with MT1-MMP (MMP14) (Itoh and Nagase, 1995). In turn, activated MMP-2 can activate pro-MMP-9 (Tjahajawati *et al.*, 2020). MT1-MMP was expressed in non-malignant monkey kidney epithelial BS-C-1 cells and incubated with and without TIMP2 and pro-MMP-2 (Tjahajawati *et al.*, 2020). Gelatin zymography of supernatant revealed presence of TIMP2 was required for activation of pro-MMP-2, and both TIMP2 and MMP-2 were required for activation of MMP-9. Increasing concentrations of TIMP2 led to increased activation of MMP-2 and MMP-9 in a dose dependent manner up to 10nM, however addition of 50nM of TIMP2 or TIMP1 were inhibitory for activation of either protease (Tjahajawati *et al.*, 2020). At high levels, TIMP2 saturates the MT1-MMP molecules and leaves none available to cleave and activate MMP-2. Our results show cytokine-stimulation reduced endothelial cell expression of TIMP1 and TIMP2, and increased MMP-2 activation. This suggests that even with the downregulation, there was still enough TIMP2 present to facilitate MMP2 activation. To confirm if our results are in line with the previous data, TIMP2 expression should be measured using fully-quantitative methods. Furthermore, to confirm if our increase in MMP-2 activation is due to decreased TIMP2, future

experiments should be performed to investigate levels of MMP-2 activation in the presence of an MT-MMP inhibitor.

### *3.3.4. Controversy of MMP9 expression in endothelial cells*

Whether MMP-9 protein is found in unstimulated endothelial cells is controversial. Some studies report MMP9+ vesicles present in microvascular ECs (Nguyen, Arkell and Jackson, 1998; Taraboletti et al., 2002) however several studies have been unable to detect any MMP-9 expression in unstimulated ECs (Wang et al., 2006; Kargozaran et al., 2007). In some cases, MMP-9 protein expression was restricted to very early-passage (P0-1) cells (Arkell and Jackson, 2003). In this study, MMP-9 was secreted by P0 HUVEC, however by P2 there was no detectable MMP-9 under unstimulated conditions (Arkell and Jackson, 2003). In agreement with this, we could not detect MMP-9 in the cell lysates of HDBEC at passage 5.

MMP-9 has also previously been identified in large vesicles released from HUVEC following incubation with high serum media, however this was serum-dependent and MMP-9 could not be detected at lower serum concentrations (0% or 2.5%) (Taraboletti et al., 2002). FBS also contains vast amounts of vesicles and these findings have not been validated in studies using vesicle-depleted FBS. In our experiments, HDBEC are grown in low serum (2%) media which may contribute to the difference in MMP-9 expression detected.

Despite not detecting MMP-9 protein in endothelial cell lysates, we did detect MMP-9 in cultured cell media via ELISA and observed that it was significantly increased following cytokine-stimulation. Despite this, we could only detect MMP-9 at very low levels (1-25 pg/ml) which is at the limits of detection using ELISA. The fact we could only detect MMP-9 in the secretome but not in the lysates supports the literature that MMPs are produced in the cell as a latent zymogen that is rapidly

secreted and activated once in the extracellular environment (Rosenblum et al., 2007). In contrast, we could not detect differences between MMP-9 in the endothelium secretome compared to the media only control via gelatin zymography. The lowest sensitivity for gelatin zymography is ≈ 10pg/ml hence may not be sensitive enough to detect these changes (Kleiner and Stetlerstevenson, 1994; Snoek-van Beurden and Von Den Hoff, 2005). Overall, our results show MMP-9 transcription and secretion are increased following cytokine-stimulation in HDBEC, which may provide a novel mechanism of regulation of PEPITEM production.

### *3.3.5. Regulation of MMP expression and the PEPITEM pathway*

In the context of PEPITEM, these changes in MMP-2 and MMP-9 may have significant functional effects. Endothelial MMP-9 expression levels and MMP-2 activity are significantly increased after 24 hours of cytokine-stimulation. When investigating PEPITEM function using *in vitro* transmigration assays, endothelial cells are cytokine-stimulated for 24 hours to allow for upregulation of adhesion receptors required to facilitate lymphocyte transmigration, which allows these assays to mimic the initial stages of leukocyte recruitment (Munir, Rainger, *et al.*, 2015). Therefore, all experiments on PEPITEM function have been performed when endothelial MMP-9 and active MMP-2 is most abundant, potentially contributing towards PEPITEM cleavage. Under inflammatory conditions *in vivo*, increased MMP-9 expression and MMP-2 activity after 24 hours may be a further way to limit chronic inflammation by increasing the amount of PEPITEM produced 24 hours after an inflammatory stimulus, mediating resolution of inflammation.

### *3.3.6. Protease expression in B-cells*

Using a protease array, we detected constitutive expression of several MMPs and cathepsin proteases in B-cells that were not changed following adiponectin

treatment. Previously, primary human PBMC-derived B-cells cultured for 8 hours were found to be particularly enriched for MMP-11 and had high RNA expression of MMP -2, -7, -14 and -17 (Bar-O*r et al*., 2003). B-cells were also shown to have significant expression of MMP-9, however expression was much higher in monocytes (Bar-O*r et al*., 2003). Our protease array only looked at a subset of MMP proteins and did not include MMP-11, -14 or -7, however there was no significant variation between the MMPs it could detect. Due to the roles MMPs play in tumor progression and invasion, much of the literature surrounding MMP expression in B-cells is from a cancer context. For example, it has also been shown B-cell chronic lymphocytic leukaemia cells (B-CLL) upregulate MMP-9 in response to binding TNFα-activated HUVECs mediated by α4β1 integrin and PI3K-Akt, which facilitates B-CLL transendothelial migration and invasion (Redondo-Muñ Oz *et al.*, 2006).

Interestingly, we detected MMP-9 in both B-cell lysates and supernatants, whilst MMP-2 was only detected in the supernatants suggesting there is rapid secretion of this protease from the B-cell. Notably, these array experiments were performed on primary B-cells isolated from leukocyte reduction system (LRS) cones due to our inability to extract sufficient protein content from 100ml of peripheral blood purified B-cells. T-cells isolated from LRS cones have been found to have subtle functional differences compared to buffy coats, including an increase of surface CD44, higher cytokine production, and increased IFNγ production variability between donors (Tremblay and Houtman, 2014), which may be the case for B-cells too. To overcome this limitation, we validated MMP-9 expression in primary B-cells derived from buffy coats using ELISA and found similar results to the protease array using LRS cones. In the context of the PEPITEM pathway, there are many cell types present at the site of T cell extravasation. Both *in vivo* and *in vitro,* there are

circulating lymphocytes and endothelial cells and any of these could be the cellular origin of the protease(s) responsible for cleaving 14-3-3ζ.

### *3.3.7. Limitations*

Whilst this data provides novel information about potential methods of cleavage and regulation of PEPITEM from 14-3-3ζ, there are limitations. Most significantly, the sample sizes from the EndoDB datasets are relatively small (n=2-3) and validation of these findings would be required. Importantly, the protease prediction servers Prosper and ProCleave used for the initial *in silico* screening of cleavage sites within the 14-3-3ζ sequence is based on computer modelling and future work needs to be test the function of MMP-2, MMP-9 and cathepsin-G before we can conclusively suggest which protease(s) are involved in 14-3-3ζ cleavage. It is also worth noting that a limitation of experiments when investigating gelatinase expression in cell secretomes is that both MMP-2 and MMP-9 are present in the serum added to cell culture media. To overcome this issue, we used media controls to confirm there was no cross reactivity between our ELISA kits and the bovine serum used in cell culture, however gelatin zymography cannot differentiate between human-bovine gelatinases. We were unable to culture the endothelium in serum-free media as stimulation with TNFα would result in cell death, therefore for these experiments we had to set the media control as a background measurement. As our endothelium were grown in low-serum media (2%), there was very little background signal from the media.

## 3.4. Conclusions

Taken together, we identify MMP-2 as our most likely candidate for cleavage of 14-3-3ζ into PEPITEM due to 1) MMP-2 having the highest cleavage probability score, 2) the resulting peptide very strongly resembling PEPITEM and 3) having high

expression in endothelial cells and secretion from B-cells. We have also identified a novel mechanism of PEPITEM regulation under inflammatory conditions, in the form of protease regulation. Inflammation triggers upregulation of endothelial MMP-9 expression, and downregulation of the endogenous MMP inhibitors TIMP1 and TIMP2. Concomitantly, we have shown an increase in cleavage of MMP-2 from the pro- to the active- form. Finally, we have shown B-cells can also contribute to the extracellular MMP-2 or MMP-9 likely to be involved in PEPITEM processing. It is yet to be determined the exact cell type of origin for MMP-2 / MMP-9 in *in vitro* PEPITEM cleavage, and functional assays are required to identify which of these proteases is involved in cleavage of 14-3-3ζ.

# Chapter 4. INVESTIGATING PEPITEM

## CLEAVAGE FROM 14-3-3ζ

## 4.1. Introduction

In the previous chapter, we identified potential cleavage sites for MMP-2, MMP-9 and cathepsin-G within the 14-3-3ζ sequence using computer modelling. Although a useful tool, this could not conclusively reveal if these proteases would cleave PEPITEM physiologically. Here, we investigated the functional roles of MMP-2, MMP-9 and cathepsin-G in PEPITEM cleavage using a well-established *in vitro* static adhesion assay and genetic silencing of proteases in the endothelium. (McGettrick *et al.*, 2009; Chimen *et al.*, 2015; Munir *et al.*, 2015).

B-cell research requires multiple blood donors and time-consuming B-cell isolation preparation, therefore we also investigated the use of the Raji B-cell line and evaluate their use as a model for primary B-cells in the PEPITEM pathway. This would allow us to develop a more high-throughput assay and allow future gene silencing work that is not possible on primary B-cells.

## 4.2. Results

### *4.2.1. Establishing optimal conditions for lymphocyte adhesion and transmigration across endothelium*

To determine reproducibility of lymphocyte recruitment and transmigration across cytokine-stimulated HDBEC, peripheral blood lymphocytes (PBL) from healthy donors were treated with adiponectin (AQ; 10 µg/ml) or PEPITEM (20 ng/ml) and incubated with cytokine-stimulated HDBEC for 10, 15, and 20 minutes. We observed no difference in PBL adhesion across any of the time points (Figure A,B). We observed a ~40% and 55% reduction in lymphocyte migration when PBL were treated with adiponectin compared to untreated (control) PBL at 15 and 20 minutes respectively (Figure 4.1A,C). PEPITEM treatment significantly reduced migration

(~45%) compared to control PBL only at the 20 minute time point (Figure 4.1A,C). Thus the 20 minute incubation period was used for all future static transmigration assay experiments.

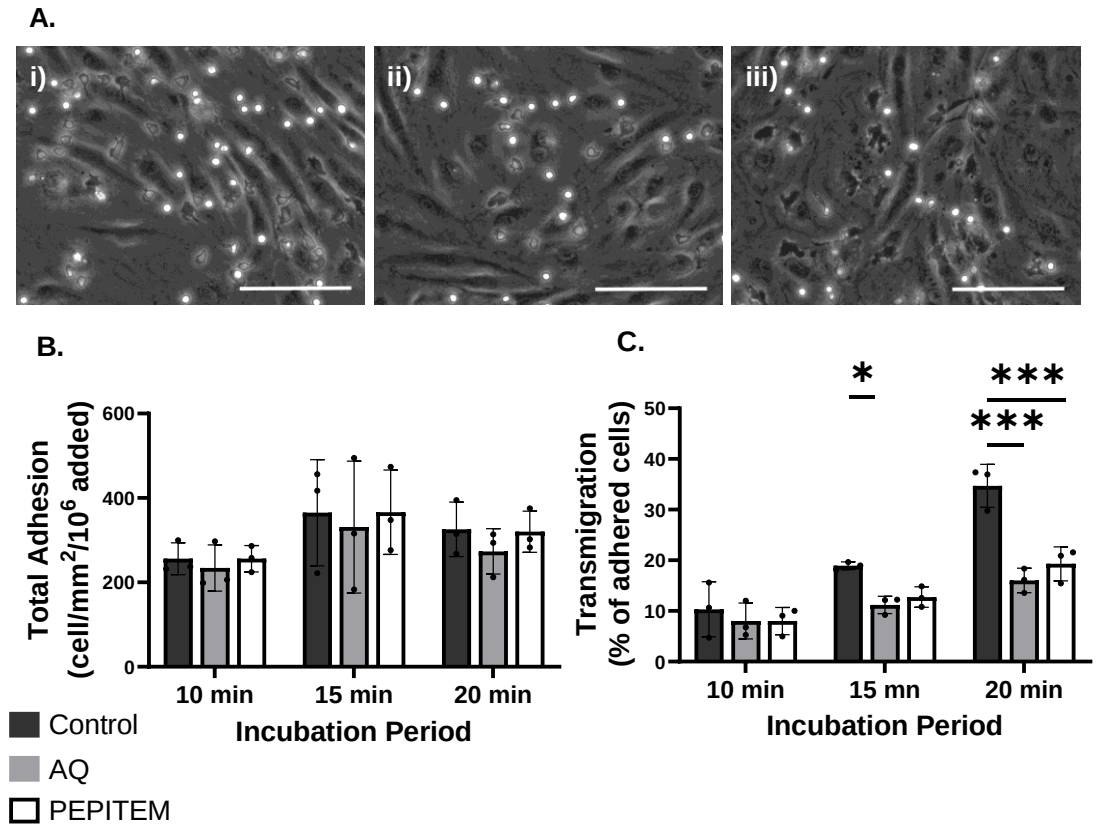


**Figure 4.1- Effect of incubation period of lymphocyte adhesion and migration**

HDBEC were simulated with TNFα and IFNγ for 24 hours. PBL were left untreated (control, grey bars), treated with adiponectin (AQ; 10µg/ml, light grey bars) for 1 hour or PEPITEM (20ng/ml, white bars) immediately before use. HDBEC were washed and incubated with 1x $10^6$ PBL prior to fixing and imaging. (A) Representative image taken following (i) 10 (ii) 15 and (iii) 20 minutes of PBL incubation. (B) The number of adherent PBL at each time point expressed as the number of cells/$mm^2$/$10^6$ cells added. (C) Lymphocyte transmigration at each time point expressed as the percentage of adherent cells that had transmigrated. ANOVA showed significant effect of treatment ($p<0.0001$) on lymphocyte transmigration. Data are shown as mean ± SEM, for n=3 independent experiments using a different blood donor in each experiment. * = P≤0.05, ** = P≤0.01, and *** = P≤0.001 compared to untreated control at respective times by Dunnett's multiple comparisons post-test. Scale bar = 100 μm.

### *4.2.2. Characterising Raji B-cells and assessing their use as a model for the PEPITEM pathway*

Experiments using primary B-cells require multiple blood donors and time-consuming PBL isolation. Another limitation is that B-cell numbers are lower than other leukocyte subpopulations within the blood (5-10% of total PBMC) (Kleiveland, 2015), meaning vast amounts of blood are required for B-cell isolation. Identifying a B-cell line that produces PEPITEM in response to adiponectin and can therefore act as a model system would overcome these limitations. Importantly, a B-cell line model would also allow for future gene silencing experiments, which would be impossible to accomplish in primary lymphocytes. Raji cells are a human B-lymphoblastic cell line derived almost 60 years ago from a patient with Burkitt's lymphoma (Karpova et al., 2004). This cell line is positive for the Epstein-Barr Virus (EBV), however no viral DNA synthesis occurs. Raji cells are a well-established immortalised B-cell line and have been used in many B-cell lymphoma studies (Dallegri et al., 1984; Karpova et al., 2004; Czuczman et al., 2008). To investigate their suitability as a model in the PEPITEM pathway, we characterised their expression of adiponectin receptors

As previously published, approximately 80% of blood B-cells (CD19+ PBMC) expressed the adiponectin receptors 1 and 2 (Figure 4.2A-B). This result was similar for AR2 expression on Raji cells, however, a significantly larger proportion of the Raji cells (~90%) expressed AR1 (Figure 4.2A-B). Moreover, whilst no significant differences were observed in the MFI values for either receptors between B-cells and Raji cells, there tended to be greater MFI values detected on both cell types for AR1 compared to than AR2 (Figure 4.2C-D). This expression pattern did not correlate with passage number (Figure 4.3).

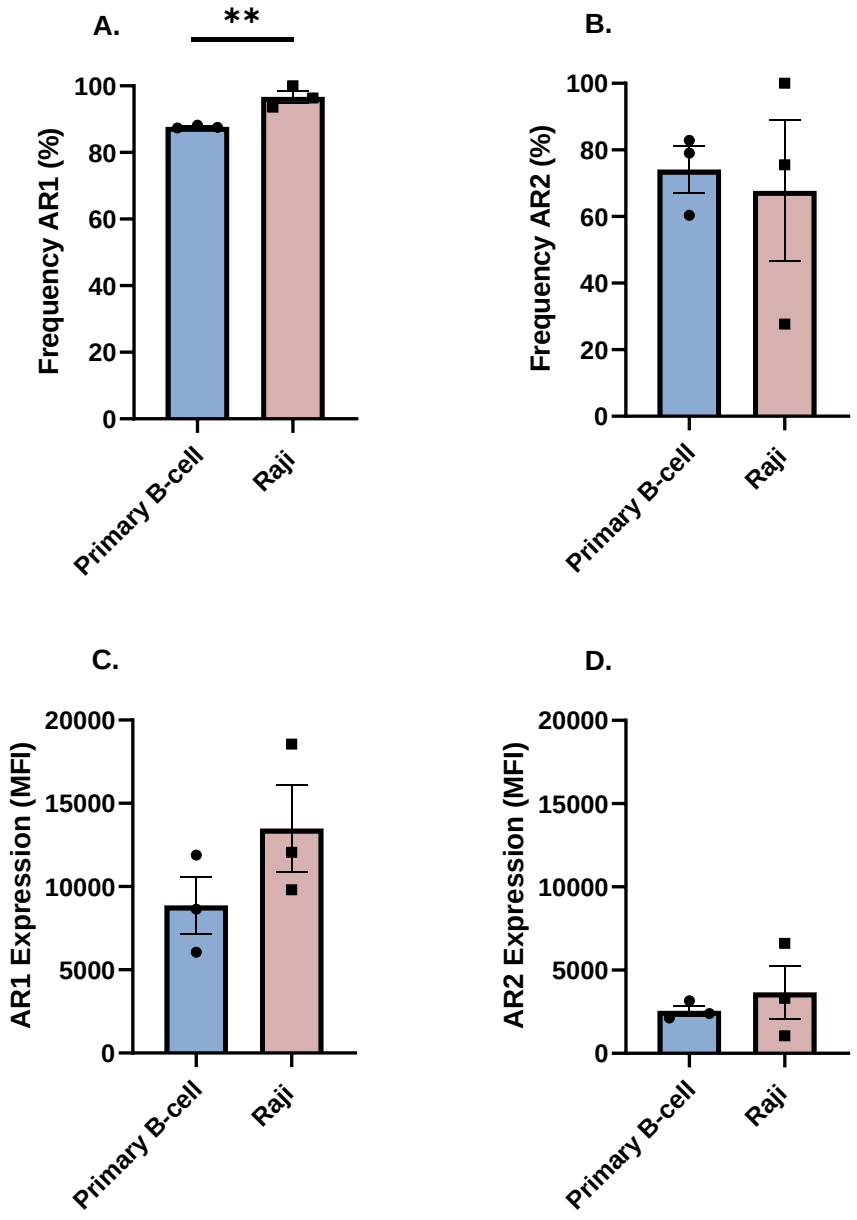


**Figure 4.2- Adiponectin receptor expression in Raji cells and CD19+ PBMC**

Expression of adiponectin receptors 1 (AR1) and 2 (AR2) in Raji B-cells and CD19+ PBMC was quantified using flow cytometry. Frequency of (A) CD19+AR1+ and (B) CD19+AR2+ PBMC and Raji B-cells. Mean Fluorescence Intensity (MFI) of (C) AR1 and (D) AR2 in CD19+ PBMC and CD19+ Raji B-cells. Data are shown as mean ± SEM, n=3 independent experiments for PBMC using a different blood donor in each experiment, and n=9 independent experiments for Raji cells. Normality was confirmed by Shapiro-Wilk test. * = P≤0.05, ** = P≤0.01 using unpaired t-test.

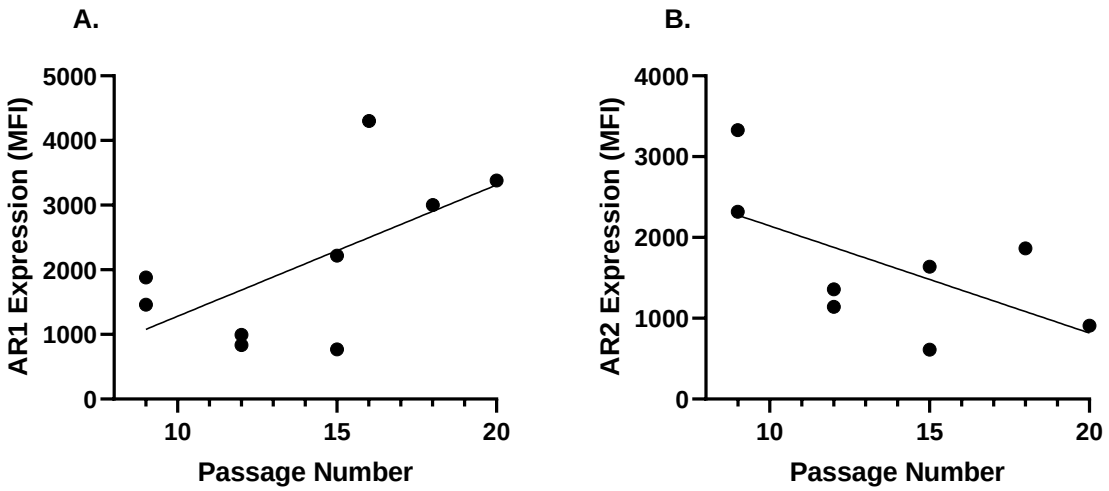


**Figure 4.3 - Adiponectin receptor expression in Raji cells across passages**

Expression of adiponectin receptors in Raji B-cells across several passages was quantified using flow cytometry. Mean Fluorescence Intensity (MFI) of (A) adiponectin receptor 1 (AR1) and (B) adiponectin receptor 2 (AR2) in CD19+ Raji B-cells were plotted against passage number of Raji cells. Data represent mean of n=9 independent experiments with linear regression analysis. The equation of the line was calculated as (A) y = 202.8x - 746.6 and R2 = 0.3861 (B) Y = -132.5x + 3468 and $R^2$ = 0.3710

We next investigated whether adiponectin-treated Raji B-cells were able inhibit PBL transmigration to the same extent as seen with primary B-cells. We have previously shown adiponectin does not reduce PBL transmigration in the absence of B-cells, however inhibition is restored with the addition of B-cells or B-cell supernatants (Chimen *et al.*, 2015). We reproduced this experiment and substituted Raji B-cells instead of primary B-cells to investigate if they can be used as a model for the PEPITEM pathway. Freshly isolated PBL were depleted of B-cells using anti-CD19 microbeads (PBL depleted), leaving an average of 0.15% B cells remaining in the sample (Figure 4.4A). B-cells were negatively selected from PBMC resulting in 98.9% purity (Figure 4.4B). As expected, depleting B-cells from PBL prevented the reduction in PBL transmigration seen with adiponectin compared to control PBL (Figure 4.5B). The addition of negatively sorted B-cells, or B-cell supernatants, back into the depleted PBL pool restored the effect of adiponectin (Figure 4.5). However, when isolated Raji B-cells or Raji B-cell supernatants were added into the B-cell depleted PBL, the effect of adiponectin was not restored (Figure 4.5B). Notably, the addition of Raji B-cells into the depleted PBL pool decreased PBL transmigration compared to the control PBL in the absence of adiponectin, suggesting that Raji cells may constitutively inhibit PBL transmigration (Figure 3.5B). These data suggests Raji cells do not secrete PEPITEM in response to adiponectin stimulation and therefore cannot be used as a suitable model for B-cells in PEPITEM research. For future B-cell experiments, primary B-cells are used.

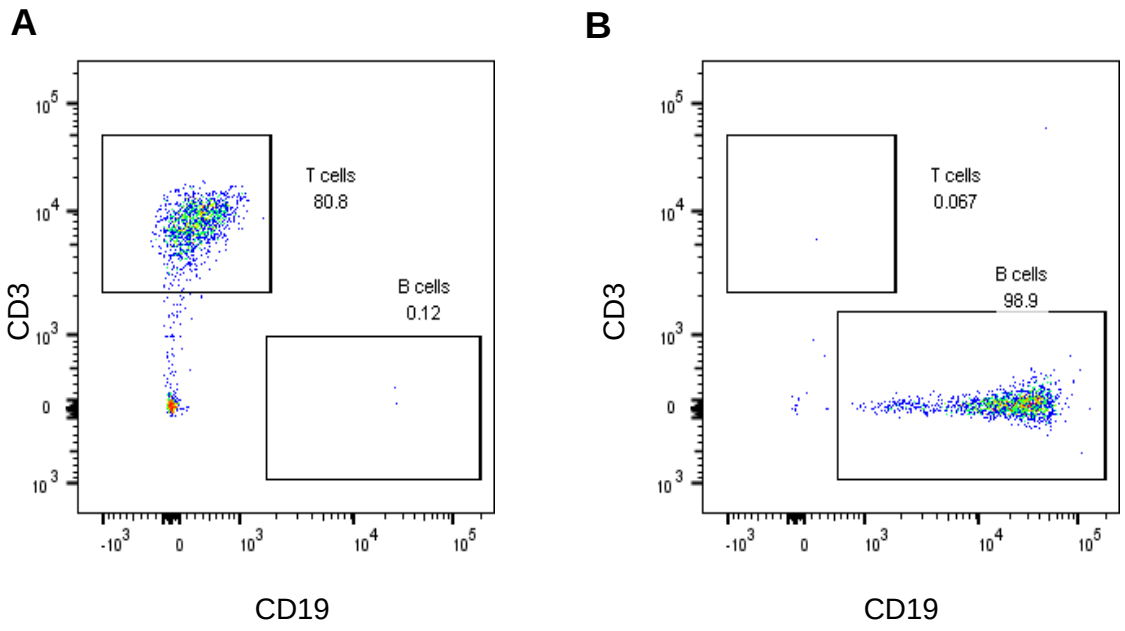


**Figure 4.4 – Representative dot plots of B cell depletion and B cell selection**

PMBC were isolated from peripheral blood from young, healthy donors and B-cells were (A) depleted using negative selection or (B) isolated using an enrichment kit. Flow cytometry data depicting the purity of samples is shown following gating on live cells. Representative plots depicting frequency of CD3+CD19- T cells and CD3-CD19+ B-cells.

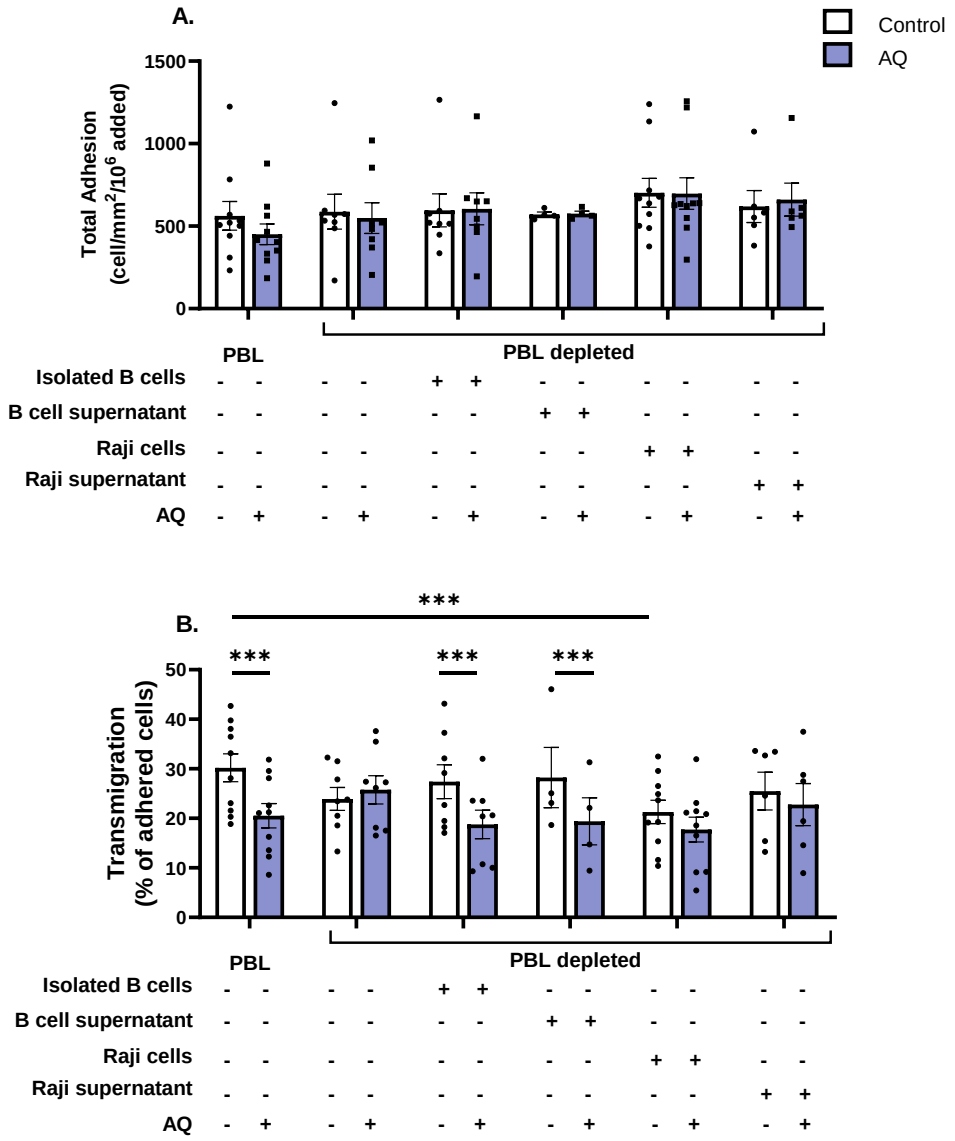


**Figure 4.5 - Effect of adiponectin-stimulated Raji cells on PBL transmigration**

HDBEC were stimulated with TNFa and IFNy for 24 hours. PBL and Raji cells were treated with (blue bars) or without (white bars) adiponectin for one hour prior to assay. HDBEC were washed and incubated with 1x $10^6$ PBL for 20 minutes at 37°C, 5% CO2. Images of 8 random fields were acquired and analysed offline. (A) The number of adherent PBLs expressed as the number of cells/$mm^2$/$10^6$ cells added. (B) Lymphocyte transmigration expressed as the percentage of adherent cells that had transmigrated. ANOVA showed significant effect of B-cell and adiponectin treatment on lymphocyte transmigration, $p<0.0001$. Data are shown as mean ± SEM, for n=8 independent experiments using a different blood donor in each experiment. Normality was confirmed by Shapiro-Wilk test. * = P≤0.05 compared to untreated PBL control by Dunnett's multiple comparisons post-test.

### *4.2.3. Investigating proteases involved in cleavage of PEPITEM from 14-3-3ζ using static migration assays*

To investigate proteases involved in the cleavage of PEPITEM from 14-3-3ζ, we incubated PBL with or without adiponectin in the presence of broad-spectrum matrix metalloproteinase (MMP) inhibitors GM6001, marimastat, or the endogenous inhibitors TIMP1 or TIMP2 for one hour prior to the *in vitro* static transmigration assay. There was no difference in PBL adhesion with adiponectin or following protease inhibitor treatment (Figure 4.6A). We observed a significant reduction in lymphocyte transmigration (~40%) when PBL were treated with adiponectin alone, or when treated with adiponectin in the presence of the DMSO or ethanol vehicle controls (Figure 4.6B). However, there was no reduction in lymphocyte transmigration following adiponectin treatment in combination with any of the broad-spectrum protease inhibitors tested (Figure 4.6B). These data suggested cleavage by MMPs is required for PEPITEM to be produced from 14-3-3ζ, however as there was significant overlap between the inhibitors' targets we next needed to identify which MMP was involved.

In the previous chapter, we used computational analysis to identify potential cleavage sites within the 14-3-3ζ sequence. Cathepsin-G, MMP-2 and MMP-9 were identified as proteases of interest as they had potential cleavage sites flanking PEPITEM. Thus, we decided to use specific inhibitors against each of these proteases in the static adhesion assay to identify if they are involved in the cleavage of 14-3-3ζ into PEPITEM. We incubated PBL with or without adiponectin in the presence of cathepsin G inhibitor (600nM), MMP-9 inhibitor (50nM), or MMP-2 inhibitor (17μM) one hour prior to the in vitro static transmigration assay. There was no difference in PBL adhesion with adiponectin or inhibitor treatment (Figure

4.7A,C). We observed a significant reduction in lymphocyte transmigration (~40%) when PBL were treated with adiponectin alone, or with adiponectin in the presence of the DMSO vehicle control (Figure 4.7B,D). In the presence of a cathepsin G inhibitor, there was significant reduction in PBL transmigration following adiponectin stimulation (Figure 4.7B). This suggests cathepsin-G is not involved in PEPITEM production. However, there was no reduction in PBL transmigration between adiponectin-stimulated and control PBL in the presence of an MMP-9 inhibitor (Figure 4.7B). Taken together, these data suggest MMP-9 is likely to be involved in cleavage of 14-3-3ζ into PEPITEM as blockade of MMP-9 inhibited the actions of adiponectin. Addition of an MMP-2 inhibitor did not inhibit the actions of adiponectin (Figure 4.7D). However, inhibition of MMP-2 led to significantly reduced migration of PBL compared to untreated control (Figure 4.7D). Therefore, MMP-2 plays a role in the transendothelial migration of leukocytes.

**Table 4.1 – List of protease inhibitor targets**

| Protease Inhibitor | Targets | EC50 (nM) |
|---|---|---|
| **GM6001** | MMP-1 | 0.4 |
| | MMP-2 | 0.5 |
| | MMP-3 | 27 |
| | MMP-7 | 3.7 |
| | MMP-8 | 0.1 |
| | MMP-9 | 0.2 |
| | MMP-12 | 3.6 |
| | MMP-14 | 3.4 |
| | MMP-26 | 0.36 |
| **Marimastat** | MMP-1 | 5 |
| | MMP-2 | 6 |
| | MMP-3 | 200 |
| | MMP-7 | 13 |
| | MMP-9 | 3 |
| | MMP-14 | 9 |
| **TIMP1** | All MMPs except transmembrane MMPs (MMP-14, MMP-16, MMP-17, MMP-18, MMP-24, MMP-26) | |
| **TIMP2** | All MMPs | |

MMP: matrix metalloproteinase; TIMP1: tissue inhibitor of metalloproteinase

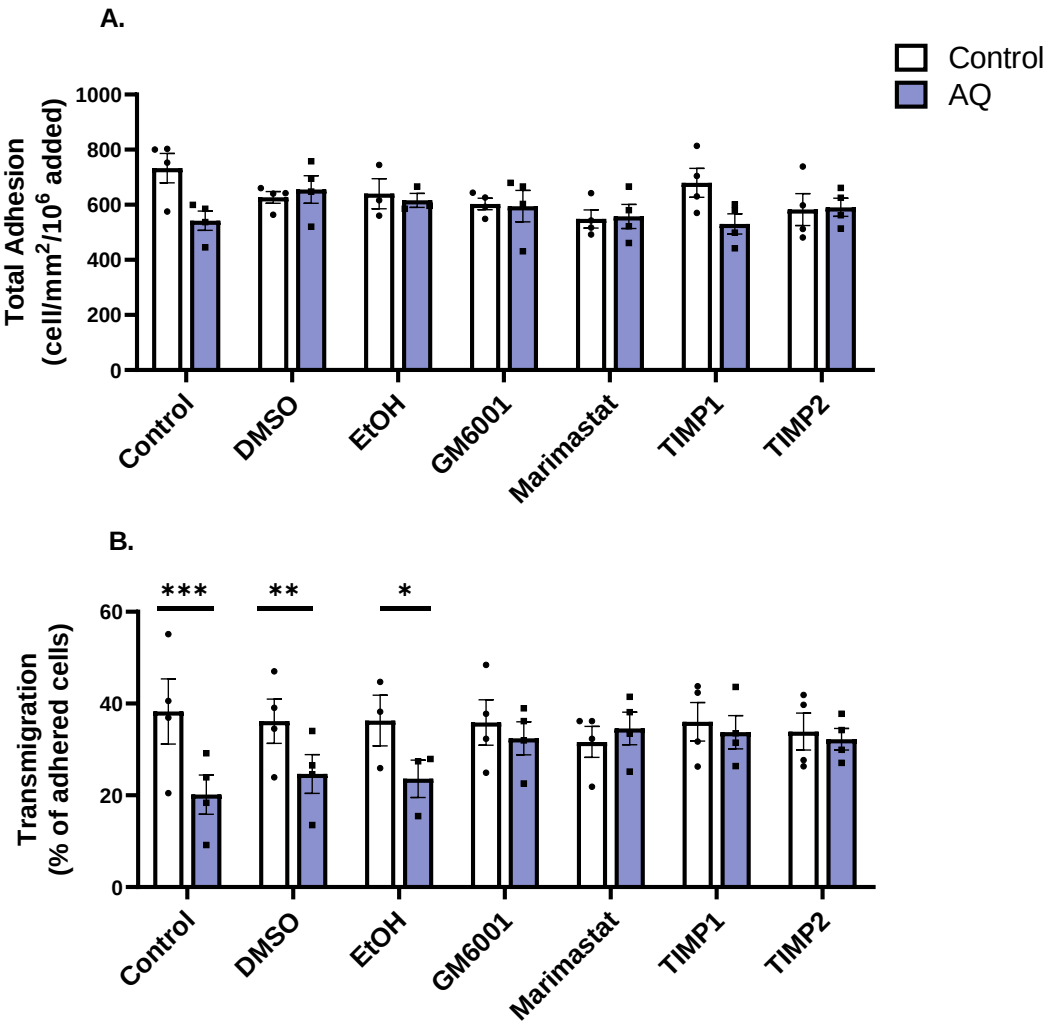


**Figure 4.6 - Effect of broad-spectrum protease inhibitors on PBL adhesion and transmigration**

HDBEC were simulated with TNFα and IFNγ for 24 hours. PBL were treated with (blue bars) or without (white bars) adiponectin for one hour prior to assay. HDBEC were treated with MMP inhibitors for one hour prior to assay. HDBEC were washed and incubated with 1x $10^6$ PBL for 20 minutes at 37°C, 5% CO2 prior to fixing and imaging. Images of 8 random fields were acquired and analysed offline. (A) The number of adherent PBL expressed as the number of cells/mm2/$10^6$ cells added. (B) Lymphocyte transmigration expressed as the percentage of adherent cells that had transmigrated. ANOVA showed significant effect of adiponectin treatment ($p<0.05$), but not inhibitor treatment on lymphocyte transmigration and no effect of either treatments on adhesion. Data are shown as mean ± SEM for n=4 independent experiments using a different blood donor in each experiment. Normality was confirmed by Shapiro-Wilk test. * = P≤0.05, ** = P≤0.01, and *** = P≤0.001 compared to untreated control in each group by Dunnett's multiple comparisons post-test.

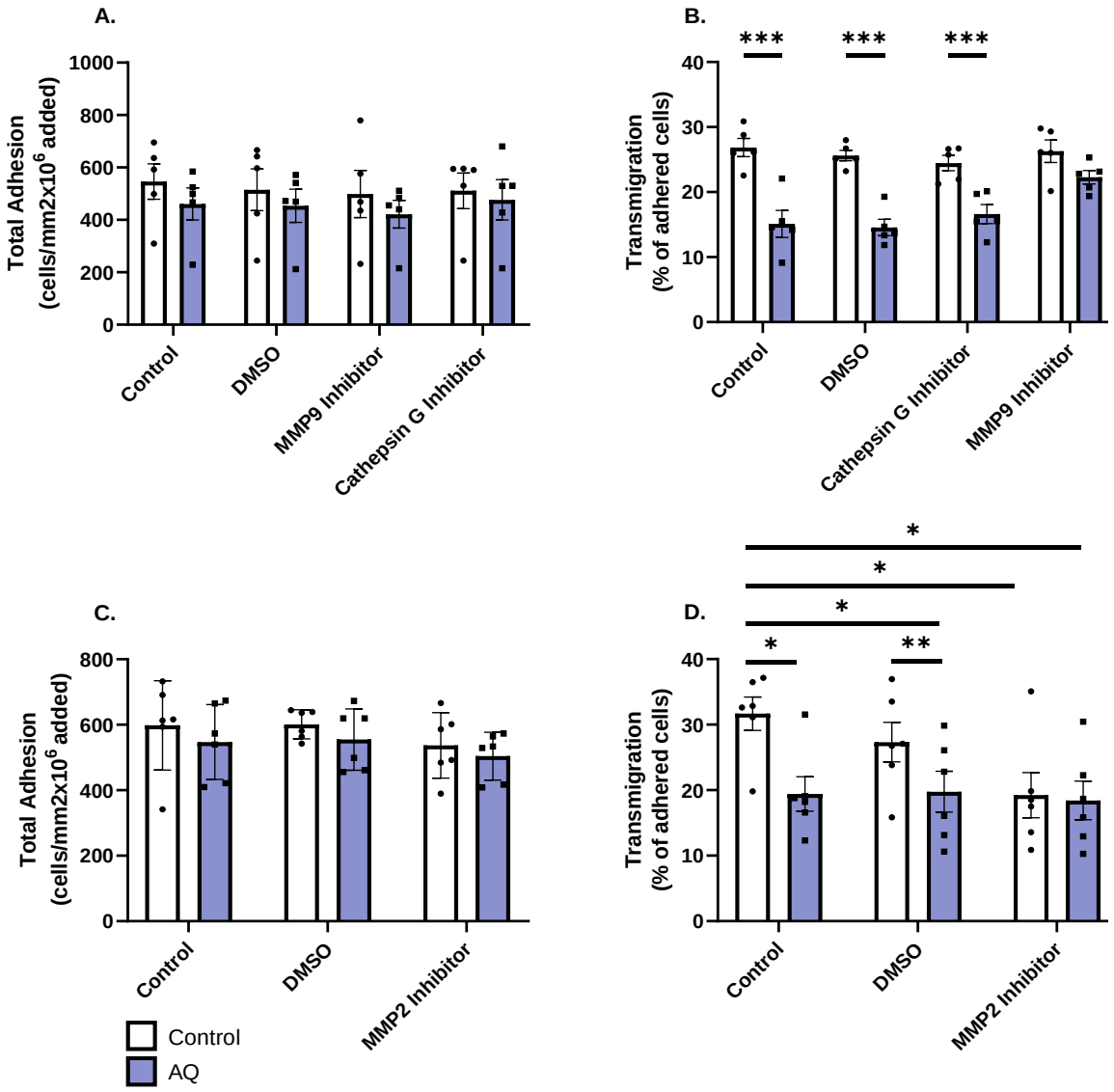


**Figure 4.7 - Effect of MMP-9 inhibitor and cathepsin G inhibitor on PBL adhesion and transmigration**

HDBEC were simulated with TNFα and IFNγ for 24 hours. PBL were treated with (blue bars) or without (white bars) adiponectin for one hour prior to assay. HDBEC were treated with MMP inhibitors for one hour prior to assay. HDBEC were washed and incubated with 1x $10^6$ PBL for 20 minutes at 37°C, 5% CO2 prior to fixing and imaging. Images of 8 random fields were acquired and analysed offline. (A) The number of adherent PBL expressed as the number of cells/$mm^2$/$10^6$ cells added. (B) Lymphocyte transmigration expressed as the percentage change of adherent cells that had transmigrated between control and adiponectin treatment. ANOVA showed significant effect of adiponectin treatment $p<0.0001$. Data are shown as mean ± SEM for (A,B) n=5 (C,D) n=6 independent experiments using a different blood donor in each experiment. Normality was confirmed by Shapiro-Wilk test. * = P≤0.05, ** = P≤0.01, and *** = P≤0.001 compared to adiponectin untreated control in each group by Dunnett's multiple comparisons post-test.

### *4.2.4. Inhibition of MMP-9 in endothelial cells*

We next wanted to find out whether the endothelial cells alone could be facilitating this cleavage, as under the standard assay design there are also several lymphocyte types present. To do this, we incubated 14-3-3ζ alone with the cytokine-stimulated endothelial cells for 1 hour prior to washing off and addition of lymphocytes. In this context, 14-3-3ζ would need to be broken down into functional peptide and act with the endothelium to result in continuous release of S1P after the addition of the lymphocytes. We also used adiponectin, PEPITEM, and 14-3-3ζ treated lymphocytes as our positive controls as these should result in reduced lymphocyte transmigration.

As expected, there was no difference in lymphocyte adhesion when either the lymphocytes or the endothelial cells were treated with adiponectin, PEPITEM, 14-3-3ζ, or any of the protease inhibitors (Figure 4.8A). When PBL were treated with adiponectin, PEPITEM, or 14-3-3ζ, we observed a significant reduction in lymphocyte transmigration compared to untreated control (Figure 4.8B). There was an equal reduction in PBL transmigration when the endothelial cells were pre-treated with 14-3-3ζ prior to the assay (Figure 4.8B). Addition of either GM6001 (broad-spectrum protease inhibitor) or a specific MMP-9 inhibitor reversed this reduction in transmigration and returned levels of transmigration to the same level as untreated control (Figure 4.8B). These data suggest the endothelial cell secretome must contain MMP-9, which is able to break down 14-3-3ζ into functional PEPITEM, and when MMP-9 is blocked, whole 14-3-3ζ protein is unable to mediate functional effects of lymphocyte transmigration.

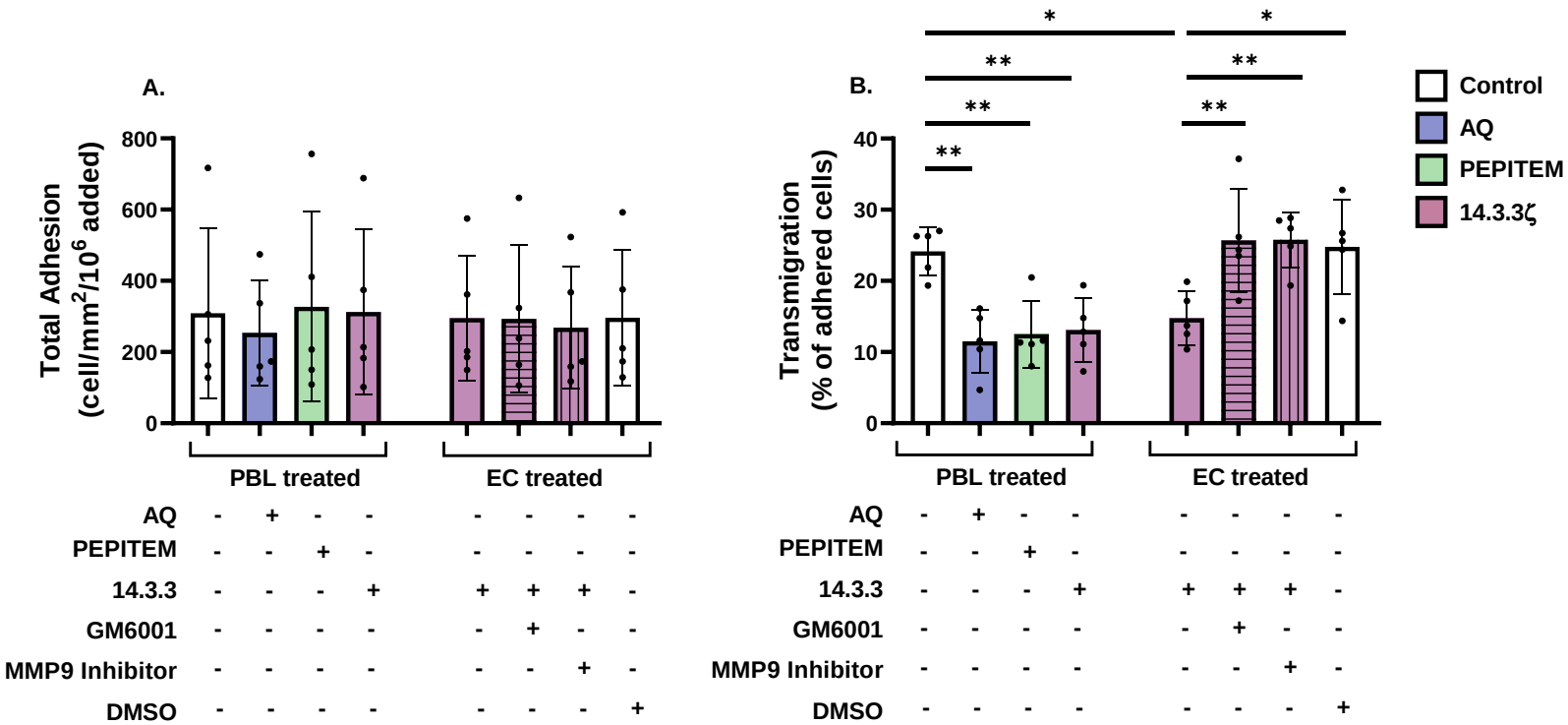


**Figure 4.8 - The effect of 14-3-3ζ pre-incubation with EC on PBL transmigration**

HDBEC were stimulated with TNFα and IFNγ for 24 hours. PBL were left untreated (control), or treated with adiponectin (AQ; 10µg/ml) for 1 hour prior to assay, or with PEPITEM (20ng/ml) or 14-3-3ζ (10ng/ml) immediately before the assay. Control and treated PBL were added to cytokine-stimulated EC. In some conditions (EC treated), EC were pre-treated for 1 hour with either 14-3-3ζ (10ng/ml), 14-3-3ζ (10ng/ml) + GM6001 (10nM), 14-3-3ζ (10ng/ml) + MMP-9 inhibitor (50nm), or DMSO vehicle control (0.000001%) prior to addition of untreated PBL. HDBEC were washed and incubated with 1x $10^6$ PBL for 20 minutes at 37°C, 5% CO2 prior to fixing and imaging. Images of 8 random fields were acquired and analysed offline. (A) The number of adherent PBL expressed as the number of cells/$mm^2$/$10^6$ cells added. (B) Lymphocyte transmigration expressed as the percentage of adherent cells that had transmigrated. ANOVA showed significant effect of treatment on lymphocyte transmigration, $p<0.05$. Data are shown as mean ± SEM for n=5 independent experiments using a different blood donor in each experiment. * = P≤0.05, ** = P≤0.01, and *** = P≤0.001 compared to untreated PBL or EC control by Dunnett's multiple comparisons post-test.

### *4.2.5. Knockdown of MMP-2 and MMP-9 in endothelium*

Inhibiting MMP-2 in the PBL and endothelium led to reduced lymphocyte migration and did not confirm if MMP-2 is involved in the cleavage of PEPITEM. Therefore, we explored if loss of MMP-2 or MMP-9 altered lymphocyte transmigration in response to 14-3-3ζ. MMP-2 or MMP-9 expression was knocked down in endothelial cells using 4 different individual MMP-2 or MMP-9 specific siRNA oligomers. We measured gene and protein expression of each protease 72 hours after treatment with the siRNA oligomers and after 24 hours of cytokine stimulation.

Endothelial cells showed a significant decrease in MMP-2 gene expression after treatment with 3 out of the 4 MMP-2 specific siRNA oligomers (Figure 4.9A), whilst MMP-2 protein expression was significantly reduced with all 4 of the MMP-2 specific siRNA oligomers when compared to cells treated with control siRNA only (Figure 4.9B). MMP-9 gene expression was significantly reduced compared to control siRNA when endothelial cells were treated with MMP-9 specific siRNA oligomers 3 and 4 (Figure 4.9C), whilst protein expression was significantly reduced with oligomers 1 and 4 (Figure 4.9D). We selected MMP-2 siRNA-1 and MMP-9 siRNA-4 to use for future gene silencing experiments as they both had the most successful knockdown efficacy and also the least variation in expression of the other gene (i.e, MMP-2 siRNA-1 did not affect MMP-9 expression and vice versa) (Figure 4.9).

To confirm if MMP-2 or MMP-9 are required for cleavage of 14-3-3ζ into PEPITEM, we knocked down MMP-2 or MMP-9 in endothelial cells and incubated these cells with 14-3-3ζ for one hour prior to running the transmigration assay. The lipofectamine, control siRNA, or either of the knockdowns had no effect on lymphocyte adhesion (Figure 4.10A). As expected, incubating the endothelial cells

with 14-3-3ζ led to a significant reduction in lymphocyte transmigration in the untreated endothelium, lipofectamine only control, or with control siRNA (Figure 4.10B). However, endothelial cells that did not express MMP-2 or MMP-9 had similar levels of PBL transmigration as control endothelial cells, both with and without incubation with 14-3-3ζ (Figure 4.10B). These data suggest both MMP-2 and MMP-9 are required for cleavage of 14-3-3ζ into PEPITEM, and they cannot act redundantly to overcompensate for absence of the other.

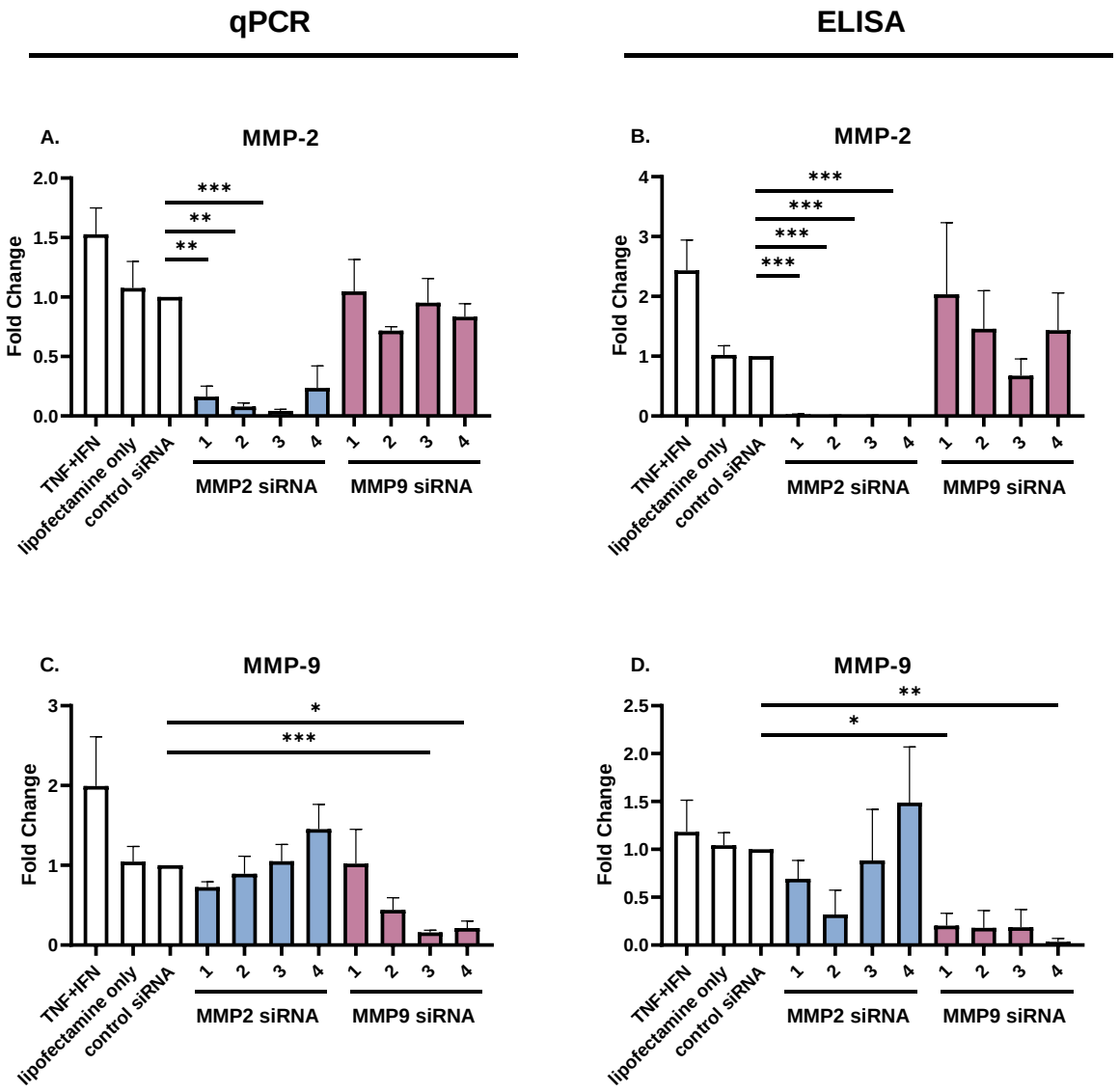


**Figure 4.9 – Validation of MMP-2 and MMP-9 knockdown by siRNA**

HDBEC were untreated (control) or treated with lipofectamine only, a scrambled control siRNA, or a siRNA oligomer specific to MMP-2 or MMP-9 for 4 hours at 37°C, 5% CO2. Media was replaced with HDBEC media for 24 hours before being simulated with TNFα and IFNγ for 24 hours. Cells were lysed and RNA isolated from cultures were analysed by qPCR for expression of (A) MMP-2 and (C) MMP-9 Supernatants were collected analysed by ELISA for protein expression of (B) MMP-2 and (D) MMP-9. Data are mean ± SEM from n=4-8 independent experiments using a different blood donor in each experiment. Data are displayed as fold change ($2^{-\Delta\Delta Ct}$) to control siRNA. * = P≤0.05, ** = P≤0.01, and *** = P≤0.001 compared to control siRNA in each group by Dunnett's multiple comparisons post-test.

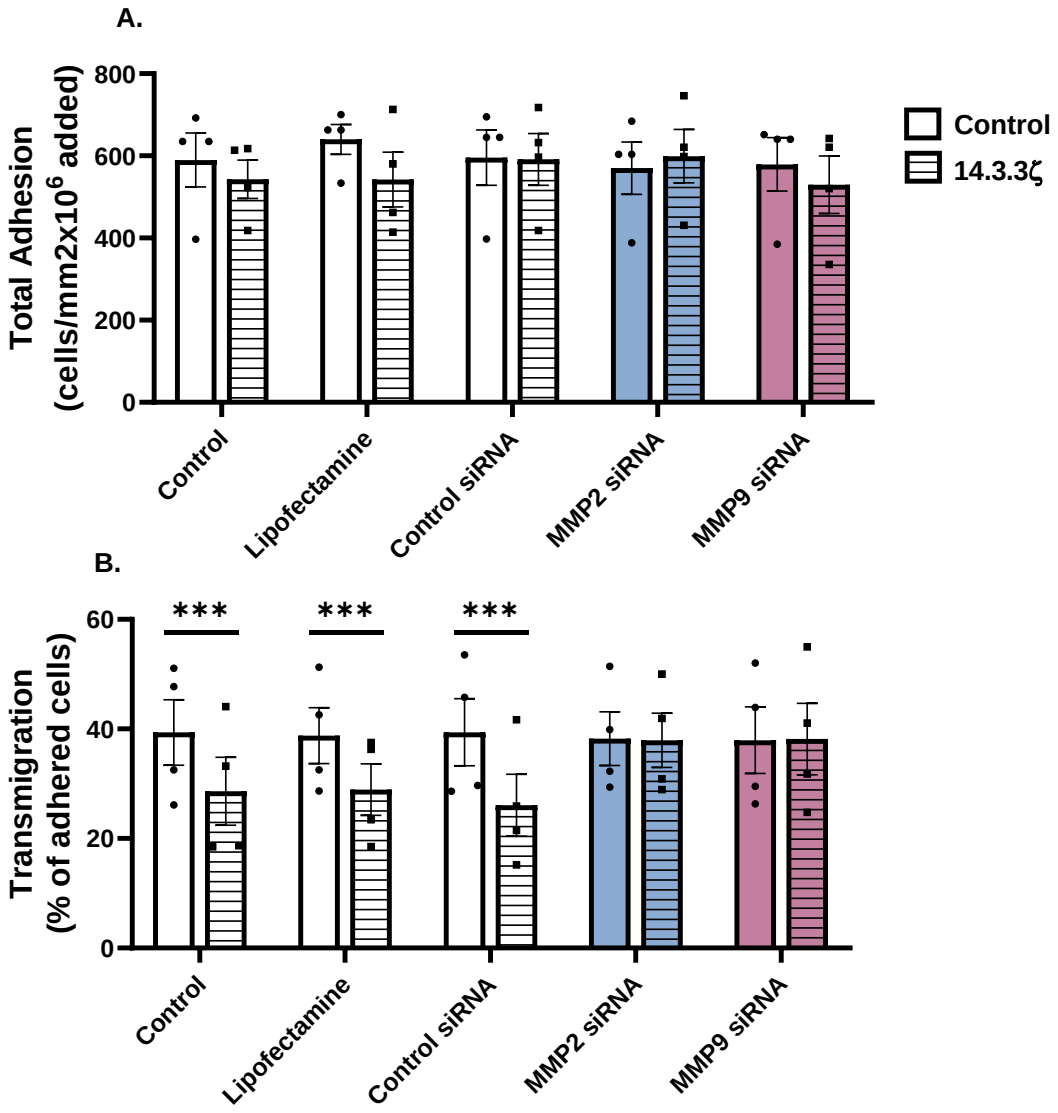


**Figure 4.10 – Effect of 14-3-3ζ on lymphocyte transmigration following endothelial cell knockdown of MMP-2 or MMP-9**

HDBEC were untreated (control) or treated with lipofectamine only, a scrambled control siRNA, or a siRNA oligomer specific to MMP-2 or MMP-9 for 4 hours at 37°C, 5% CO2. Media was replaced with HDBEC media for 24 hours before being simulated with TNFα and IFNγ for 24 hours. EC were incubated for 1 hour with either M199 (control) or 14-3-3ζ (10ng/ml) prior to addition of untreated PBL. Images of 8 random fields were acquired and analysed offline. (A) The number of adherent PBL expressed as the number of cells/$mm^2$/$10^6$ cells added. (B) Lymphocyte transmigration expressed as the percentage change of adherent cells that had transmigrated between control and adiponectin treatment. ANOVA showed significant effect of treatment $p<0.0001$. Data are shown as mean ± SEM for n=4 independent experiments using a different blood donor in each experiment. Normality was confirmed by Shapiro-Wilk test. * = P≤0.05, ** = P≤0.01, and *** = P≤0.001 compared to untreated control in each group by Dunnett's multiple comparisons post-test.

### *4.2.6. Further cleavage of PEPITEM into smaller functional peptides*

Previous work (unpublished) has identified two functional trimers within the PEPITEM sequence, SVT and QGA. As we discovered both MMP-2 and MMP-9 are required for cleavage of 14-3-3ζ into the PEPITEM 14-amino acid sequence, we investigated if these proteases are involved in further cleavage of PEPITEM into functional trimers. Using the static transmigration assay, we incubated lymphocytes with PEPITEM, PEPITEM + GM6001, or PEPITEM + MMP-9 inhibitor and measured lymphocyte adhesion and transmigration.

PEPITEM alone or in conjunction with MMP-9 or GM6001 had no effect on total lymphocyte adhesion (Figure 4.11A). As expected, PEPITEM lead to a significant reduction in lymphocyte transmigration (Figure 4.11B). Interestingly, lymphocyte transmigration returned to control levels when treated with PEPITEM in conjunction with GM6001 (Figure 4.11B). Importantly, addition of an MMP-9 inhibitor did not return transmigration to control levels (Figure 4.11B). DMSO was used as a vehicle control for the protease inhibitors and had no effect on lymphocyte transmigration compared to PEPITEM. (Figure 4.11B). Therefore, PEPITEM does need to be further proteolytically cleaved into functional peptides in order to inhibit lymphocyte transmigration, however MMP-9 is not involved in this cleavage.

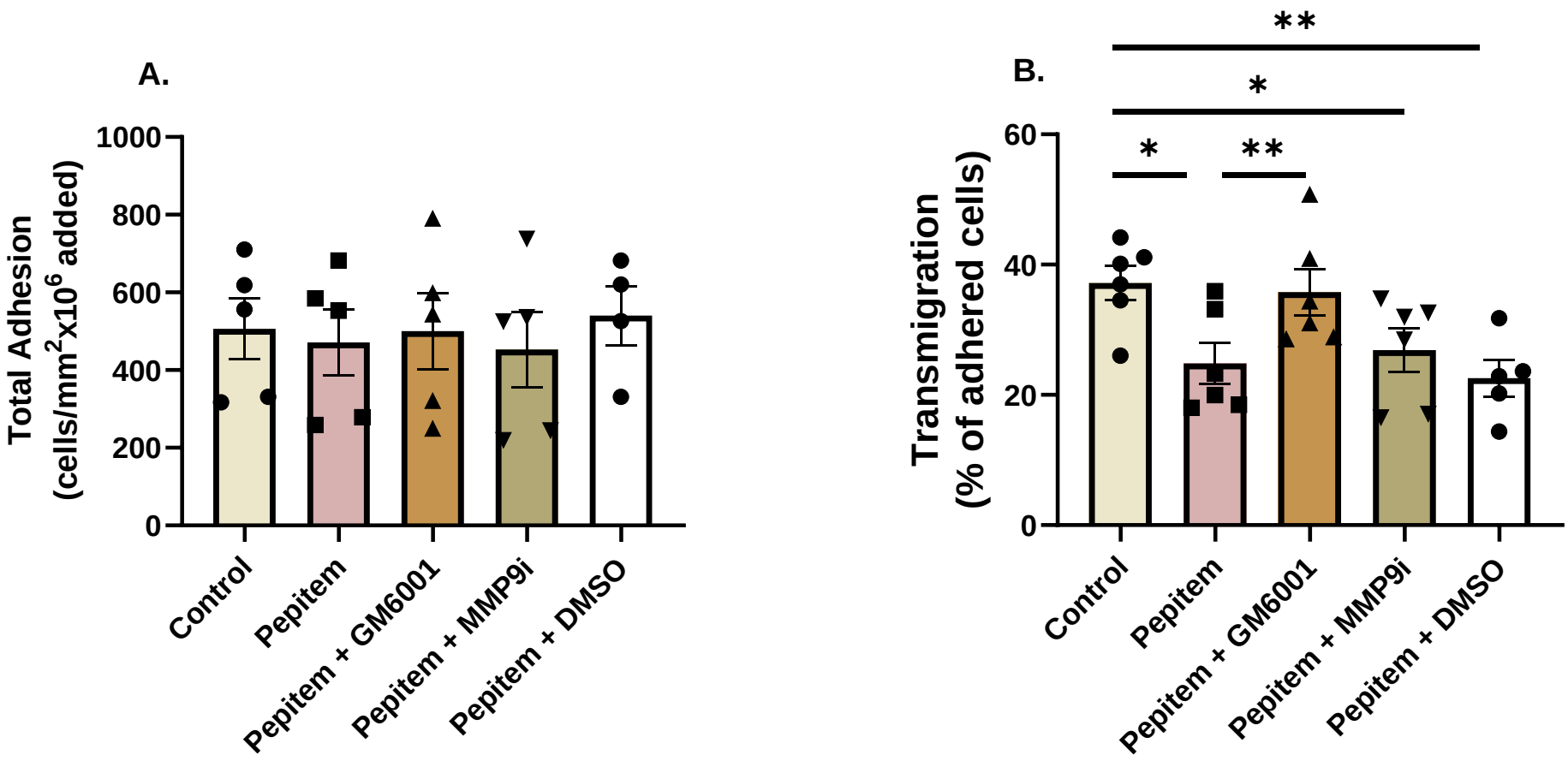


**Figure 4.11 – Investigating role of MMP-9 on further processing of PEPITEM**

HDBEC were stimulated with TNFα and IFNγ for 24 hours. PBL were left untreated (control) or treated with PEPITEM (20ng/ml), GM6001 (10nM) or MMP-9 inhibitor (50nm), or DMSO vehicle control (0.000001%). HDBEC were washed and incubated with 1x $10^6$ PBL for 20 minutes at 37°C, 5% CO2 prior to fixing and imaging. Images of 8 random fields were acquired and analysed offline. (A) The number of adherent PBL expressed as the number of cells/$mm^2$/$10^6$ cells added. (B) Lymphocyte transmigration expressed as the percentage of adherent cells that had transmigrated. ANOVA showed significant effect of treatment on lymphocyte transmigration, $p<0.05$. Data are shown as mean ± SEM for n=5 independent experiments using a different blood donor in each experiment. * = P≤0.05 and ** = P≤0.01 by Dunnett's multiple comparisons post-test.

## 4.3. Discussion

PEPITEM is derived from the larger, parent protein 14-3-3ζ, yet the proteases involved in this cleavage or where this cleavage occurs has remained unknown. Here, we have shown that the adiponectin-mediated regulation of lymphocyte transmigration was lost when used in the presence of broad-spectrum MMP inhibitors or a specific MMP-9 inhibitor. By adapting the experimental design of the static adhesion assay, we have shown that the endothelium have the ability to cleave 14-3-3ζ into functional peptide in the absence of any other cell type. Importantly, we have shown that 14-3-3ζ function was lost when endothelial MMP-2 or MMP-9 activity was blocked using competitive inhibitors or via gene silencing. Furthermore, we discovered a novel role for MMP-2 in supporting T-cell trafficking across inflamed endothelium. We also explored the use of a lymphoblastoid-like cell line (LCL) as a model for primary B-cells in the PEPITEM pathway and discovered that despite their abundant expression of adiponectin receptors, they could not functionally replace primary B-cells in the PEPITEM pathway. Taken together, these data strongly indicate non-redundant roles for both MMP-2 and MMP-9 in cleavage of 14-3-3ζ into PEPITEM and show the requirement for further cleavage of PEPITEM into functional, smaller peptides.

### *4.3.1. B-cell lines as a model for the PEPITEM pathway*

We investigated the use of Raji cells as a model for B-cells in the PEPITEM pathway. Primary human B cells are difficult to transduce and therefore we aimed to identify a genetically tractable model for investigating PEPITEM *in vitro*. There are many cancerous B-cell lines frequently used in immunology research (Klinker *et al.*, 2014; Van Belle *et al.*, 2016; Tan *et al.*, 2018), and Raji cells appeared to be a good potential model cell line for our studies as they are readily susceptible to lentiviral

transduction (Feederle et al., 2000; Winiarska et al., 2017). Raji cells also have high expression of the co-receptor CD19, which decreases the threshold for BCR activation (Carter and Fearon, 1992). Therefore, Raji cells would have been a useful tool for future project aims investigating extracellular vesicle release from B-cells (chapter 5), a process that is induced by BCR stimulation.

We identified expression of adiponectin receptors 1 and 2 on Raji cells, however, we found they are not able to regulate T-cell trafficking in response to adiponectin. Expression of these receptors has previously been identified in Raji cells using semi-quantitative qPCR (Jasinski-Bergner et al., 2017). In this study they also looked for expression of CDH13 (T-cadherin), an alternate receptor for adiponectin, however this was not expressed in Raji cells (Jasinski-Bergner et al., 2017). Notably, western blot of cell lysates revealed Raji cells contained homo-trimers of adiponectin, whilst all isoforms of adiponectin were absent from primary B-cells (Jasinski-Bergner et al., 2017). We identified AR1 and AR2 expression on 80% of B-cells, which is in line with previous studies (Chimen *et al.*, 2015). B-cells have much higher expression of both adiponectin receptors than other lymphocytes (Chimen *et al.*, 2015) and are the only lymphocytes that release PEPITEM in response to adiponectin. Similarly, B-cells isolated from individuals with type-1-diabetes and rheumatoid arthritis have significantly lower levels of adiponectin receptors expressed on their surface and subsequently there is no PEPITEM in serum from these patients (Chimen *et al.*, 2015). Therefore, it is evident that expression of adiponectin receptors correlates to PEPITEM release and is an important regulator of the pathway. As Raji cells express adiponectin receptors but cannot regulate T-cell trafficking in response to adiponectin, Raji cells may have

different downstream signalling pathways following adiponectin stimulation that does not result in the release of PEPITEM.

### *4.3.2. Adiponectin signalling via adiponectin receptors*

Depending on biological context, adiponectin can mediate both pro- and anti-inflammatory effects. One mechanism is via modulating NFκB nuclear translocation (Jung *et al.*, 2012; Wang *et al.*, 2016). In one study, the monocytic cell lines U-937 and THP-1 responded to both native and globular adiponectin by increasing nuclear translocation of the NFκB p65 subunit (Haugen and Drevon, 2007). In contrast, p65 DNA binding did not change in response to either adiponectin isoform in Raji cells, which may be due to their constitutively high levels of p65 DNA binding (Haugen and Drevon, 2007). Notably, the B-cell line Ramos had constitutive low levels of p65 DNA binding, which remained low following adiponectin stimulation, suggesting p65 nuclear translocation does not occur in LCLs in response to adiponectin stimulation (Haugen and Drevon, 2007). Lack of NFκB nuclear translocation in response to adiponectin may possibly explain the inability of Raji cells to regulate T-cell trafficking. To investigate this, the response of NFκB in primary B-cells would need to be characterised.

Immediately downstream of the adiponectin receptors AdipoR1 and AdipoR2 is the adaptor protein phosphotyrosine interacting with pH domain and leucine zipper 1 (APPL1) (Mao *et al.*, 2006). Adiponectin binding to AR1/AR2 leads to activation of APPL1, inducing activation of several intracellular signalling pathways, namely peroxisome-proliferator-activated-receptor α (PPARα), p38 mitogen-activated protein kinase (p38 MAPK) and adenosine monophosphate-activated protein kinase (AMPK) pathways (Mao *et al.*, 2006; Cheng *et al.*, 2007). Subsequently, these signalling

pathways converge on activation of cAMP response element-binding protein (CREB) transcription factor. Another consequence of APPL1 activation is increased calcium influx into the cells (Iwabu *et al.*, 2010) causing activation of the calcium/calmodulin-dependent protein kinase kinase (CAMKK)-dependent pathways and activation of the transcription factor ATF-1. Both Creb and ATF-1 activation leads to *YWHAZ* (14-3-3ζ) transcription. Previous work from our lab (Hopkin, 2023) has shown APPL1 is present in primary B-cells but is lost in aged B-cells resulting in a loss of PEPITEM response in older adults. It is not known if this pathway is functional in Raji cells and how it may differ from primary B-cells. This pathway needs to be further characterised in Raji cells to elucidate why Raji cells cannot regulate T-cell trafficking in response to adiponectin.

Another potential explanation for why Raji cells were unable to respond to adiponectin in the same way as primary B-cells may be due to their expression of the transcriptional activator EBV nuclear antigen 1 (EBVNA1) (Satoh, Kawana and Yamamoto, 2013). Chromatin immunoprecipitation followed by sequencing (ChIP-Seq) identified several members of the adiponectin signalling pathway to be EBNA-1 target genes, including; AMPK, APPL1, P38 MAPK, PPAR, Creb, and even 14-3-3ζ and 14-3-3γ (Satoh, Kawana and Yamamoto, 2013). Therefore, EBVNA1 offers another level of 14-3-3 transcriptional regulation that is not seen in primary (EBV negative) B-cells. In contrast to our results, these data may suggest Raji cells should have more 14-3-3ζ transcription than primary B-cells. Quantification of 14-3-3ζ in Raji cells would need to be performed to confirm this. If in fact Raji cells have more transcription of 14-3-3ζ than primary B-cells, it may be post-translational processing of 14-3-3ζ into PEPITEM or secretion of PEPITEM itself that may be defective in Raji cells, resulting in their inability to regulate T-cell trafficking. To investigate fully why

Raji cells do not functionally respond to adiponectin the same as primary B-cells derived from PBMC, first we need to identify if 14-3-3ζ/PEPITEM is being secreted in response to adiponectin. This can be done by western blotting of 14-3-3ζ or LC/MS of the Raji secretome to detect PEPITEM. If there is no 14-3-3ζ secretion, further experiments can be done to identify which of the above pathways may be involved.

### *4.3.3. Potential uses of alternative B-cell lines as a model for B-cells in the PEPITEM pathway*

There are differences in intracellular signalling and function between different lymphoblastoid cell lines (LCL). Cancerous B cell lines can exhibit abnormalities in Ig and cytokine production (Van Belle et al., 2016). A study comparing several Burkett lymphoma lines, Daudi, Namalwa, Raji and Ramos identified significant differences in activation between these cell types. Raji cells were one of the least responsive cell types to stimulation with a TLR9 agonist and exhibited limited upregulation of CD40, CD69, CD70, CD80, CD83, CD86 and MHC class I and class II molecules following 24 hours of stimulation (Van Belle et al., 2016). Conversely, Namalwa cells had significant upregulation of several of these markers and closely mimicked polyclonal human B-cells in induction of activation markers after TLR9 stimulation (Van Belle et al., 2016). As previously mentioned, Ramos cells have much lower levels of p65 DNA binding than Raji cells, which may lead to differences in response to adiponectin (Haugen and Drevon, 2007). Therefore, it is worth identifying how different B-cell lines respond to adiponectin as they may have differential responses. In this case, an alternate B-cell line may be able to respond to adiponectin and secrete PEPITEM and act as a model of primary B cells in the PEPITEM pathway.

We do not know which B-cell types are involved in PEPITEM secretion and regulation of T-cell trafficking. Primary B-cells used in our studies are isolated from circulating peripheral blood, of which the B cell population is predominantly composed of naive B cells (66%) and of memory B cells (33%), whilst there are very low circulating levels of plasma cells (Caraux et al., 2010). Before further investigation into different B-cell lines as use as a model in the PEPITEM pathway, more research is required to identify the subset/s of B-cells involved in this pathway. This could help us identify the most suitable cell line to use.

Alternatively, EBV infection has been shown to increase sensitivity of B-cells to genetic engineering (Bovia et al., 2003; Winiarska et al., 2017). Primary B-cells cultured in culture media from B95.8 cell lines that contain EBV significantly increased the transduction of the primary B-cells by HIV vectors (Bovia et al., 2003). More recently, infection of primary human B-cells with EBV resulted in the generation of lymphoblastoid cell lines that could be transduced using lentiviruses (Winiarska et al., 2017). Infecting B-cells with EBV led to an increase in CD27+ memory pool and induced class switching to IgG or IgA, further highlighting the functional differences between primary B-cells and lymphoblastoid cells (Winiarska et al., 2017). Despite these differences, infecting B-cells with EBV could be a potential mechanism to enable genetic engineering of B-cells, which would be invaluable for future work on understanding the signalling pathways involved in PEPITEM secretion.

#### *4.3.4. Functional roles of protease inhibitors on lymphocyte migration*

As expected, we observed inhibition of leukocyte trafficking with adiponectin and PEPITEM treatment, although this was only significant after 15-20 minute incubation of the PBL with cytokine-stimulated endothelium. Previously adiponectin

has inhibited PBL trafficking following incubation with EC in as little as 6 minutes (Chimen *et al.*, 2015). The differences between this and our data could be due to the donor of endothelial cells used and their responsiveness to the cytokine treatment. TNFα and IFNγ upregulate expression of adhesion molecules on the surface of the EC which is essential for leukocyte transmigration. To normalise between experiments with different EC donors, expression profiles of adhesion molecules should be characterised in each donor following treatment with TNFα and IFNγ.

Previous published work (Apta 2015) showed extracellular recombinant 14-3-3ζ has a similar efficacy to PEPITEM in inhibiting lymphocyte transmigration, suggesting 14-3-3ζ may be cleaved into PEPITEM in the extracellular environment. We have demonstrated genetic silencing of MMP-2 or MMP-9 in the EC abolished the functional effect of 14-3-3ζ, highlighting the requirement for both proteases in cleavage of 14-3-3ζ into a functional peptide. In contrast, only specific inhibition of MMP-9 abolished the functional effect of adiponectin. Inhibition of MMP-2 led to a significant reduction in PBL transmigration in the absence of adiponectin. The key difference between these experimental designs is that the inhibitors blocked MMP activity in both the PBL and the EC, suggesting MMP-2 is required in the PBL for efficient transendothelial migration.

MMP-2 has been reported to regulate cell migration in varying contexts (Dubois *et al.*, 1999; Esparza *et al.*, 2004; Song *et al.*, 2015), however this is a novel observation for the role of MMP-2 of T-cell trafficking across endothelial cell layers. In a murine model of EAE, MMP-2 and MMP-9 are present at the blood brain barrier and modulate activity of cytokines to promote leukocyte migration into the CNS (Song et al., 2015). Reduced leukocyte migration across the blood brain barrier and into the CNS prevents the Th1 and Th17 mediated demyelination essential for the

pathophysiology of EAE (Song et al., 2015). Furthermore, MMP-2 and MMP-9 knockout mice are typically resistant to EAE development (Dubois et al., 1999; Agrawal et al., 2006). Unexpectedly, one study found MMP-2 KO mice treated with myelin oligodendrocyte glycoprotein (MOG) to induce EAE had earlier disease onset and higher clinical scores than wild-type (WT), due to increased perivascular and parenchymal mononuclear cell infiltrates (Esparza *et al.*, 2004). *In vitro*, these MMP-2 deficient MOG-specific T cells exhibited increased transmigration through mouse brain endothelium (b.End5 cell line) (Esparza *et al.*, 2004). This increase in T-cell transmigration *in vivo* and *in vitro* was found to be due to overcompensation of MMP-9. MMP-$2^{-/-}$ T cells had a 2.76 fold increase in MMP-9 mRNA expression and the secretome demonstrated a 3-fold increase in MMP-9 gelatinolytic activity (Esparza *et al.*, 2004). Notably, there was also an increase in MMP-9 expression in lung-derived microvascular endothelial cells isolated from these MMP-$2^{-/-}$ mice, but there was no change in MMP-9 expression in fibroblasts isolated from the same animals (Esparza *et al.*, 2004). Therefore, overcompensation for loss of MMP-2 by MMP-9 is a cell-specific phenomenon. In light of this, we need to test for activity of other MMPs in our PBL and endothelial cell population to confirm if the decrease in lymphocyte trafficking seen with the MMP-2 inhibitor is directly due to MMP-2 inhibition or potential over compensation with other proteases.

MMP-2 is upregulated during allergic inflammation and is essential for egress of inflammatory cells into the airway lumen (Corry *et al.*, 2004). BALB/c mice challenged with ovalbumin and C56Bl/6 mice challenged with complete aspergillus antigen have enhanced expression of MMP-2 protein in the bronchoalveolar lavage compared to untreated control (Corry *et al.*, 2004). Inhibition of MMPs with GM6001 or specific knock-down of MMP-2 inhibited inflammatory cell egress, leading to an

accumulation of inflammatory cells in the lung parenchyma, and subsequently increased susceptibility of MMP-2$^{-/-}$ mice to asphyxiation and death (Corry *et al.*, 2004). This was due to increased levels of the Th2 cytokines IL-4 and IL-13 in MMP-2 KO mice, which are both involved in pathology of allergic airway disease (Doucet *et al.*, 1998). As MMP-2 is known to regulate leukocyte trafficking through regulation of cytokines, we should also investigate cytokine profiles of PBL and endothelial cells treated with the MMP-2 inhibitor to investigate any changes in cytokine expression that could be causing the reduced lymphocyte migration seen with the addition of an MMP-2 inhibitor.

It is well documented that the MMP-9 inhibitor (CAS 1177749-58-4) is not truly specific and exhibits cross reactivity with other MMPs. At high concentrations, this inhibitor can inhibit MMP-1 ($IC_{50}$ = 1.05 µM) and MMP-13 ($IC_{50}$ = 113 nM). We overcame this cross reactivity by using a concentration that should be specific for MMP-9 (50 nM, $IC_{50}$ = 5 nM). This concentration has been used previously to inhibit 10 ng/mL of exogenous MMP-9 added to a mouse vascular smooth muscle cell line (Shih et al., 2021). Inhibition of MMP-9 using the CAS 1177749-58-4 MMP-9 inhibitor reversed the increase in cell migration that was seen with the addition of MMP-9 (Shih et al., 2021). Similarly, another study showed 10 nM of this inhibitor could reverse the IL-17 mediated increase in cell migration, which is known to be MMP-9 dependent (Xu *et al.*, 2014). In other studies, concentrations as low as 4 nM have been used to fully inhibit the increase in MMP-9 activity induced by high glucose-homocysteine in retinal endothelial cells (Mohammad and Kowluru, 2020). Importantly, in none of these studies did they report measuring the activity of other MMPs to confirm there was no cross-reactivity. Future work should use titration experiments to identify the lowest concentration of the inhibitor that can be used to

still fully inhibit MMP-9 activity in HDBEC. Activity of other MMPs, particularly MMP-1 and MMP-13, should also be measured to exclude potential cross-reactivity issues.

### *4.3.5. Potential mechanisms of action of MMP-2 and MMP-9*

We have identified the requirement for both MMP-2 and MMP-9 in cleavage of 14-3-3ζ into functional peptide. There are several possible routes for their action. Firstly, MMP-2 and MMP-9 could both be directly acting on the 14-3-3ζ sequence, i.e., one may cleave at the start of the sequence and the other at the end, and without either of these proteases functional PEPITEM cannot be produced. Secondly, there could be a stepwise sequence of activation requiring both of these proteases. MMPs exist in latent pro-MMP forms and cleavage of their pro-domain is required for their activation. Many MMPs can activate other MMPs, and MMP-2 is a known activator of MMP-9 in a process that is tightly regulated by TIMPs (Tjahajawati *et al.*, 2020). This is unlikely to be the case however as in the previous chapter we found MMP-2 is much more abundant than MMP-9 in endothelial cells, and typically the activator is the limiting factor and would be more likely to be present at low amounts (Camire, 2021; Postler, 2021). Also, each MMP has several routes of activation and MMP-9 is known to cleaved by several other proteases, such as MMP-3, MMP-7, MMP-10, MMP-13, cathepsin G and plasmin (Christensen and Shastri, 2015), and therefore knocking down MMP-2 in EC *in vitro* may not lead to complete abolishment of MMP-9 activation. However, to provide a greater understanding of the role of MMP-2 in MMP-9 activation we could investigate protease activity of the knockdown endothelial supernatants. If there is a sequence of MMP-2 to MMP-9 activation, then there should be no MMP-9 activity in the MMP-2 knockdowns. Similarly, there should still be active MMP-2 in the MMP-9 knockdowns. Similarly, addition of pro-MMP-9 into the MMP-2 knockdown should not

cause 14-3-3ζ cleavage or result in MMP-9 activation. Another method could be to incubate 14-3-3ζ with active MMP-2 and MMP-9 independently and use LC/MS to investigate cleavage products. However, this was unavailable to us as the current LC/MS protocol requires proteolytic degradation which would interfere with our results.

The final scenario is that PEPITEM has to be further cleaved into functional peptides to suppress lymphocyte transmigration, and one of the MMPs may be required for this further cleavage. Previous work from our lab using amino acid substitutions in the form of an alanine sweep has identified two active pharmacophores in the PEPITEM sequence, the tripeptides SVT and QGA (unpublished). These tripeptides both display greater efficacy than PEPITEM or 14-3-3ζ at regulating T-cell trafficking. It was previously not known if PEPITEM has to be cleaved *in vitro* into these active trimers for PEPITEM to mediate its effect, here we have shown that further cleavage of PEPITEM is essential for immuno-regulation as incubating lymphocytes with PEPITEM and GM6001 (the broad spectrum MMP inhibitor) results in loss of the PEPITEM effect. Notably, the MMP-9 inhibitor did not fully reverse the effect of PEPITEM. Therefore, MMP-2 may be the protease involved in further cleavage of PEPITEM. To investigate this further, we would need to perform a static transmigration assay and treat the PBL with both PEPITEM and a specific MMP-2 inhibitor.

### *4.3.6. Limitations*

Whilst these data provide a novel understanding of the mechanisms of PEPITEM production, there are several limitations. Namely, we used functional readouts for identifying PEPITEM formation as we have no way of currently detecting

PEPITEM in culture. PEPITEM is a small peptide (14 amino acids) for which there is no antibody readily available, limiting our ability to detect it using quantitative methods, such as ELISA. Previously, PEPITEM has been detected in B-cell supernatants and human serum using LC/MS, however sample preparation requires peptide fragmentation that would interfere with our results and not be a suitable method for our research question. Therefore, we utilised functional readouts as a method of PEPITEM measurement.

Another limitation of MMP research is the cross reactivity seen between inhibitors. The MMP-9 inhibitor used in our experiments is known to cross-react with MMP-1 and MMP-13 at higher concentrations. To overcome this, we utilised a concentration that should be specific for MMP-9. However, to be sure there is no cross-reactivity between MMP-2 and MMP-9, gelatin zymography should be performed on the endothelial cell and PBL supernatants to confirm activity of MMP-2 remains in the presence of the MMP-9 inhibitor, and vice versa.

Another key limitation of these results is that in physiological conditions, lymphocyte transendothelial migration is a complex process and is influenced by many factors, including immune cell cross talk, shear stress, and circulating mediators. The *in vitro* static transmigration assay used in this chapter is a good model for leukocyte recruitment during inflammation, however, does not fully mimic the complex inflammatory environment due to lack of these factors. Future *in vivo* experiments may help to provide a more physiological understanding of the involvement of MMPs in PEPITEM production. MMP-2 and MMP-9 knockout mice are viable but are smaller than their wild type littermates and do exhibit reduced angiogenesis and altered inflammatory responses (Mautino *et al.*, 1997; Esparza *et al.*, 2004). Previous *in vivo* experiments have shown PEPITEM is able to prevent the

effects of zymosan-induced peritonitis (Hopkin, 2023), use of MMP-2 and MMP-9 KO mice in this model of inflammation would provide a further understanding of the roles played by each of these proteases.

### *4.3.7. Conclusion*

The main aims of this chapter were to identify a model for B-cells in the PEPITEM pathway, and to identify the protease(s) involved in 14-3-3ζ into functional peptide. We characterised the Raji B-cell line and found it was unable to respond to adiponectin in the same way as primary PMBC-derived B-cells. Therefore, for the B-cell experiments in this thesis we have utilised primary B-cells. Future work should investigate responses of other B-cell lines to adiponectin, and use 14-3-3ζ quantification to see if any secrete 14-3-3ζ protein. EBV negative LCLs may be more applicable for this as many pathways downstream of adiponectin signalling are modulated by the EBVNA1 transcriptional activator. We have also shown MMP-2 and MMP-9 are both independently required for cleavage of 14-3-3ζ into a functional immunoregulatory peptide. Future work is required to identify how these proteases work in conjunction to cleave a functional peptide from 14-3-3ζ, investigating whether this is due to a stepwise sequence of activation or independent cleavage from both the proteases.

# Chapter 5. INVESTIGATING MECHANISMS OF 14-3-3Z SECRETION

## 5.1. Introduction

PEPITEM is derived from the parent protein 14-3-3ζ and is released from the B-cell following adiponectin stimulation. However, the mechanism by which PEPITEM is secreted from the B-cell remains unknown. In the previous chapters, we have shown recombinant extracellular 14-3-3ζ can inhibit lymphocyte transmigration with a similar efficacy as PEPITEM itself, however we can prevent this function by inhibiting protease activity. We have also shown 14-3-3ζ can be cleaved extracellularly by the endothelium, suggesting the whole 14-3-3ζ protein could be being released from the B-cells which is then being cleaved into PEPITEM extracellularly.

14-3-3ζ is typically a cytosolic protein, however it has been identified in extracellular environments in certain pathological conditions, including in the secretome of tumour associated monocytes/macrophages (Kobayashi et al, 2008). Proteins in the 14-3-3ζ family do not contain a signal recognition sequence for vesicular trafficking and therefore are not directed to the ER for packaging into secretory vesicles as part of the classical secretory pathway. Despite this, treating B-cells with an inhibitor of the classical secretory pathway (Brefeldin-A) prevented the adiponectin-mediated effect on lymphocyte transmigration, suggesting PEPITEM may be secreted via the classical pathway (Chimen et al, 2015).

14-3-3ζ has also been identified in exosomes from several cell types (Kruger et al, 2014; Zhang et al, 2016; Keerthikumar et al, 2016) and can have functional effects on the recipient cells. Exosomes derived from human umbilical cord mesenchymal stem cells are 14-3-3ζ+ which could regulate skin cell proliferation and restricted excessive collagen deposition in a mouse burn model (Zhang et al, 2016). Hepatocarcinoma-derived 14-3-3ζ+ exosomes can be “swallowed” by tumour

infiltrating T-cells resulting in impaired activation, proliferation, and anti-tumour functions (Wang et al, 2018). 14-3-3ζ+ vesicles have been identified in exosomes derived from the EBV-transformed B-cell line (RN), however, 14-3-3ζ has never been identified in primary B-cell-derived exosomes. Therefore, we sought to identify if B-cells were secreting 14-3-3ζ+ positive extracellular vesicles as a mechanism of PEPITEM release.

In this chapter, we aim to explore whether 14-3-3ζ is being secreted from B-cells following adiponectin stimulation. We also aim to elucidate the mechanism of release by inhibiting the classical secretory pathway and characterising B-cell derived extracellular vesicles.

## 5.2. Results

### *5.2.1. 14-3-3ζ secretion from adiponectin stimulated B-cells*

To investigate the hypothesis that 14-3-3ζ is released from adiponectin-stimulated B-cells, we measured 14-3-3ζ expression in B-cell supernatants following adiponectin stimulation. Using a western blot, we detected significantly more 14-3-3ζ protein in supernatants of B-cells stimulated with adiponectin compared to unstimulated control (Figure 5.1). This data shows that B-cells secrete whole 14-3-3ζ protein following adiponectin stimulation which must then be cleaved into PEPITEM extracellularly. As 14-3-3ζ is a non-classically secreted protein, we investigated B-cell derived extracellular vesicles as a potential mechanism of secretion.

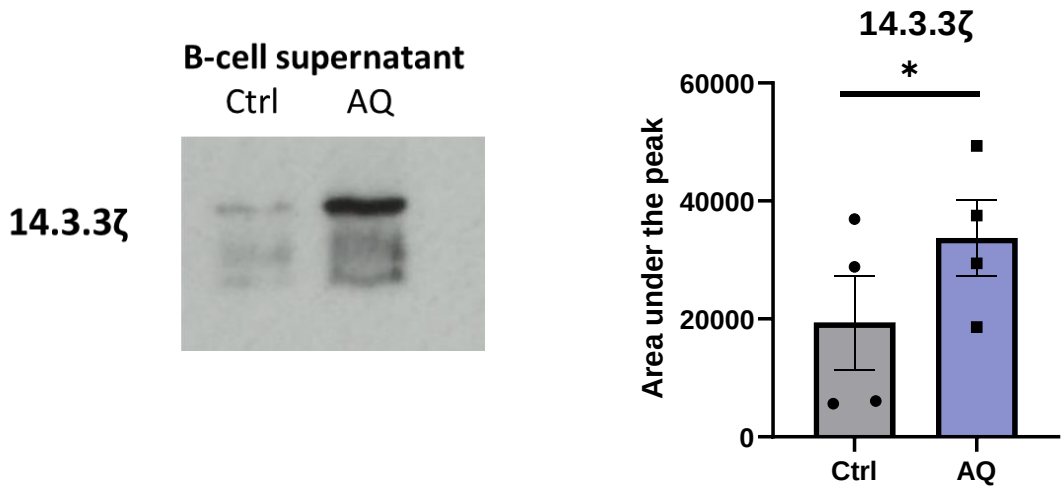


**Figure 5.1 – Western Blot of B cell supernatants following adiponectin stimulation**

Supernatants were collected from B-cells that were either left untreated (grey bar) or stimulated with adiponectin (blue bar) for 1 hour. Total 14-3-3ζ content was measured by western blot (representative image of 4 independent experiments). Data are shown as mean ± SEM, n=4 independent experiments using a different blood donor in each experiment. * = P≤0.05, ** = P≤0.01 using unpaired t-test.

### *5.2.2. B-cell agonists in B-cell extracellular vesicle release*

Proteins from the 14-3-3ζ family have been found in extracellular vesicles (EVs) from varying cell types. To investigate if B-cells are secreting 14-3-3ζ associated with EVs following adiponectin stimulation, EV release from primary B cells was quantified using flow cytometry. B cells were stained with PKH26, a lipophilic membrane dye, which would be carried over to any vesicles budding from the plasma membrane. B-cell supernatants were analysed for expression of small particles positive for PKH26. Previously, platelet derived vesicles have been detected in this way (Chimen *et al.*, 2020)

As previously described (Chimen *et al.*, 2020), to enable detection of small extracellular vesicles, the detection threshold was decreased to 20,000 FSC-H. Unstimulated B-cells were used to set the FSC/SSC gate (Figure 5.1A). Setting the threshold detection limit this low will result in high background from the machine (Figure 5.1A), so to overcome this and only visualise small particles derived from B-cells, the detection threshold was increased to 2,500 fluorescence intensity of PKH26 (Figure 5.1B). Once the limits were set, we measured expression of PKH26+ particles in B-cell supernatants. B-cells were left untreated (control), or stimulated with adiponectin, or with classical inducers of B-cell extracellular vesicle release, CD40 + IL-4, or PMA. In all of the unstimulated and stimulated B-cell supernatants, we observed a population of PKH26+ particles that sat outside of the cell gate, suggesting they are smaller than B-cells (Figure 5.1C). This population contained ~40% of all particles detected, and there was no difference in population size (Figure 5.1C) or PKH26 MFI (Figure 5.1D) between control or stimulated B-cells

To confirm this population is representative of extracellular vesicles, we confirmed it was not platelet contamination by staining for CD41. We also stained B-cells for CD19 to investigate if this population could represent B-cells which had not been correctly removed from the supernatant and had slightly changed shape after freeze thawing. After staining for CD41 and CD19, we collected the cells via centrifugation. Supernatants were collected and ran either on the same day, or the following day after being frozen overnight at -80°C, on the FacsVia at threshold detection 20,000 FSC. In this case, we detected CD41+ particles which could represent platelet-derived vesicles suggesting there was some platelet contamination in our B-cell preparation. However, this was a distinct population from the PKH26+ population previously identified (Figure 5.3A). We observed a population of CD19+ particles in both the fresh and frozen supernatants. In the fresh supernatants, this population matched the cell gate from the B-cells, and in the frozen sample, this population had migrated slightly to the left and fell outside the cell gate. This data suggests the PKH26+ population we observed previously are representative of B-cells that had not been efficiently spun down in sample preparation.

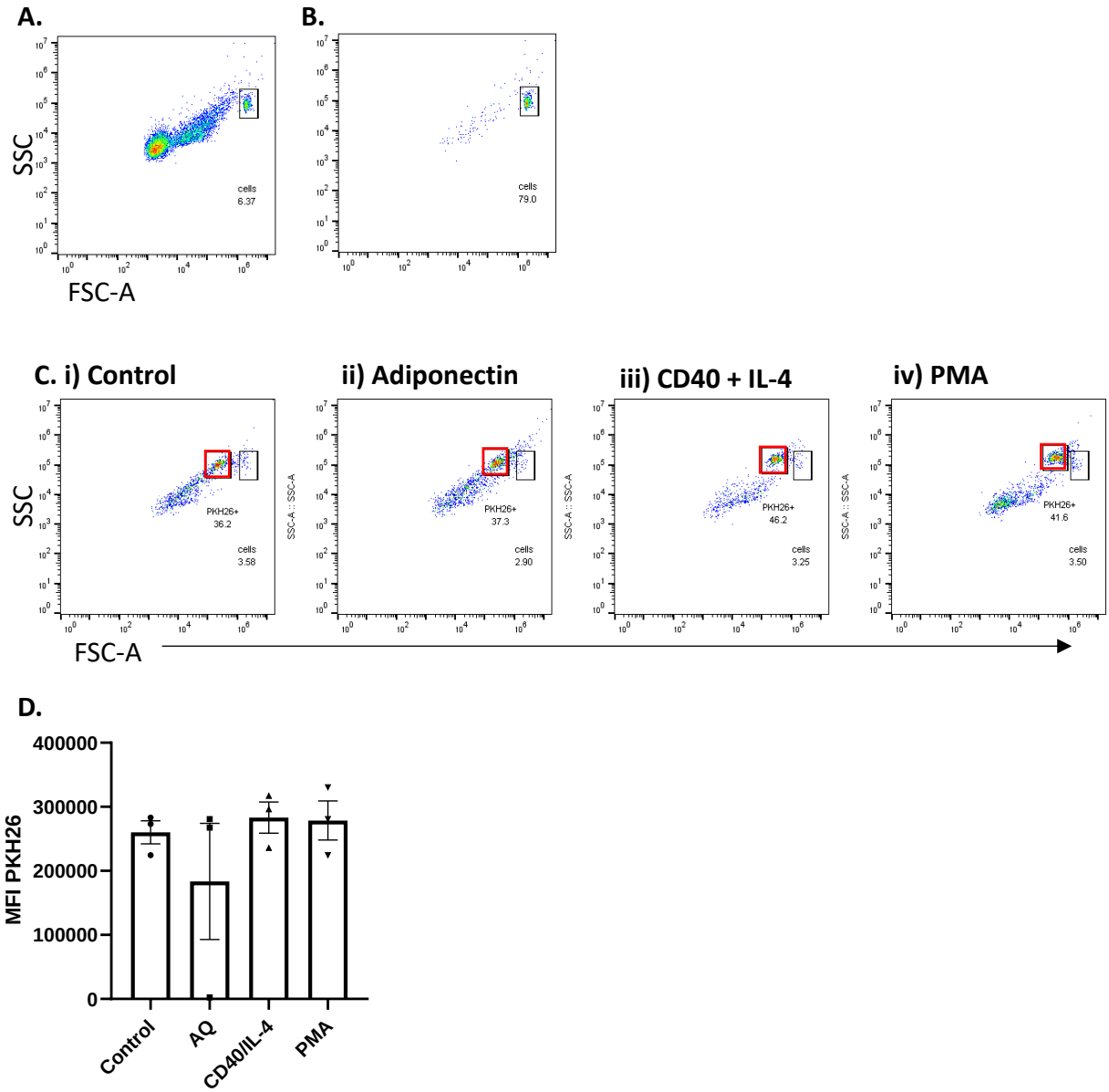


**Figure 5.2 Flow cytometry analysis of B-cell supernatants**

B-cells were stained with lipid dye PKH26 and either (i) left untreated, or treated with (ii) adiponectin, (iii) CD40 + IL-4, or (iv) PMA. Supernatants were collected and frozen at -80°C until future use, and cells were fixed with 2% FA and ran on the FacsVia flow cytometer the following day. (A,B) Forward vs side scatter representative plot for untreated cells when the size threshold for detection was set to (A) 20,000 FSC-H and (B) 2,500 fluorescence intensity of PKH26. (C) Forward vs side scatter representative plot from B-cell supernatants. (D) Median Fluorescence Intensity (MFI) values of PKH26.

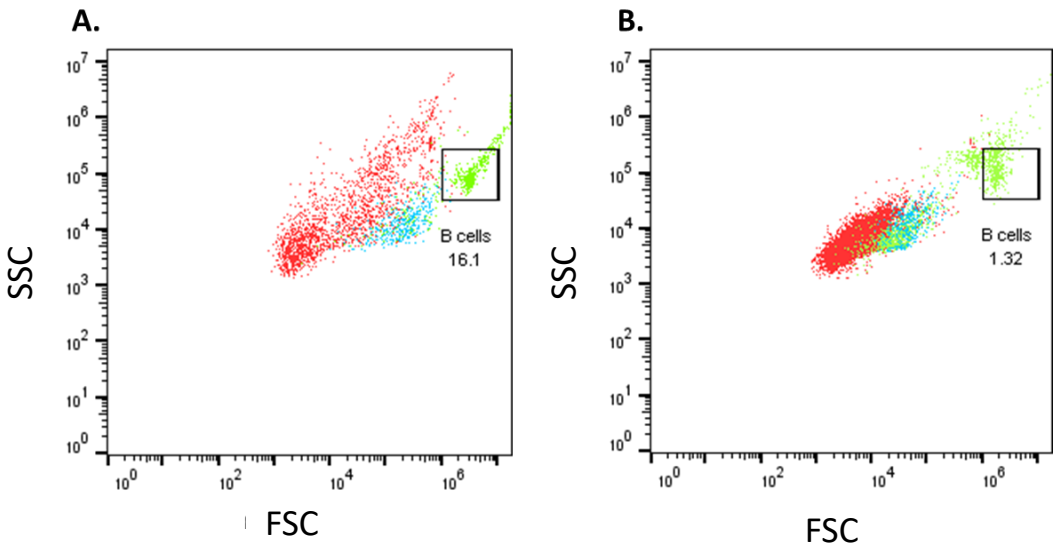


**Figure 5.3 – Effect of freeze thawing B-cell supernatants**

B-cells were stained for platelet marker CD41 (blue) and B cell marker CD19 (green). Unstained particles are shown in red. Cells were collected by centrifugation and supernatant s collected and acquired by FacsVia on (A) the same day as isolated or (B) the following day after freezing at -80°C.

### *5.2.3. Optimisation of B-cell supernatant preparations*

After identifying B-cells remaining in the supernatant preparations, we investigated ways to optimise our sample preparation and reduce B-cell contamination. PBMCs from freshly isolated peripheral blood were stained with B-cell and T-cell markers (CD19 and CD3 respectively). Subsequent to staining, cells were collected by centrifugation at 250 g for 5 minutes. Both the cell sample and the supernatant were immediately analysed on the FacsVia, set at a standard threshold of 80,000 FSC-H. Following gating on lymphocytes, the cell sample showed approximately 70% CD3+ T cells, 1% CD19+ B-cells, and 25% double negative cells (Figure 5.4A). The supernatant sample, which should not have contained any cells, showed 65% CD3+ T cells, 10% CD19+ B-cells, and 25% double negative (Figure 5.4B). This data showed we were not fully removing the cells during centrifugation, and B-cells in particular were difficult to remove with our current centrifugation protocol.

To overcome this, alternate centrifugation steps were trialled. PBMC were centrifuged at 250 g, 500 g, 750 g and 1000 g for either 10 minutes, or twice for 5 minutes. A single 10 minute spin led to 2443, 1553, 184 and 622 lymphocytes remaining in the supernatant at speeds of 250 g, 500 g, 750 g and 1000 g respectively (Figure 5.5) (Table 5.1). Numbers of cells in the supernatant was lower when supernatants were spun twice for 5 minutes, with supernatant being transferred to a fresh Eppendorf between spins. In this case, only 511 lymphocytes were remaining when spun at 250 g, and this decreased to 69, 14 and 37 lymphocytes present after centrifugation at 500 g, 750 g, and 1000 g respectively (Figure 5.6) (Table 5.1). Thus, for all future B-cell supernatant preparations, we centrifuged B-cells twice for 5 minutes at 750 g.

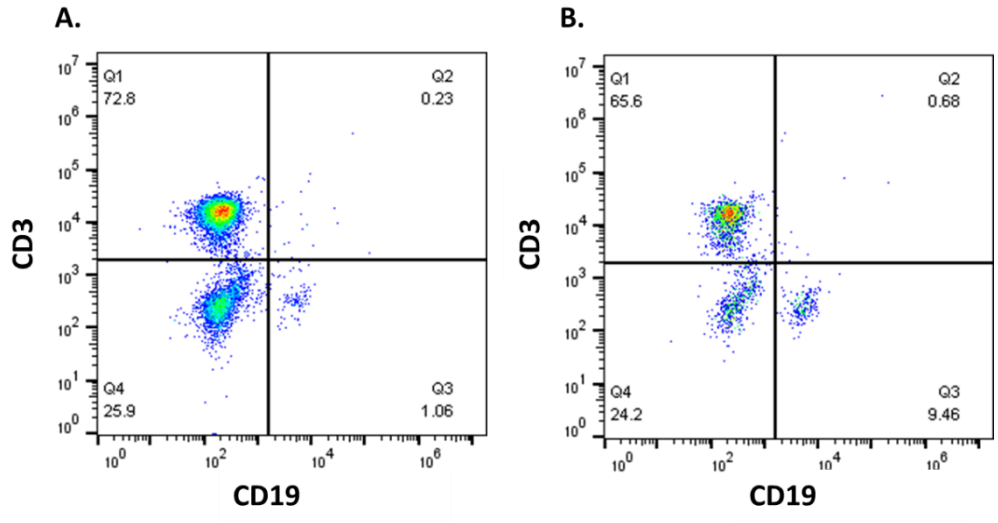


**Figure 5.4 – Flow cytometry analysis of supernatant following centrifugation for cell pelleting**

PBMC were isolated from peripheral blood and stained with B cell marker (CD19) and T-cell marker (CD3). Cells were collected via centrifugation at 250g for 5 minutes and both (A) cells and (B) supernatant were analysed using flow cytometry. Data represent n=1 experiment.

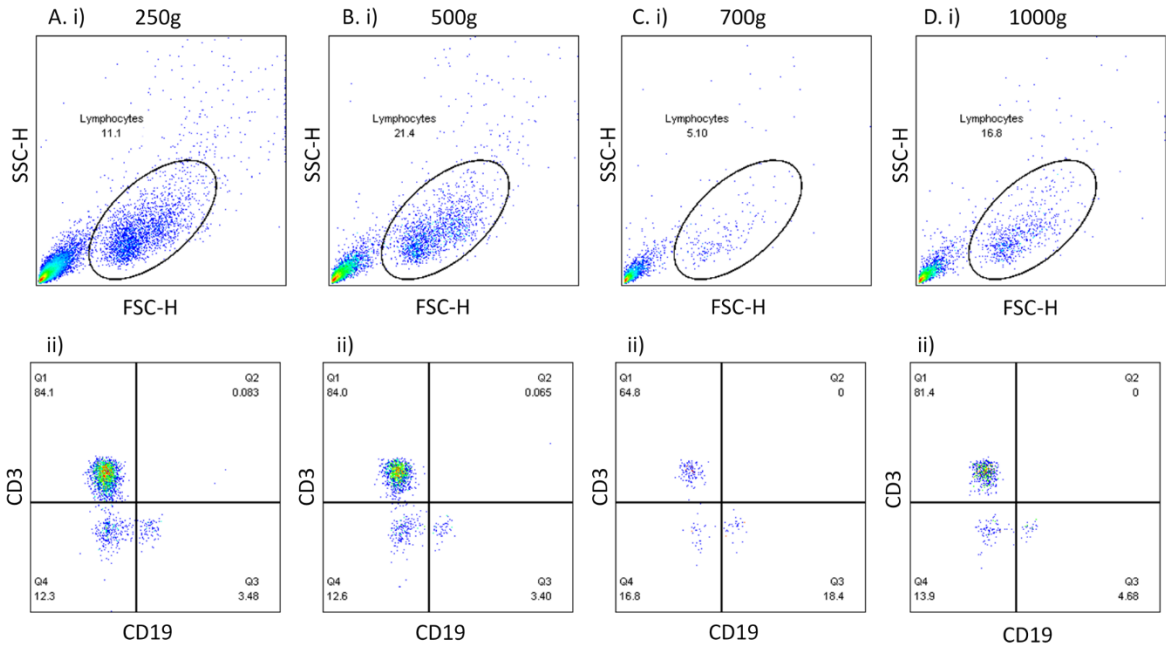


**Figure 5.5 - Flow cytometry analysis of PBL supernatants following different centrifugation forces for cell pelleting**

PBMC were isolated from peripheral blood and stained with B cell marker (CD19) and T-cell marker (CD3). Cells were collected via centrifugation at (A) 250 g, (B) 500 g, (C) 750 g or (D) 1000 g for 10 minutes and supernatants were analysed using flow cytometry. Representative images of (i) lymphocyte gate on forward vs side scatter plots and (ii) CD19 (B-cells) and CD3 (T-cells).

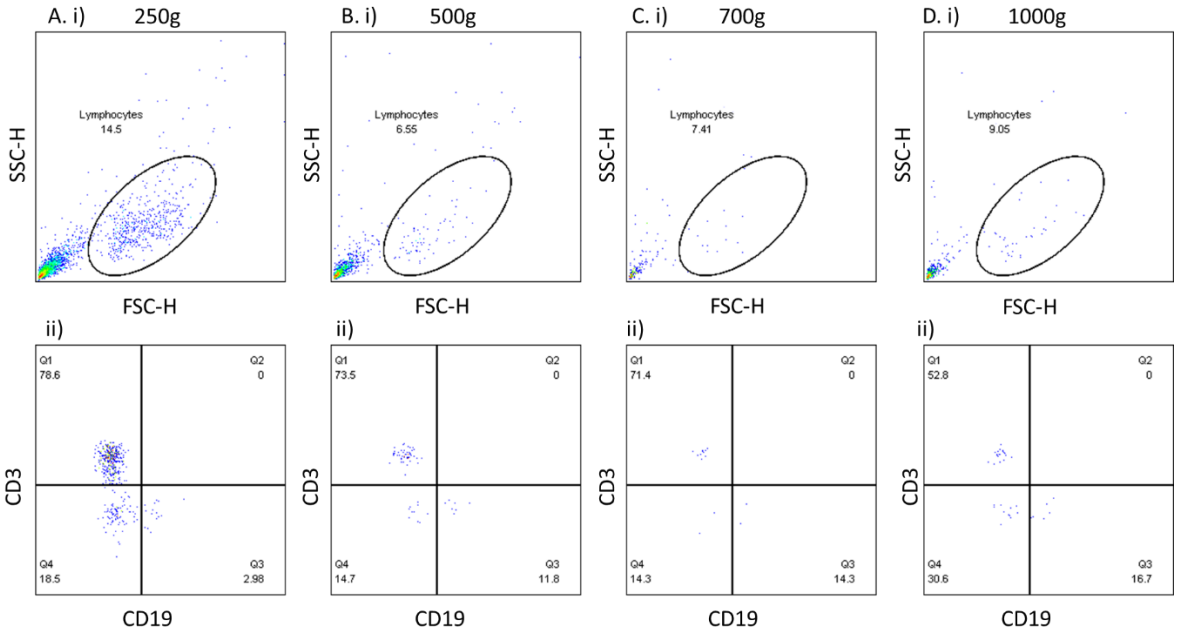


**Figure 5.6 - Flow cytometry analysis of PBL supernatants following different centrifugation forces for cell pelleting**

PBMC were isolated from peripheral blood and stained with B cell marker (CD19) and T-cell marker (CD3). Cells were collected via centrifugation at (A) 250 g, (B) 500 g, (C) 750 g or (D) 1000 g twice for 5 minutes with supernatant transferred to a fresh Eppendorf between spins, and supernatants were analysed using flow cytometry. Representative images of (i) lymphocyte gate on forward vs side scatter plots and (ii) CD19 (B-cells) and CD3 (T-cells).

**Table 5.1 – Total cell numbers recorded by flow cytometry following cell pelleting at different centrifuge speeds**

| Spin Time (minutes) | Spin Speed (g) | #Cells | #Lymphocytes | %B cells | #B cells |
|---|---|---|---|---|---|
| **5 x 2** | 250 | 3533 | 511 | 2.98 | 15 |
| | 500 | 1054 | 69 | 11.8 | 8 |
| | 750 | 189 | 14 | 14.3 | 2 |
| | 1000 | 409 | 37 | 16.7 | 6 |
| **10** | 250 | 22065 | 2443 | 3.48 | 84 |
| | 500 | 7246 | 1553 | 3.4 | 52 |
| | 750 | 3605 | 184 | 18.4 | 33 |
| | 1000 | 3702 | 622 | 4.68 | 29 |

Total cell, lymphocyte, and B-cell numbers in the supernatant of PBMC samples after cells have been collected via centrifugation. # = number

### *5.2.4. Characterising size and concentration of B-cell derived extracellular vesicles*

Nanoparticle tracking analysis (NTA) is a light-scattering technique where particles in suspension are illuminated by a laser beam and the scattered light is focussed onto an image sensor enabling movement of individual particles to be tracked. NTA was used to investigate size and concentration of B cell derived EV under resting conditions and following adiponectin-stimulation. NTA can be performed on many different devices and several publications are available addressing device-dependent NTA measurement variations (Kramberger *et al.*, 2012; Bachurski *et al.*, 2019). To increase accuracy of our results, we ran the same samples on two Nanosight models on the same day, the older LM10 and the newer NS300.

Using either model of nanosight, no significant difference was observed in size or concentration of vesicles released from control or AQ stimulated B-cells (Figure 5.7, Figure 5.8). Using the LM10, NTA identified vesicles in B-cell supernatants with a mean size of 273nm and concentration of $2.5x10^9$ (Figure 5.7). Interestingly, the NS300 recorded the same vesicles to have a significantly smaller mean size of 178nm and significantly lower concentration of $2.45 \times 10^8$ (Figure 5.9). Taken together, these data show adiponectin stimulation does not affect concentration or size of vesicles released from B-cells.

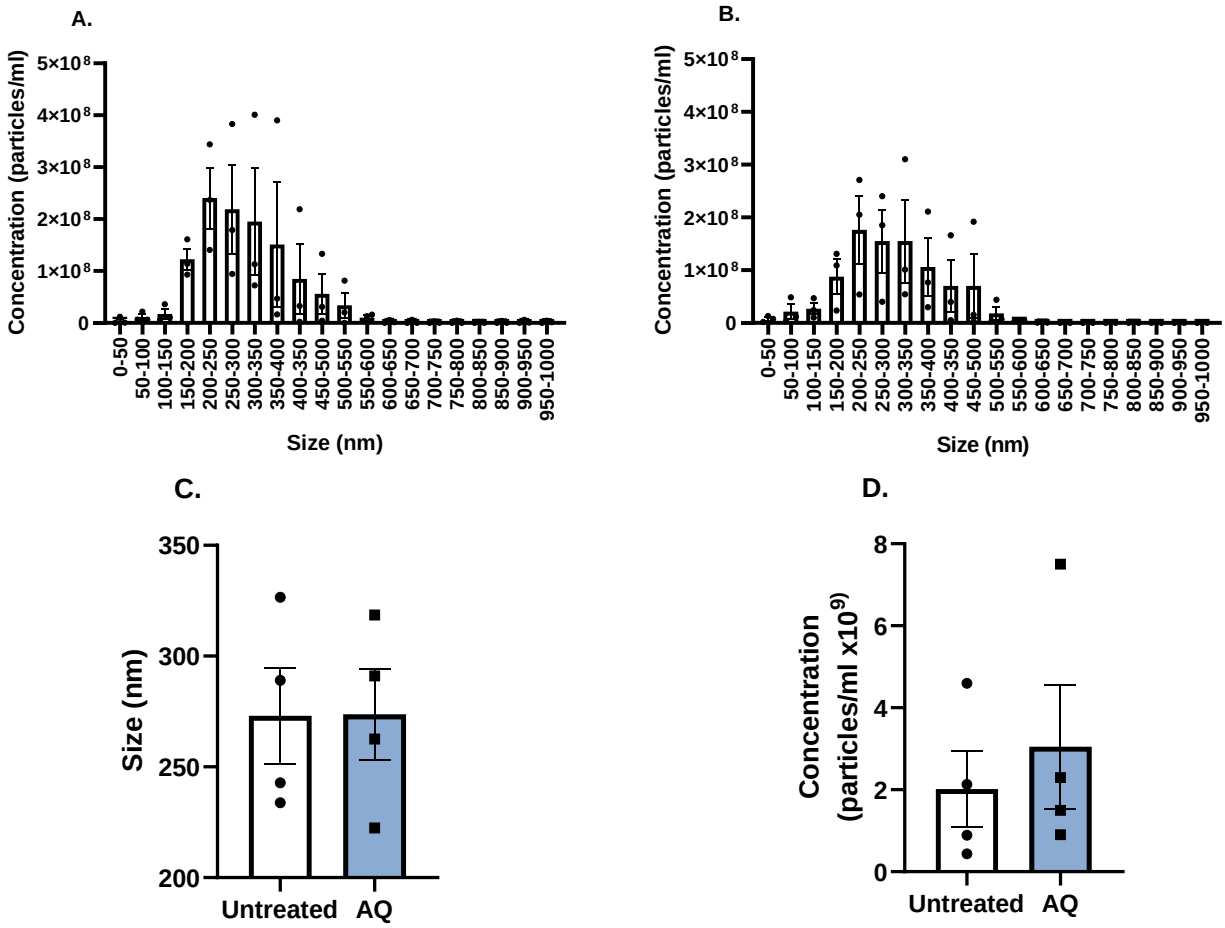


**Figure 5.7 – Size and concentration of B-cell derived extracellular vesicles measured using LM10**

B cells ($10x10^6$/ml) were stimulated with or without AQ (10 ug/ml) for 1 hour before cells were pelleted by centrifugation at 2000 g for 20 minutes. Supernatants were collected and subjected to a 13,000 g spin for 2 minutes to remove apoptotic bodies and large debris. Supernatants were diluted 1:5 in sterile filtered P-BSA (0.15%) to allow particle concentration to fall within the linear range of the LM10 nanosight (1-$10x10^8$/ml). Sixty-second videos (30 frames per second) were recorded from five different fields of view per sample. Videos were recorded with the camera level set at 13 and camera gain set at 1, and analysed with detection threshold set at 8. The mean size and particle concentration are calculated by the Nanoparticle Tracking Analysis software 2.2. Graphs showing concentration of particles within 50nm size ranges in (A) resting and (B) AQ-stimulated B cell supernatants. (C) Total mean size ± SEM of all vesicles is shown in untreated (control) and AQ-stimulated supernatants. (D) Total concentration ± SEM of all vesicles is shown in untreated (control) and AQ-stimulated supernatants (N=4). No significance determined using paired student's t-test. NS = $P > 0.05$.

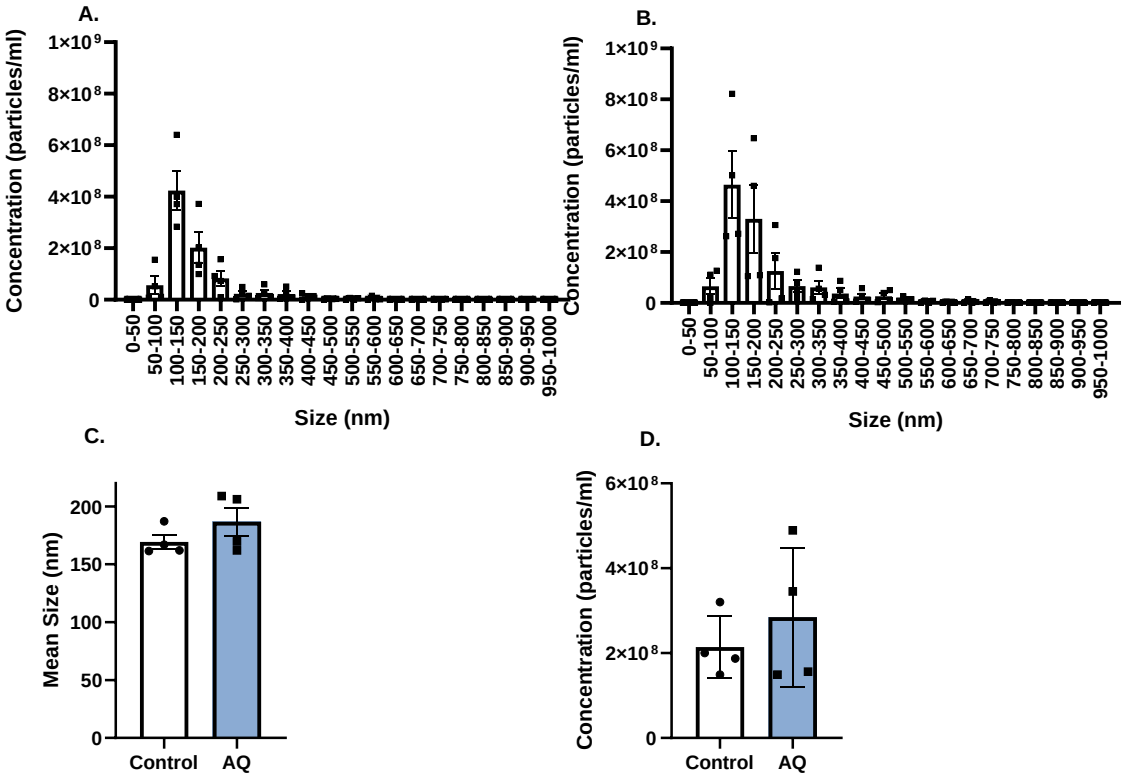


**Figure 5.8 - Size and concentration of B-cell derived extracellular vesicles measured using NS300**

B cells ($10x10^6$/ml) were stimulated with or without AQ (10 ug/ml) for 1 hour before cells were pelleted by centrifugation at 2000 g for 20 minutes. Supernatants were collected and subjected to a 13,000 g spin for 2 minutes to remove apoptotic bodies and large debris. Supernatants were diluted 1:5 in sterile filtered P-BSA (0.15%) to allow particle concentration to fall within the linear range of the NS300 nanosight (1-$10x10^8$/ml). Sixty-second videos (30 frames per second) were recorded from five different fields of view per sample. Videos were recorded with the camera level set at 13 and camera gain set at 1, and analysed with detection threshold set at 8. The mean size and particle concentration are calculated by the Nanoparticle Tracking Analysis software 2.2. Graphs showing concentration of particles within 50nm size ranges in (A) resting and (B) AQ-stimulated B cell supernatants. (C) Total mean size of all vesicles is shown in untreated (control) and AQ-stimulated supernatants. (D) Total concentration of all vesicles is shown in untreated (control) and AQ-stimulated supernatants (N=4). No significance determined using paired student's t-test. NS = P > 0.05.

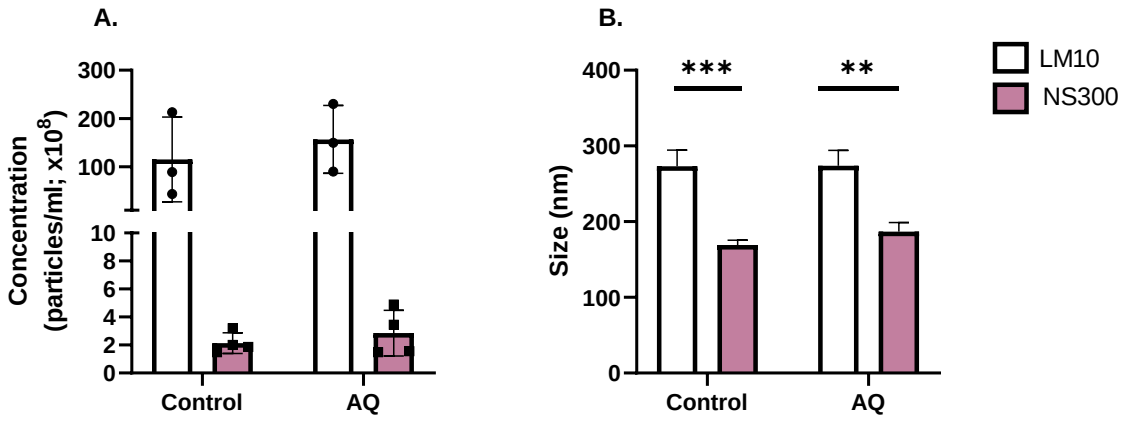


**Figure 5.9 – Comparison of LM10 and NS300**

B cells ($10x10^6$/ml) were stimulated with or without AQ (10 ug/ml) for 1 hour before cells were pelleted by centrifugation at 2000 g for 20 minutes. Supernatants were collected and subjected to a 13,000 g spin for 2 mins to remove apoptotic bodies and large debris. Supernatants were diluted 1:5 in sterile filtered P-BSA (0.15%) to allow particle concentration to fall within the linear range of the nanosight ($1\text{-}10x10^8$/ml). Sixty-second videos (30 frames per second) were recorded from five different fields of view per sample. Videos were recorded with the camera level set at 13 and camera gain set at 1, and analysed with detection threshold set at 8. The mean size and particle concentration are calculated by the Nanoparticle Tracking Analysis software 2.2. (A) Total concentration of all vesicles is shown in untreated (control) and AQ-stimulated supernatants (n=3-4) (B) Total mean size of all vesicles is shown in untreated (control) and AQ-stimulated supernatants (n=4). ** = ≤0.01 and P*** = P≤0.001 by paired student's t-test.

### *5.2.5. Investigating cargo of B-cell derived extracellular vesicles using western blot*

As we observed no significant difference in amount of vesicle release between unstimulated and adiponectin-stimulated B-cells, we next investigated if there were changes in amount of 14-3-3ζ present in the EVs. Exosomes are highly enriched in the tetraspanins CD9, CD63 and CD81 (Andreu and Yáñez-Mó, 2014) and have been identified by MISEV 2018 guidelines as proteins that can be analysed to demonstrate presence of EVs (Théry *et al.*, 2018). Calnexin is an endoplasmic reticulum protein abundant in cell lysates which can be used as a vesicle "exclusion marker" (Théry *et al.*, 2018). Therefore, we investigated our isolated EVs for expression of the tetraspanins and calnexin as positive and negative markers of EVs (respectively).

Supernatants from isolated B-cells were ultracentrifuged overnight to pellet EVs, which were subjected to western blotting for EV-associated tetraspanins, CD9, CD63 and CD81, calnexin, and 14-3-3ζ. All three samples expressed CD9 and CD63, however did not express CD81 or calnexin, and there was no difference between expression of these proteins between control and adiponectin-stimulated B-cells (Figure 5.10). There was very little expression of 14-3-3ζ in extracellular vesicles isolated from either sample (Figure 5.11).

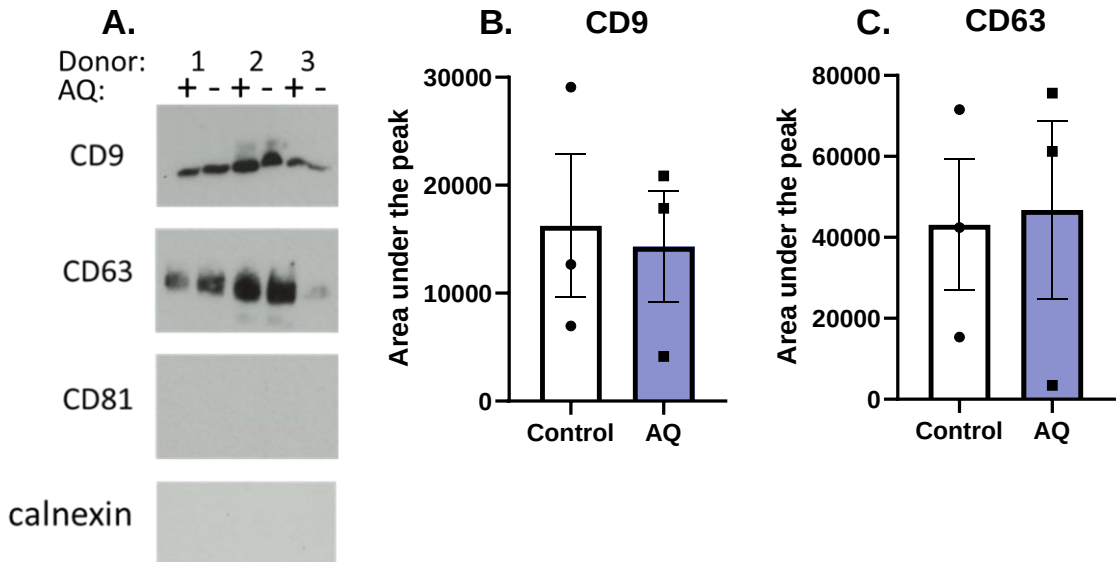


**Figure 5.10 - Expression of classical exosome-associated tetraspanins in isolated B-cell derived extracellular vesicles measured by western blot**

B cells ($10x10^6$/ml) were stimulated with or without AQ (10ug/ml) for 1 hour before cells were pelleted by centrifugation at 2000g for 20 minutes. Supernatants were collected and subjected to a 13,000g spin for 2 mins to remove apoptotic bodies and large debris, before being ultracentrifuged at 100,000g for 16 hours to pellet the extracellular vesicles. (A) EV pellets were lysed and subject to western blotting for exosomal tetraspanins CD9, CD63 and CD81, and exclusion marker calnexin. Data are shown as mean ± SEM, n=3 independent experiments using a different blood donor in each experiment. (A) Western blots from 3 donors. Area under the curve for (B) CD9 and (C) CD63. No significance determined using paired student's T-test. NS = $P > 0.05$.

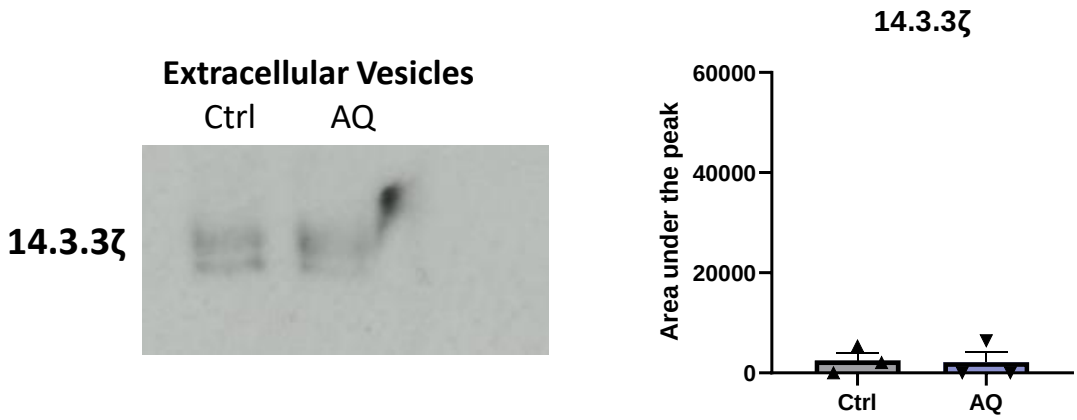


**Figure 5.11 – 14-3-3ζ expression in isolated B-cell derived extracellular vesicles measured by western blot**

B cells ($10x10^6$/ml) were stimulated with or without AQ (10 ug/ml) for 1 hour before cells were pelleted by centrifugation at 2000 g for 20 minutes. Supernatants were collected and subjected to a 13,000 g spin for 2 mins to remove apoptotic bodies and large debris, before being ultracentrifuged at 100,000 g for 16 hours to pellet the extracellular vesicles. EV pellets were lysed and subject to western blotting for expression of 14-3-3ζ. Data are shown as mean ± SEM, n=3 independent experiments using a different blood donor in each experiment. No significance determined using paired student's T-test. NS = P > 0.05.

### *5.2.1. Investigating cargo of B-cell derived extracellular vesicles using immuno-affinity capture and fluorescent staining*

To further investigate vesicle 14-3-3ζ expression, we utilised a method of immuno-affinity capture and fluorescent staining (Price *et al.*, 2023). Using the Exoview, EVs are immobilised onto capture chips expressing antibodies against CD9, CD63 and CD81. Captured EVs were then labelled with B-cell marker (CD19) and our protein of interest (14-3-3ζ). There was no difference between total particles captured between control and adiponectin-stimulated B-cells (Figure 5.12A). However, significantly different numbers of particles were captured by different capture antibodies. The smallest number of vesicles were captured by CD81, and the highest number of particles were captured by CD9 (Figure 5.12A). There were very few (<100) 14-3-3ζ positive EVs captured by any of the capture chips (Figure 5.12B), further supporting the evidence that 14-3-3ζ is not present on B-cell derived vesicles. CD19 was present on vesicles captured from all capture antibodies and from both control and adiponectin-stimulated B-cells (Figure 5.12C) (Figure 5.13).

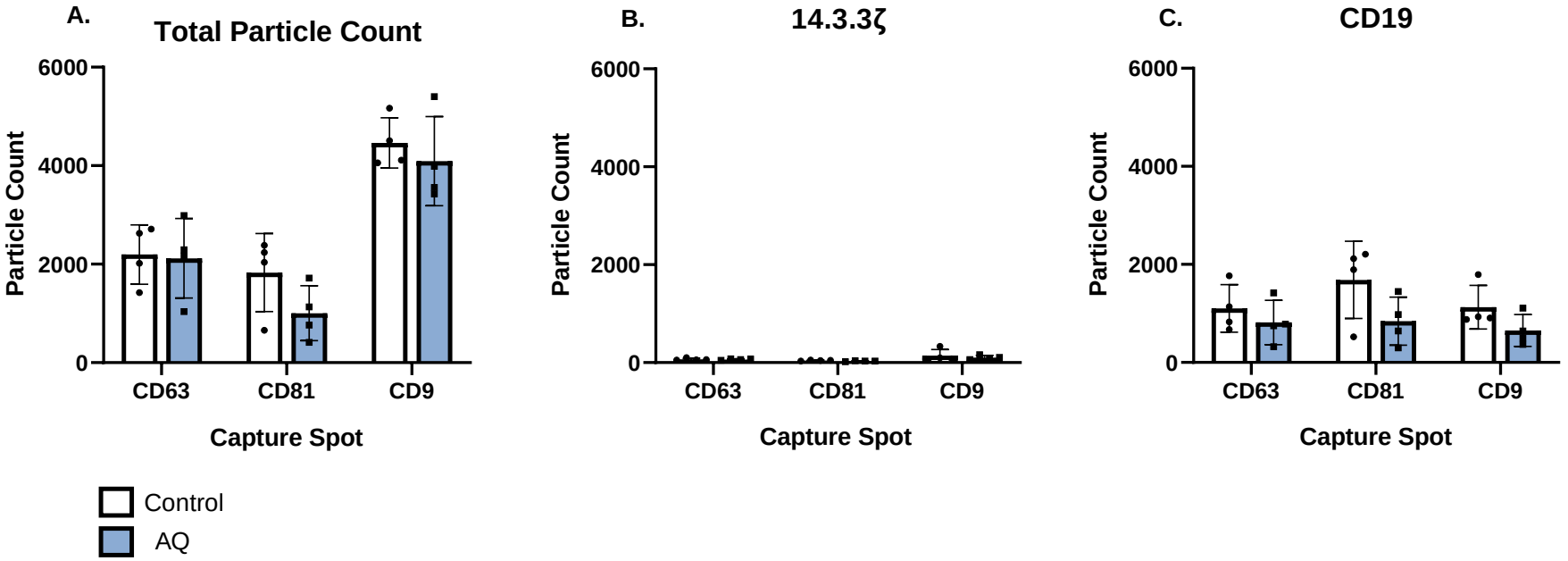


**Figure 5.12 - ExoView analysis of B-cell derived exosomes**

B cells ($10x10^6$/ml) were cultured for 1 hour before cells were pelleted by centrifugation and supernatants were collected. Supernatants were diluted 1:2 in incubation buffer and exosomes were captured on exoview tetraspanin chips expressing CD63, CD81, and CD9. (A) Total particle count on each tetraspanin chip. Exosomes were permeabilised and stained for (B) 14-3-3ζ (red) and (C) CD19 (blue). Data showing mean particle count ± SEM, n=4 independent experiments using a different blood donor in each experiment. Two-way ANOVA showed significant effect of capture spot on particle count, $p<0.0001$. * = $P\leq0.05$, ** = $P\leq0.01$, and *** = $P\leq0.001$ by Dunnett's multiple comparisons post-test.

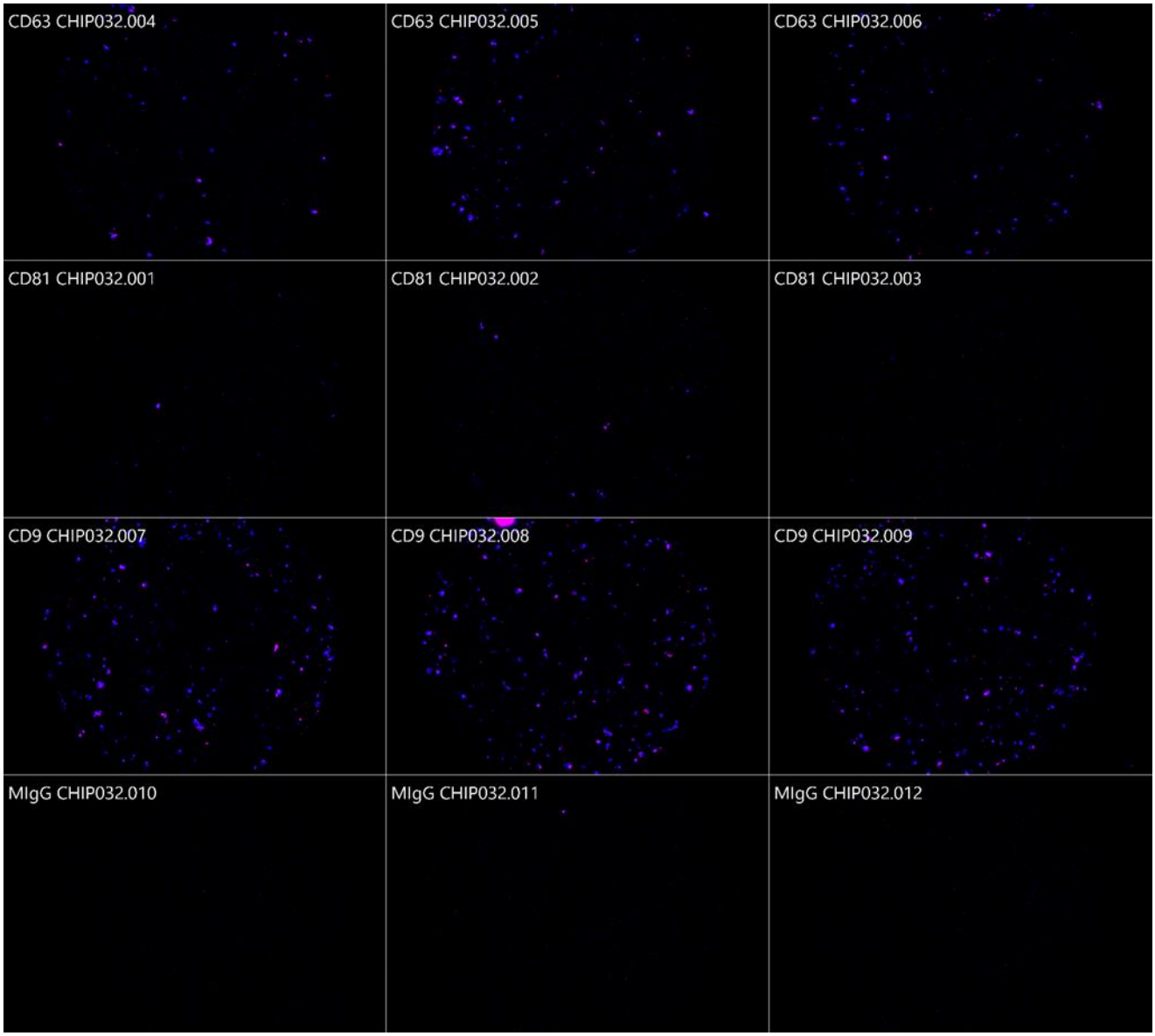


**Figure 5.13 – Fluorescent images of B-cell derived exosomes captured by ExoView**

B cells ($10x10^6$/ml) were cultured for 1 hour before cells were pelleted by centrifugation and supernatants were collected. Supernatants were diluted 1:2 in incubation buffer and exosomes were captured on exoview tetraspanin chips expressing CD63, CD81, CD9, and IgG control. Exosomes were permeabilised and stained for CD19 (blue) and 14-3-3ζ (red). Representative image from n=4 independent experiments using a different blood donor in each experiment.

### *5.2.2.* 14-3-3ζ *release via the classical secretory pathway*

It has previously been shown the effect of adiponectin on PBL transmigration is lost when used in the presence of brefeldin-A, an inhibitor of the classical secretory pathway (Chimen *et al.*, 2015). However, it is not known if this loss of function is due to inhibition of 14-3-3ζ secretion. Therefore, to investigate if 14-3-3ζ is being secreted from the B-cells via the classical secretory pathway, we performed western blotting on supernatants of adiponectin-stimulated B-cells. Adiponectin stimulation led to high amounts of 14-3-3ζ present in the B-cell supernatant (Figure 5.14). Addition of Brefeldin-A at 10ug/ml did not have a significant effect on 14-3-3ζ release, however at the higher concentration (100ug/ml) there was significantly reduced 14-3-3ζ present in the supernatant (Figure 5.14). Taken together, this data suggest 14-3-3ζ release is regulated via the classical secretory pathway as blockage of classical secretion results in reduced 14-3-3ζ presence in the B-cell secretome.

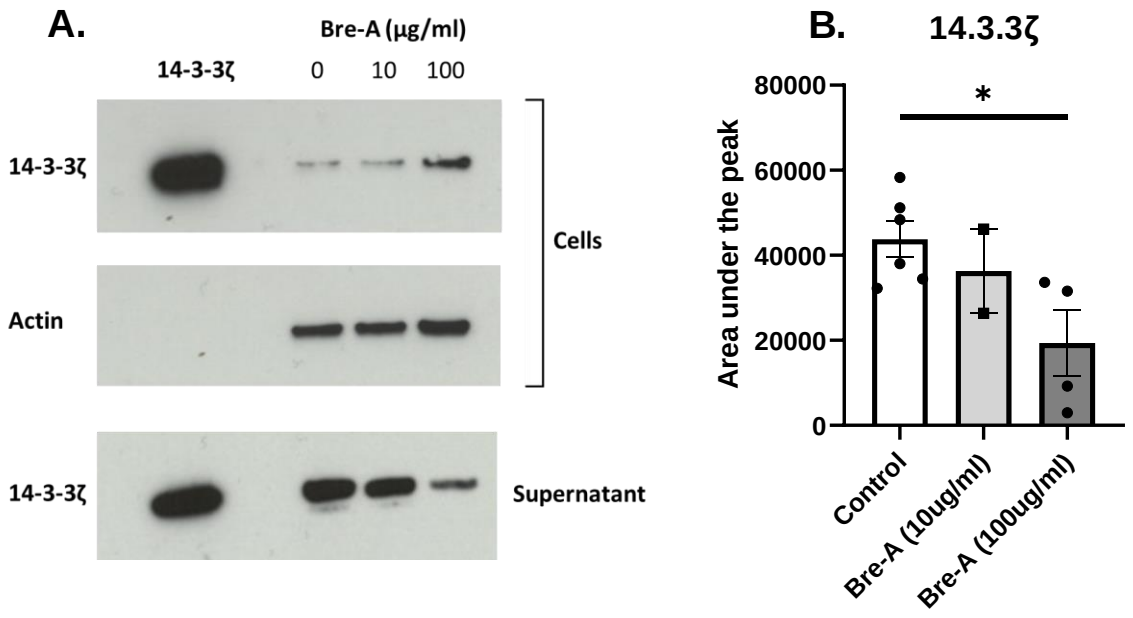


**Figure 5.14 – Western blot of B cell supernatants following Brefeldin-A treatment**

B-cells were stimulated with adiponectin (10 ug/ml) for one hour either in the absence of (control, white bars) or presence of brefeldin-A (Bre-A) at 10ug/ml or 100ug/ml. Cells were pelleted by centrifugation and lysed, supernatants were concentrated using vacuum centrifugation and lysed. Cells and supernatants were subjected to western blot for 14-3-3ζ. (A) Representative image of western blot, (B) Total 14-3-3ζ protein content in B-cell supernatants. Data are mean ± SEM. One-way ANOVA found significant effect of Brefeldin-A treatment on 14-3-3ζexpression, $P<0.05$. * = $P \leq 0.05$ by Dunnett's multiple comparisons test.

## 5.3. Discussion

PEPITEM is a homeostatic regulator of transendothelial migration that was thought to be secreted from B-cells following adiponectin stimulation. In this chapter, we have shown that in response to adiponectin, B cells secrete whole 14-3-3ζ protein which must then be further cleaved in the extracellular environment. As 14-3-3ζ proteins lack a traditional signal recognition peptide and are typically found in the cytoplasm, it was unclear how 14-3-3ζ secretion was occurring. Previous reports have shown 14-3-3ζ to be an exosomal protein (Buschow *et al.*, 2010), however we have shown adiponectin does not affect B-cell derived EV secretion or EV protein content, and we could not detect 14-3-3ζ in vesicles derived from B-cells. Notably, we identified 14-3-3ζ secretion to be regulated at least partly via the classical secretory pathway as blockade of protein transport from endoplasmic reticulum to golgi complex reduced levels of extracellular 14-3-3ζ. Taken together, our results suggest a novel mechanism involved in the PEPITEM pathway, as we have identified 14-3-3ζ to be released via the classical secretory pathway in response to adiponectin stimulation.

### *5.3.1. B-cell 14-3-3ζ secretion*

Using western blot analysis, we observed secretion of whole 14-3-3ζ protein from B-cells following adiponectin stimulation. Many intracellular roles of 14-3-3ζ are known, however roles for extracellular 14-3-3ζ in physiological conditions are yet to be elucidated. In pathology, monocytes and macrophages infected with HIV-1 virus *in vitro* secrete 14-3-3ζ (Ciborowsk*i et al*., 2007) and 14-3-3ζ is secreted from tumour-associated monocytes/macrophages in the ascetic fluid of patients with endothelial ovarian cancer (Kobayashi *et al.*, 2009). Interestingly, the 14 amino acid sequence of PEPITEM was detected via mass spec in these patients, as well as two

other peptides unique to the zeta isoform of 14-3-3. However, peptide fragmentation was used in sample preparation and PEPITEM can be produced via trypsin cleavage (Chimen *et al*., 2015). No mechanism for 14-3-3ζ secretion from these macrophages was suggested.

More recently, it was found macrophages stimulated with TNFα undergo swelling followed by necropoptosis which results in secretion of 14-3-3η into the extracellular space (Trimova *et al.*, 2020). Macrophages are known to release IL-1β following gasdermin D-dependent pyroptosis in a similar mechanism following inflammasome activation (Kayagaki *et al.*, 2015; Martin-Sanchez *et al.*, 2016), therefore this could represent a mechanism for 14-3-3ζ secretion from macrophages in other pathologies. However, no mechanism of activation-induced cell death leading to specific protein secretion has been identified in B-cells. Co-activation of IFN, toll-like receptor 7 (TLR-7) and the B-cell receptor (BCR) induces healthy B-cells to become hyperactive and increase cell death (Fan et al, 2014), however whether this cell death led to protein release was not investigated. To investigate this as a potential mechanism of 14-3-3ζ release, viability of B-cells following adiponectin-stimulation should be investigated. If cell death is initiated following adiponectin-stimulation, gasdermin-D inhibitors should be used to identify if this is the mechanism of action.

### *5.3.2. Flow cytometry for EV analysis*

Previously, flow cytometry has been used to investigate platelet derived EV (PEV) using lipid dyes (Chimen *et al.*, 2020). Platelets were labelled with PKH67 and stimulated with cross linked collagen related peptide (CRP-XL) to induce PEV production and analysed using an Accuri C6 flow cytometer. In this method, 500nm

and 900nm microspheres were used to set gates for microvesicles of different sizes. The supernatant containing PEV showed a large population of GP1ba+ vesicles within the 500-900nm range, however the flow cytometer failed to detect anything smaller than 500nm (Chimen *et al.*, 2020).

In this study, PEV were also characterised using NTA and the Exoview and amounts of PEV recorded between these varied to extreme levels, with flow cytometry detecting a fraction of the total PEV recorded using nanosight and exoview. The highest number of vesicles detected by nanosight were in the size range 150-200nm, which is significantly smaller than the limits of flow cytometry detection. The Exoview, which captures vesicles via tetraspanins often enriched on exosomes, recorded vesicles with an even smaller size range, peaking in 50-75nm. Variations in size recordings is dependent on isolation methods (immuno-affinity capture compared to ultracentrifugation) and device detection limits.

The size limitation of flow cytometry detection may be why we did not observe many vesicles using flow cytometry, as NTA recorded B-cell derived EV much smaller than 500nm. Flow cytometry can be used to detect small vesicles by binding to streptavidin-coated beads to capture biotinylated antibodies and subsequent staining of bead-bound EVs (Morales-Kastresana and Jones, 2017). More novel imaging flow cytometry devices are also being used which allow detection of small (<200nm), fluorescently labelled EVs (Gomez *et al.*, 2023), but these were not available to us for these studies.

### *5.3.3. B-cell agonists and EV release*

When investigating the use of flow cytometry for B-cell derived EV characterisation, we used positive controls CD40 and IL-4, and PMA, which are

known to stimulate EV release (Saunderson *et al.*, 2008). B-cell derived EV play important roles in immunological signalling due to their high levels of MHC class I and class II complexes, as well as components of the BCR complex (Muntasell, Berger and Roche, 2007; Saunderson *et al.*, 2008). Activated B-cells recycle surface pMHC-II complexes and release them through exosomes, which can stimulate primed CD4 T-cells (Muntasell, Berger and Roche, 2007). Antigen-specific T-cells in turn can stimulate B-cells and initiate exosome release, creating a positive feedback loop of exosome release (Muntasell, Berger and Roche, 2007). B-cells also secrete MHC+ exosomes in response to BCR and TLR9 stimulation, but not IL-4 alone (Arita *et al.*, 2008). Our data revealed adiponectin stimulation did not lead to increased amounts of B-cell EV release. As adiponectin induces the PEPITEM pathway, a regulator of immunity, it makes sense this does not also lead to increased EV release which would act in a pro-inflammatory manner.

### *5.3.4. Limitations of nanoparticle tracking analysis*

We investigated EV release from B-cells as a potential mechanism of 14-3-3ζ secretion. Our data showed B-cells constitutively secrete vesicles and vesicle secretion does not change in response to adiponectin stimulation. Using nanoparticle tracking analysis, we observed a discrepancy between vesicle size and concentration recorded between different machines. The LM10 recorded significantly more vesicles than the NS300, and recorded a larger mean size than its counterpart. NTA is a light-scattering technique which records particles moving in Brownian motion, however standardisation between instruments is still lacking (Gardine*r et al*., 2013). To limit our inter-machine discrepancy, we followed the standardisation protocol laid out by Gardiner et al, 2013. Despite this, discrepancies have been recorded between different NTA models and even between the same machine on

different days. A study measuring the same sample of Ad5 virus every day for 4 consecutive days at the same settings revealed the LM10 has up to a 14% inter-day variations in concentration recordings (Kramberger *et al.*, 2012). Using microbeads of known size and concentration, the LM10 was also found to underestimate particle concentration by 15% (Kramberger *et al.*, 2012). In another study comparing NTA output between different NTA devices, the NanoSight NS300 exhibited a 2-fold overestimation of particle concentration and a much larger coefficient of variation compared to a different device, the ZetaView (Bachurski *et al.*, 2019). These studies, along with our data, highlight inaccuracies that can be recorded using nanoparticle tracking analysis and shows the need for use of microbeads for correct standardisation between recordings made on separate devices, but also to limit variations on the same machine. Reasons for such high discrepancies between recordings include device sensitivity to temperature and external vibrations, as well as incorrect recordings of sample viscosity, cleanliness of the optical glass surface, and duration of measurements (Gardiner *et al.*, 2013).

### *5.3.5. 14-3-3ζ and vesicles*

We did not observe the presence of 14-3-3ζ in B-cell derived EVs using western blotting or fluorescent labelling following immuno-affinity capture of exosomes. Several 14-3-3ζ proteins have been identified in exosomes derived from cancer cells (Keerthikumar et al., 2016). 14-3-3ζ has also previously been identified in exosomes derived from EBV-transformed B-cell lines via mass spectrometry (Buschow *et al.*, 2010), however 14-3-3ζ has never been identified in EV derived from primary B-cells. 14-3-3ζ is often upregulated in cancers (Neal and Yu, 2010), which may explain why we did not detect 14-3-3ζ on EV released from healthy B-cells.

Using two different methods, we isolated B-cell derived EVs and stained for classical EV markers, CD9, CD63 and CD81. Western blotting EVs isolated via ultracentrifugation revealed CD63 and CD9 positive vesicles, but no CD81 was detected in this way. In accordance with International Society for Extracellular Vesicles guidelines (MISEV 2018), we also tested purity of these EV samples by staining for the endoplasmic reticulum marker, calnexin. The absence of calnexin from our samples reveals EV purity. Using immuno-affinity capture and fluorescent staining via the Exoview, vesicles were captured from all capture chips including the chips coated in anti-CD81, although notably at lower amounts than CD9 and CD63. Taken together, it appears B-cell derived EV are positive for all three of the classical exosomal tetraspanins, but CD81 is expressed at lower amounts.

Overall, in an ever-growing field of EV research with adapting techniques there needs to be rigid standardisation to support reliable and accurate data reporting. The International Society for Extracellular Vesicles have released guidelines which are updated regularly to help support the advancement of this field (Théry *et al.*, 2018).

### *5.3.6. Classical secretory pathway*

We discovered 14-3-3ζ secretion from adiponectin-stimulated B-cells was inhibited with the addition of an inhibitor of the classical secretory pathway, brefeldin-A. This supports previous findings from our lab that show brefeldin-A inhibits the function of adiponectin on lymphocyte transmigration (Chime*n et al*., 2015). Importantly, this poses a question as 14-3-3ζ lacks any signal recognition particle which is required secretion via the classical secretory pathway (Liu *et al.*, 1995). The two requirements for unconventional protein secretion are 1) lack of a classical signal sequence and 2) secretion is not affected by using inhibitors of classical

secretion (such as brefeldin-A) (Cohen, Chirico and Lipke, 2020). Before now, there are very few reports of proteins that lack a signal recognition particle yet whose secretion is blocked with brefeldin-A. For example, human CKLF-like MARVEL transmembrane domain-containing 5 (CMTM5-v1), a secreted protein which has various roles in regulation of the autoimmune system, is associated with small vesicles (<100nm) however has no co-localisation with CD63 or the golgi complex (Li et al, 2009). Notably, secretion of CMTM5-v1 is inhibited by brefeldin-A, but not by wortmanin, which inhibits the formation of multivesicular bodies (Li et al, 2009). The study reports that the CMTM5-v1 containing vesicles are similar in size and density to that of exosomes, however they have a different secretory pathway from exosomes (Li et al, 2009). Similarly, another report showed brefeldin-A inhibited secretion of TNFR1 exosome-like vesicles, similar to those found containing CMTM5-v1 (Islam et al., 2007). Our data is the first report of a non-classical secreted protein blocked by brefeldin-A, which is not secreted associated with vesicles.

There is no definite route of unclassical protein secretion which makes it difficult to investigate. One hypothesis for the mechanism of 14-3-3 release is it may be secreted in a complex with, or bound to, another classically secreted protein which contains a signal recognition particle. However this protein would also need to be selectively secreted following adiponectin stimulation and nothing other than PEPITEM was identified in the initial mass spec screen (Chimen et al, 2015). Future work should use computational modelling to identify potential binding partners of 14-3-3ζ and highlight any potential carriers. Importantly, future work should also follow the experimentally-based guide by Cohen et al (2020) to rule out other pathways of unconventional secretion including; secretion via a specific transporter, translocating

across the plasma membrane directly by binding to the PM or through liposomes or entering the lumen of a multivesicular body or autophagosome.

### *5.3.7. Limitations*

As previously mentioned, the most significant limitation of EV research surrounds a lack of standardised protocols for isolation and characterisation of small nanoparticles. To overcome this, we followed the MISEV2018 guidelines in our experimental design and analysis and published protocol standardisation for nanoparticle tracking analysis (Gardiner et al, 2013). Another limitation was an inability to show functionally vesicles are not involved in the PEPITEM pathway. For this, depletion experiments would be required involving overnight centrifugation of B-cell supernatants before addition of vesicle free B-cell supernatants and into the static transmigration assay.

All B-cell experiments require vast amounts of blood and time consuming isolation steps, and follow on experiments have to be completed on the same day. This means many of these experiments have low numbers of biological replicates (n=3-4). Many studies on EV research use cell-lines to overcome this limitation, however these are not always physiologically relevant as we have shown in the previous chapter.

### *5.3.8. Conclusions*

Here, we have shown B-cells secrete whole 14-3-3ζ protein into the extracellular environment following stimulation with adiponectin. We have shown the mechanism of release of 14-3-3ζ is via the classical secretory pathway and is not in association with microvesicles. Notably, as 14-3-3ζ lacks the requirements for classical secretion, we have identified a novel route of unclassical secretion which is

also blocked by brefeldin-A. Future work is required to elucidate this mechanism of release further, with a focus on identifying potential carrier proteins that may be able to associate with 14-3-3ζ and facilitate transport out of the cell.

# Chapter 6. GENERAL DISCUSSION

## 6.1. Summary of Findings

This thesis aimed to identify the protease(s) involved in PEPITEM cleavage and investigate their regulation in endothelial cells. By using computational modelling and *in vitro* inhibitor studies, we identified non-redundant roles for both MMP-2 and MMP-9 in cleavage of 14-3-3ζ into PEPITEM. Using publicly available transcriptomics datasets and in house gene and protein expression studies, we investigated regulation of MMP-2 and MMP-9 in inflamed endothelium. We identified a novel mechanism of MMP-2 regulation in response to inflammatory stimuli by downregulation of endogenous inhibitors. The final part of this thesis aimed to explore the mechanism of PEPITEM secretion. We discovered whole, intact 14-3-3ζ was secreted from the B-cell in response to adiponectin which is then cleaved into PEPITEM extracellularly. To explore mechanisms of secretion, we investigated B-cell derived EV and classical protein secretion. The main findings from this thesis are as follows:

- Inflammation regulates endothelial cell MMP-2 and MMP-9 expression and function. MMP-9 is expressed at low levels in unstimulated EC, and transcription and translation are increased in response to TNFα stimulation. MMP-2 is expressed constitutively but activity is increased in response to TNFα, likely in consequence of downregulation of the endogenous inhibitors TIMP1 and TIMP2.
- MMP-2 and MMP-9 are both independently required for cleavage of 14-3-3ζ into functional peptide. Inhibition or silencing of either protease abolishes the inhibitory effect of 14-3-3ζ on leukocyte trafficking.

- PEPITEM needs to be further proteolytically cleaved into smaller, functional peptides to exert an immunoregulatory effect. Protease inhibition prevents PEPITEM from having an effect on T-cell transendothelial migration.
- MMP-2 has a role in leukocyte migration and inhibition of MMP-2 in both the leukocyte population and the endothelial cells results in significantly reduced transmigration of leukocytes.
- Adiponectin stimulated B cells secrete whole 14-3-3ζ protein, which is cleaved into PEPITEM in the extracellular environment. Despite being an unconventionally secreted protein, 14-3-3ζ secretion is reduced in the presence of an inhibitor of the classical secretory pathway highlighting a novel mechanism of secretion of unconventional proteins.
- B-cell EV release is not under the regulation of adiponectin signalling

In conclusion, we report that 14-3-3ζ is secreted via the classical secretory pathway and subsequently cleaved by MMP-2 and MMP-9 to generate PEPITEM once in the extracellular environment. A graphical summary of this thesis can be found in Figure 6.1.

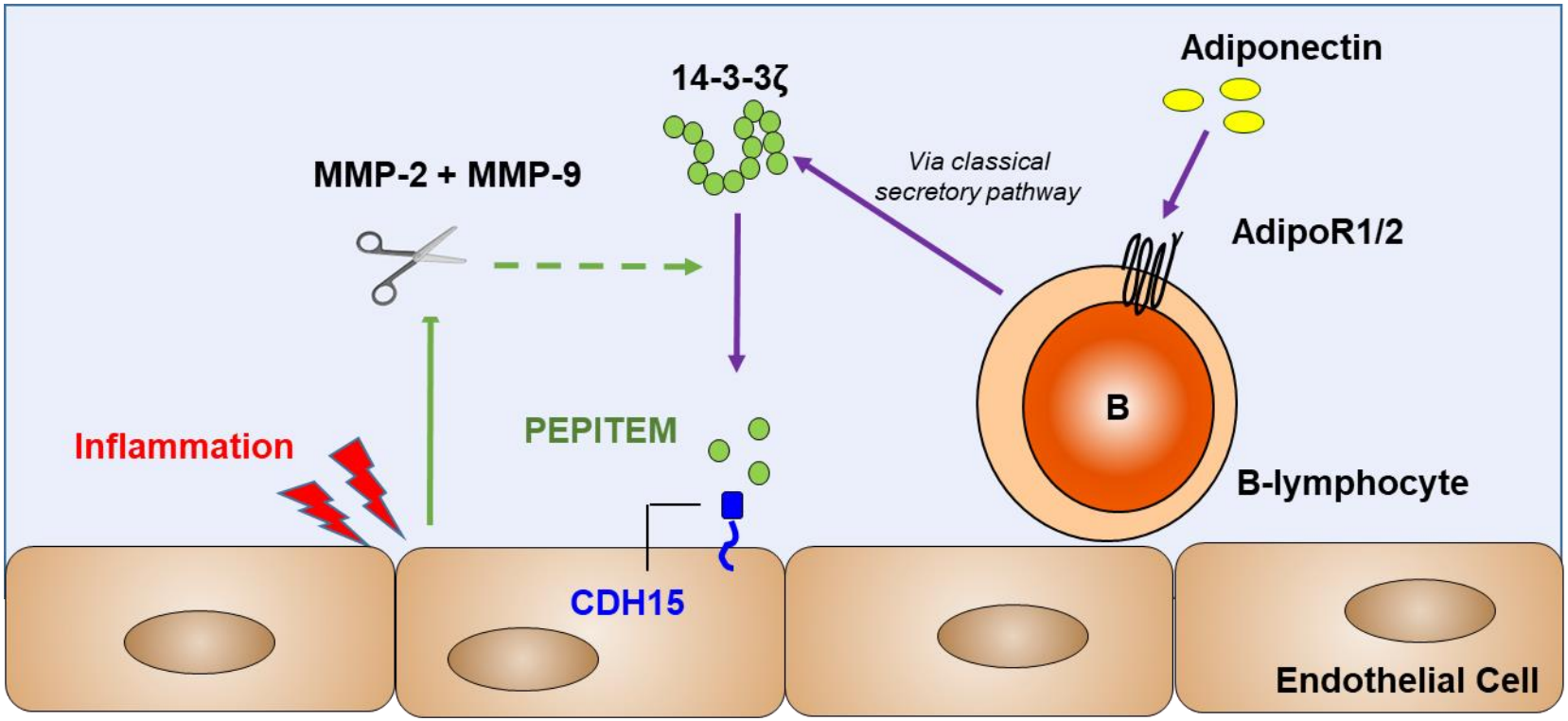


**Figure 6.1 – Updated understanding of the induction of the PEPITEM pathway**

Adiponectin binds to adiponectin receptors (AdipoR1 / AdipoR2) on the surface on B-cells. B-cells secrete 14-3-3ζ via the classical secretory pathway. Inflamed endothelium produce and secrete the proteases MMP2 and MMP9 which are both required to proteolytically cleave 14-3-3ζ into PEPITEM and other active peptides. These functional peptides bind to CDH15 on the surface on the endothelial cells and triggers the downstream effects of the PEPITEM pathway. CDH15: cadherin-1

## 6.2. Significance of findings

T-cell driven autoimmune diseases such as RA, psoriasis, and T1D have a significant impact on patients' quality of life as well as having a huge economic burden on individuals and health care systems. Current treatments are often expensive, limited in efficacy, and can have life-threatening side effects (Bullock *et al.*, 2018). The PEPITEM pathway may represent a promising therapeutic gateway in inflammatory disease, and addition of exogenous PEPITEM may be able to reduce the chronic inflammation seen in these patients.

T-cell targeted therapies are actively used in treatment for certain inflammatory conditions and target different areas of T-cell biology. Abaptacept is a human fusion protein approved for treatment of RA and juvenile idiopathic arthritis (Kuek, Hazleman and Östör, 2007). T-cell activation requires important co-stimulatory signals in conjunction with TCR engagement. CD28 expressed on T-cells binds to CD80/CD86 on antigen presenting cells and mediates activation via the MAPK, AKT and NFκB pathways (Alegre, Frauwirth and Thompson, 2001). Cytotoxic T lymphocyte-associated antigen (CTLA4) is an inhibitory counterpart also present on the T-cell surface that binds CD80/CD86 to acts as an immune checkpoint and regulate the immune response (Alegre, Frauwirth and Thompson, 2001). Abatacept is made up of the extracellular region of CTLA-4 and attached to an Ig-G Fc region which inhibits CD28 signaling by occupying the CD80 and CD86 receptors (Liu, Yu and Hu, 2021).

Natalizumab is an existing T-cell therapy for relapsing remitting multiple sclerosis that inhibits T-cell migration into brain tissue. Like PEPITEM, it works by inhibiting interactions between leukocyte integrins and adhesion molecules on endothelial

cells. Natalizumab binds α4β1-integrin and blocks its interaction with VCAM-1 (Hutchinson, 2007). However, Natalizumab is not approved for other inflammatory conditions due to an increased risk of progressive multifocal leukoencephalopathy (Bloomgren *et al.*, 2012). Other T-cell directed biologics include Teplizumab, a monoclonal antibody which binds to CD3 on the TCR and is used to delay the onset of T1D (Masharani and Becker, 2010), and Iscalimab, an anti-CD40 antibody currently in development for inhibition of organ transplant rejection (Espié *et al.*, 2020).

Despite extensive progress in the field of inflammatory biology, these treatments are still far from ideal. Antibody-based therapies can have serious side effects including increased risk of infections and neurological diseases (Bullock *et al.*, 2018). Biologics also show limited success in long-term treatment and have expensive production costs, which puts strain on individuals and health care systems due to the long-term use needed in chronic conditions (Tanaka, 2021). Therefore, there is a clear need for more efficient, cost-effective, and less toxic therapeutics for chronic inflammatory disease.

PEPITEM represents a therapeutic strategy that would overcome many of these hurdles, due to its high efficacy at low concentrations, safety demonstrated in short-term *in vivo* animal studies, and would be more cost-effective than antibody production. In addition, the PEPITEM pathway is known to be dysregulated in conditions such as T1D and RA, and the therapeutic strategy in these cases would focus on restoration of a homeostatic pathway rather than inhibition of a pathological process.

One of the biggest limitations of using PEPITEM as a therapeutic is its short half-life. Due to its small size (14-amino acids), PEPITEM is rapidly cleared by the kidneys. Intravenous administration of radiolabelled PEPITEM in wild-type mice revealed a circulatory half-life of <2 minutes (Apta, 2015). For use as a therapeutic, the half-life would need to be increased to be able to mediate its effects on the target. Current methods to increase therapeutic half-life of proteins include addition of polyethylene glycol (PEG), which would increase the molecular weight and reduce elimination by the kidneys, and would also protect the protein from enzymatic degradation (Zaman et al, 2019). Previous work in our lab has synthesised pegylated-PEPITEM and shown it has a similar efficacy in vitro to the native peptide (Apta, 2015), although further work is required to investigate its pharmacokinetic properties *in vivo*. Another method to increase time of drug in circulation is via carrier mediated delivery, which acts to slowly release the therapeutic over a longer period of time (Zaman *et al.*, 2019). *In vivo* experiments have been performed using PEPITEM contained in liposomes and similar functional effects were observed when PEPITEM-liposomes were given twice-weekly compared to daily intraperitoneal (IP) injections (Lewis, 2021). In contrast, every-other-day IP injections failed to show any functional effect (Lewis, 2021). Therefore, delivery of PEPITEM in liposomes may represent a method of increasing availability of PEPITEM therapeutically.

Using amino acid substitutions and peptide truncations, two active pharmacophores have been identified in the PEPITEM sequence, SVT and QGA (unpublished). These are currently being investigated as potential therapeutics, however, further *in vitro* and *in vivo* studies are required to elucidate the pharmacokinetics and pharmacodynamics of these trimers compared to PEPITEM.

Route of administration is another key decision of drug development. Oral delivery is often the most desirable route as it is non-invasive and can be managed by the patient. However, in the case of PEPITEM this may be problematic due to its rapid renal clearance. For certain conditions, such as inflammation of the skin or eye, topical administration may be applicable. This would eliminate the need to consider the effects of gut absorption and entrance into the blood stream on bioavailability, and would provide a much more direct route of administration. PEPITEM has also been shown previously to mediate beneficial effects in animal models of eye inflammation (Chimen *et al.*, 2015). Indeed, in a model of LPS-induced autoimmune uveitis in C57Bl6 wild type mice, PEPITEM reduced the number of T-cells in the ocular infiltrate (Chimen *et al.*, 2015). Therefore, further investigation into the function of PEPITEM in topical conditions may provide the most convenient method of using PEPITEM as a therapeutic.

### 6.3. Future Directions

Our studies have provided a greater understanding of the mechanisms surrounding PEPITEM production and release. However, additional work is still needed to further understand the biology of the PEPITEM pathway and to fully unlock its therapeutic potential.

*Cleavage of 14-3-3ζ into active peptides:*

- Determine if MMP-2 is responsible for further cleavage of PEPITEM into smaller active peptides using *in vitro* transmigration assays, and identify the sequence of these peptides

- Elucidate the specific areas of the 14-3-3ζ sequence that MMP-2 and MMP-9 are cleaving, and identify if there is a stepwise sequence of activation of these proteases
- Investigate leukocyte trafficking in response to 14-3-3ζ in MMP-2 and MMP-9 knockout mice

*Mechanisms of 14-3-3ζ secretion*

- Investigate if 14-3-3ζ is being secreted associated with a classically secreted protein / complex
- Elucidate the exact mechanism of 14-3-3ζ export from the B-cell

*Therapeutic potential of PEPITEM*

- Develop synthetic versions of PEPITEM / smaller pharmacophores with increased half-life
- Formulate a carrier-mediated delivery system to deliver PEPITEM therapeutically
- Further investigate PEPITEM in the context of topical inflammatory conditions as this seems the most viable route of PEPITEM administration

# REFERENCES


Abbitt, K. B. and Nash, G. B. (2003) 'Rheological properties of the blood influencing selectin-mediated adhesion of flowing leukocytes', *American journal of physiology. Heart and circulatory physiology*, 285(1). doi: 10.1152/AJPHEART.00408.2002.

Admyre, C. *et al.* (2007) 'Exosomes with immune modulatory features are present in human breast milk', *Journal of immunology (Baltimore, Md. : 1950)*, 179(3), pp. 1969–1978. doi: 10.4049/JIMMUNOL.179.3.1969.

Agrawal, S. *et al.* (2006) 'Dystroglycan is selectively cleaved at the parenchymal basement membrane at sites of leukocyte extravasation in experimental autoimmune encephalomyelitis', *The Journal of Experimental Medicine*, 203(4), p. 1007. doi: 10.1084/JEM.20051342.

Alberts, B. *et al.* (2002) 'B Cells and Antibodies', in *Molecular Biology of the Cell*. 4th Editio. Garland Science. Available at: https://www.ncbi.nlm.nih.gov/books/NBK26884/ (Accessed: 29 September 2023).

Alegre, M.-L., Frauwirth, K. A. and Thompson, C. B. (2001) 'T-CELL REGULATION BY CD28 AND CTLA-4', 1. Available at: www.nature.com/reviews/immunol (Accessed: 12 September 2023).

Alon, R., Hammer, D. A. and Springer, T. A. (1995) 'Lifetime of the P-selectin-carbohydrate bond and its response to tensile force in hydrodynamic flow', *Nature 1995 374:6522*, 374(6522), pp. 539–542. doi: 10.1038/374539a0.

Andersson, M. *et al.* (2005) 'Differential global gene expression response patterns of human endothelium exposed to shear stress and intraluminal pressure', *Journal of vascular research*, 42(5), pp. 441–452. doi: 10.1159/000087983.

Andreu, Z. and Yáñez-Mó, M. (2014) 'Tetraspanins in extracellular vesicle formation and function', *Frontiers in Immunology*, 5(SEP), p. 109543. doi: 10.3389/FIMMU.2014.00442/BIBTEX.

Von Andrian, U. H. *et al.* (1993) 'L-Selectin Mediates Neutrophil Rolling in Inflamed Venules Through Sialyl Lewisx-Dependent and -Independent Recognition Pathways', *Blood*, 82(1), pp. 182–191. doi: 10.1182/BLOOD.V82.1.182.BLOODJOURNAL821182.

von Andrian, U. H. and Mackay, C. R. (2000) 'T-cell function and migration. Two sides of the same coin', *The New England journal of medicine*, 343(14), pp. 1020–1034. doi: 10.1056/NEJM200010053431407.

Apta, B. (2016) *Investigating the Structure and Function of PEPITEM, a Novel Inhibitor of T cell Transmigration*.

Apta, B. H. R. (2015) *Investigating the Structure and Function of PEPITEM, a Novel Inhibitor of T cell Transmigration*. University of Birmingham. Available at: https://etheses.bham.ac.uk/id/eprint/6762/11/Apta16PhD.pdf.

Arita, S. *et al.* (2008) 'B cell activation regulates exosomal HLA production', *European journal of immunology*, 38(5), pp. 1423–1434. doi: 10.1002/EJI.200737694.

Arkell, J. and Jackson, C. J. (2003) 'Constitutive secretion of MMP9 by early-passage cultured human endothelial cells', *Cell Biochemistry and Function*, 21(4), pp. 381–386. doi: 10.1002/CBF.1037.

Arnaout, M. A., Mahalingam, B. and Xiong, J.-P. (2005) 'INTEGRIN STRUCTURE, ALLOSTERY, AND BIDIRECTIONAL SIGNALING', *http://dx.doi.org/10.1146/annurev.cellbio.21.090704.151217*, 21, pp. 381–410. doi: 10.1146/ANNUREV.CELLBIO.21.090704.151217.

Bachurski, D. *et al.* (2019) 'Extracellular vesicle measurements with nanoparticle tracking analysis – An accuracy and repeatability comparison between NanoSight NS300 and ZetaView'. doi: 10.1080/20013078.2019.1596016.

Balashov, K. E. *et al.* (1999) 'CCR5+ and CXCR3+ T cells are increased in multiple sclerosis and their ligands MIP-1α and IP-10 are expressed in demyelinating brain lesions', *Proceedings of the National Academy of Sciences of the United States of America*, 96(12), p. 6873. doi: 10.1073/PNAS.96.12.6873.

Bar-Or, A. *et al.* (2003) 'Analyses of all matrix metalloproteinase members in leukocytes emphasize monocytes as major inflammatory mediators in multiple sclerosis', *Brain*, 126(12), pp. 2738–2749. doi: 10.1093/BRAIN/AWG285.

Barker, K. S. *et al.* (2008) 'Transcriptome Profile of the Vascular Endothelial Cell Response to Candida albicans', *The Journal of Infectious Diseases*, 198(2), pp. 193–202. doi: 10.1086/589516.

Barlowe, C. *et al.* (1994) 'COPII: a membrane coat formed by Sec proteins that drive vesicle budding from the endoplasmic reticulum', *Cell*, 77(6), pp. 895–907. doi: 10.1016/0092-8674(94)90138-4.

Van Belle, K. *et al.* (2016) 'Comparative In Vitro Immune Stimulation Analysis of Primary Human B Cells and B Cell Lines', *Journal of immunology research*, 2016. doi: 10.1155/2016/5281823.

Benbow, U. and Brinckerhoff, C. E. (1997) 'The AP-1 site and MMP gene regulation: what is all the fuss about?', *Matrix biology : journal of the International Society for Matrix Biology*, 15(8–9), pp. 519–526. doi: 10.1016/S0945-053X(97)90026-3.

Bevilacqua, M. P. *et al.* (1987) 'Identification of an inducible endothelial-leukocyte adhesion molecule (inflammation/cytokine/endotoxin/neutrophil/HL-60 cell)', *Proc. Nail. Acad. Sci. USA*, 84, pp. 9238–9242.

Bixel, G. *et al.* (2004) 'Mouse CD99 participates in T-cell recruitment into inflamed skin', *Blood*, 104(10), pp. 3205–3213. doi: 10.1182/blood-2004-03-1184.

Björklund, M. and Koivunen, E. (2005) 'Gelatinase-mediated migration and invasion of cancer cells', *Biochimica et biophysica acta*, 1755(1), pp. 37–69. doi: 10.1016/J.BBCAN.2005.03.001.

Bleul, C. C. *et al.* (1996) 'A highly efficacious lymphocyte chemoattractant, stromal cell-derived factor 1 (SDF-1)', *The Journal of Experimental Medicine*, 184(3), p. 1101. doi: 10.1084/JEM.184.3.1101.

Bloomgren, G. *et al.* (2012) 'Risk of natalizumab-associated progressive multifocal leukoencephalopathy', *The New England journal of medicine*, 366(20), pp. 1870–1880. doi: 10.1056/NEJMOA1107829.

Bond, M. *et al.* (2001) 'Inhibition of transcription factor NF-κB reduces matrix

metalloproteinase-1, -3 and -9 production by vascular smooth muscle cells', *Cardiovascular Research*, 50(3), pp. 556–565. doi: 10.1016/S0008-6363(01)00220-6/2/50-3-556-GR5.GIF.

Bovia, F. *et al.* (2003) 'Efficient transduction of primary human B lymphocytes and nondividing myeloma B cells with HIV-1-derived lentiviral vectors', *Blood*, 101(5), pp. 1727–1733. doi: 10.1182/BLOOD-2001-12-0249.

Bradfield, P. F. *et al.* (2003) 'Rheumatoid fibroblast-like synoviocytes overexpress the chemokine stromal cell-derived factor 1 (CXCL12), which supports distinct patterns and rates of CD4+ and CD8+ T cell migration within synovial tissue', *Arthritis and rheumatism*, 48(9), pp. 2472–2482. doi: 10.1002/ART.11219.

Brew, K. and Nagase, H. (2010) 'The tissue inhibitors of metalloproteinases (TIMPs): An ancient family with structural and functional diversity', *Biochimica et Biophysica Acta - Molecular Cell Research*. NIH Public Access, pp. 55–71. doi: 10.1016/j.bbamcr.2010.01.003.

Briggs, M. R. *et al.* (1986) 'Purification and biochemical characterization of the promoter-specific transcription factor, Sp1', *Science (New York, N.Y.)*, 234(4772), pp. 47–52. doi: 10.1126/SCIENCE.3529394.

Brooks, P. C. *et al.* (1996) 'Localization of matrix metalloproteinase MMP-2 to the surface of invasive cells by interaction with integrin αvβ3', *Cell*, 85(5), pp. 683–693. doi: 10.1016/S0092-8674(00)81235-0.

Bullock, J. *et al.* (2018) 'Rheumatoid Arthritis: A Brief Overview of the Treatment', *Medical principles and practice : international journal of the Kuwait University, Health Science Centre*, 27(6), pp. 501–507. doi: 10.1159/000493390.

Buschow, S. I. *et al.* (2010) 'MHC class II-associated proteins in B-cell exosomes and potential functional implications for exosome biogenesis', *Immunology and Cell Biology*, 88(8), pp. 851–856. doi: 10.1038/icb.2010.64.

Camire, R. M. (2021) 'Blood Coagulation Factor X: Molecular Biology, Inherited Disease, and Engineered Therapeutics', *Journal of Thrombosis and Thrombolysis*, 52(2), pp. 383–390. doi: 10.1007/s11239-021-02456-w.

Caraux, A. *et al.* (2010) 'Circulating human B and plasma cells. Age-associated changes in counts and detailed characterization of circulating normal CD138- and CD138+ plasma cells', *Haematologica*, 95(6), pp. 1016–1020. doi: 10.3324/HAEMATOL.2009.018689.

Carman, C. V and Springer, T. A. (2003) 'Integrin avidity regulation: are changes in affinity and conformation underemphasized?', *Current Opinion in Cell Biology*, 15, pp. 547–556. doi: 10.1016/j.ceb.2003.08.003.

Carter, R. H. and Fearon, D. T. (1992) 'CD19: lowering the threshold for antigen receptor stimulation of B lymphocytes', *Science (New York, N.Y.)*, 256(5053), pp. 105–107. doi: 10.1126/SCIENCE.1373518.

Chakraborti, S. *et al.* (2003) 'Regulation of matrix metalloproteinases: an overview', *Molecular and cellular biochemistry*, 253(1–2), pp. 269–285. doi: 10.1023/A:1026028303196.

Cheng, K. K. Y. *et al.* (2007) 'Adiponectin-induced endothelial nitric oxide synthase activation and nitric oxide production are mediated by APPL1 in endothelial cells',

*Diabetes*, 56(5), pp. 1387–1394. doi: 10.2337/DB06-1580.

Cheng, X. and Kao, H. Y. (2012) 'Microarray analysis revealing common and distinct functions of promyelocytic leukemia protein (PML) and tumor necrosis factor alpha (TNFα) signaling in endothelial cells', *BMC Genomics*, 13(1), p. 453. doi: 10.1186/1471-2164-13-453.

Cheng, X. W. *et al.* (2007) 'Mechanisms underlying the impairment of ischemia-induced neovascularization in matrix metalloproteinase 2-deficient mice', *Circulation Research*, 100(6), pp. 904–913. doi: 10.1161/01.RES.0000260801.12916.b5.

Chimen, M. *et al.* (2015) 'Homeostatic regulation of T cell trafficking by a B cell-derived peptide is impaired in autoimmune and chronic inflammatory disease', *Nature Medicine*, 21(5), pp. 467–475. doi: 10.1038/nm.3842.

Chimen, M. *et al.* (2020) 'Appropriation of GPIbα from platelet-derived extracellular vesicles supports monocyte recruitment in systemic inflammation', *Haematologica*, 105(5), pp. 1248–1261. doi: 10.3324/HAEMATOL.2018.215145.

Choi, D. S. *et al.* (2007) 'Proteomic analysis of microvesicles derived from human colorectal cancer cells', *Journal of proteome research*, 6(12), pp. 4646–4655. doi: 10.1021/PR070192Y.

Christensen, J. and Shastri, V. P. (2015) 'Matrix-metalloproteinase-9 is cleaved and activated by Cathepsin K', *BMC Research Notes 2015 8:1*, 8(1), pp. 1–8. doi: 10.1186/S13104-015-1284-8.

Ciborowski, P. *et al.* (2007) 'Investigating the human immunodeficiency virus type 1-infected monocyte-derived macrophage secretome'. doi: 10.1016/j.virol.2007.01.013.

Lo Cicero, A., Stahl, P. D. and Raposo, G. (2015) 'Extracellular vesicles shuffling intercellular messages: for good or for bad', *Current opinion in cell biology*, 35, pp. 69–77. doi: 10.1016/J.CEB.2015.04.013.

Clarke, M. C. H. *et al.* (2010) 'Vascular Smooth Muscle Cell Apoptosis Induces Interleukin-1–Directed Inflammation', *Circulation Research*, 106(2), pp. 363–372. doi: 10.1161/CIRCRESAHA.109.208389.

Clayton, A. *et al.* (2004) 'Adhesion and signaling by B cell-derived exosomes: the role of integrins', *The FASEB Journal*, 18(9), pp. 977–979. doi: 10.1096/fj.03-1094fje.

Cohen, M. J., Chirico, W. J. and Lipke, P. N. (2020) 'Through the back door: Unconventional protein secretion', *The Cell Surface*, 6, p. 100045. doi: 10.1016/J.TCSW.2020.100045.

Constantin, G. *et al.* (2000) 'Chemokines Trigger Immediate β2 Integrin Affinity and Mobility Changes: Differential Regulation and Roles in Lymphocyte Arrest under Flow', *Immunity*, 13(6), pp. 759–769. doi: 10.1016/S1074-7613(00)00074-1.

Corry, D. B. *et al.* (2004) 'Overlapping and independent contributions of MMP2 and MMP9 to lung allergic inflammatory cell egression through decreased CC chemokines', *FASEB journal : official publication of the Federation of American Societies for Experimental Biology*, 18(9), pp. 995–997. doi: 10.1096/FJ.03-1412FJE.

Coulet, M. *et al.* (2023) 'Identification of Small Molecules Affecting the Secretion of Therapeutic Antibodies with the Retention Using Selective Hook (RUSH) System', *Cells*, 12(12), p. 1642. doi: 10.3390/cells12121642.

Curbishley, S. M. *et al.* (2005) 'CXCR3 Activation Promotes Lymphocyte Transendothelial Migration across Human Hepatic Endothelium under Fluid Flow', *The American Journal of Pathology*, 167(3), p. 887. doi: 10.1016/S0002-9440(10)62060-3.

Czuczman, M. S. *et al.* (2008) 'Acquirement of Rituximab Resistance in Lymphoma Cell Lines Is Associated with Both Global CD20 Gene and Protein Down-Regulation Regulated at the Pretranscriptional and Posttranscriptional Levels', *Clinical Cancer Research*, 14(5), pp. 1561–1570. doi: 10.1158/1078-0432.CCR-07-1254.

Dallegri, F. *et al.* (1984) 'Antibody-dependent killing of tumor cells by polymorphonuclear leukocytes. Involvement of oxidative and nonoxidative mechanisms', *Journal of the National Cancer Institute*, 73(2), pp. 331–339. doi: 10.1093/JNCI/73.2.331.

Dame, T. M. *et al.* (2007) 'IFN-γ Alters the Response of Borrelia burgdorferi-Activated Endothelium to Favor Chronic Inflammation', *The Journal of Immunology*, 178(2), pp. 1172–1179. doi: 10.4049/JIMMUNOL.178.2.1172.

Denzer, K. *et al.* (2000) 'Exosome: From internal vesicle of the multivesicular body to intercellular signaling device', *Journal of Cell Science*, 113(19), pp. 3365–3374. doi: 10.1242/jcs.113.19.3365.

Denzer, Kristin *et al.* (2000) 'Follicular Dendritic Cells Carry MHC Class II-Expressing Microvesicles at Their Surface', *The Journal of Immunology*, 165(3), pp. 1259–1265. doi: 10.4049/jimmunol.165.3.1259.

Dimitrov, S. *et al.* (2009) 'Cortisol and epinephrine control opposing circadian rhythms in T cell subsets', *Blood*, 113(21), pp. 5134–5143. doi: 10.1182/blood-2008-11-190769.

Ding, J. *et al.* (2016) 'Pore-forming activity and structural autoinhibition of the gasdermin family', *Nature 2016 535:7610*, 535(7610), pp. 111–116. doi: 10.1038/nature18590.

Dolo, V. *et al.* (1999) 'Matrix-degrading proteinases are shed in membrane vesicles by ovarian cancer cells in vivo and in vitro', *Clinical & experimental metastasis*, 17(2), pp. 131–140. doi: 10.1023/A:1006500406240.

Doucet, C. *et al.* (1998) 'Interleukin (IL) 4 and IL-13 act on human lung fibroblasts. Implication in asthma', *The Journal of clinical investigation*, 101(10), pp. 2129–2139. doi: 10.1172/JCI741.

Doyle, L. M. and Wang, M. Z. (2019) 'Overview of Extracellular Vesicles, Their Origin, Composition, Purpose, and Methods for Exosome Isolation and Analysis', *Cells*, 8(7). doi: 10.3390/CELLS8070727.

Dubois, B. *et al.* (1999) 'Resistance of young gelatinase B-deficient mice to experimental autoimmune encephalomyelitis and necrotizing tail lesions', *The Journal of clinical investigation*, 104(11), pp. 1507–1515. doi: 10.1172/JCI6886.

Dunn, J. *et al.* (2014) 'Flow-dependent epigenetic DNA methylation regulates endothelial gene expression and atherosclerosis', *The Journal of Clinical Investigation*, 124(7), p. 3187. doi: 10.1172/JCI74792.

England, H. *et al.* (2014) 'Release of Interleukin-1 or Interleukin-1 Depends on Mechanism of Cell Death *'. doi: 10.1074/jbc.M114.557561.

Escola, J. M. *et al.* (1998) ‘Selective enrichment of tetraspan proteins on the internal vesicles of multivesicular endosomes and on exosomes secreted by human B-lymphocytes’, *The Journal of biological chemistry*, 273(32), pp. 20121–20127. doi: 10.1074/JBC.273.32.20121.

Esparza, J. *et al.* (2004) ‘MMP-2 null mice exhibit an early onset and severe experimental autoimmune encephalomyelitis due to an increase in MMP-9 expression and activity’, *FASEB journal : official publication of the Federation of American Societies for Experimental Biology*, 18(14), pp. 1682–1691. doi: 10.1096/FJ.04-2445COM.

Espié, P. *et al.* (2020) ‘First-in-human clinical trial to assess pharmacokinetics, pharmacodynamics, safety, and tolerability of iscalimab, an anti-CD40 monoclonal antibody’, *American journal of transplantation : official journal of the American Society of Transplantation and the American Society of Transplant Surgeons*, 20(2), pp. 463–473. doi: 10.1111/AJT.15661.

Etzioni, A. *et al.* (1992) ‘Recurrent Severe Infections Caused by a Novel Leukocyte Adhesion Deficiency’, *New England Journal of Medicine*, 327(25), pp. 1789–1792. doi: 10.1056/NEJM199212173272505.

Fan, D. and Kassiri, Z. (2020) ‘Biology of Tissue Inhibitor of Metalloproteinase 3 (TIMP3), and Its Therapeutic Implications in Cardiovascular Pathology’, *Frontiers in Physiology*, 11, p. 661. doi: 10.3389/FPHYS.2020.00661.

Feederle, R. *et al.* (2000) ‘The Epstein-Barr virus lytic program is controlled by the co-operative functions of two transactivators’, *The EMBO journal*, 19(12), pp. 3080–3089. doi: 10.1093/EMBOJ/19.12.3080.

Finger, E. B. *et al.* (1996) ‘Adhesion through L-selectin requires a threshold hydrodynamic shear’, *Nature*, 379(6562), pp. 266–269. doi: 10.1038/379266A0.

Forthal, D. N. (2015) ‘Functions of Antibodies’, in Crowe Jr, J. ., Boraschi, D., and Rappuoli, R. (eds) *Antibodies for Infectious Disease*, pp. 23–48. Available at: https://onlinelibrary.wiley.com/doi/abs/10.1128/9781555817411.ch2 (Accessed: 29 September 2023).

Garcia-Guzman, M. *et al.* (1999) ‘Cell adhesion regulates the interaction between the docking protein p130(Cas) and the 14-3-3 proteins’, *The Journal of biological chemistry*, 274(9), pp. 5762–5768. doi: 10.1074/JBC.274.9.5762.

Gardiner, C. *et al.* (2013) ‘Extracellular vesicle sizing and enumeration by nanoparticle tracking analysis’, *Journal of Extracellular Vesicles*, 2(1). doi: 10.3402/JEV.V2I0.19671.

Ginestra, A. *et al.* (1997) ‘Urokinase plasminogen activator and gelatinases are associated with membrane vesicles shed by human HT1080 fibrosarcoma cells’, *The Journal of biological chemistry*, 272(27), pp. 17216–17222. doi: 10.1074/JBC.272.27.17216.

Goldsmith, H. and Spain, S. (1984) ‘Margination of leukocytes in blood flow through small tubes’, *Microvascular research*, 27(2), pp. 204–222. doi: 10.1016/0026-2862(84)90054-2.

Gomez, N. E. *et al.* (2023) ‘PBMC-derived extracellular vesicles in a smoking-related inflammatory disease model’, *European Journal of Immunology*, 53(6), p. 2250143. doi: 10.1002/EJI.202250143.

Gonzalez, A. M., Cyrus, B. F. and Muller, W. A. (2016) 'Targeted Recycling of the Lateral Border Recycling Compartment Precedes Adherens Junction Dissociation during Transendothelial Migration', *The American journal of pathology*, 186(5), pp. 1387–1402. doi: 10.1016/J.AJPATH.2016.01.010.

Gotsch, U. *et al.* (1994) 'Expression of P-selectin on endothelial cells is upregulated by LPS and TNF-alpha in vivo', *Cell adhesion and communication*, 2(1), pp. 7–14. doi: 10.3109/15419069409014198.

Groom, J. R. and Luster, A. D. (2011) 'CXCR3 in T cell function', *Experimental cell research*, 317(5), p. 620. doi: 10.1016/J.YEXCR.2010.12.017.

Hamze, A. B. *et al.* (2007) 'Constraining specificity in the N-domain of tissue inhibitor of metalloproteinases-1; gelatinase-selective inhibitors', *Protein science : a publication of the Protein Society*, 16(9), pp. 1905–1913. doi: 10.1110/PS.072978507.

Han, D. C., Rodriguez, L. G. and Guan, J. L. (2001) 'Identification of a novel interaction between integrin beta1 and 14-3-3beta', *Oncogene*, 20(3), pp. 346–357. doi: 10.1038/SJ.ONC.1204068.

Haugen, F. and Drevon, C. A. (2007) 'Activation of Nuclear Factor-B by High Molecular Weight and Globular Adiponectin'. doi: 10.1210/en.2007-0370.

Hazrati, A. *et al.* (2022) 'Immune cells-derived exosomes function as a double-edged sword: role in disease progression and their therapeutic applications', *Biomarker research*, 10(1). doi: 10.1186/S40364-022-00374-4.

He, W.-T. *et al.* (2015) 'Gasdermin D is an executor of pyroptosis and required for interleukin-1β secretion', *Nature Publishing Group*, 25, pp. 1285–1298. doi: 10.1038/cr.2015.139.

Hong, J. *et al.* (2007) 'Anthrax edema toxin inhibits endothelial cell chemotaxis via Epac and Rap1', *The Journal of biological chemistry*, 282(27), pp. 19781–19787. doi: 10.1074/JBC.M700128200.

Hopkin, S. J. (2023) 'PEPITEM, a regulator of leukocyte trafficking in ageing', (May).

Hosseini-Beheshti, E. *et al.* (2012) 'Exosomes as biomarker enriched microvesicles: characterization of exosomal proteins derived from a panel of prostate cell lines with distinct AR phenotypes', *Molecular & cellular proteomics : MCP*, 11(10), pp. 863–885. doi: 10.1074/MCP.M111.014845.

Hottenrott, M. C. *et al.* (2013) 'N-Octanoyl Dopamine Inhibits the Expression of a Subset of κB Regulated Genes: Potential Role of p65 Ser276 Phosphorylation', *PLOS ONE*, 8(9), p. e73122. doi: 10.1371/JOURNAL.PONE.0073122.

Hunter, M. C., Teijeira, A. and Halin, C. (2016) 'T cell trafficking through lymphatic vessels', *Frontiers in Immunology*, 7(DEC), p. 613. doi: 10.3389/FIMMU.2016.00613/BIBTEX.

Hutchinson, M. (2007) 'Natalizumab: A new treatment for relapsing remitting multiple sclerosis', *Therapeutics and Clinical Risk Management*, 3(2), pp. 259–268.

Indraccolo, S. *et al.* (2007) 'Identification of Genes Selectively Regulated by IFNs in Endothelial Cells', *The Journal of Immunology*, 178(2), pp. 1122–1135. doi: 10.4049/JIMMUNOL.178.2.1122.

Itoh, Y. *et al.* (2001) 'Homophilic complex formation of MT1-MMP facilitates proMMP-

2 activation on the cell surface and promotes tumor cell invasion', *The EMBO Journal*, 20(17), p. 4782. doi: 10.1093/EMBOJ/20.17.4782.

Itoh, Y. (2015) 'Membrane-type matrix metalloproteinases: Their functions and regulations', *Matrix Biology*, 44–46, pp. 207–223. doi: 10.1016/J.MATBIO.2015.03.004.

Itoh, Y. and Nagase, H. (1995) 'Preferential inactivation of tissue inhibitor of metalloproteinases-1 that is bound to the precursor of matrix metalloproteinase 9 (progelatinase B) by human neutrophil elastase', *The Journal of biological chemistry*, 270(28), pp. 16518–16521. doi: 10.1074/JBC.270.28.16518.

Iwabu, M. *et al.* (2010) 'Adiponectin and AdipoR1 regulate PGC-1alpha and mitochondria by Ca(2+) and AMPK/SIRT1', *Nature*, 464(7293), pp. 1313–1319. doi: 10.1038/NATURE08991.

Jaczewska, J. *et al.* (2014) 'TNF-α and IFN-γ promote lymphocyte adhesion to endothelial junctional regions facilitating transendothelial migration', *Journal of Leukocyte Biology*, 95(2), p. 265. doi: 10.1189/JLB.0412205.

Jasinski-Bergner, S. *et al.* (2017) 'Adiponectin and Its Receptors Are Differentially Expressed in Human Tissues and Cell Lines of Distinct Origin', *Obesity facts*, 10(6), pp. 569–583. doi: 10.1159/000481732.

Johnson *et al.* (1993) 'Adhesion molecule expression in human synovial tissue', *Arthritis and rheumatism*, 36(2), pp. 137–146. doi: 10.1002/ART.1780360203.

Johnson, L. A. *et al.* (2006) 'An inflammation-induced mechanism for leukocyte transmigration across lymphatic vessel endothelium', *The Journal of Experimental Medicine*, 203(12), p. 2763. doi: 10.1084/JEM.20051759.

Johnstone, R. M. *et al.* (1987) 'THE JOURNAL OF BIOLOGICAL CHEMISTRY Vesicle Formation during Reticulocyte Maturation ASSOCIATION OF PLASMA MEMBRANE ACTIVITIES WITH RELEASED VESICLES (EXOSOMES)*', 262, pp. 9412–9420. doi: 10.1016/S0021-9258(18)48095-7.

Jose, P. J. *et al.* (1994) 'Eotaxin: a potent eosinophil chemoattractant cytokine detected in a guinea pig model of allergic airways inflammation', *The Journal of experimental medicine*, 179(3), pp. 881–887. doi: 10.1084/JEM.179.3.881.

Jung, M. Y. *et al.* (2012) 'Adiponectin Induces Dendritic Cell Activation via PLCγ/JNK/NF-κB Pathways, Leading to Th1 and Th17 Polarization', *The Journal of Immunology*, 188(6), pp. 2592–2601. doi: 10.4049/jimmunol.1102588.

Jung, T. *et al.* (1988) 'Down-regulation of homing receptors after T cell activation', *Journal of immunology*, 141, pp. 4110–4117.

Jung, U. and Ley, K. (1999) 'Mice lacking two or all three selectins demonstrate overlapping and distinct functions for each selectin', *Journal of immunology*, 162(11), pp. 6755–6762.

Kappelmayer, J. *et al.* (2004) 'The emerging value of P-selection as a disease marker', *Clinical Chemistry and Laboratory Medicine*, 42(5), pp. 475–486. doi: 10.1515/CCLM.2004.082/MACHINEREADABLECITATION/RIS.

Kargozaran, H. *et al.* (2007) 'A role for endothelial-derived matrix metalloproteinase-2 in breast cancer cell transmigration across the endothelial-basement membrane barrier', *Clinical and Experimental Metastasis*, 24(7), pp. 495–502. doi:

10.1007/S10585-007-9086-6/FIGURES/5.

Karpova, M. B. *et al.* (2004) ‘Raji revisited: cytogenetics of the original Burkitt’s lymphoma cell line’, *Leukemia 2005 19:1*, 19(1), pp. 159–161. doi: 10.1038/sj.leu.2403534.

Kayagaki, N. *et al.* (2015) ‘Caspase-11 cleaves gasdermin D for non-canonical inflammasome signalling’, *Nature 2015 526:7575*, 526(7575), pp. 666–671. doi: 10.1038/nature15541.

Keerthikumar, S. *et al.* (2015) ‘Proteogenomic analysis reveals exosomes are more oncogenic than ectosomes’, *Oncotarget*, 6(17), pp. 15375–15396. doi: 10.18632/ONCOTARGET.3801.

Keerthikumar, S. *et al.* (2016) ‘ExoCarta: A Web-Based Compendium of Exosomal Cargo’, *Journal of molecular biology*, 428(4), pp. 688–692. doi: 10.1016/J.JMB.2015.09.019.

Khan, S. *et al.* (2019) ‘EndoDB: a database of endothelial cell transcriptomics data’, *Nucleic Acids Research*, 47(D1), pp. D736–D744. doi: 10.1093/NAR/GKY997.

Kim, C. H. and Broxmeyer, H. E. (1999) ‘Chemokines: Signal lamps for trafficking of T and B cells for development and effector function’, *Journal of Leukocyte Biology*, 65(1), pp. 6–15. doi: 10.1002/JLB.65.1.6.

Kindt, T. J., Osborne, B. A. and Goldsby, R. A. (2006) ‘Inflammation Represents a Complex Sequence of Events That Stimulates Immune Responses’, in *Kuby Immunology*. Sixth Edition. New York: W. H. Freeman & Co, pp. 7–9. Available at: https://www.amazon.co.uk/Immunology-Osborne-Barbara-Goldsby-Paperback/dp/B010WFJBDE (Accessed: 2 November 2021).

Kirk, S. J. *et al.* (2010) ‘Biogenesis of secretory organelles during B cell differentiation’, *Journal of Leukocyte Biology*, 87(2), pp. 245–255. doi: 10.1189/JLB.1208774.

Kjeldsen, L. *et al.* (1993) ‘Structural and Functional Heterogeneity Among Peroxidase-Negative Granules in Human Neutrophils: Identification of a Distinct Gelatinase-Containing Granule Subset by Combined Immunocytochemistry and Subcellular Fractionation’, *Blood*, 82(10), pp. 3183–3191. doi: 10.1182/BLOOD.V82.10.3183.3183.

Kleiner, D. E. and Stetlerstevenson, W. G. (1994) ‘Quantitative zymography: Detection of picogram quantities of gelatinases’, *Analytical Biochemistry*, 218(2), pp. 325–329. doi: 10.1006/ABIO.1994.1186.

Kleiveland, C. R. (2015) ‘Peripheral Blood Mononuclear Cells’, *The Impact of Food Bioactives on Health: In Vitro and Ex Vivo Models*, pp. 161–167. doi: 10.1007/978-3-319-16104-4_15.

Klinker, M. W. *et al.* (2014) ‘Human B cell-derived lymphoblastoid cell lines constitutively produce Fas ligand and secrete MHCII+FasL+ killer exosomes’, *Frontiers in Immunology*, 5(APR), p. 70905. doi: 10.3389/FIMMU.2014.00144/BIBTEX.

Knight, B. E. *et al.* (2019) ‘TIMP-1 Attenuates the Development of Inflammatory Pain Through MMP-Dependent and Receptor-Mediated Cell Signaling Mechanisms’, *Frontiers in Molecular Neuroscience*, 12, p. 220. doi:

10.3389/FNMOL.2019.00220/BIBTEX.

Kobayashi, R. *et al.* (2009) '14-3-3 Zeta protein secreted by tumor associated monocytes/macrophages from ascites of epithelial ovarian cancer patients', *Cancer Immunology, Immunotherapy*, 58(2), pp. 247–258. doi: 10.1007/S00262-008-0549-7/FIGURES/5.

Kramberger, P. *et al.* (2012) 'Evaluation of nanoparticle tracking analysis for total virus particle determination', *Virology Journal*, 9(1), pp. 1–10. doi: 10.1186/1743-422X-9-265/FIGURES/4.

Kuek, A., Hazleman, B. L. and Östör, A. J. K. (2007) 'Immune-mediated inflammatory diseases (IMIDs) and biologic therapy: A medical revolution', *Postgraduate Medical Journal*. BMJ Publishing Group, pp. 251–260. doi: 10.1136/pgmj.2006.052688.

Kunkel, E. J. and Ley, K. (1996) 'Distinct Phenotype of E-Selectin–Deficient Mice', *Circulation Research*, 79(6), pp. 1196–1204. doi: 10.1161/01.RES.79.6.1196.

Kuravi, S. J. *et al.* (2014) 'Podocytes regulate neutrophil recruitment by glomerular endothelial cells via IL-6-mediated crosstalk', *Journal of immunology (Baltimore, Md. : 1950)*, 193(1), pp. 234–243. doi: 10.4049/JIMMUNOL.1300229.

Laronha, H. and Caldeira, J. (2020) 'Structure and Function of Human Matrix Metalloproteinases', *Cells*, 9(5). doi: 10.3390/CELLS9051076.

Lawrence, M. B. *et al.* (1997) 'Threshold levels of fluid shear promote leukocyte adhesion through selectins (CD62L,P,E)', *The Journal of cell biology*, 136(3), pp. 717–727. doi: 10.1083/JCB.136.3.717.

Lewis, J. W. (2021) 'CHARACTERISING THE THERAPEUTIC POTENTIAL OF PEPITEM IN AGE-RELATED BONE LOSS, SKELETAL REMODELLING AND REPAIR'.

Ley, K. *et al.* (1995) 'Sequential contribution of L- and P-selectin to leukocyte rolling in vivo.', *Journal of Experimental Medicine*, 181(2), pp. 669–675. doi: 10.1084/JEM.181.2.669.

Ley, K. *et al.* (2007) 'Getting to the site of inflammation: The leukocyte adhesion cascade updated', *Nature Reviews Immunology*. Nature Publishing Group, pp. 678–689. doi: 10.1038/nri2156.

Liang, B. *et al.* (2013) 'Characterization and proteomic analysis of ovarian cancer-derived exosomes', *Journal of proteomics*, 80, pp. 171–182. doi: 10.1016/J.JPROT.2012.12.029.

Liu, D. *et al.* (1995) 'Crystal structure of the zeta isoform of the 14-3-3 protein', *Nature*, 376(6536), pp. 191–194. doi: 10.1038/376191A0.

Liu, M., Yu, Y. and Hu, S. (2021) 'A review on applications of abatacept in systemic rheumatic diseases', *International Immunopharmacology*, 96, p. 107612. doi: 10.1016/J.INTIMP.2021.107612.

Liu, P., Sun, M. and Sader, S. (2006) 'Matrix metalloproteinases in cardiovascular disease', *Can J Cardiol*, 22, p. 25.

Liu, T. *et al.* (2014) 'Single-cell imaging of caspase-1 dynamics reveals an all-or-none inflammasome signaling response', *Cell reports*, 8(4), pp. 974–982. doi: 10.1016/J.CELREP.2014.07.012.

Liu, X. *et al.* (2016) 'Inflammasome - activated gasdermin D causes pyroptosis by forming membrane pores', *Nature*, 535(7610), p. 153. doi: 10.1038/NATURE18629.

Löffek, S., Schilling, O. and Franzke, C. W. (2011) 'Biological role of matrix metalloproteinases: a critical balance', *European Respiratory Journal*, 38(1), pp. 191–208. doi: 10.1183/09031936.00146510.

Lu, J. *et al.* (2009) '14-3-3zeta Cooperates with ErbB2 to promote ductal carcinoma in situ progression to invasive breast cancer by inducing epithelial-mesenchymal transition', *Cancer cell*, 16(3), pp. 195–207. doi: 10.1016/J.CCR.2009.08.010.

Luscinskas, F. W., Ding, H. and Lichtman, A. H. (1995) 'P-selectin and vascular cell adhesion molecule 1 mediate rolling and arrest, respectively, of CD4+ T lymphocytes on tumor necrosis factor alpha-activated vascular endothelium under flow', *The Journal of Experimental Medicine*, 181(3), p. 1179. doi: 10.1084/JEM.181.3.1179.

Ma, L. *et al.* (2012) 'CD31 exhibits multiple roles in regulating T lymphocyte trafficking in vivo', *Journal of immunology (Baltimore, Md. : 1950)*, 189(8), pp. 4104–4111. doi: 10.4049/JIMMUNOL.1201739.

Mackay, C. R., Marston, W. and Dudler, L. (1992) 'Altered patterns of T cell migration through lymph nodes and skin following antigen challenge', *European journal of immunology*, 22(9), pp. 2205–2210. doi: 10.1002/EJI.1830220904.

Mambula, S. S. and Calderwood, S. K. (2006) 'Heat shock protein 70 is secreted from tumor cells by a nonclassical pathway involving lysosomal endosomes', *Journal of immunology (Baltimore, Md. : 1950)*, 177(11), pp. 7849–7857. doi: 10.4049/JIMMUNOL.177.11.7849.

Manes, T. D. and Pober, J. S. (2011) 'Identification of endothelial cell junctional proteins and lymphocyte receptors involved in transendothelial migration of human effector memory CD4+ T cells', *Journal of immunology (Baltimore, Md. : 1950)*, 186(3), pp. 1763–1768. doi: 10.4049/JIMMUNOL.1002835.

Manning, J. E. *et al.* (2021) 'Insights Into Leukocyte Trafficking in Inflammatory Arthritis - Imaging the Joint', *Frontiers in cell and developmental biology*, 9. doi: 10.3389/FCELL.2021.635102.

Mao, X. *et al.* (2006) 'APPL1 binds to adiponectin receptors and mediates adiponectin signalling and function', *Nature Cell Biology*, 8(5), pp. 516–523. doi: 10.1038/ncb1404.

Martin-Sanchez, F. *et al.* (2016) 'Inflammasome-dependent IL-1β release depends upon membrane permeabilisation', *Cell death and differentiation*, 23(7), pp. 1219–1231. doi: 10.1038/CDD.2015.176.

Masharani, U. B. and Becker, J. (2010) 'Teplizumab therapy for type 1 diabetes', *Expert Opinion on Biological Therapy*. doi: 10.1517/14712591003598843.

Matsubara, H. *et al.* (2020) 'PEPITEM/Cadherin 15 Axis Inhibits T Lymphocyte Infiltration and Glomerulonephritis in a Mouse Model of Systemic Lupus Erythematosus', *The Journal of Immunology*, 204(8), pp. 2043–2052. doi: 10.4049/JIMMUNOL.1900213.

Mautino, G. *et al.* (1997) 'Increased Release of Matrix Metalloproteinase-9 in Bronchoalveolar Lavage Fluid and by Alveolar Macrophages of Asthmatics', *American Journal of Respiratory Cell and Molecular Biology*, 17(5), pp. 583–591. doi:

10.1165/ajrcmb.17.5.2562.

Mazanet, M. M., Neote, K. and Hughes, C. C. W. (2000) ‘Expression of IFN-Inducible T Cell α Chemoattractant by Human Endothelial Cells Is Cyclosporin A-Resistant and Promotes T Cell Adhesion: Implications for Cyclosporin A-Resistant Immune Inflammation’, *The Journal of Immunology*, 164(10), pp. 5383–5388. doi: 10.4049/JIMMUNOL.164.10.5383.

McCandless, E. E. *et al.* (2008) ‘CXCR4 antagonism increases T cell trafficking in the central nervous system and improves survival from West Nile virus encephalitis’, *Proceedings of the National Academy of Sciences of the United States of America*, 105(32), p. 11270. doi: 10.1073/PNAS.0800898105.

McEver, R. P. *et al.* (1989) ‘GMP-140, a platelet alpha-granule membrane protein, is also synthesized by vascular endothelial cells and is localized in Weibel-Palade bodies.’, *Journal of Clinical Investigation*, 84(1), p. 92. doi: 10.1172/JCI114175.

McGettrick, H. M. *et al.* (2009) ‘Fibroblasts from different sites may promote or inhibit recruitment of flowing lymphocytes by endothelial cells’, *European Journal of Immunology*, 39(1), pp. 113–125. doi: 10.1002/EJI.200838232.

McGettrick, H. M., Buckley, Chris D., *et al.* (2010) ‘Influence of stromal cells on lymphocyte adhesion and migration on endothelial cells’, *Methods in molecular biology (Clifton, N.J.)*, 616, p. 49. doi: 10.1007/978-1-60761-461-6_4.

McGettrick, H. M., Buckley, Christopher D., *et al.* (2010) ‘Stromal cells differentially regulate neutrophil and lymphocyte recruitment through the endothelium’, *Immunology*, 131(3), p. 357. doi: 10.1111/J.1365-2567.2010.03307.X.

McGettrick, M. *et al.* (2009) ‘Direct observations of the kinetics of migrating T cells suggest active retention by endothelial cells with continual bidirectional migration’, *Journal of leukocyte biology*, 85(1), pp. 98–107. doi: 10.1189/JLB.0508301.

McInnes, I. B. and Gravallese, E. M. (2021) ‘Immune-mediated inflammatory disease therapeutics: past, present and future’, *Nature reviews. Immunology*, 21(10), pp. 680–686. doi: 10.1038/S41577-021-00603-1.

Mehana, E. S. E., Khafaga, A. F. and El-Blehi, S. S. (2019) ‘The role of matrix metalloproteinases in osteoarthritis pathogenesis: An updated review’, *Life Sciences*, 234, p. 116786. doi: 10.1016/J.LFS.2019.116786.

Middleton, J. *et al.* (2002) ‘Leukocyte extravasation: chemokine transport and presentation by the endothelium’, *Blood*, 100(12), pp. 3853–3860. doi: 10.1182/BLOOD.V100.12.3853.

Miguel Angel, del P. *et al.* (1998) ‘The two poles of the lymphocyte: specialized cell compartments for migration and recruitment’, *Cell adhesion and communication*, 6(2–3), pp. 125–133. doi: 10.3109/15419069809004468.

Mittelbrunn, M. *et al.* (2011) ‘Unidirectional transfer of microRNA-loaded exosomes from T cells to antigen-presenting cells’, *Nature communications*, 2(1). doi: 10.1038/NCOMMS1285.

Mohammad, G. and Kowluru, R. A. (2020) ‘Homocysteine Disrupts Balance between MMP-9 and Its Tissue Inhibitor in Diabetic Retinopathy: The Role of DNA Methylation’, *International journal of molecular sciences*, 21(5), pp. 1–15. doi: 10.3390/ijms21051771.

Mohammed, R. N. *et al.* (2016) 'L-selectin Is Essential for Delivery of Activated CD8+ T Cells to Virus-Infected Organs for Protective Immunity', *Cell Reports*, 14(4), pp. 760–771. doi: 10.1016/j.celrep.2015.12.090.

Morales-Kastresana, A. and Jones, J. C. (2017) 'Flow Cytometric Analysis of Extracellular Vesicles', *Methods Molecular Biology*, 1545, pp. 215–225. doi: 10.1007/978-1-4939-6728-5_16.

Morelli, C. *et al.* (2004) 'Activity of the Matrix Metalloproteinase-9 Promoter in Human Normal and Tumor Cells', *Journal of Cellular Physiology*, 199(1), pp. 126–133. doi: 10.1002/jcp.10450.

Muller, W. A. (2003) 'Leukocyte–endothelial-cell interactions in leukocyte transmigration and the inflammatory response', *Trends in Immunology*, 24(6), pp. 326–333. doi: 10.1016/S1471-4906(03)00117-0.

Muller, W. A. (2011) 'Mechanisms of Leukocyte Transendothelial Migration', *Annual review of pathology*, 6, p. 323. doi: 10.1146/ANNUREV-PATHOL-011110-130224.

Mun, G. I. *et al.* (2009) 'Differential gene expression in young and senescent endothelial cells under static and laminar shear stress conditions', *Free radical biology & medicine*, 47(3), pp. 291–299. doi: 10.1016/J.FREERADBIOMED.2009.04.032.

Munier, C. C., Ottmann, C. and Perry, M. W. D. (2021) '14-3-3 modulation of the inflammatory response', *Pharmacological Research*, 163, p. 105236. doi: 10.1016/J.PHRS.2020.105236.

Munir, H., Ed Rainger, G., *et al.* (2015) 'Analyzing the Effects of Stromal Cells on the Recruitment of Leukocytes from Flow', *Journal of Visualized Experiments : JoVE*, (95), p. 52480. doi: 10.3791/52480.

Munir, H., Rainger, G. E., *et al.* (2015) 'Analyzing the Effects of Stromal Cells on the Recruitment of Leukocytes from Flow', *Journal of Visualized Experiments : JoVE*, (95), p. 52480. doi: 10.3791/52480.

Muntasell, A., Berger, A. C. and Roche, P. A. (2007) 'T cell-induced secretion of MHC class II–peptide complexes on B cell exosomes', *The EMBO Journal*, 26(19), p. 4263. doi: 10.1038/SJ.EMBOJ.7601842.

Murphy, G. *et al.* (1994) 'Assessment of the role of the fibronectin-like domain of gelatinase A by analysis of a deletion mutant.', *Journal of Biological Chemistry*, 269(9), pp. 6632–6636. doi: 10.1016/S0021-9258(17)37419-7.

Nagase, H. (1997) 'Activation mechanisms of matrix metalloproteinases', *Biological Chemistry*, 378, pp. 151–160. Available at: https://typeset.io/papers/activation-mechanisms-of-matrix-metalloproteinases-5bvqr7ipn5 (Accessed: 11 January 2023).

Nagase, H., Visse, R. and Murphy, G. (2006) 'Structure and function of matrix metalloproteinases and TIMPs', *Cardiovascular Research*. Oxford Academic, pp. 562–573. doi: 10.1016/j.cardiores.2005.12.002.

Nagaset, H. and Woessner, J. F. (1999) 'Matrix metalloproteinases', *Journal of Biological Chemistry*, 274(31), pp. 21491–21494. doi: 10.1074/jbc.274.31.21491.

Neal, C. L. and Yu, D. (2010) '14-3-3Z As a Prognostic Marker and Therapeutic Target for Cancer', *Expert Opinion on Therapeutic Targets*, 14(12), pp. 1343–1354. doi: 10.1517/14728222.2010.531011.

Nguyen, M., Arkell, J. and Jackson, C. J. (1998) 'Active and Tissue Inhibitor of Matrix Metalloproteinase-free Gelatinase B Accumulates within Human Microvascular Endothelial Vesicles', *Journal of Biological Chemistry*, 273(9), pp. 5400–5404. doi: 10.1074/JBC.273.9.5400.

O'Connor, L., Gilmour, J. and Bonifer, C. (2016) 'Focus: Epigenetics: The Role of the Ubiquitously Expressed Transcription Factor Sp1 in Tissue-specific Transcriptional Regulation and in Disease', *The Yale Journal of Biology and Medicine*, 89(4), p. 513. Available at: /pmc/articles/PMC5168829/ (Accessed: 27 September 2023).

Obsilova, V. and Obsil, T. (2022) 'Structural insights into the functional roles of 14-3-3 proteins', *Frontiers in Molecular Biosciences*, 9. doi: 10.3389/FMOLB.2022.1016071.

Oksvold, M. P. *et al.* (2014) 'Expression of B-cell surface antigens in subpopulations of exosomes released from B-cell lymphoma cells', *Clinical therapeutics*, 36(6). doi: 10.1016/J.CLINTHERA.2014.05.010.

Ortega, M. A. *et al.* (2022) 'Immune-Mediated Diseases from the Point of View of Psychoneuroimmunoendocrinology', *Biology*, 11(7). doi: 10.3390/BIOLOGY11070973.

Pallis, M. *et al.* (1993) 'Distribution of cell adhesion molecules in skeletal muscle from patients with systemic lupus erythematosus', *Annals of the rheumatic diseases*, 52(9), pp. 667–671. doi: 10.1136/ARD.52.9.667.

Park, J. E. *et al.* (2010) 'Hypoxic tumor cell modulates its microenvironment to enhance angiogenic and metastatic potential by secretion of proteins and exosomes', *Molecular & cellular proteomics : MCP*, 9(6), pp. 1085–1099. doi: 10.1074/MCP.M900381-MCP200.

Parsonage, G. *et al.* (2005) 'A stromal address code defined by fibroblasts', *Trends in immunology*, 26(3), pp. 150–156. doi: 10.1016/J.IT.2004.11.014.

Patten, D. A. *et al.* (2017) 'Human liver sinusoidal endothelial cells promote intracellular crawling of lymphocytes during recruitment: A new step in migration', *Hepatology*, 65(1), pp. 294–309. doi: 10.1002/HEP.28879/SUPPINFO.

Peinado, H. *et al.* (2012) 'Melanoma exosomes educate bone marrow progenitor cells toward a pro-metastatic phenotype through MET', *Nature medicine*, 18(6), pp. 883–891. doi: 10.1038/NM.2753.

Piali, L. *et al.* (1998) 'The chemokine receptor CXCR3 mediates rapid and shear-resistant adhesion-induction of effector T lymphocytes by the chemokines IP10 and Mig'. doi: 10.1002/(SICI)1521-4141(199803)28:03.

Pober, J. S. and Cotran, R. S. (1990) 'Cytokines and endothelial cell biology', *https://doi.org/10.1152/physrev.1990.70.2.427*, 70(2), pp. 427–451. doi: 10.1152/PHYSREV.1990.70.2.427.

Postler, T. S. (2021) 'A most versatile kinase: The catalytic subunit of PKA in T-cell biology', *International Review of Cell and Molecular Biology*, 361, pp. 301–318. doi: 10.1016/BS.IRCMB.2021.01.005.

Pozzobon, T. *et al.* (2016) 'CXCR4 signaling in health and disease', *Immunology Letters*, 177, pp. 6–15. doi: 10.1016/J.IMLET.2016.06.006.

Price, J. M. J. *et al.* (2023) 'Detection of tissue factor-positive extracellular vesicles

using the ExoView R100 system', *Research and practice in thrombosis and haemostasis*, 7(4). doi: 10.1016/J.RPTH.2023.100177.

Qazi, K. R. *et al.* (2009) 'Antigen-loaded exosomes alone induce Th1-type memory through a B cell–dependent mechanism', *Blood*, 113(12), pp. 2673–2683. doi: 10.1182/BLOOD-2008-04-153536.

Qin, S. *et al.* (1998) 'The chemokine receptors CXCR3 and CCR5 mark subsets of T cells associated with certain inflammatory reactions.', *Journal of Clinical Investigation*, 101(4), p. 746. doi: 10.1172/JCI1422.

Qu, Y. (2009) 'Related Content Nonclassical IL-1β Secretion Stimulated by P2X7 Receptors Is Dependent on Innammasome Activation and Correlated with Exosome Release in Murine Macrophages P2X7 Receptor-Dependent Blebbing and the Activation of Rho-Effector Kinases, Caspases, and IL-1β Release Inhibitory Effects of Chloride on the Activation of Caspase-1, IL-1β Secretion, and Cytolysis by the P2X7 Receptor', *J Immunol*, 182(8), p. 5052. doi: 10.4049/jimmunol.0802968.

Quintero-Fabián, S. *et al.* (2019) 'Role of Matrix Metalloproteinases in Angiogenesis and Cancer', *Frontiers in Oncology*, 9, p. 1370. doi: 10.3389/FONC.2019.01370/BIBTEX.

Rainger, G. *et al.* (1996) 'Prolonged E-selectin induction by monocytes potentiates the adhesion of flowing neutrophils to cultured endothelial cells', *British Journal of Haematology*, 92(1), pp. 192–199. doi: 10.1046/J.1365-2141.1996.00308.X.

Rainger, G. *et al.* (2001) 'A novel system for investigating the ability of smooth muscle cells and fibroblasts to regulate adhesion of flowing leukocytes to endothelial cells', *Journal of immunological methods*, 255(1–2), pp. 73–82. doi: 10.1016/S0022-1759(01)00427-6.

Raposo, G. *et al.* (1996) 'B lymphocytes secrete antigen-presenting vesicles', *The Journal of Experimental Medicine*, 183(3), p. 1161. doi: 10.1084/JEM.183.3.1161.

Ratitong, B., Marshall, M. and Pearlman, E. (2021) 'β-Glucan-stimulated neutrophil secretion of IL-1α is independent of GSDMD and mediated through extracellular vesicles', *Cell reports*, 35(7), p. 109139. doi: 10.1016/J.CELREP.2021.109139.

Redondo-Muñ Oz, J. *et al.* (2006) 'MMP-9 in B-cell chronic lymphocytic leukemia is up-regulated by 41 integrin or CXCR4 engagement via distinct signaling pathways, localizes to podosomes, and is involved in cell invasion and migration'. doi: 10.1182/blood-2006-03-007294.

Roomi, M. W. *et al.* (2017) 'Modulation of MMP-2 and MMP-9 secretion by cytokines, inducers and inhibitors in human glioblastoma T-98G cells', *Oncology reports*, 37(3), pp. 1907–1913. doi: 10.3892/OR.2017.5391.

Rosenblum, G. *et al.* (2007) 'Molecular Structures and Dynamics of the Stepwise Activation Mechanism of a Matrix Metalloproteinase Zymogen: Challenging the Cysteine Switch Dogma'. doi: 10.1021/ja073941l.

Roukens, M. G. *et al.* (2010) 'Control of endothelial sprouting by a Tel–CtBP complex', *Nature Cell Biology 2010 12:10*, 12(10), pp. 933–942. doi: 10.1038/ncb2096.

Ryan, G. B. and Majno, G. (1977) 'Acute inflammation. A review.', *The American Journal of Pathology*, 86(1), p. 183. Available at:

https://www.ncbi.nlm.nih.gov/pmc/articles/PMC2032041/ (Accessed: 2 November 2021).

Sallusto, F., Mackay, C. R. and Lanzavecchia, A. (1997) 'Selective expression of the eotaxin receptor CCR3 by human T helper 2 cells', *Science (New York, N.Y.)*, 277(5334), pp. 2005–2007. doi: 10.1126/SCIENCE.277.5334.2005.

Sánchez-Madrid, F. and del Pozo, M. A. (1999) 'Leukocyte polarization in cell migration and immune interactions', *The EMBO journal*, 18(3), pp. 501–511. doi: 10.1093/EMBOJ/18.3.501.

Satoh, J. I., Kawana, N. and Yamamoto, Y. (2013) 'Molecular network of chromatin immunoprecipitation followed by deep sequencing-based (ChIP-Seq) Epstein-Barr virus nuclear antigen 1-target cellular genes supports biological implications of Epstein-Barr virus persistence in multiple sclerosis', *Clinical and Experimental Neuroimmunology*, 4(2), pp. 181–192. doi: 10.1111/CEN3.12035.

Saunderson, S. C. *et al.* (2008) 'Induction of exosome release in primary B cells stimulated via CD40 and the IL-4 receptor', *Journal of immunology (Baltimore, Md. : 1950)*, 180(12), pp. 8146–8152. doi: 10.4049/JIMMUNOL.180.12.8146.

Saunderson, S. C. *et al.* (2014) 'CD169 mediates the capture of exosomes in spleen and lymph node', *Blood*, 123(2), p. 208. doi: 10.1182/BLOOD-2013-03-489732.

Saunderson, S. C. and McLellan, A. D. (2017) 'Role of Lymphocyte Subsets in the Immune Response to Primary B Cell-Derived Exosomes', *Journal of immunology (Baltimore, Md. : 1950)*, 199(7), pp. 2225–2235. doi: 10.4049/JIMMUNOL.1601537.

Schweighofer, B. *et al.* (2009) 'The VEGF-induced transcriptional response comprises gene clusters at the crossroad of angiogenesis and inflammation', *Thrombosis and haemostasis*, 102(3), pp. 544–554. doi: 10.1160/TH08-12-0830.

Shih, Y. C. *et al.* (2021) 'Mmp-9 deletion attenuates arteriovenous fistula neointima through reduced perioperative vascular inflammation', *International Journal of Molecular Sciences*, 22(11). doi: 10.3390/ijms22115448.

Shimizu, Y. *et al.* (1991) 'Four molecular pathways of T cell adhesion to endothelial cells: roles of LFA-1, VCAM-1, and ELAM-1 and changes in pathway hierarchy under different activation conditions', *The Journal of Cell Biology*, 113(5), p. 1203. doi: 10.1083/JCB.113.5.1203.

Snoek-van Beurden, P. A. M. and Von Den Hoff, J. W. (2005) 'Zymographic techniques for the analysis of matrix metalloproteinases and their inhibitors', *BioTechniques*, 38(1), pp. 73–83. doi: 10.2144/05381RV01/ASSET/IMAGES/LARGE/FIGURE5.JPEG.

Song, J. *et al.* (2015) 'Focal MMP-2 and MMP-9 activity at the blood-brain barrier promotes chemokine-induced leukocyte migration', *Cell reports*, 10(7), pp. 1040–1054. doi: 10.1016/J.CELREP.2015.01.037.

Springer, T. (1995) 'Traffic signals on endothelium for lymphocyte recirculation and leukocyte emigration', *Annual review of physiology*, 57, pp. 827–872. doi: 10.1146/ANNUREV.PH.57.030195.004143.

Stow, J. L. and Murray, R. Z. (2013) 'Intracellular trafficking and secretion of inflammatory cytokines', *Cytokine & Growth Factor Reviews*, 24, pp. 227–239. doi: 10.1016/j.cytogfr.2013.04.001.

Strindhall, J., Lundblad, A. and Pahlsson, P. (1997) 'Interferon-γ Enhancement of E-Selectin Expression on Endothelial Cells is Inhibited by Monensin', *Scandinavian Journal of Immunology*, 46(4), pp. 338–343. doi: 10.1046/J.1365-3083.1997.D01-135.X.

Suehiro, J. I. *et al.* (2010) 'Vascular endothelial growth factor activation of endothelial cells is mediated by early growth response-3', *Blood*, 115(12), pp. 2520–2532. doi: 10.1182/BLOOD-2009-07-233478.

Tada, Y. *et al.* (2003) 'Acceleration of the Onset of Collagen-Induced Arthritis by a Deficiency of Platelet Endothelial Cell Adhesion Molecule 1', *Arthritis and Rheumatism*, 48(11), pp. 3280–3290. doi: 10.1002/ART.11268.

Tan, K. T. *et al.* (2018) 'Profiling the B/T cell receptor repertoire of lymphocyte derived cell lines', *BMC Cancer*, 18(1), pp. 1–13. doi: 10.1186/S12885-018-4840-5/FIGURES/6.

Tanaka, Y. (2021) 'Recent progress in treatments of rheumatoid arthritis: an overview of developments in biologics and small molecules, and remaining unmet needs', *Rheumatology (Oxford, England)*, 60(Suppl 6), pp. VI12–VI20. doi: 10.1093/RHEUMATOLOGY/KEAB609.

Taraboletti, G. *et al.* (2002) 'Shedding of the Matrix Metalloproteinases MMP-2, MMP-9, and MT1-MMP as Membrane Vesicle-Associated Components by Endothelial Cells', *The American Journal of Pathology*, 160(2), p. 673. doi: 10.1016/S0002-9440(10)64887-0.

Tedder, T. F., Steeber, D. A. and Pizcueta, P. (1995) 'L-selectin-deficient mice have impaired leukocyte recruitment into inflammatory sites.', *Journal of Experimental Medicine*, 181(6), pp. 2259–2264. doi: 10.1084/JEM.181.6.2259.

Théry, C. *et al.* (2018) 'Minimal information for studies of extracellular vesicles 2018 (MISEV2018): a position statement of the International Society for Extracellular Vesicles and update of the MISEV2014 guidelines', *Journal of Extracellular Vesicles*, 7(1). doi: 10.1080/20013078.2018.1535750.

Tjahajawati, S. *et al.* (2020) 'Matrix levels of metalloproteinase-2 (MMP-2) and toxicity evaluation of carbonate apatite-based endodontic sealer in rat subcutaneous implantation', *Heliyon*, 6(7), p. e04330. doi: 10.1016/j.heliyon.2020.e04330.

Trimova, G. *et al.* (2020) 'Tumour necrosis factor alpha promotes secretion of 14-3-3η by inducing necroptosis in macrophages', *Arthritis Research and Therapy*, 22(1), pp. 1–11. doi: 10.1186/S13075-020-2110-9/FIGURES/6.

Tsou, P. S. *et al.* (2018) 'EZH2 Modulates the DNA Methylome and Controls T Cell Adhesion Through Junctional Adhesion Molecule A in Lupus Patients', *Arthritis & rheumatology (Hoboken, N.J.)*, 70(1), pp. 98–108. doi: 10.1002/ART.40338.

La Venuta, G. *et al.* (2015) 'The Startling Properties of Fibroblast Growth Factor 2: How to Exit Mammalian Cells without a Signal Peptide at Hand', *The Journal of biological chemistry*, 290(45), pp. 27015–27020. doi: 10.1074/JBC.R115.689257.

Viemann, D. *et al.* (2006) 'TNF induces distinct gene expression programs in microvascular and macrovascular human endothelial cells', *Journal of Leukocyte Biology*, 80(1), pp. 174–185. doi: 10.1189/JLB.0905530.

Viotti, C. (2016) 'ER to Golgi-Dependent Protein Secretion: The Conventional

Pathway', *Methods in molecular biology (Clifton, N.J.)*, 1459, pp. 3–29. doi: 10.1007/978-1-4939-3804-9_1.

Wada, Y. *et al.* (2009) 'A wave of nascent transcription on activated human genes', *Proceedings of the National Academy of Sciences of the United States of America*, 106(43), pp. 18357–18361. doi: 10.1073/PNAS.0902573106.

Walter, P. and Blobel, G. (1982) 'Mechanism of protein translocation across the endoplasmic reticulum', *Biochemical Society symposium*, 47, pp. 183–191. Available at: https://pubmed.ncbi.nlm.nih.gov/6100822/ (Accessed: 1 August 2023).

Wang, L. *et al.* (2006) 'Matrix Metalloproteinase 2 (MMP2) and MMP9 Secreted by Erythropoietin-Activated Endothelial Cells Promote Neural Progenitor Cell Migration', *Journal of Neuroscience*, 26(22), pp. 5996–6003. doi: 10.1523/JNEUROSCI.5380-05.2006.

Wang, X. *et al.* (2016) 'Adiponectin improves NF-κB-mediated inflammation and abates atherosclerosis progression in apolipoprotein E-deficient mice', *Lipids in Health and Disease*, 15(1), pp. 1–14. doi: 10.1186/s12944-016-0202-y.

Wang, X. *et al.* (2018) '14-3-3ζ delivered by hepatocellular carcinoma-derived exosomes impaired anti-tumor function of tumor-infiltrating T lymphocytes', *Cell Death & Disease 2018 9:2*, 9(2), pp. 1–14. doi: 10.1038/s41419-017-0180-7.

Winiarska, M. *et al.* (2017) 'Selection of an optimal promoter for gene transfer in normal B cells', *Molecular Medicine Reports*, 16(3), p. 3041. doi: 10.3892/MMR.2017.6974.

Wong, D. and Dorovini-Zis, K. (1992) 'Upregulation of intercellular adhesion molecule-1 (ICAM-1) expression in primary cultures of human brain microvessel endothelial cells by cytokines and lipopolysaccharide', *Journal of Neuroimmunology*, 39(1–2), pp. 11–21. doi: 10.1016/0165-5728(92)90170-P.

Wong, M. X. *et al.* (2005) 'The inhibitory co-receptor, PECAM-1 provides a protective effect in suppression of collagen-induced arthritis', *Journal of clinical immunology*, 25(1), pp. 19–28. doi: 10.1007/S10875-005-0354-7.

Wragg, J. W. *et al.* (2014) 'Shear Stress Regulated Gene Expression and Angiogenesis in Vascular Endothelium', *Microcirculation*, 21(4), pp. 290–300. doi: 10.1111/MICC.12119.

Wubbolts, R. *et al.* (2003) 'Proteomic and biochemical analyses of human B cell-derived exosomes. Potential implications for their function and multivesicular body formation', *The Journal of biological chemistry*, 278(13), pp. 10963–10972. doi: 10.1074/JBC.M207550200.

Wuthrich, R. P. (1992) 'Vascular cell adhesion molecule-i (VCAM-1) expression in murine lupus nephritis', *Kidney International*, 42, pp. 903–914. doi: 10.1038/ki.1992.367.

Xu, B. *et al.* (2014) 'Promotion of lung tumor growth by interleukin-17', *American Journal of Physiology - Lung Cellular and Molecular Physiology*, 307(6), pp. L497–L508. doi: 10.1152/ajplung.00125.2014.

Yan, C. and Boyd, D. D. (2007) 'Regulation of matrix metalloproteinase expression expression', *Journal of Cellular Physiology*, 211(1), pp. 19–26. doi: 10.1002/jcp.20948.

Yáñez-Mó, M. *et al.* (2015) ‘Biological properties of extracellular vesicles and their physiological functions’, *Journal of Extracellular Vesicles*, 4(2015), pp. 1–60. doi: 10.3402/JEV.V4.27066.

Yosef, G., Hayun, H. and Papo, N. (2021) ‘Simultaneous targeting of CD44 and MMP9 catalytic and hemopexin domains as a therapeutic strategy’, *Biochemical Journal*, 478(5), p. 1139. doi: 10.1042/BCJ20200628.

Yoshizaki, T. *et al.* (1998) ‘The expression of matrix metalloproteinase 9 is enhanced by Epstein-Barr virus latent membrane protein 1’, *Proceedings of the National Academy of Sciences of the United States of America*, 95(7), pp. 3621–3626. doi: 10.1073/PNAS.95.7.3621.

Yu, Q. and Stamenkovic, I. (1999) ‘Localization of matrix metalloproteinase 9 to the cell surface provides a mechanism for CD44-mediated tumor invasion’, *Genes & Development*, 13(1), p. 35. doi: 10.1101/GAD.13.1.35.

Zaman, R. *et al.* (2019) ‘Current strategies in extending half-lives of therapeutic proteins’, *Journal of controlled release : official journal of the Controlled Release Society*, 301, pp. 176–189. doi: 10.1016/J.JCONREL.2019.02.016.

Zhang, M. *et al.* (2015) ‘Translocation of interleukin-1β into a vesicle intermediate in autophagy- mediated secretion’, *eLife*, 4(NOVEMBER2015). doi: 10.7554/ELIFE.11205.001.

Zhang, Y. *et al.* (2019) ‘Exosomes: biogenesis, biologic function and clinical potential’, *Cell & Bioscience 2019 9:1*, 9(1), pp. 1–18. doi: 10.1186/S13578-019-0282-2.